[redacted]

NASA Contractor Report 165928

AIRCRAFT SURFACE COATINGS

ENERGY EFFICIENT TRANSPORT PROGRAM

BOEING COMMERCIAL AIRPLANE COMPANY
P.O. BOX 3707, SEATTLE, WA 98124

Contract NAS1-15325, Task 4.4

National Aeronautics and
Space Administration

Langley Research Center
Hampton, Virginia 23665

NASA Contractor Report 165928

AIRCRAFT SURFACE COATINGS

ENERGY EFFICIENT TRANSPORT PROGRAM

BOEING COMMERCIAL AIRPLANE COMPANY
P.O. BOX 3707, SEATTLE, WA 98124

Contract NAS1-15325, Task 4.4
June 1982

325

ıor
ese
t-

National Aeronautics and
Space Administration

Langley Research Center
Hampton, Virginia 23665

FOREWORD

This is the final report on surface coatings work accomplished under Task 4.4, Aircraft Surface Coatings, Contract NAS1-15325. This task is a continuation of work initiated under Contract NAS1-14742 and reported in documents CR 158954 and CR 159288.

Technical investigations were conducted from January 1980 to February 1982. D. B. Middleton, in the Aircraft Energy Efficiency Project Office (ACEEPO), Langley Research Center, was the NASA technical monitor. The work was done by the Preliminary Design department of the Vice President-Engineering organization, Boeing Commercial Airplane Company, and by Avco Systems Division, as a major subcontractor. Participating personnel were:

Boeing

G. W. Hanks
Program Manager

H. R. Gelbach
Systems Technology

R. L. Kreitinger
Project Manager

D. George-Falvy
Aerodynamics Technology

L. R. Elvigan
Materials Technology

J. S. Kautzky
Economic Analysis

M. J. Omoth
Systems Technology

Avco

R. M. Rouleau
Project Manager

Special acknowledgement is given to Dennis Parks and Jeff Swindells of Continental Airlines and to Ralph Stockton and Ed Robertson of Delta Air Lines for their cooperation in managing and reporting the flight service evaluations for their respective airlines.

The project is indebted to Jim Hall of the NASA-Langley Terminal Configured Vehicle Project Office (TCVPO) and the personnel who participated in the drag measurement flight tests for their expertise and total cooperation.

Principal measurements and calculations used during this study were in customary units.

CONTENTS

FIGURES

TABLES

1.0 SUMMARY

Previous work on aircraft surface coatings, reported in NASA CR 158954 (ref. 1) and CR 159288 (ref. 2), led to the selection of liquid spray-on elastomeric polyurethanes as best candidate materials. Further work on three commercially available products of this type, CAAPCO B-274, Chemglaze M313 and Astrocoat Type I, is reported in this document. Drag measurement flight tests, airline service evaluations, and additional laboratory tests were conducted. A cost/benefit assessment was made, based on test results. Principal conclusions from the current study were:

Drag Measurement Flight Tests

- CAAPCO applied to the wing upper surface in place of rough Corogard (average measured roughness 160μin) reduced airfoil section profile drag 2.4%, which is equivalent to about 0.4% airplane drag in cruise. The estimated drag reduction from CAAPCO applied to both wing and empennage surfaces is about 0.6%.

- A badly eroded wing leading edge on the 737 could cause a drag penalty of about 0.3% at cruise.

Airline Service Evaluations

- When properly applied to leading edges, CAAPCO and Chemglaze have an erosion life of about 6500 and 5000 flight-hours, respectively. The erosion life of Astrocoat is significantly less.

- CAAPCO requires an epoxy primer for best adhesion. Chemglaze can be satisfactorily applied over either a wash primer or an epoxy primer.

Laboratory Tests

- Leading-edge coatings do not significantly affect thermal anti-icing system performance.

- Coatings applied from the leading edge to the rear spar will not cause precipitation static interference with communication and navigation equipment.

- A lightning-strike analysis should be performed before applying coatins to wing areas containing fuel that are immediately above wing-mounted engines.

- Composite leading edges (fiberglass-epoxy, graphite-epoxy, Kevlar-epoxy and hybrid Kevlar-graphite-epoxy) were found to have very short erosion lives. When protected by a 9-mil coating, the best specimen in rain erosion tests was CAAPCO on fiberglass-epoxy with an erosion durability roughly equivalent to uncoated 2024 ST aluminum.

- In laboratory tests, the coatings with a polyurethane enamel topcoat provided corrosion protection equal to, or better than, current systems. Long-term effects of the operating environment were not evaluated.

Cost/Benefit Assessment

- The net annual benefit per 737-200 airplane, from coatings applied from leading edge to rear spar of the empennage surfaces and wing upper surface, was estimated to be \$10 000 to \$20 000, depending upon fuel price and annual utilization.

- Coatings applied only from the leading edge to front spar would not produce dollar benefits from reduced fuel burn. Operators with extreme erosion problems might benefit from reduced parts replacement costs and improved low-speed handling qualities.

It is recommended that industry pursue any long-term corrosion-protection investigations necessary to fully qualify these coatings for application to the jet transport fleet.

2.0 INTRODUCTION

Under the energy efficient transport (EET) element of the NASA-sponsored Aircraft Energy Efficiency (ACEE) program, surface coatings were investigated to find smooth, durable materials that would reduce airplane drag and would protect external surfaces from erosion and/or corrosion. Three principal areas of investigation were followed during the program, as shown in Figure 1. Three series of laboratory tests were conducted; leading candidate materials were evaluated in revenue service by Continental Airlines (CO) and by Delta Air Lines (DL); and drag changes due to coatings were measured in flight tests conducted at NASA-Langley Research Center.

The first series of laboratory tests identified three elastomeric polyurethane spray-on coatings as the best potential candidates out of a field of 9 liquid coatings and 60 film-adhesive systems. Two of the candidate coatings, CAAPCO B-274 and Chemglaze M313, were applied to the leading edges of wing slats and the horizontal tail of a CO 727 and flown 14 months in the Air Micronesia route system. Results of the initial laboratory tests and details of the coating application to the CO 727 are reported in Reference 1.

During the second series of laboratory tests, most of the effort was directed toward evaluating and reducing the susceptibility of elastomeric polyurethanes to synthetic-type hydraulic fluids, such as Skydrol or Hyjet IV. During these tests and in

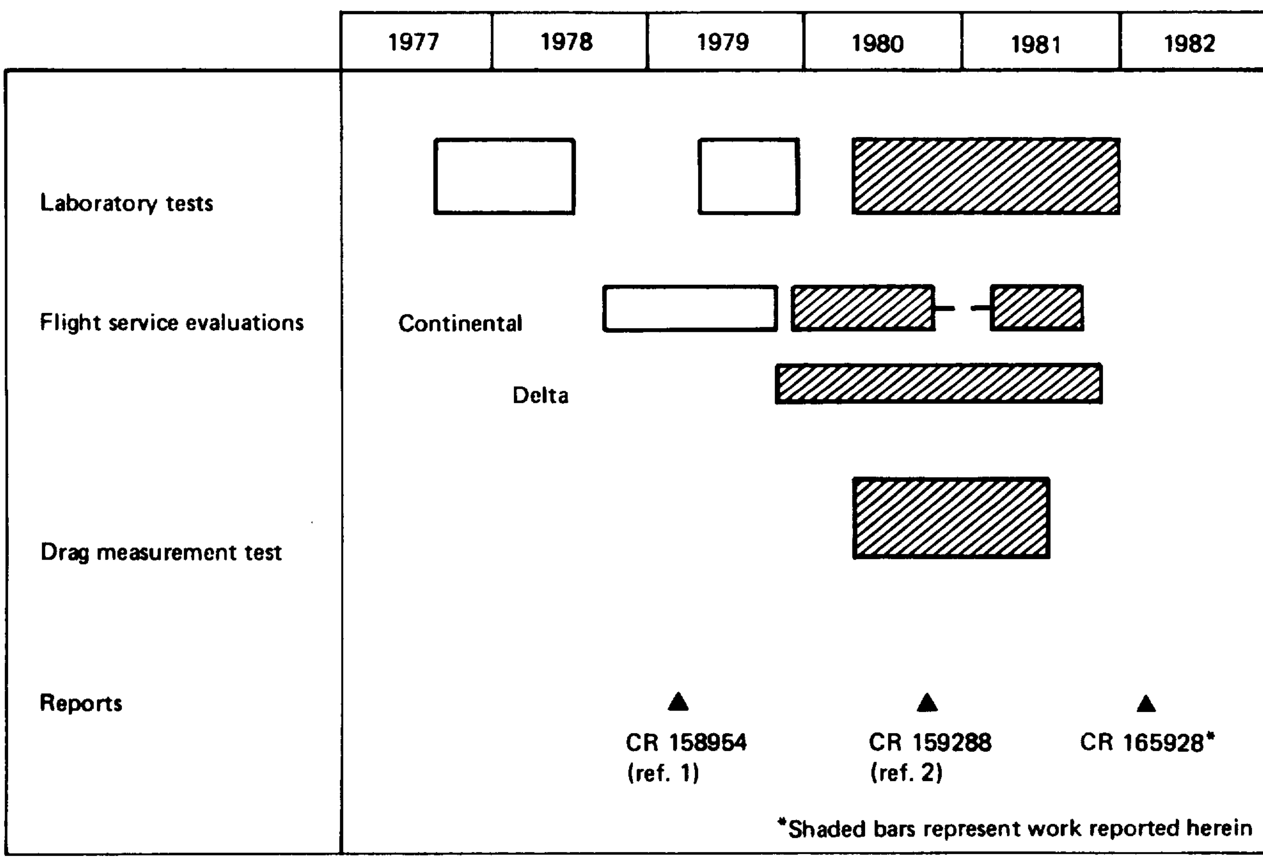

Figure 1. Aircraft Surface Coatings Program

subsequent testing, Astrocoat Type I was included as a reference material with the other two candidate elastomeric polyurethanes. Limited testing also was conducted on the four best films identified in the earlier tests (Tradlon, Kapton, Kynar, and UHMW Polyolefin) in combination with additional adhesives. Because of the difficulty anticipated in bonding films to large areas with compound curvature and because of their relatively short erosion life, further work with films was discontinued.

Results of the second laboratory test series and the CO flight service evaluation are reported in Reference 2. Also reported are descriptions of the coating application to a DL 727 for service evaluation and the coating reapplication to the CO 727 for a second service evaluation by that airline.

The shaded bars in Figure 1 represent parts of the total program reported in this document. The drag measurement flight tests conducted at NASA-Langley Research Center are reported in Section 4.1, with the test data analysis methods described in Appendix A. Results of the DL service evaluation and the second CO evaluation are covered in Section 4.2. Section 4.3 reports the various laboratory tests in the final series, designed to evaluate the compatibility of elastomeric polyurethane coatings with the airline transport operating environment. Icing tests, lightning and precipitation static analyses, erosion protection and corrosion protection tests were conducted. Icing test data are presented in Appendix B; corrosion test methods are described in Appendix C.

Section 5.0 contains an assessment of the economic merit of applying coatings to an airline transport and recommendations based on both technical and economic considerations.

The work reported in this document was accomplished under Contract NAS1-15325.

NOTE:

> Certain commercial materials are identified in this document in order to specify adequately which materials were investigated in the research effort. In no case does such identification imply recommendation or endorsement of the product by NASA or Boeing, nor does it imply that the materials are necessarily the only ones or the best ones available for the purpose.

3.0 ABBREVIATIONS AND SYMBOLS

ACEE	Aircraft Energy Efficiency program
AFB	Air Force base
AFML	Air Force Materials Laboratory
ASTM	American Society for Testing and Materials
c	chord
C	coulomb, charge transfer
C_d	section drag coefficient
C_D	airplane drag coefficient
C_l	section lift coefficient
C_L	airplane lift coefficient
CMI	continuous maximum icing
CO	Continental Airlines
c_p	local static pressure
DA	dry air
DL	Delta Air Lines
e	freestream condition (subscript)
EET	energy efficient transport
FAR	Federal Aviation Regulation
FOD	foreign object damage
FTMS	Federal Test Methods Standard
h_p	pressure altitude
ID	inside diameter
IMI	intermittent maximum icing
kPa	kilopascal (pounds force per square inch)
L	liter

M	Mach number
M	freestream Mach number
m	meter, magnification factor
mA	milliampere
max	maximum
MEK	methyl ethyl ketone
MIBK	methyl isobutyl ketone
M_{MO}	Mach number, maximum operating
NASA	National Aeronautics and Space Administration
P_o	atmospheric pressure
P_s	static pressure
P_v	velocity pressure
Q_B	average current multiplied by time
Q_C	maximum current
Q_T	total charge in coulombs
r_a	surface roughness
ref.	reference
R/m, R/ft	freestream unit Reynolds number
S_D	distance between spars
S_{REF}	reference area
T	time, total temperature
TAI	thermal anti-icing
T/C	thermocouple
TCV	Terminal Configured Vehicle
T_D	dwell time
u/U_e	velocity ratio
UHMW	ultrahigh molecular weight
UV	ultraviolet

V	aircraft velocity
V_{MO}	velocity, maximum operating
WBL	wing buttock line
W/δ	weight to pressure ratio
y	distance from surface
x/c	chord thickness ratio
Δ	difference
θ	corrected momentum thickness
ρ	air density

4.0 STUDY RESULTS

The four areas of investigation—drag measurement test, flight service evaluations, environmental (laboratory) tests, and cost/benefit assessment—are described in this section and the results are presented. Additional information on some of the unique tests is contained in the appendixes.

4.1 DRAG MEASUREMENT TEST

A flight test program was conducted at NASA-Langley Research Center to investigate the effects of surface coatings on airplane drag. The tests were flown on the B737 Terminal Configured Vehicle (TCV) shown in Figure 2. The airplane provided a test surface on the inboard wing that was free of leading-edge devices that might affect upper surface boundary layer flow and influence test results. The test surface also provided a representative jet transport airfoil section on which measurements could be taken at full-scale Reynolds numbers.

Because the three elastomeric polyurethanes being investigated (CAAPCO, Chemglaze, and Astrocoat) had nearly identical surface smoothness characteristics, only CAAPCO was used in the program. It was believed that testing the other two materials would give redundant results with increased expense. CAAPCO was compared to Corogard paint, bare, and enamel paint surfaces in the test series.

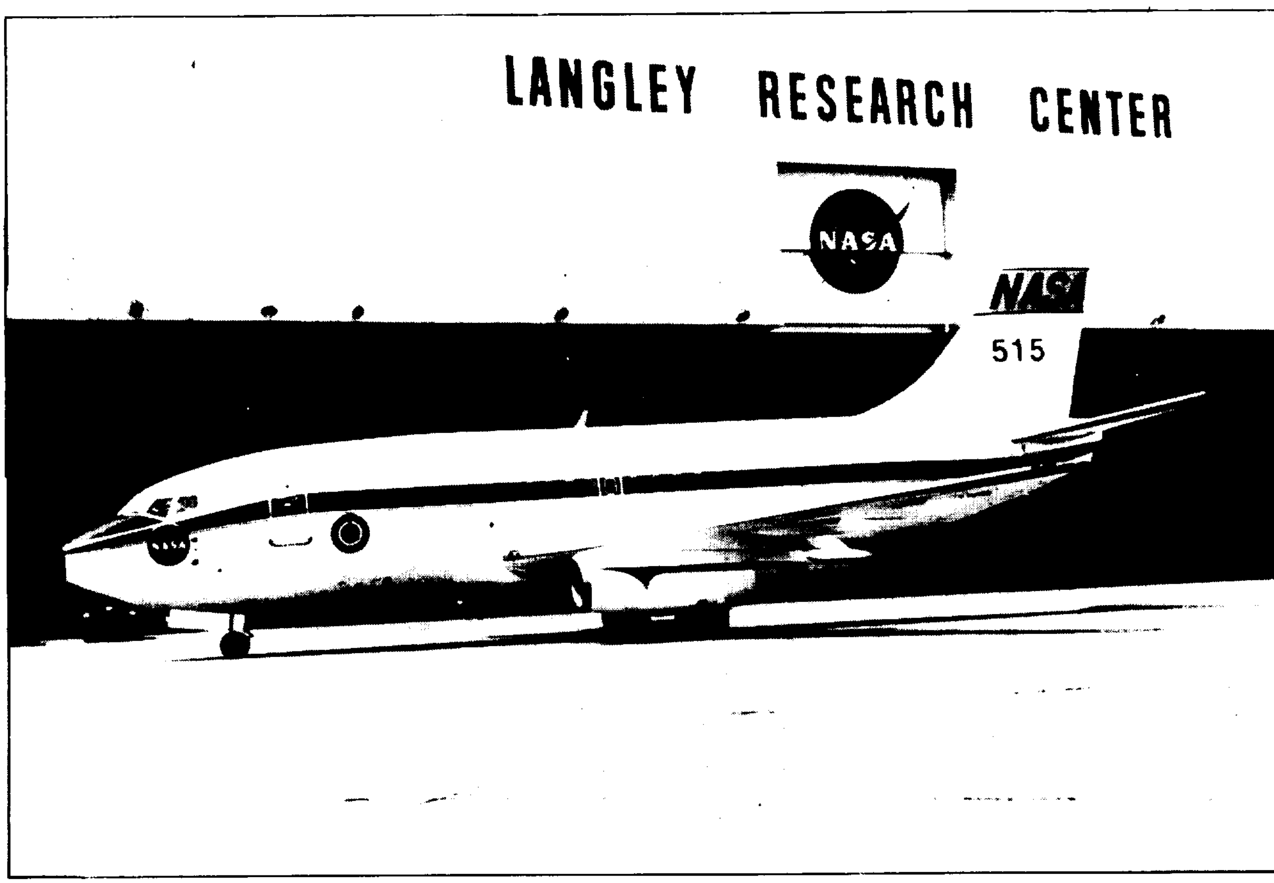

Figure 2. Test Airplane: NASA TCV B737 Research Aircraft

4.1.1 TEST DESCRIPTION

This section contains a brief description of the test setup, surface configurations tested, instrumentation, test procedure, philosophy of test analysis, and data processing. Complete details are reported in Reference 3.

4.1.1.1 Test Airplane and Experimental Layout

The principal requirements for a suitable test vehicle were (1) the capability of achieving flight conditions, i.e., speed, altitude, Mach numbers, and Reynolds numbers typical of jet transport airplanes; (2) test surface characteristics representative of transport airplanes; and (3) proper instruments for high-precision data gathering.

Figure 3 shows the location of the test surface on the airplane and the principal instrumentation used. The various surface coatings were applied to a 2.03m- (80-in-) wide strip on the inboard left wing, extending between the 18% span station and the 32% span station and terminating at the aft end at the hinge line of the inboard spoiler. The same area of the right wing was stripped of paint to the bare metal surface and was retained in that condition throughout the test to provide a constant baseline reference surface. Evaluation of the various surface coatings was made principally by a side-to-side comparison from measurements taken simultaneously on the test surface and the base reference surface. This method ensured that comparison of the two surfaces was made at exactly the same flight conditions. To further validate the evaluation, the left side test surface was also tested in the bare condition and differences between the two surfaces were taken into account.

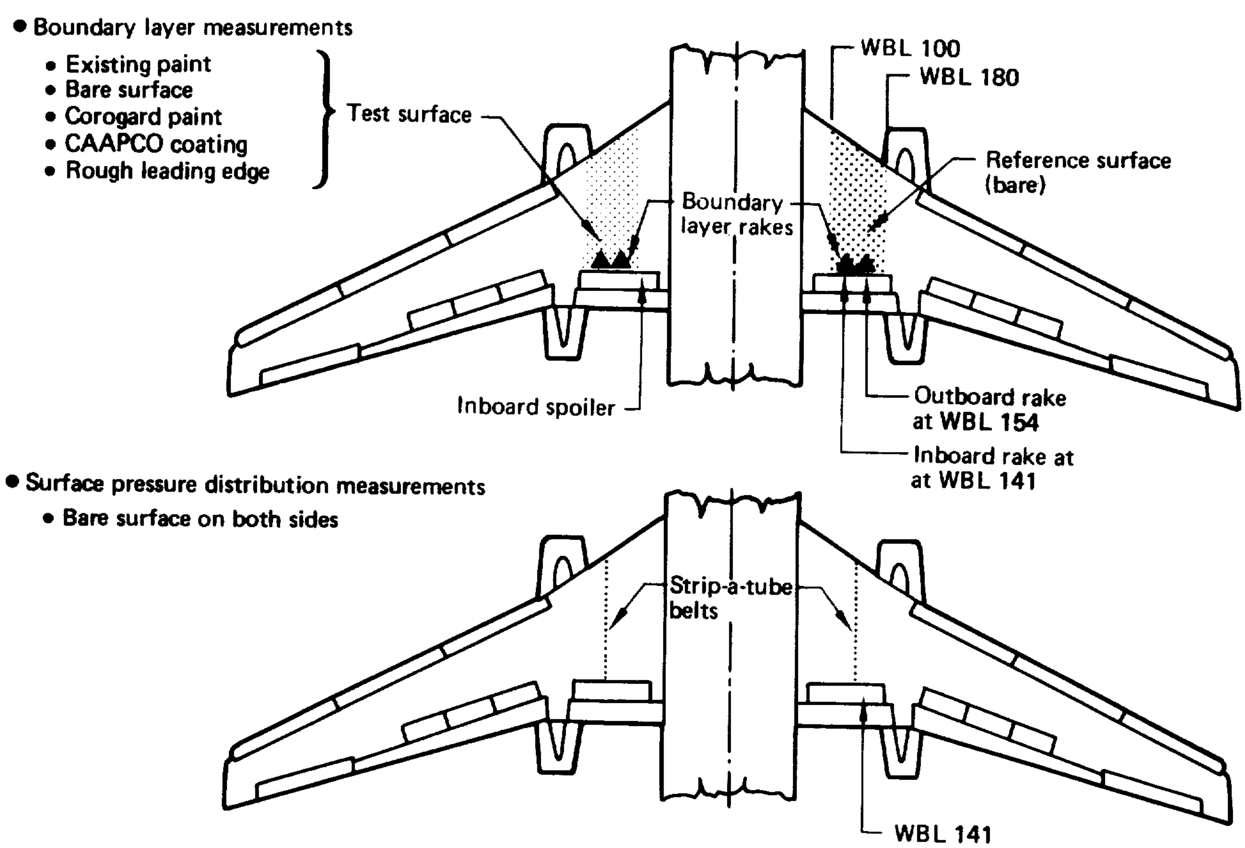

Figure 3. Experiment Layout

The principal instrumentation consisted of a pair of boundary layer rakes mounted on the wing near the downstream edge of the reference surface and test surface (73% of the local wing chord). The rakes mounted at the surface midspan (WBL 141) were the primary data source, and the outboard rakes (WBL 154) provided backup data.

Chordwise pressure distributions along the center of the test section (WBL 141) were measured during flight 2, using multitube plastic belts (Strip-a-tube) bonded to the wing surface. These measurements provided an experimental data base for the calculation of boundary layer growth along the test surface.

4.1.1.2 Surface Configurations Tested

Boundary layer measurements were made of five surface configurations: the painted surface, which existed prior to the test; the bare surface; the bare surface with rough leading edge; Corogard; and CAAPCO coating.

The existing paint on the test airplane was a nonstandard enamel coating, applied by a NASA contractor several years ago. Although there were no major discrepancies on the upper surface test section, there were numerous small lumps and specks. In general, the surface condition was typical of a medium-time airplane in airline service.

The bare metal surface shown in Figure 4a was very smooth (surface roughness, $r_a \approx$ 30 μin), however, numerous rivet heads protruded from the surface up to about 0.1 mm (0.004 in). In addition, spanwise skin butt joints across the test section had small gaps 1 to 3 mm (0.04 to 0.12 in) wide, with aerodynamic putty in the larger gaps. There were occasional skin joint mismatches of up to 0.25 mm (0.01 in). Because these surface imperfections were comparable to the thickness of the viscous sublayer, they produced some incremental drag above the profile drag of a perfectly smooth wing. The bare surface chosen as a baseline configuration, therefore, was not an ideal, hydraulically smooth surface, but one that had discrete roughness elements.

The roughened leading edge (fig. 4b) was included among the test configurations to obtain data on the effects of an eroded leading edge on drag. The simulation was accomplished by applying metallic grit to the leading edge on the left wing test surface for flight 3a. The roughened strip was about 76 mm (3 in) wide. The grit size was No. 50, 0.50 mm (0.02 in), with a nominal density of about 15 particles per square centimeter (100 particles per square inch). For a comparison to a severely eroded leading edge on an airline transport, refer to Figure 28, Section 4.2.1.2.

Corogard paint (fig. 4c) was tested to obtain an additional reference to which the CAAPCO B-274 elastomeric polyurethane surface coating could be compared. Corogard is widely used on large transport airplanes because of its excellent corrosion protection characteristics, however, it produces a certain level of roughness that varies with application techniques. Surveys reported that Corogard roughness averaged about $r_a = 150 \pm 30\ \mu$in on Boeing production airplanes. Duplication of this roughness level was intended for the present experiment; however, the coating ultimately was slightly rougher than desired, registering a mean value of about $r_a \approx 160\ \mu$in. The Corogard was applied from the front spar back to the spoiler hinge line, i.e., past the boundary layer rakes.

The CAAPCO coating (fig. 4d) applied ahead of the front spar was approximately 12-mil thick. Aft of the front spar, where erosion protection is not critical, a 5-mil

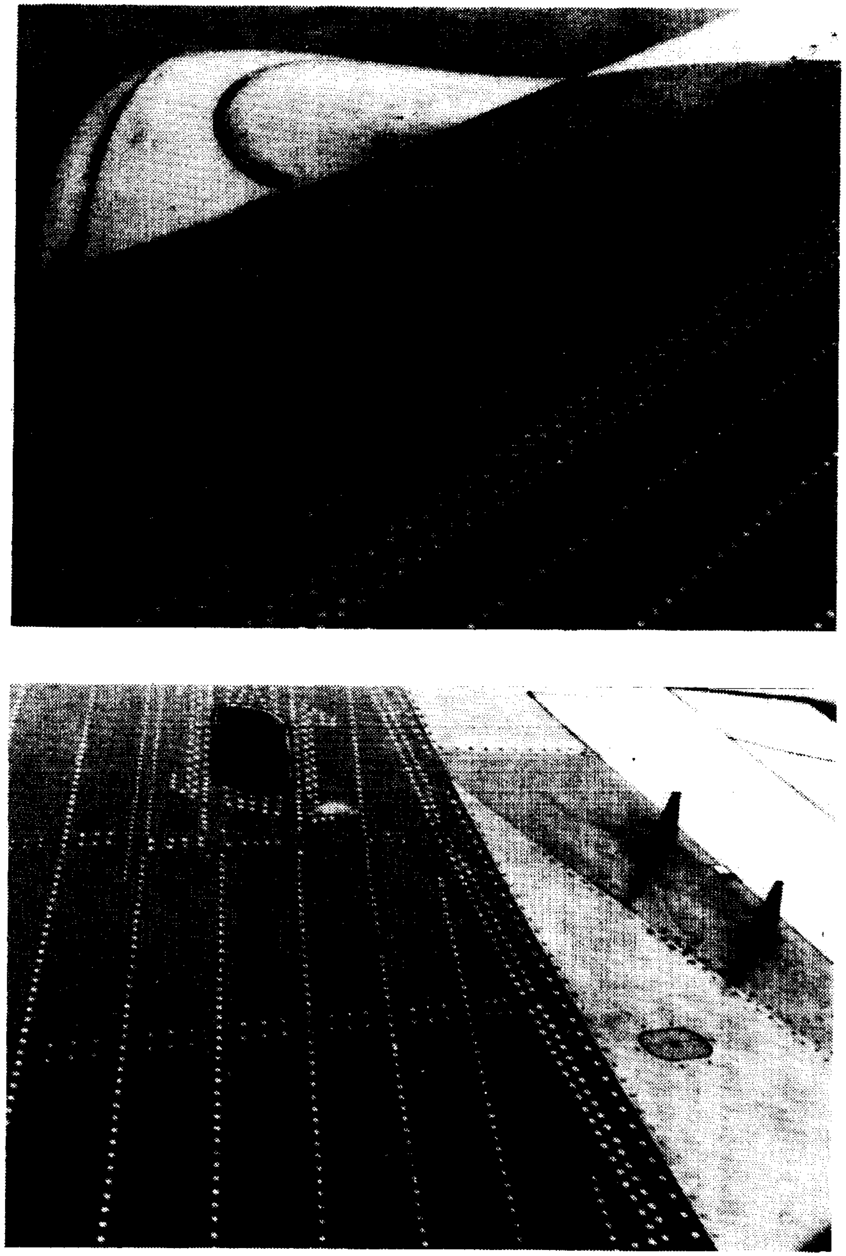

(a) Bare Metal Surface

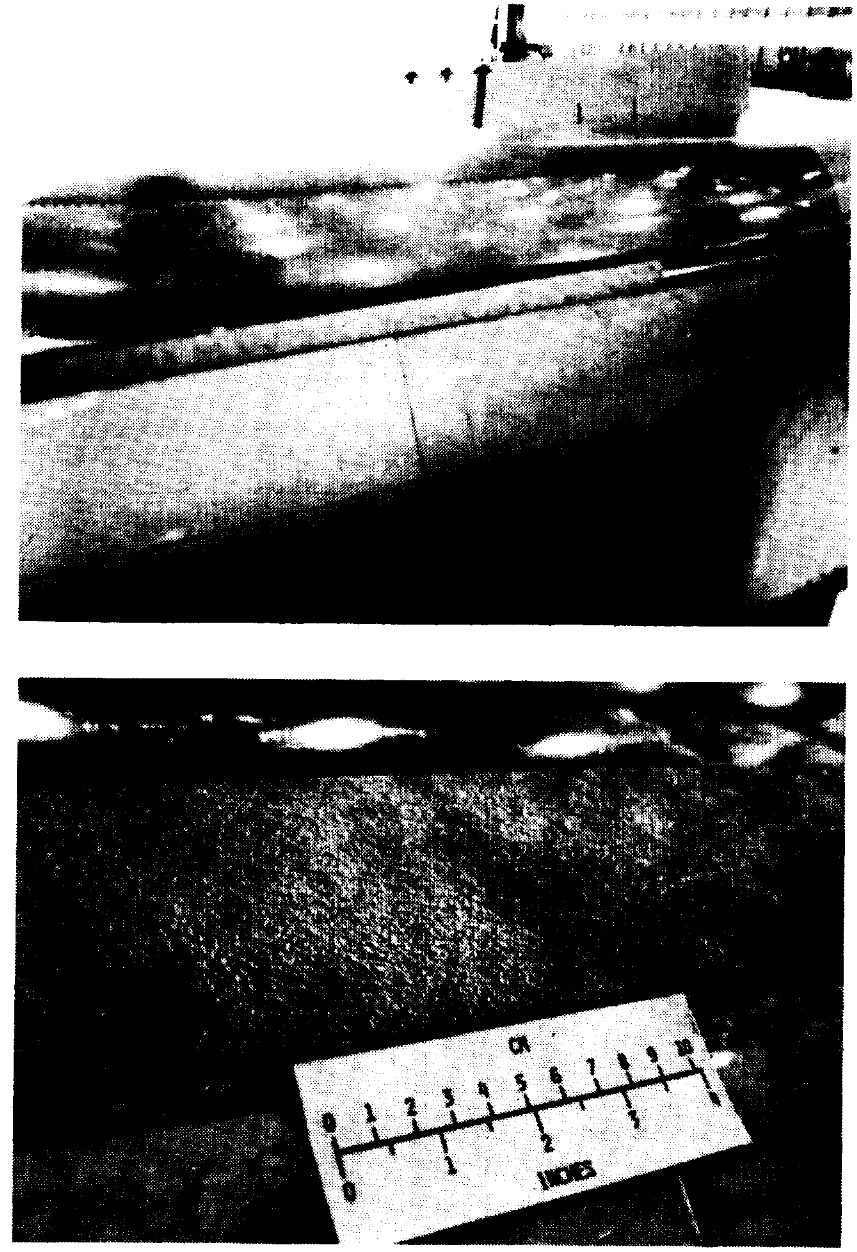

(b) Rough Leading Edge

Figure 4. Test Surfaces

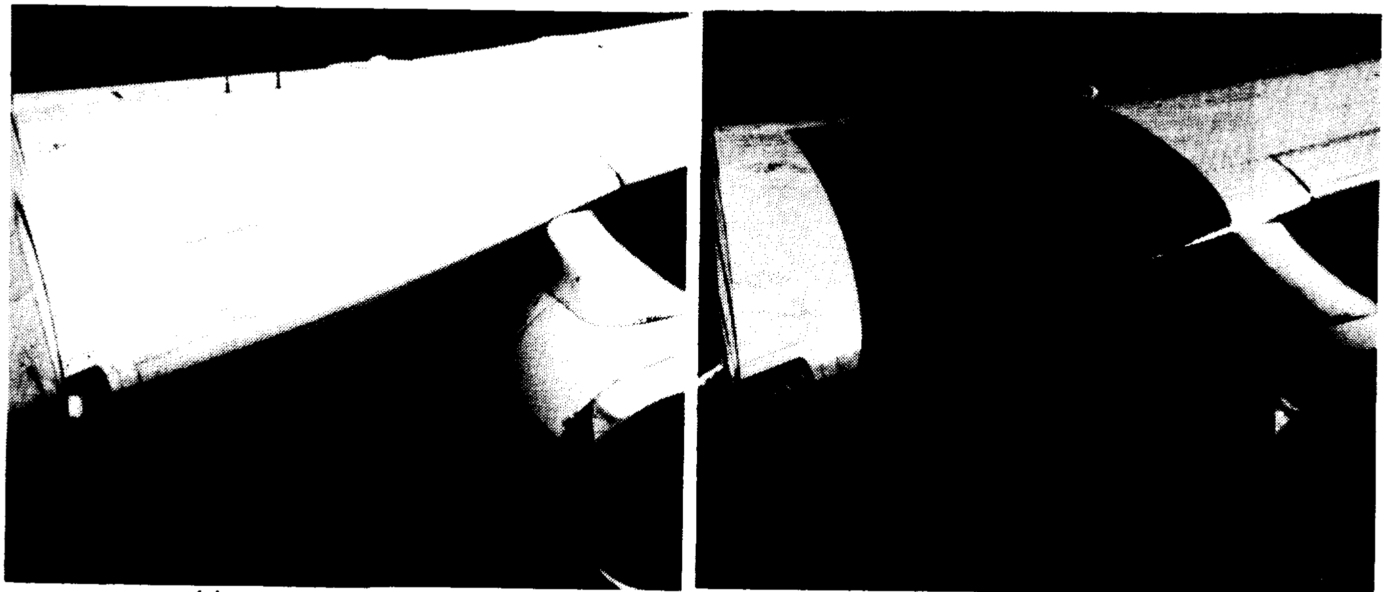

(c) Corogard Coated Surface (d) CAAPCO B-274 Coated Surface

Figure 4. Test Surfaces (Concluded)

thickness was applied. The resulting surface was fairly smooth and, to some extent, the coating faired nonflush rivet heads and skin joints. The coating was applied under a protective enclosure that had a filtered ventilation system. During coating application, the enclosure was opened and additional fans were added to improve ventilation. This caused some dust and lint particles to be deposited on the wet surface during the curing period. It is believed that higher surface quality could be achieved under properly controlled application conditions. The CAAPCO-coated test surface showed an average roughness level of $r_a \approx 10$ to 15μin.

4.1.1.3 Instrumentation

The instrumentation system consisted of four principal elements: (1) pressure sensors, including boundary layer rakes and static pressure survey belts; (2) scan-control module; (3) high-accuracy airplane reference pressure and temperature transducers; and (4) onboard recording equipment of the test airplane. A detailed description of the instrumentation elements is contained in Reference 3.

Boundary Layer Rakes—The four boundary layer rakes were the principal data sensors. Each rake had 24 total head probes and one static pressure probe. The total head probes were closely spaced near the surface, as shown in Figure 5, to obtain good definition of the boundary layer in that critical region. The probes extended to a height of 12.7 cm (5 in) above the surface.

Static Pressure Survey Belts—These belts served as supplementary data sensors and were used during flight 2. One belt was installed on each wing panel at the 25% semispan location (WBL 141) extending from the leading edge to the 73% chordline. Each belt had static ports at 18 chordwise locations along the test surface. Figure 6 shows the belt installation.

Scan-Control Module—The scan-control module contained pressure sensors and interfaces with the data recording system of the airplane. The main functions of the module were to activate and control four pressure multiplexer valves (Scanivalves)

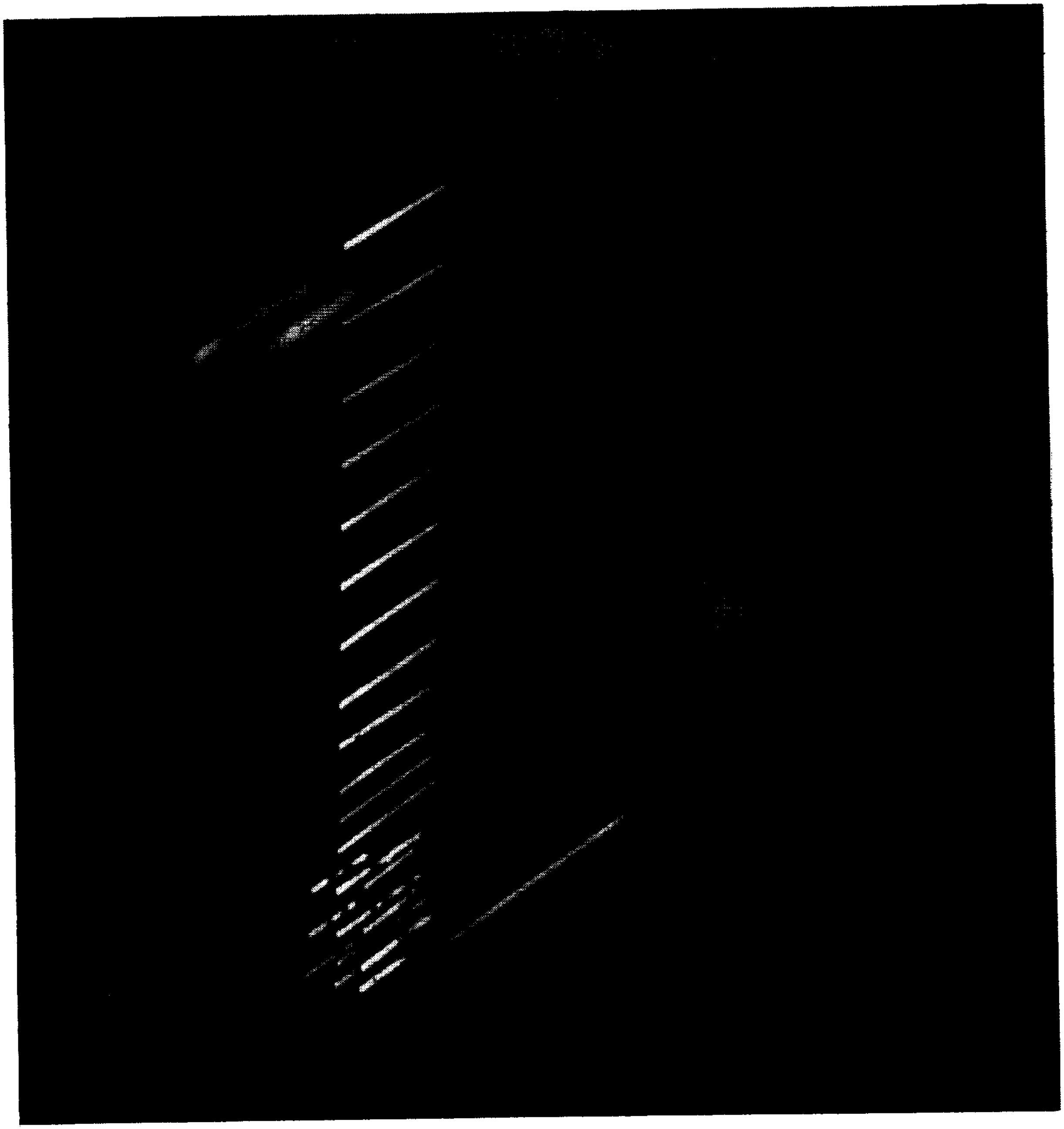

Figure 5. Boundary Layer Rake Installation

and to supply excitation voltage and signal conditioning for the pressure transducers contained in each Scanivalve. The scan-control module also contained valving that allowed cabin air to flow out the measurement ports during non-data-taking periods. This function was provided to purge the pressure measurement tubes and probes of water or ice. Provision was made for manual control of purge/operate, initiating data sequence, and selection of scanning rate. Remote control and Scanivalve position readouts also were provided for preflight checkout.

Reference Pressure and Temperature Transducers—Four high-accuracy Digiquartz transducers were used to measure the reference total, static, and impact pressures taken from the copilot's pitot static system and the freestream total temperature. These transducers were integral parts of the test airplane data acquisition system.

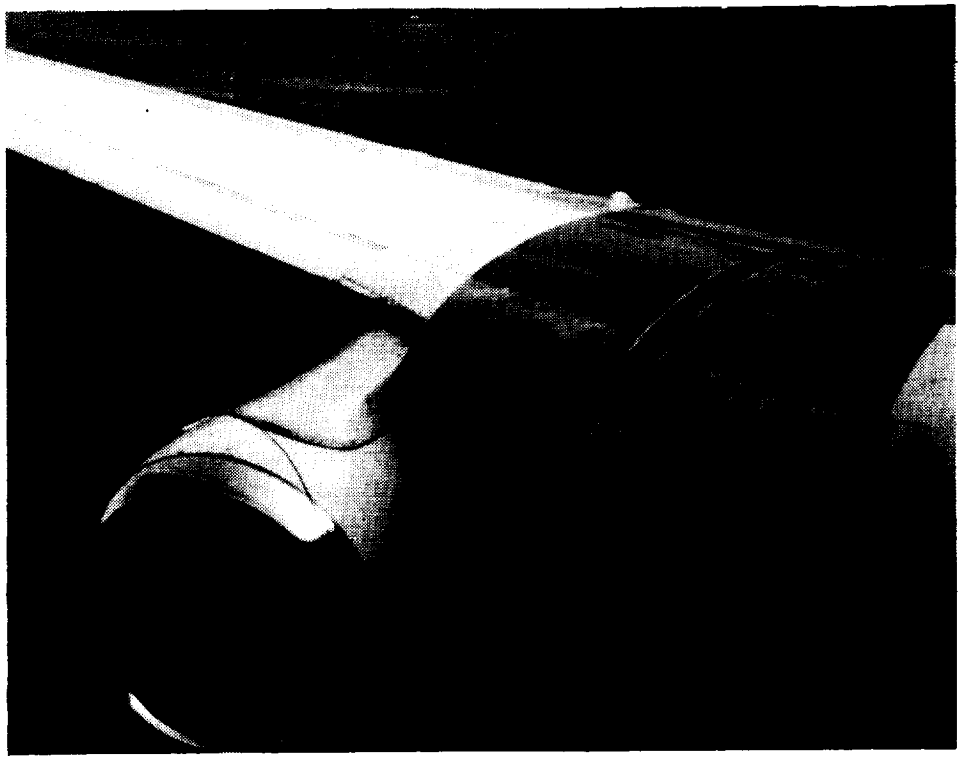

Figure 6. Static Pressure Survey Belt Installation

The total and static pressures from these sources were transmitted to one channel of each Scanivalve and recorded with the scanned rake pressure data. This arrangement provided an updated recalibration at each scanning cycle.

Onboard Data Recording Equipment—The test airplane onboard data recording equipment consisted of a 100-channel digital tape recorder and three 8-channel oscillographs for online data monitoring and quick-look data recording.

In addition to variables essential to the data analysis, other variables, such as airspeed, altitude, angle of attack, pitch and yaw angles, and fuel quantity, were recorded for identification of flight conditions.

4.1.1.4 Test Procedure

Tests evaluating surface coating drag were incorporated into the TCV flight test program on a concurrent basis and were usually performed after the airplane had completed its primary mission at the Wallops Island test site. The drag tests were flown in tightly controlled off-shore corridors designated by Air Traffic Control.

There were five test flights and one supplementary test during flight 3a, when the roughened leading edge was tested. The following flights and test configurations are listed chronologically:

Flight No.	Date	Test surfaces Left wing	Right wing	Data sources
1	2-11-80	Existing paint	Bare	Boundary layer rakes
2	1-20-81	Bare	Bare	Pressure belts
3a	1-23-81	Bare, leading-edge grit	Bare	Boundary layer rakes
3	1-23-81	Bare	Bare	Boundary layer rakes
4	1-27-81	Corogard	Bare	Boundary layer rakes
5	2-03-81	CAAPCO	Bare	Boundary layer rakes

A total of 15 test conditions was flown during each flight, except in the case of the roughened leading edge, which included only four conditions. The conditions were selected, as shown in Figure 7, to provide systematic variations of Mach number and lift coefficient throughout the cruise regime of the airplane. The following test conditions were flown:

Test condition	C_L	M	W/δ, kg	(lb)
1	0.75	0.55	149 180	(328 881)
2	0.55	0.65	152 983	(337 264)
3	0.45	0.70	145 165	(320 029)
4	0.35	0.75	129 611	(285 740)
5	0.65	0.55	129 447	(285 377)
6	0.45	0.65	125 167	(275 943)
7	0.35	0.70	112 906	(248 911)
8	0.55	0.55	109 532	(241 473)
9	0.35	0.65	97 352	(214 623)
10	0.25	0.75	92 579	(204 100)
11	0.45	0.55	89 616	(197 568)
12	0.25	0.70	80 647	(177 794)
13	0.25	0.65	69 537	(153 302)
14	0.35	0.55	69 702	(153 664)
15	0.25	0.55	49 787	(109 760)

To achieve a given combination of Mach number and lift coefficient, each condition was flown at a fixed value of W/δ determined from the formula:

$$W/\delta = 0.7\, P_o\, S_{ref}\, M^2 C_L$$

To establish a test condition, the momentary gross weight of the airplane was determined from onboard fuel gage readings. The appropriate pressure altitude to obtain the required W/δ ratio was then calculated. Finally, engine thrust was set to establish the desired Mach number.

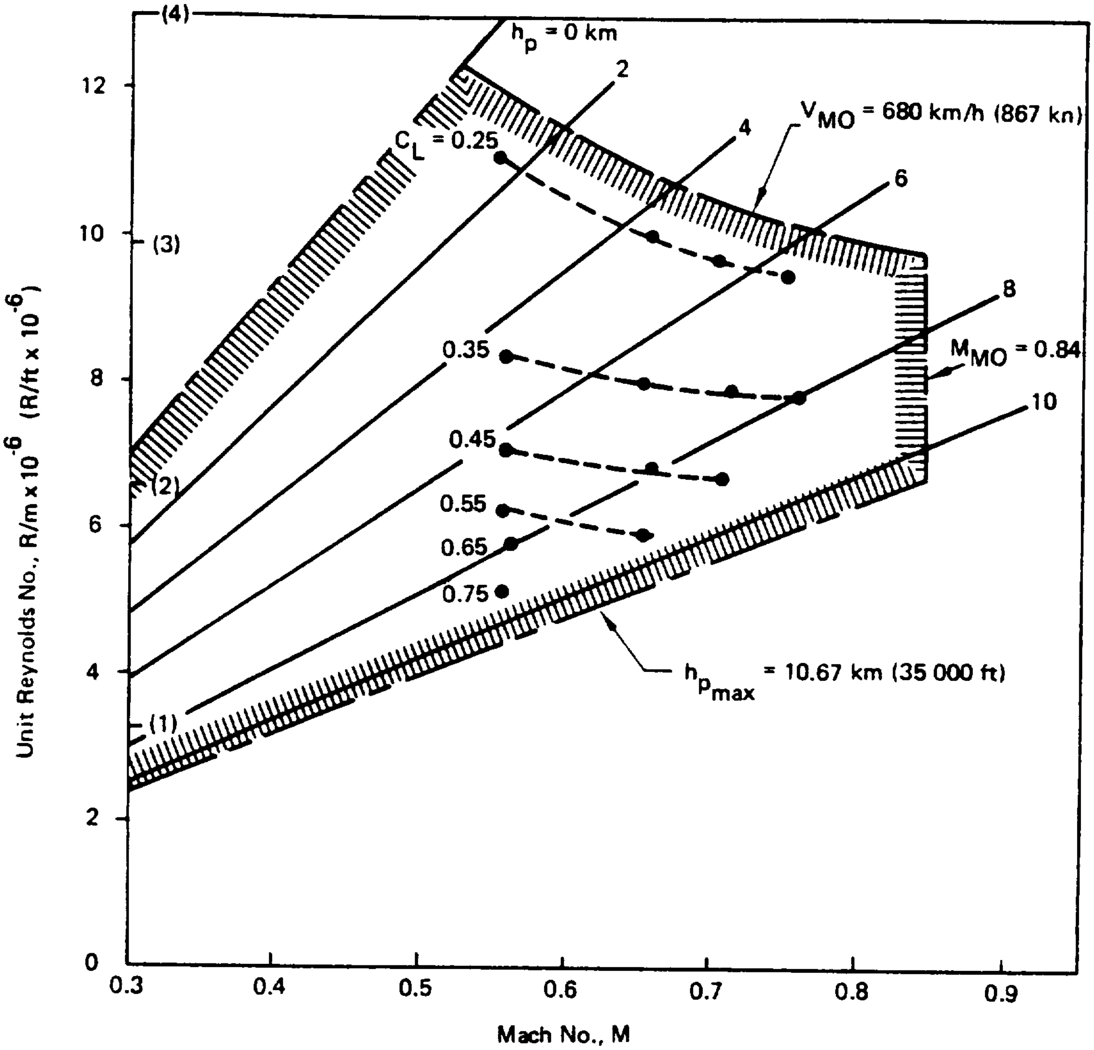

Figure 7. Range of Test Conditions

During each condition, after the airspeed and altitude were stabilized and sideslip was zeroed, a minimum of 2 minutes was allowed for data taking. This permitted at least two full scanning cycles. Airspeed and altitude were held constant during the data recording; the maximum allowable deviations from the nominal values were $\pm$5.5 km/h ($\pm$3 kn) and $\pm$7.6m ($\pm$25 ft), respectively. There were about 3 to 5 minutes between test conditions to change and stabilize speed and altitude. The usual duration of the entire test sequence was about 1 hour 20 minutes.

4.1.2 TEST RESULTS

The section pressure distributions from flight 2 were used, according to the method described in Reference 3, to convert boundary layer momentum losses measured at 73% chord of the upper surface to full-chord section profile drag increments at the measurement station. Boundary layer data from flight 3 (both test panels bare metal) were compared and a correction factor was applied to the right wing reference panel data. This permitted boundary layer changes due to coatings or paint (flights 2, 4, and 5) to be evaluated from data taken simultaneously on left and right wing panels.

Results of the boundary layer surveys and drag evaluations are presented in the following paragraphs.

4.1.2.1 Boundary Layer Surveys

Results of the boundary layer surveys are presented in the following order:

1. Bare surfaces on both panels (flight 3)
2. Corogard paint versus bare surface (flight 4)
3. CAAPCO coating versus bare surface (flight 5)
4. Rough leading edge (flight 3a)
5. Existing paint versus bare surface (flight 1)

Bare-to-Bare-Surface Comparison—A typical set of measured boundary layer profiles is presented in Figure 8. These profiles show velocity variations and momentum loss variations across the boundary layer for varying lift coefficient and constant Mach number. The measurements indicate a very orderly behavior of the boundary layer, with steady increase in the velocity defect and momentum loss as lift coefficient increases. The thickness of the boundary layer at the measurement station varies from about 50 to 80 mm (2 to 3 in). Figure 9 shows a comparison between the boundary layer profiles measured on the left and right wing panels. The profiles are nearly identical, both in terms of velocity defect and momentum defect. There is, however, a slight difference in the value of momentum thickness (derived by integration of momentum loss profile) that was consistent and, therefore, not a random error.

Figure 10 shows the corrected momentum thickness data comparing left and right sides. Considering the greatly expanded scale, differences between the two sides are very small, although at high lift coefficients the right side tends to show values slightly higher than those of the left side.

Corogard-to-Bare-Surface Comparison—Figure 11 illustrates a typical set of measured boundary layer profiles for the Corogard-coated surface and the bare reference surface. Corogard shows an increased velocity defect and momentum loss throughout the boundary layer and slightly increased local velocity (i.e., shear) next to the surface. The case shown represents an average flight condition. At lower lift coefficients (i.e., higher Reynolds numbers) the increments are higher, whereas at higher lift coefficients (i.e., lower Reynolds numbers) the Corogard surface shows little or no increment in momentum thickness relative to the bare surface. The results, in terms of adjusted momentum thickness increments and corresponding section drag coefficient increments, are presented in Figure 12. Distinct trends of increasing ΔC_d with decreasing lift coefficients are evident. This apparent dependency on lift coefficient, however, mainly reflects Reynolds number effects, as shown in Section 4.1.3.

CAAPCO-to-Bare-Surface Comparison—The CAAPCO-coated surface is compared with the bare reference surface in Figure 13. The measurements show very small differences in the velocity profiles or in the momentum loss profiles. However, when the measured momentum thickness is adjusted for differences between the reference panel and the bare test panel, the CAAPCO coating exhibits a lower momentum thickness than the bare surface. A small decrement in momentum thickness for the CAAPCO-coated surface is present throughout the entire range of test conditions. The decrements in θ and the corresponding decrements in section drag coefficient are shown in Figure 14.

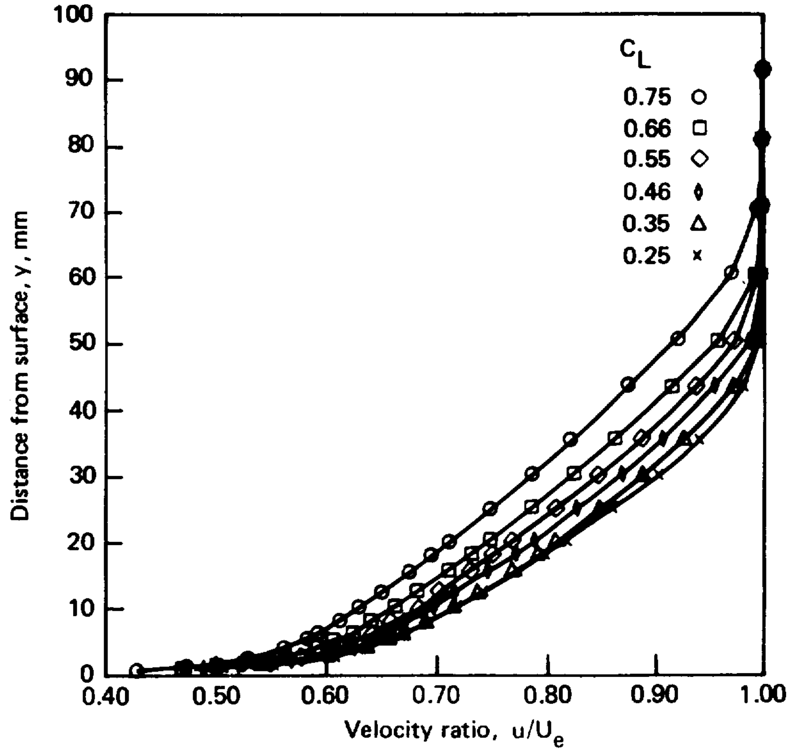

(a) Velocity Profiles

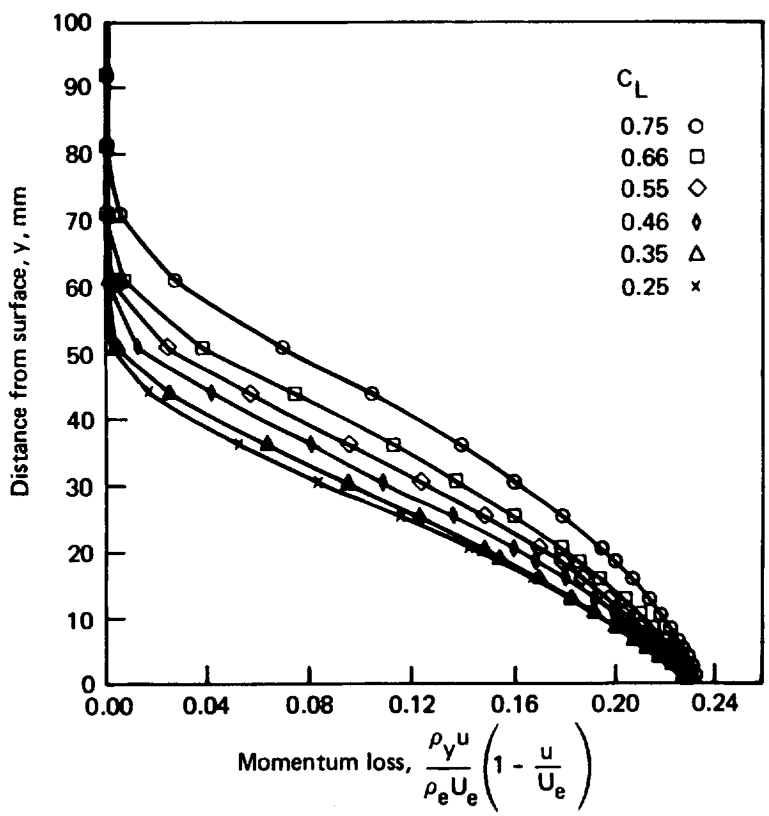

(b) Momentum Loss Profiles

Figure 8. Typical Measured Boundary Layer Profiles—Bare Surface, M = 0.55

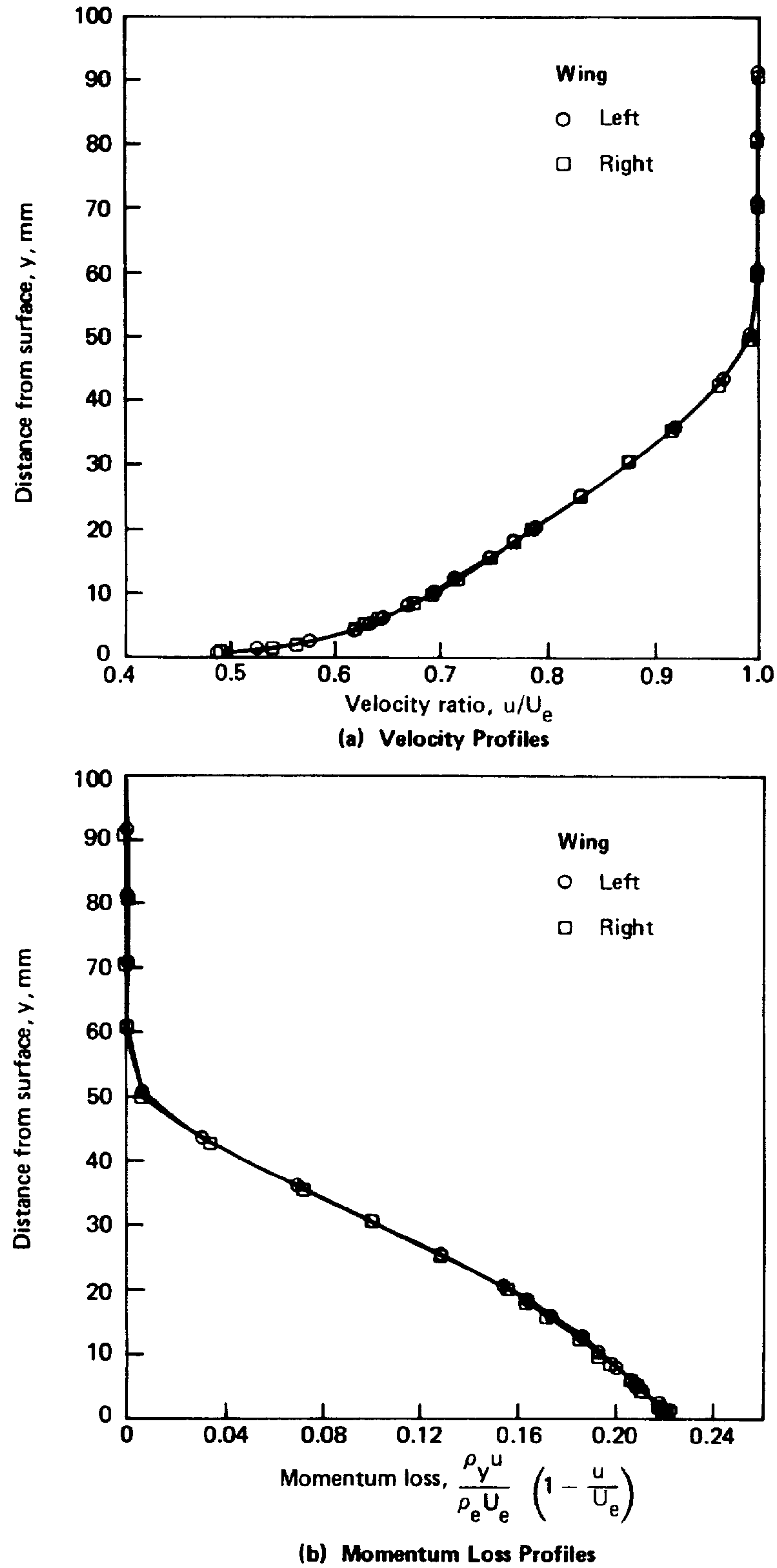

Figure 9. Comparison of Boundary Layer Profiles—Bare Left and Right Wings (Flight 3); $M = 0.702$, $C_L = 0.35$

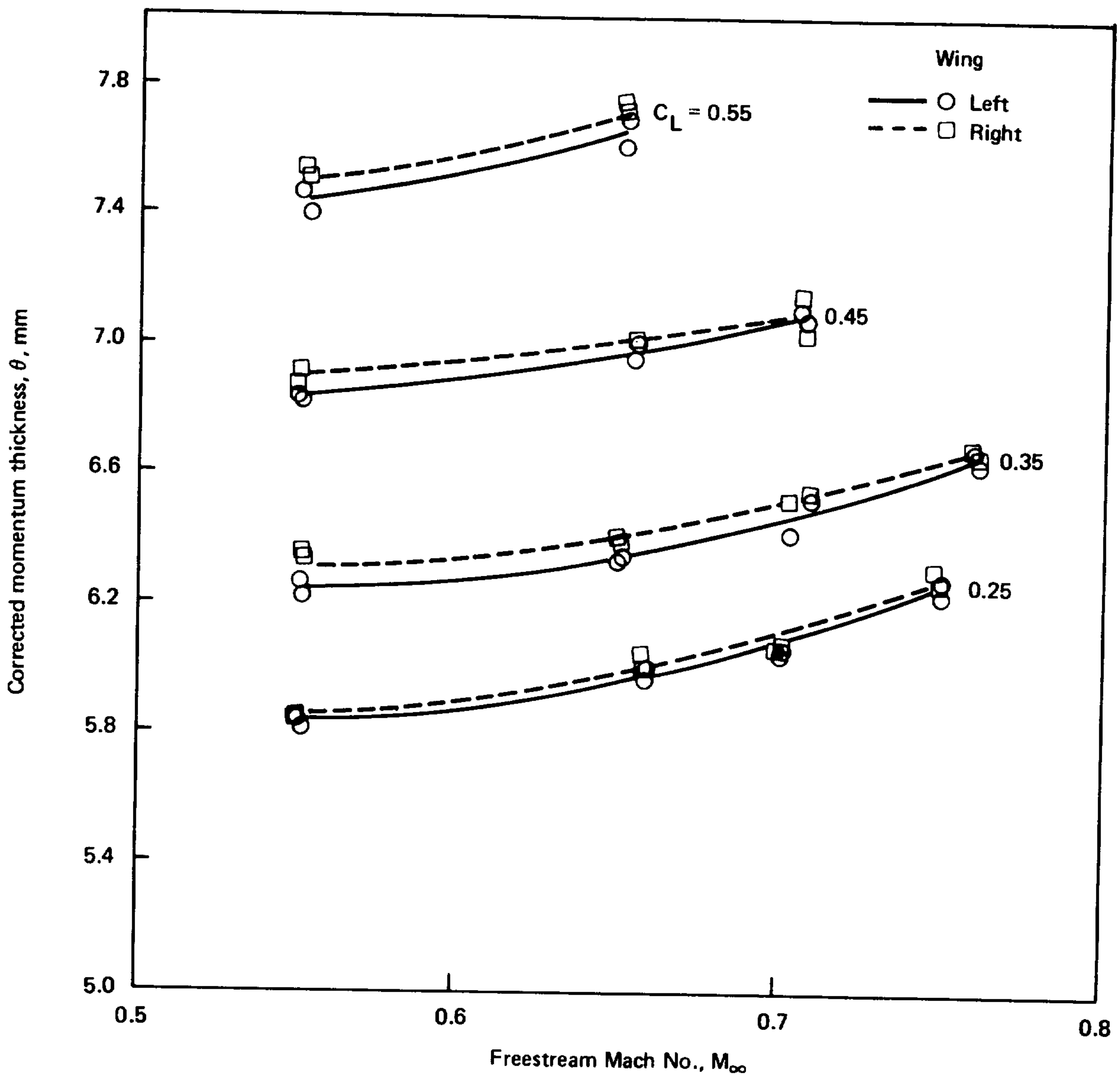

Figure 10. Corrected Momentum Thickness—Bare Surfaces

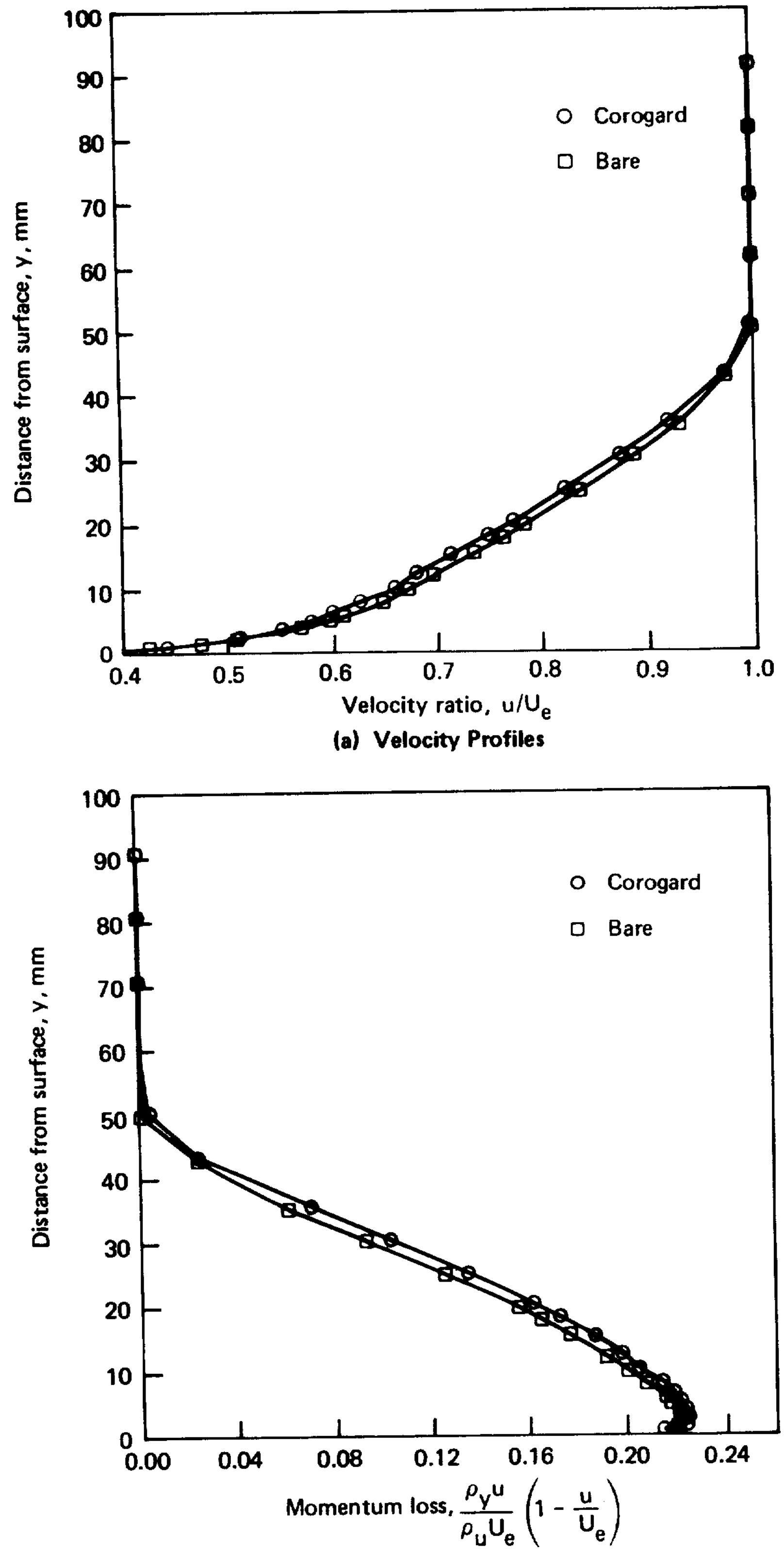

(a) Velocity Profiles

(b) Momentum Loss Profiles

Figure 11. Comparison of Boundary Layer Profiles—Corogard and Bare Surface (Flight 4); $M = 0.716$, $C_L = 0.251$

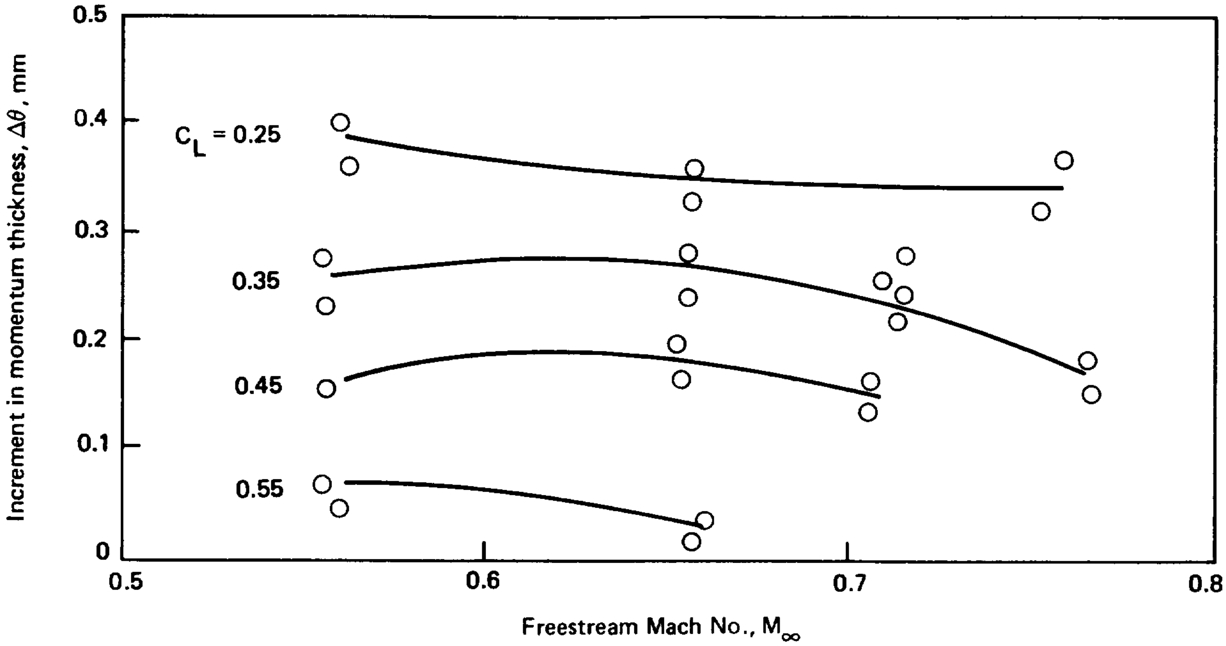

(a) Momentum Thickness Increment at x/c = 73%

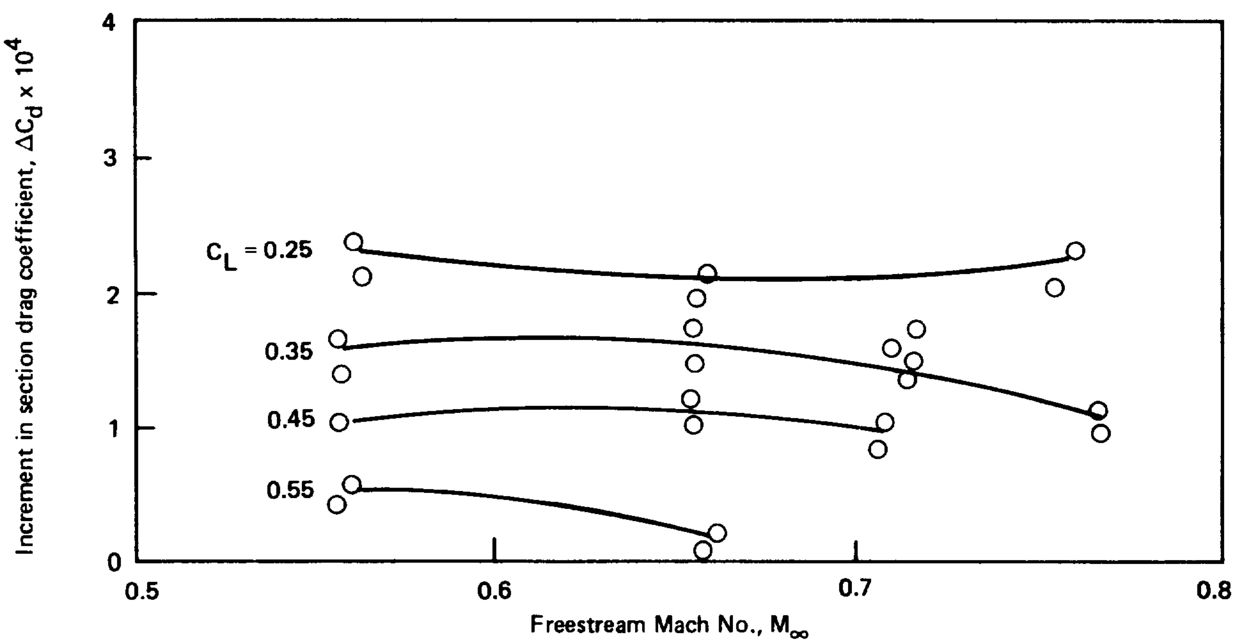

(b) Section Profile Drag Increment

Figure 12. Incremental Effect of Corogard Relative to Bare Surface (Flight 4)

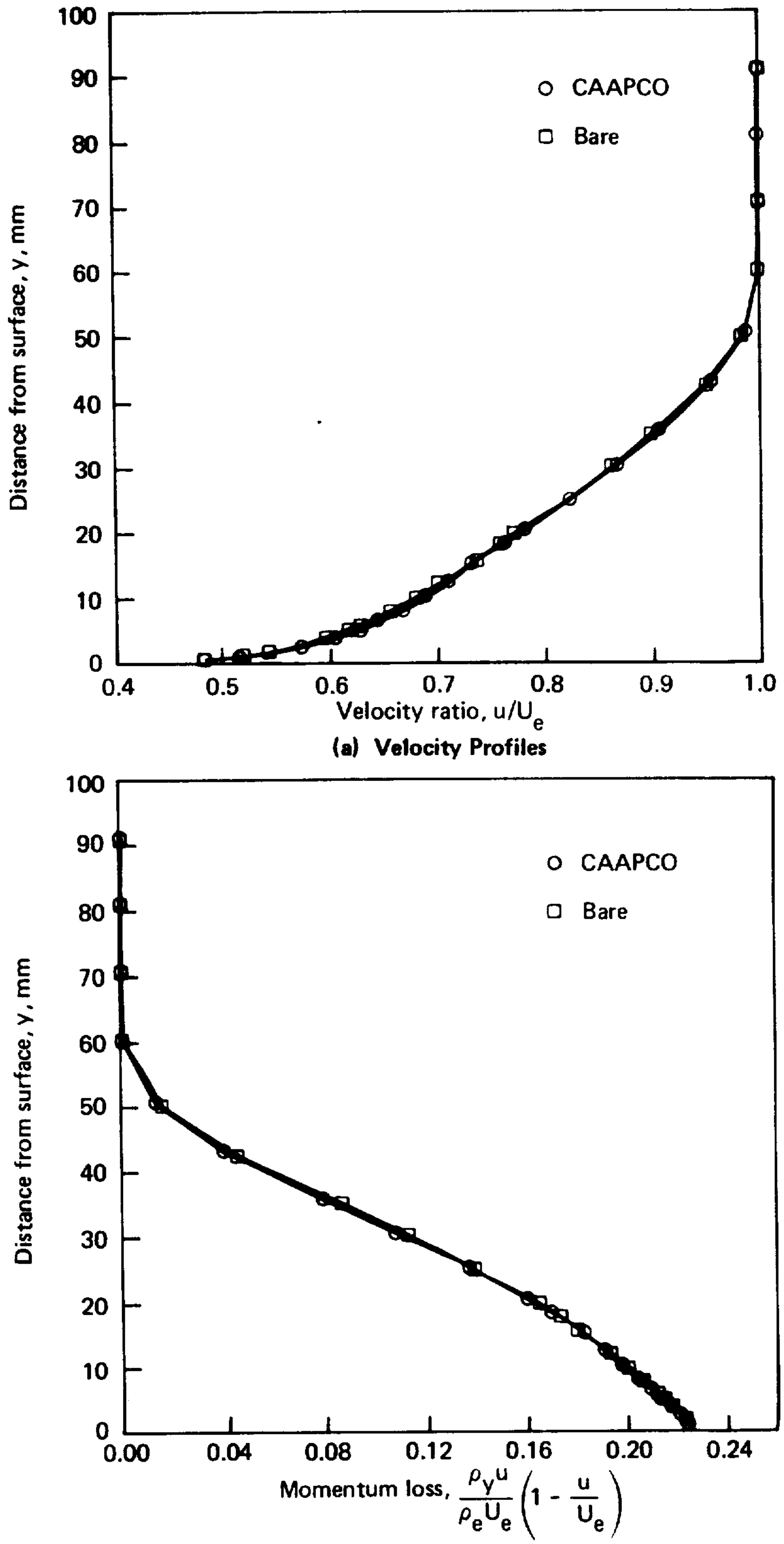

(a) Velocity Profiles

(b) Momentum Loss Profiles

Figure 13. Comparison of Boundary Layer Profiles—CAAPCO Versus Bare Surface (Flight 5); $M = 0.661$, $C_L = 0.445$

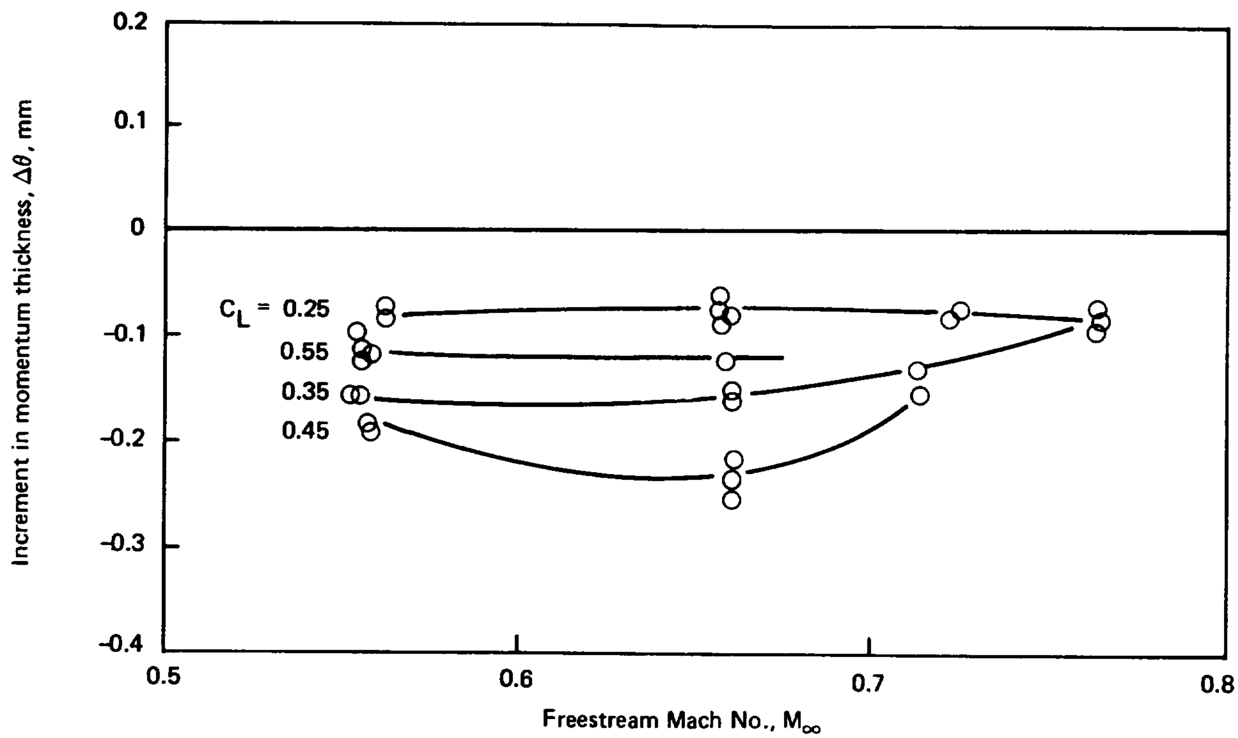

(a) Momentum Thickness Decrement at x/c = 73%

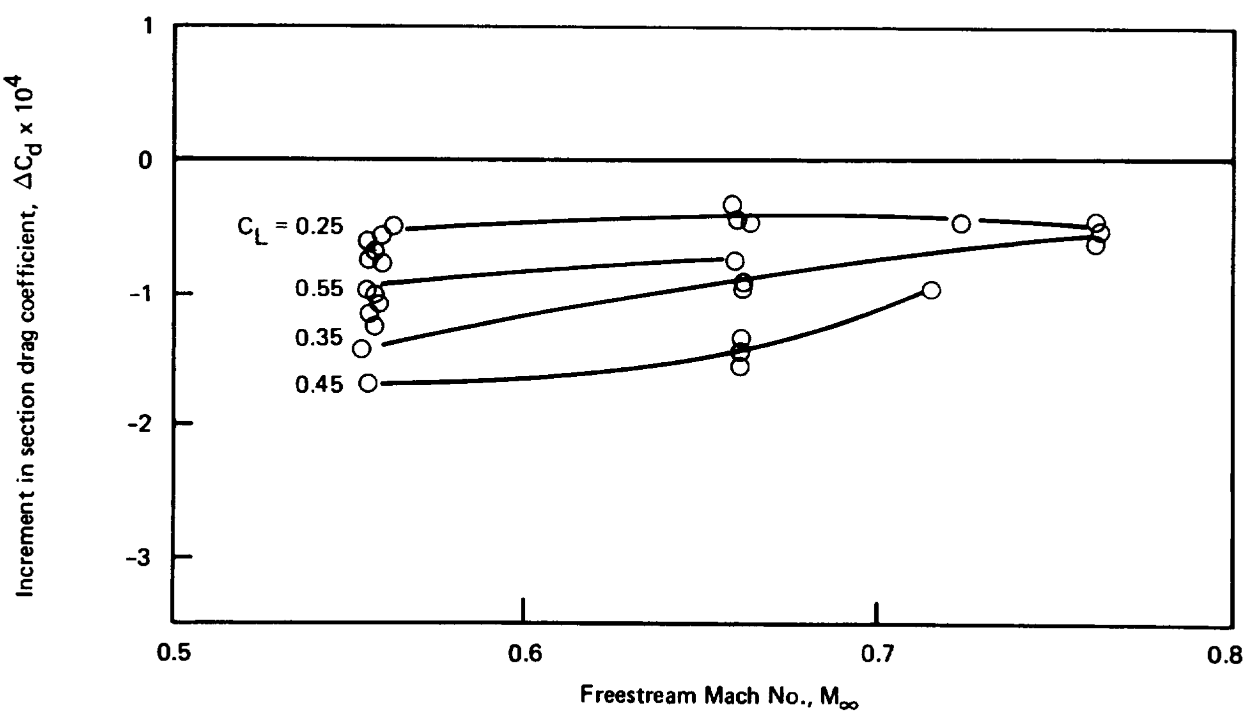

(b) Section Profile Drag Decrement

Figure 14. Effect of CAAPCO Relative to Bare Surface (Flight 5)

Bare Surface With Rough Leading Edge—The effect of a rough leading edge on boundary layer velocity profiles is presented in Figure 15. The lower portions of the profiles are essentially identical, but throughout the outer region there is a small but definite difference, which is largely due to the upstream flow conditions. The rough leading edge was tested at only 4 of the 15 selected flight conditions during a ferry flight from Langley Field to the Wallops Island test site. These four test conditions were all below altitudes of 6100m (20 000 ft).

Incremental effects of the rough leading edge relative to the bare surface are shown in Figure 16. Three data sets acquired at $C_L = 0.25$ indicate a momentum thickness increment of about $\Delta\theta = 0.08$ mm (≈ 0.003 in) and a corresponding section profile drag increment of $\Delta C_d = 0.00005$ (0.5 drag count). The fourth data set, taken at $C_L = 0.45$, indicates a $\Delta\theta = 0.18$ mm (0.007 in) and a $\Delta C_d = 0.00011$ (1.1 drag count). The larger effect of leading-edge roughness at the higher lift coefficient is expected.

Existing-Paint-to-Bare-Surface Comparison—Testing of the existing painted surface took place during the first flight, which also served to check out the instrumentation and data recording systems. The functioning of the data acquisition system was demonstrated, but there were some problems with data recording. The reference pressure readings (from the Digiquartz transducers) were not recorded during the first half of the test due to a faulty power supply, and at some conditions the rake pressures exceeded the preset scales of the recorders. For these reasons not all of the 15 test conditions flown yielded valid data, so the evaluation of this surface is not as accurate as those of the subsequent flights.

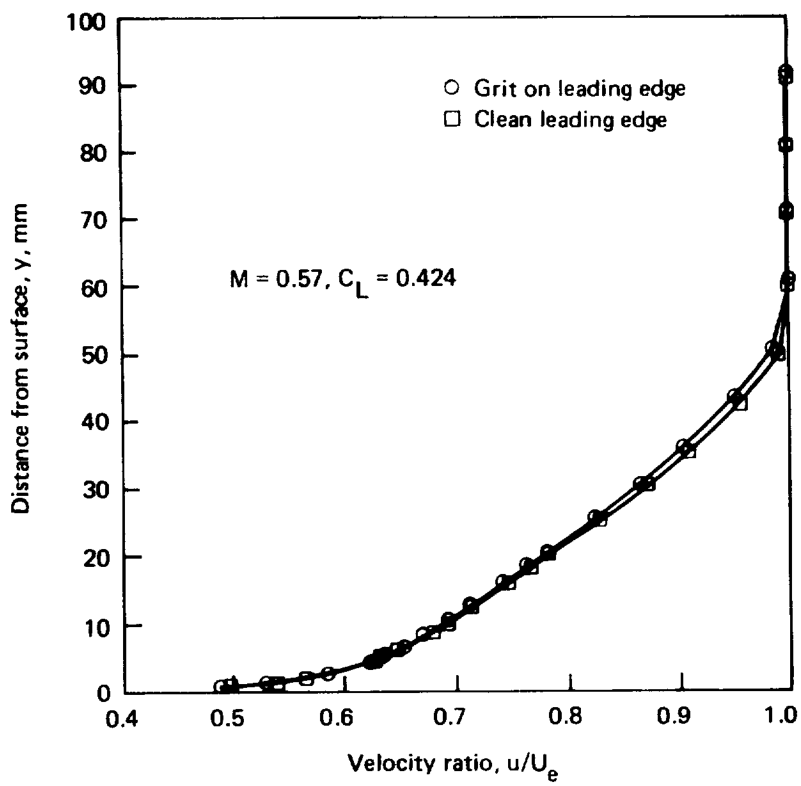

Figure 15. Typical Boundary Layer Profiles—Effect of Rough Leading Edge

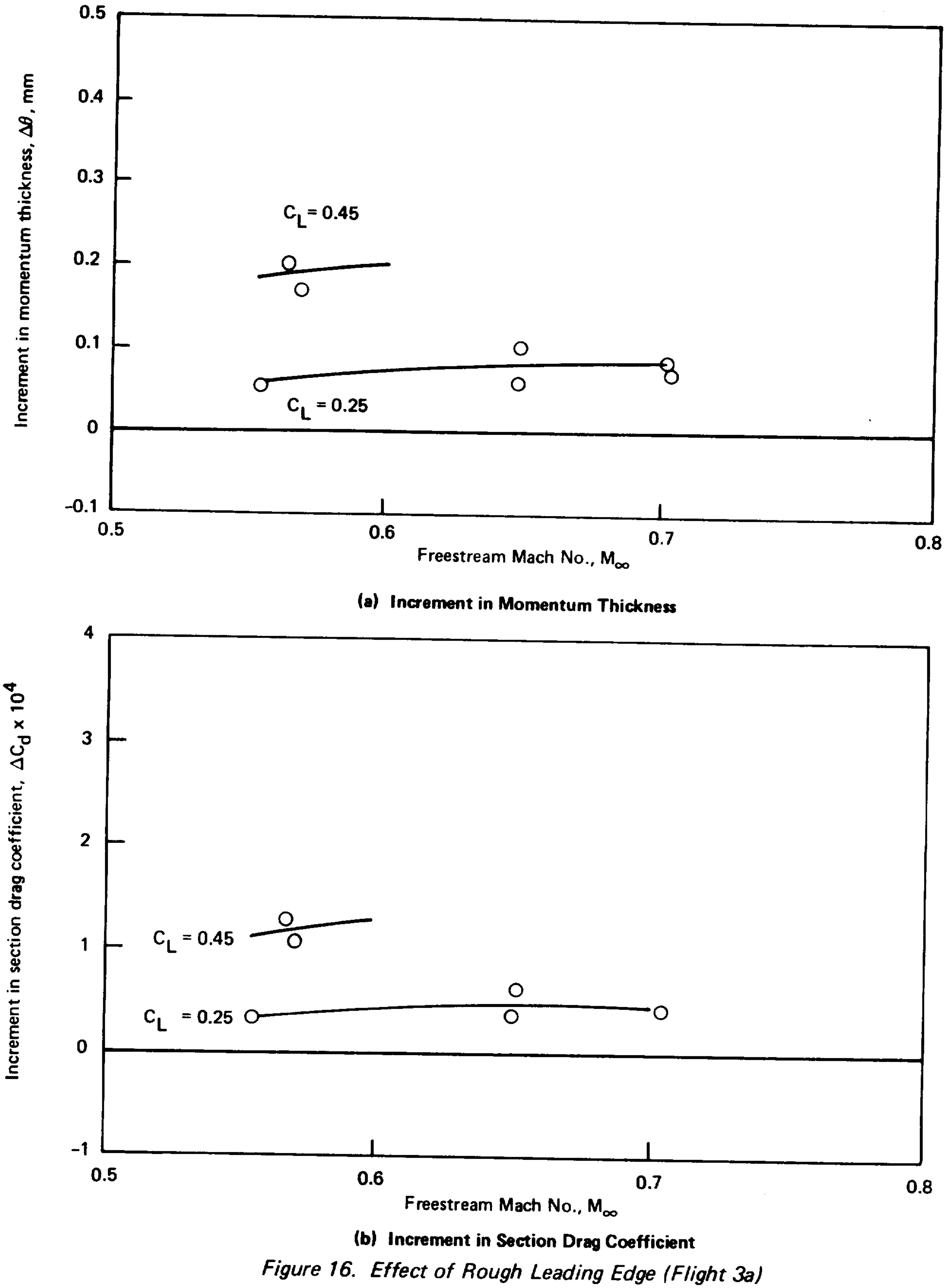

(a) Increment in Momentum Thickness

(b) Increment in Section Drag Coefficient

Figure 16. Effect of Rough Leading Edge (Flight 3a)

The painted surface showed a small increase in velocity defect compared to the bare reference surface. However, the momentum thickness data derived from the measurements indicated that the increments between the two test surfaces were not always consistent, as shown in Figure 17 for a typical set of test conditions (C_L = 0.35). The painted surface appeared to have slightly higher drag than the bare surface, although the increments are about the same magnitude as the experimental data scatter.

4.1.3 CONCLUSIONS

The test provided a set of highly accurate basic data showing the effects of various surface finishes, including bare metal, Corogard, CAAPCO, polyurethane enamel, and leading-edge roughness, on boundary layer properties. The Corogard applied at the test site was slightly rougher than is typical of factory applications. A severely eroded leading edge was simulated with No. 50 grit.

The effects of the measured boundary layer differences were converted to increments in section profile drag at the test stations on the 737 wing, and the corresponding effects on total airplane drag were estimated. These effects are presented in the following sections.

4.1.3.1 Section Drag

Final drag evaluation results for each test surface are presented in Figure 18 as section profile drag increments plotted as a function of freestream unit Reynolds number. The data were plotted in this form because classic experiments indicate that unit Reynolds number is the primary factor in distributed roughness effects.

Bare-to-bare-surface comparisons indicated a small difference in section profile drag between the left and right wing test sections, which amounted to an average of about 0.35%. No definite trends were discernible with Reynolds number, Mach number, or lift coefficient. This drag difference found on the baseline configuration was accounted for when assessing effects of the other surface coatings tested:

- CAAPCO coating produced a lower drag than the bare reference surface, about 0.75% to 2% of the section profile drag. At a typical cruise Reynolds number of 6.5 million per meter (2 million per foot), the section drag decrement is 1.4%. The 2% decrement is applicable to lower Reynolds numbers or higher lift coefficients.

- Corogard surface showed a clear trend of increasing drag with increasing unit Reynolds number when the latter exceeded a certain limit below which the surface was indicated to be hydraulically smooth. This critical Reynolds number was about 4.9 million per meter (1.5 million per foot) for the particular surface tested. At the highest Reynolds numbers of this test, the section profile drag increment was about 3.5%. At a typical cruise Reynolds number of 6.5 million per meter (2.0 x 10 million per foot) the increment was 1.2%.

- The rough leading edge test showed a drag increment amounting to about 0.65% of the section profile drag at three test conditions flown at C_L = 0.25 and about 1.6% at one condition flown at C_L = 0.45.

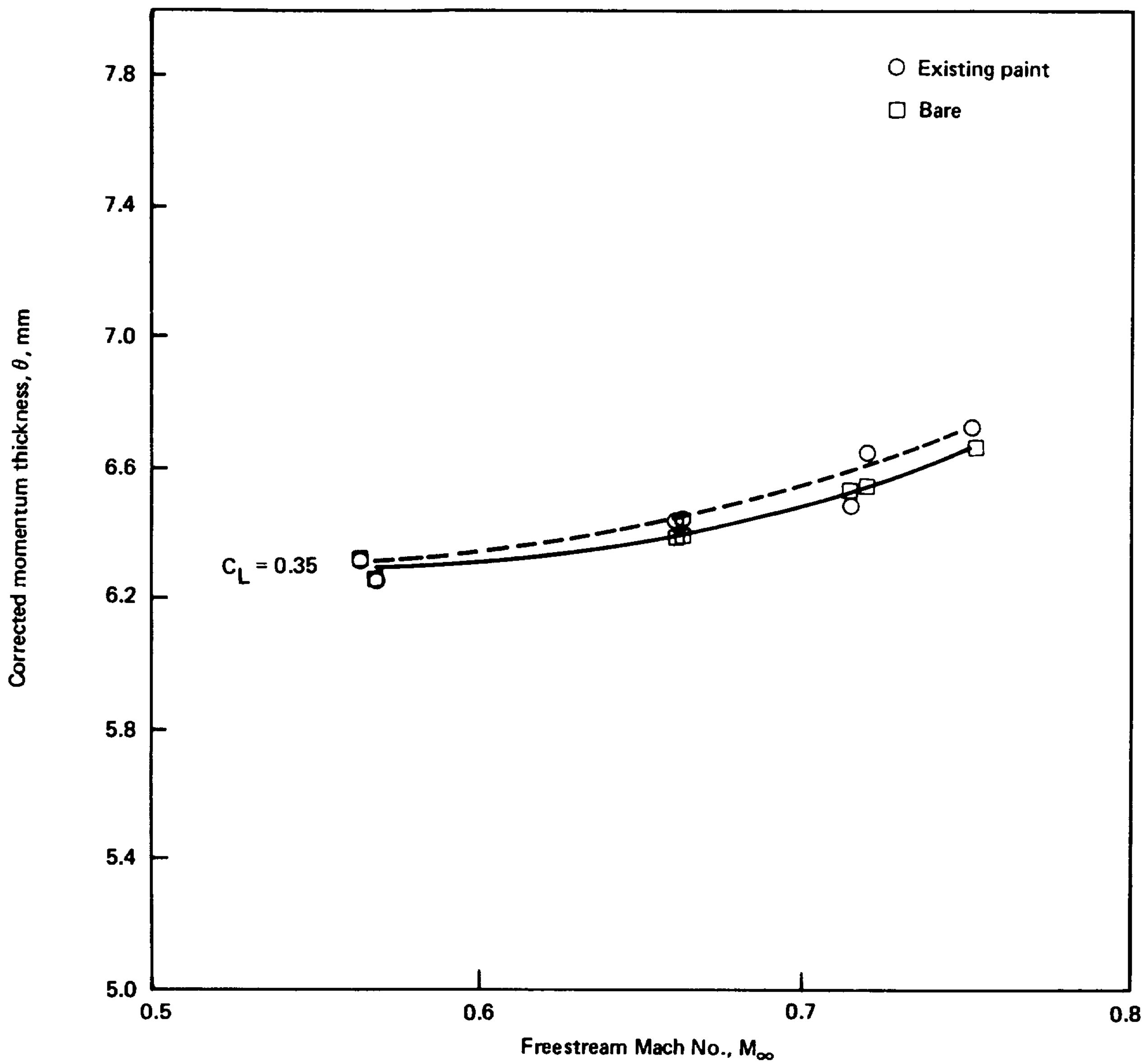

Figure 17. Corrected Momentum Thickness, Existing Paint Versus Bare Surface (Flight 1)

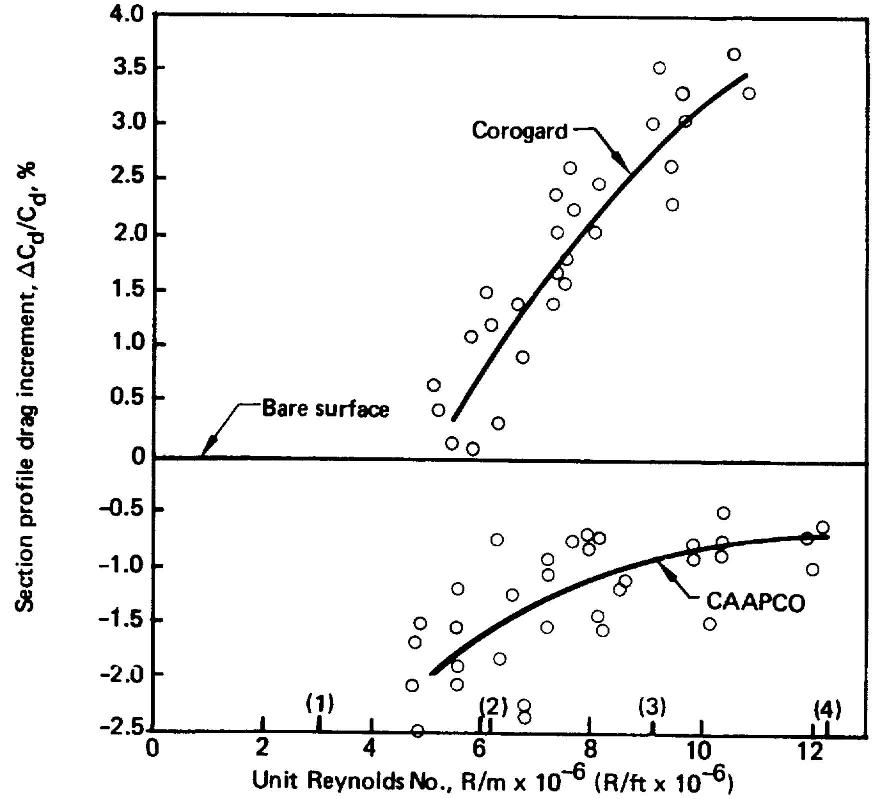

(a) CAAPCO and Corogard Relative to Bare Surface

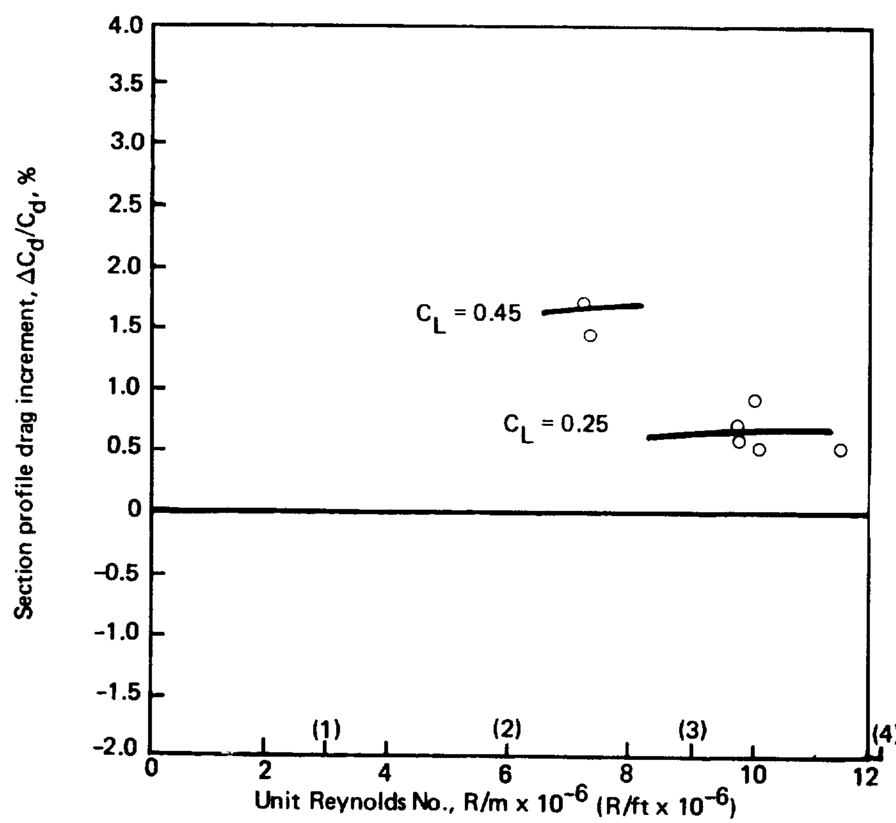

(b) Rough Leading Edge

Figure 18. Effect of Surface Coatings on Test Section Profile Drag

- The existing painted surface showed a slightly higher drag level than the bare surface. The increments, however, were of the same magnitude as the experimental scatterband, so these results were not conclusive.

4.1.3.2 Conversion to Airplane Drag

To accurately determine the effect on total airplane drag, additional measurements would have to be made at enough spanwise stations to permit integration over the entire wingspan. If, however, it is assumed that the same section drag coefficient increments occur at all spanwise stations, the total airplane drag increments can be estimated. Results of such calculations are presented in Figure 19. For the Corogard data only, an adjustment was made for differences in the amount of Corogard at various stations on production 737 airplanes. For the test airplane, 57.5% chord was covered with Corogard at the test station, while 42% is an appropriate average for the entire wing upper surface of production airplanes. This adjustment is considered appropriate because the Corogard data exhibit typical distributed roughness characteristics. For CAAPCO and the roughened leading edge, however, the data behave as if discrete roughness elements are involved. Hence the effects may not vary in a simple manner with coated areas, and the drag coefficient increments were assumed to be independent of spanwise location:

- At a typical cruise condition, $C_L = 0.45$ and $R = 6.5$ million per meter (2.0 million per foot), the total airplane drag increments relative to the bare surface for the test airplane are estimated to be:

CAAPCO	0.2% decrease
Corogard	0.2% increase
Rough leading edge	0.3% increase

- The Corogard drag increments observed at higher Reynolds numbers are equivalent to as much as 0.75% airplane drag. A precise assessment of the effects of these drag increments on the fuel consumption of an airplane in airline operation must be based on a complete mission profile analysis. The effects on fuel consumption are addressed in Section 4.4.

- As indicated by this test, CAAPCO produces a small drag benefit. The benefit is thought to result from smoothing fasteners and joints in the bare metal; therefore, this benefit may vary considerably at other span stations or for other airplanes. Before CAAPCO could be used in the inspar region, corrosion protection equivalent to Corogard would have to be thoroughly demonstrated.

4.2 FLIGHT SERVICE EVALUATIONS

Continental Airlines (CO) and Delta Air Lines (DL) conducted evaluations on the candidate coatings applied to wing slat and horizontal tail leading edges for erosion protection. Airline maintenance personnel applied the coatings with normal paint spray equipment during periods of scheduled maintenance.

4.2.1 CONTINENTAL AIRLINES EVALUATION

CO conducted two flight service evaluations of surface coatings in series. The first evaluation, flown in the Air Micronesia route system, began in September 1978 and ended in November 1979. Results from that 14-month evaluation in the harsh Pacific environment are reported in Reference 2. The second evaluation began in December

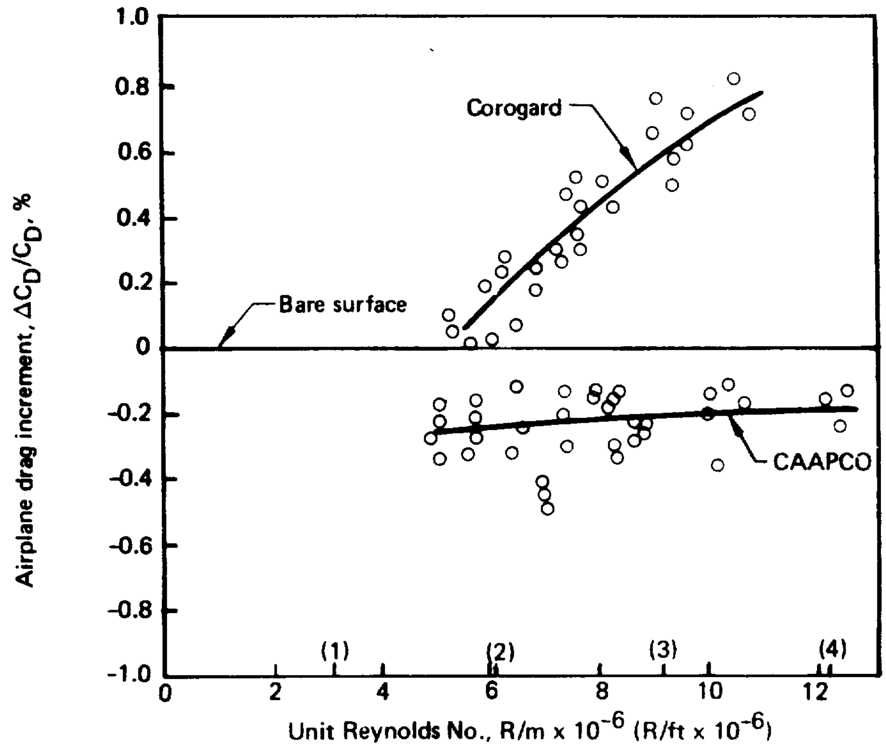

(a) CAAPCO Coating and Corogard

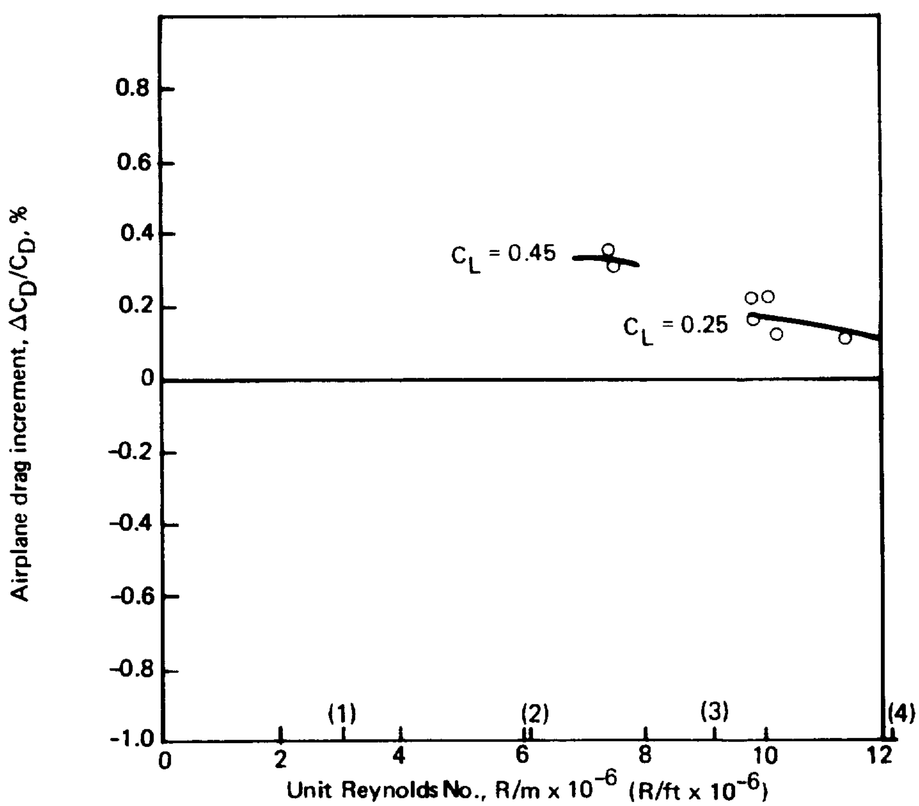

(b) Rough Leading Edge

Figure 19. Effect of Surface Coatings on Total Airplane Drag

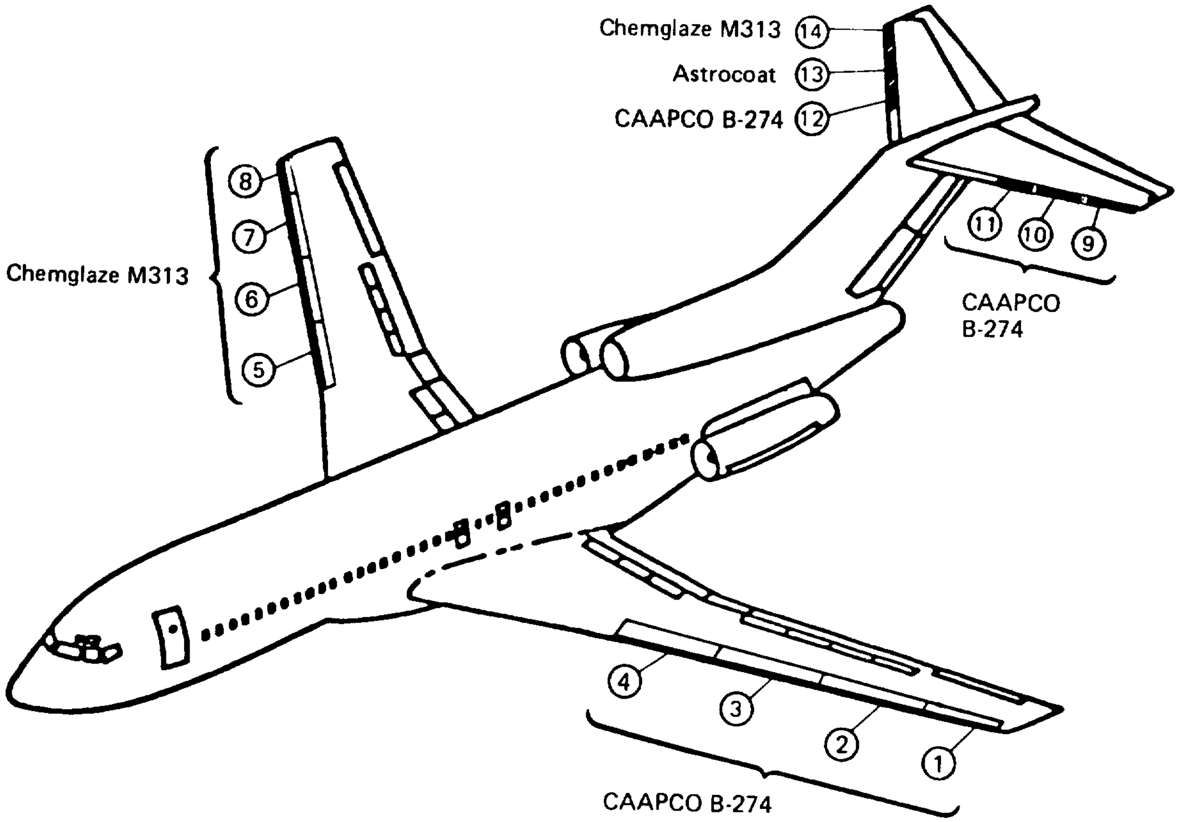

Figure 20. Continental Airlines Surface Coatings Configuration

1979 when the airplane was flying U.S. domestic routes. In October 1980, this airplane was transferred to the Air Micronesia system and was destroyed in an accident 1 month later. The right outboard horizontal tail leading edge, which had been coated in the laboratory with the three test coatings and which had been serving as a control part, was removed intact and installed on another Air Micronesia 727 until October 1981. Results of the second CO evaluation, emphasizing results on the control part, are reported in the following paragraphs.

4.2.1.1 Coating Configuration

Coatings were applied to wing slat leading edges and the outboard half of the horizontal tail leading edge (fig. 20). All field coated parts were primed with BMS 10-79 epoxy primer and coated with approximately 12 mil of either CAAPCO B-274 or Chemglaze M313. The slat coatings were a strip of constant 9.53-cm- (3.75-in-) wraparound width at the leading edge, whereas the horizontal tail coatings tapered from 28-cm- (11-in-) wraparound width at the inboard end to 15 cm (6 in) at the tip.

The right outboard horizontal tail leading edge had been coated in Avco Systems Division laboratories with 89-cm- (35-in-) long panels of each of the three candidate materials indicated in Figure 20. A 12.7-cm (5-in) strip of bare metal separated the coatings to obtain an indication of bare-metal erosion that would occur during the flight service evaluation (the part was new when coated and installed on the airplane). CO maintenance personnel coated the opposite left leading edge with CAAPCO only. The right leading edge served as a control part for comparing the durability of laboratory-applied coatings with that of coatings applied by airline personnel during scheduled maintenance.

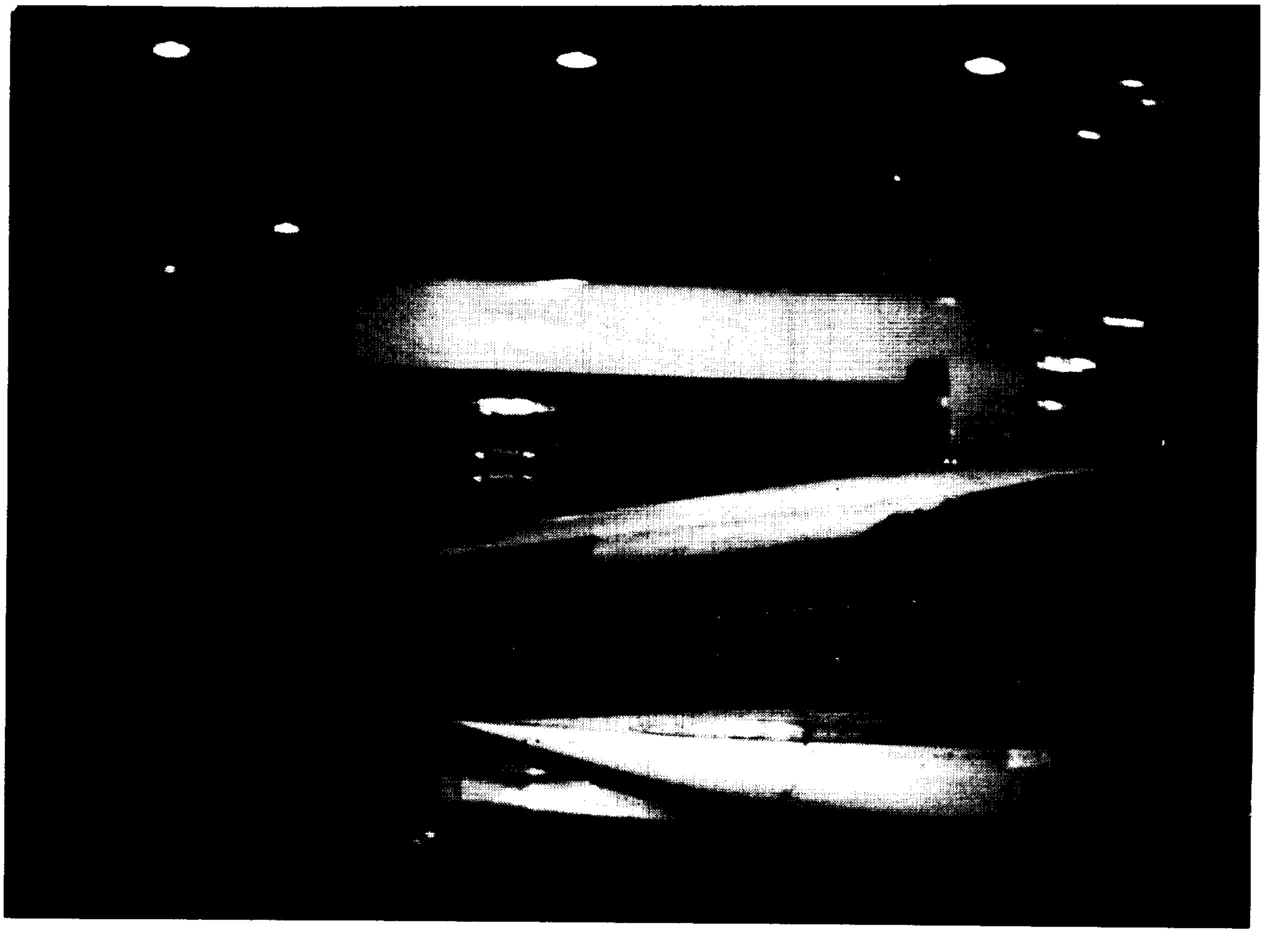

Figure 21. Slat 2 After 1200 hr—70% Coating Missing

4.2.1.2 Evaluation Results

The coating configuration described in the previous paragraphs was applied to CO 727 N18479 during the first week of December 1979. The airplane entered domestic service on 20 December. Periodic inspection reports on coating condition from CO are summarized as a function of accumulated flight-hours in Table 1.

Slat 1, coated with CAAPCO, went through the service evaluation with only slight erosion of the inboard edge. The erosion was noticed after 2000 flight-hours and received touchup repair. The other CAAPCO-coated slats (slats 2, 3, and 4) had extensive peeling during the first 1200 flight-hours, probably due to hydraulic fluid leaks reported in the left wing leading edge. Figure 21 shows slat 2 with 70% of the coating and primer missing after 1200 hours. Slats 2, 3, and 4 were stripped and recoated at 1539 flight-hours and had only very minor erosion and/or peeling at the end of the evaluation period.

The Chemglaze-coated slats (slats 5, 6, 7, and 8), with the exception of slat 5, shown at 1200 hours in Figure 22, had peeled at both ends and showed some surface crazing near the inboard end. Slat 5 was stripped and recoated at 1539 hours and was in relatively good condition for the remainder of the evaluation.

Table 1. Continental Airlines Evaluation—Summary of Inspection Reports

	ITEM	COATING	FLIGHT-HOURS-CUMULATIVE * 400 est.	730 est.	1200 est.	1539	1800 est.	2092	2160 est.	2290 est.	2435
Wing slats	1	CAAPCO	OK	OK	OK		OK	Erosion, inboard end leading edge 1.2 cm (0.5 in)	Erosion, inboard end leading edge 1.2 cm (0.5 in) Repaired	OK	Slight erosion, inboard end leading edge Peeling, outboard end at screw head
	2	CAAPCO	Extensive leading edge peeling, 23 cm (9 in) inboard end, 69 cm (27 in) center	Peeling, inboard end 51 cm (20 in)	70% coating and primer missing (fig. 4.2.2)	Recoated	OK	OK	OK	OK	Peeling, inboard end at rivet head
	3	CAAPCO	OK	Peeling, center leading edge, 8 cm (3 in)	Peeling, center leading edge, 18 cm (7 in)	Recoated	OK	OK	OK	OK	OK
	4	CAAPCO	Peeling, outboard end 5 cm (2 in)	Peeling, inboard end 8 cm (3 in), outboard end 5 cm (2 in)	Peeling, inboard end 48 cm (19 in), outboard end 5 cm (2 in)	Recoated (slight orange peel appearance)	OK	OK	Peeled spot, 1.2-cm (0.5-in) diameter outboard of flow fence	OK	Peeled spot outboard of flow fence
	5	Chemglaze	Peeling, inboard end 4 cm (1.5 in)	Peeling, inboard end 13 cm (5 in), outboard end 8 cm (3 in)	Peeling, inboard end crazing 81 cm (32 in) from inboard end (fig. 4.2.3)	Recoated	OK	OK	Edges of seven rivet heads exposed	OK	Erosion, inboard end 2.5 cm (1 in) Peeling, outboard end rivet heads
	6	Chemglaze	OK	OK	OK, except some dulling		OK	Erosion, inboard end 0.3 cm (0.12 in)	One rivet edge exposed	OK	Peeling, outboard end at fastener head
	7	Chemglaze	OK	OK	OK		OK	Erosion, inboard end 0.3 cm (0.12 in)	One rivet edge exposed	OK	Erosion beginning at inboard end
	8	Chemglaze	OK	OK	Tear beginning at inboard end 1.2 cm (0.5 in)		OK	Erosion, inboard end 0.3 cm (0.12 in)	OK	OK	Erosion beginning at inboard end
Horizontal tail leading edge	9	CAAPCO	Peeling, inboard end 1.2 cm (0.5 in)	Peeled, inboard end 1.2 cm (0.5 in)	OK		Peeling, inboard end 1.2 cm (0.5 in)	Erosion, inboard end 1.2 cm (0.5 in) (fig. 4.2.4)	Erosion, inboard end 2.5 cm (1 in) Repaired	Peeling, inboard end at repair, 1.2 cm (0.5 in) (fig. 4.2.5)	Peeled, inboard end 1.2 cm (0.5 in)
	10	CAAPCO	Peeling, inboard end 2.5 cm (1 in)	Peeled, inboard end 2.5 cm (1 in)	Small tear beginning at inboard end		Peeled, inboard end 2.5 cm (1 in)	Erosion, inboard end 2.5 cm (1 in)	Erosion, inboard end 3 cm (1.2 in) Repaired	Peeling, inboard end 1.2 cm (0.5 in)	Slight peeling, upper inboard edge corner 0.6 cm (0.25 in)
	11	CAAPCO	OK	OK	Peeled, inboard end 2.5 by 3.8 cm (1 by 1.5 in)		OK	OK	Erosion, inboard end (minor) Repaired	Peeling, inboard end 1.2 cm (0.5 in)	Peeling, upper inboard edge corner 1 cm (0.4 in)
	12	CAAPCO	OK	OK	OK		OK	OK	OK	OK	OK
	13	Astrocoat	OK	OK	OK		OK	OK	OK	OK	OK
	14	Chemglaze	OK	OK	OK		OK	OK	OK	OK	OK

*Evaluation of 727 airplane N18479 terminated at 2741 flight-hours (11-1/2 mo).
Last Continental inspection report was at 2435 flight-hours.
Evaluation of right-hand horizontal tail leading edge (parts 12, 13, 14) continued on airplane N2475.

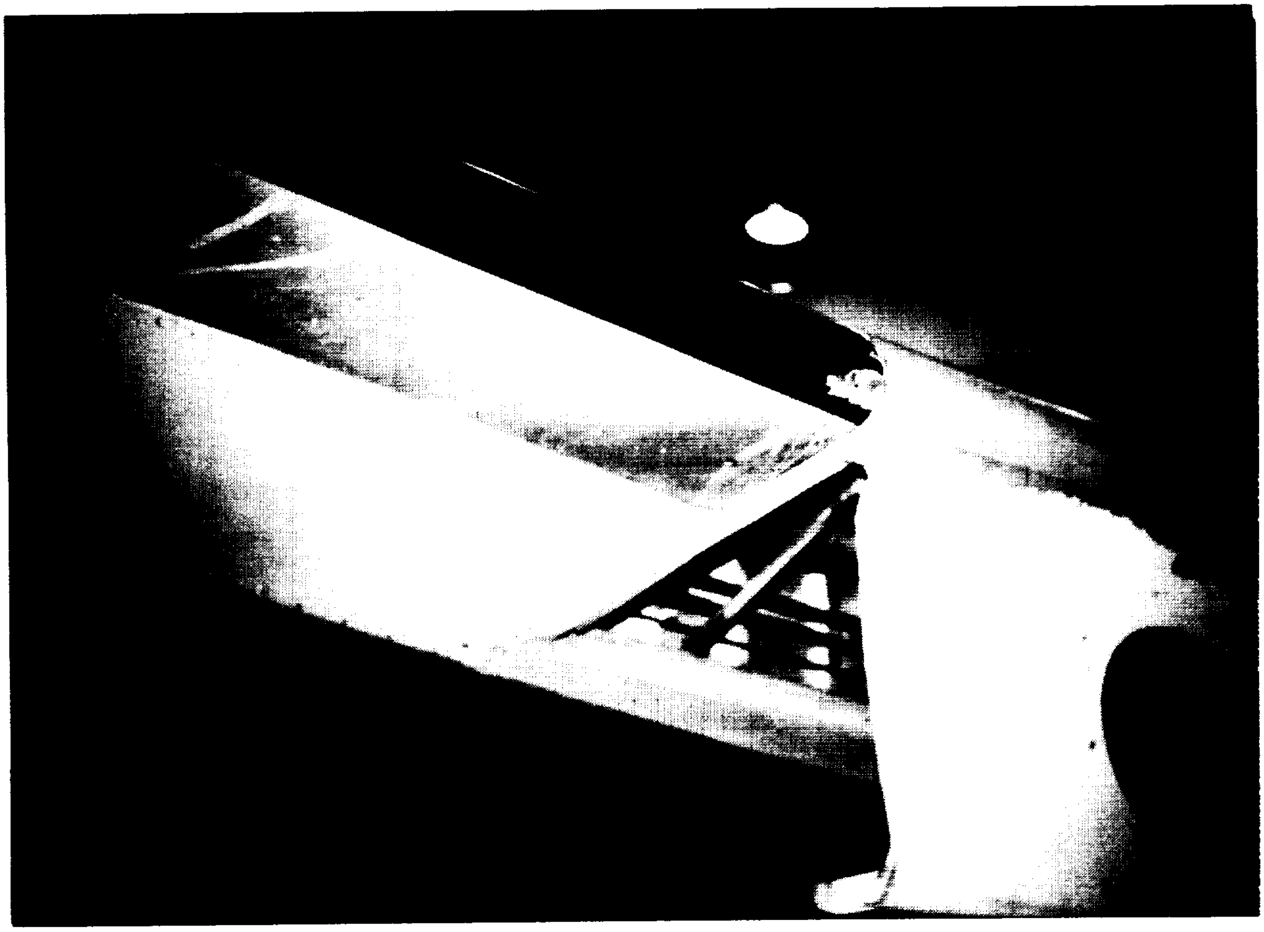

Figure 22. Slat 5 After 1200 hr—Peeling at Inboard End

The three CAAPCO-coated panels (items 9, 10, and 11) on the left outboard horizontal tail experienced early edge peeling at the inboard ends that extended about 1.2 to 2.5 cm (0.5 to 1 in) into the coated leading edge. Figure 23 shows this condition at the inboard end of item 9 after 2092 flight-hours. Shortly thereafter (at 2160 hours), touchup repair of these areas was attempted and, after a cure time of about 40 hours, the airplane returned to flight status. The next field inspection, at 2290 flight-hours, revealed that the repairs were not properly accomplished and peeling recurred, as shown in Figure 24. The touchup repairs on items 1, 9, 10, and 11 required 5 labor-hours to complete.

The last inspection was conducted at 2435 flight-hours, just before airplane N18479 was transferred to Air Micronesia service. Photos taken then (figs. 25a, b, c, d) show the generally good appearance of the coatings. The small discrepancies identified in Table 1 are not apparent.

The flight service evaluation of coatings on N18479 was terminated at 2741 flight-hours. During that time, coatings on the horizontal tail control part had not been repaired and showed no evidence of deterioration. It was decided that the evaluation of that part should continue so that the durability of laboratory-applied coatings could be assessed. The control part, therefore, was transferred to airplane N2475 and was flown an additional 8 months in Air Micronesia service.

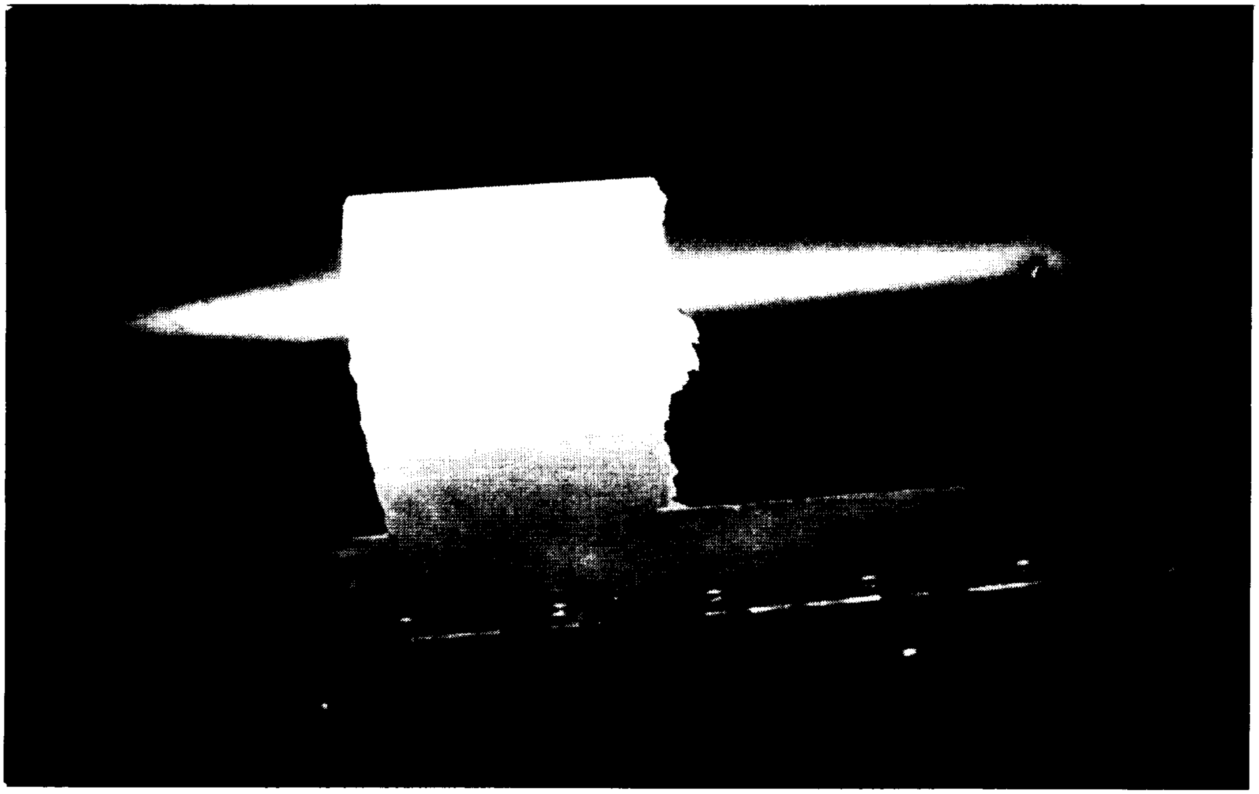

Figure 23. Erosion at Inboard End of Item 9 (2092 hr)

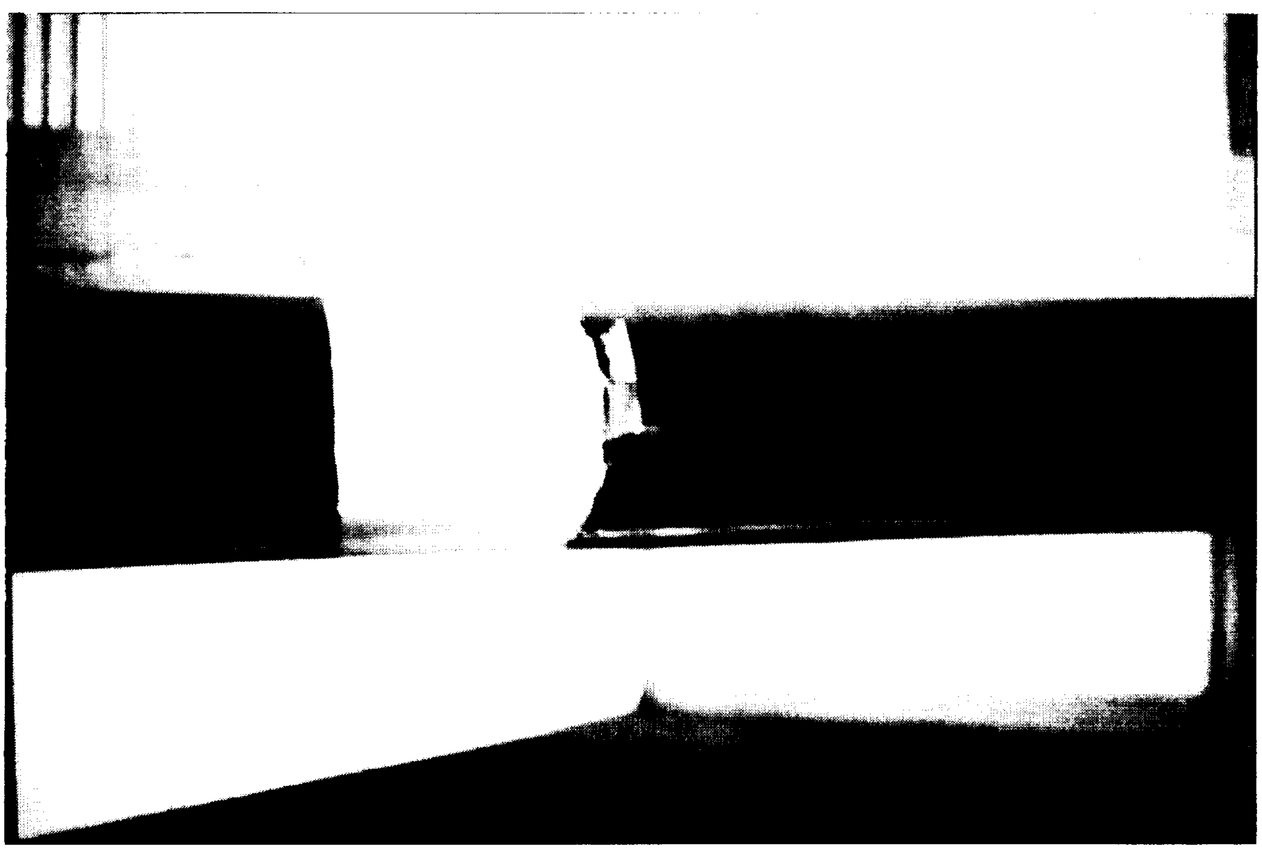

Figure 24. Peeling of Touchup Repair on Inboard End of Item 9 (2290 hr)

(a) Slats 2, 3, and 4 (CAAPCO)

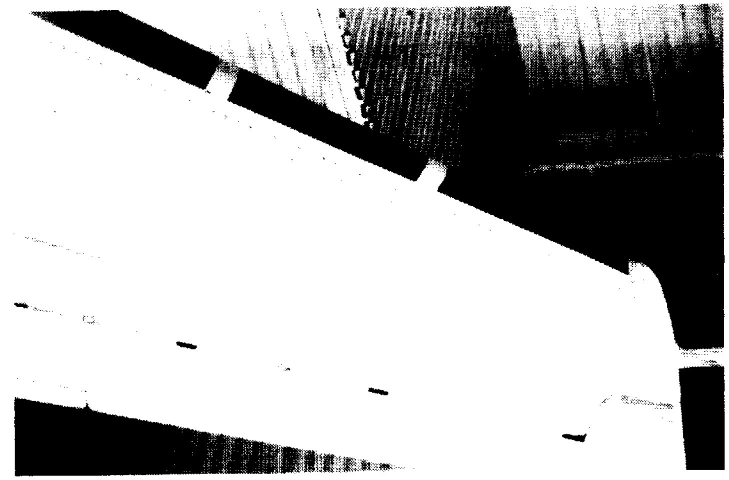

(c) Slats 5, (c) Left Horizontal Tail Leading Edge (CAAPCO)

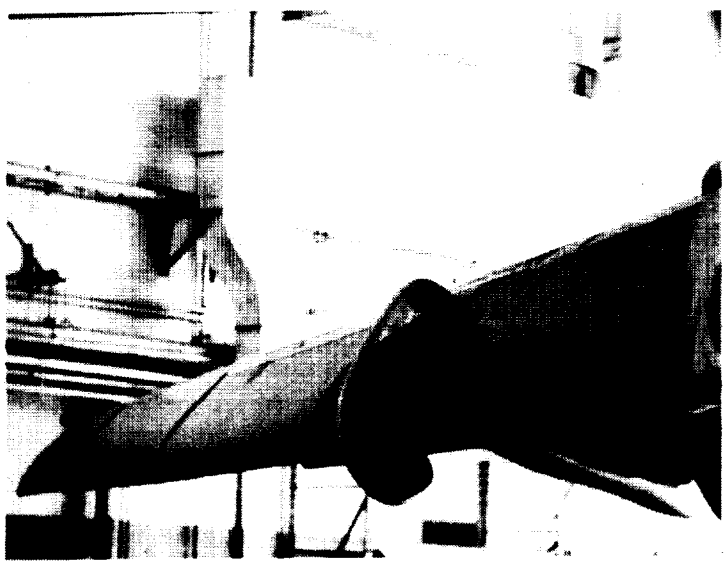

(b) Slats 5, 6, 7, and 8 (Chemglaze)

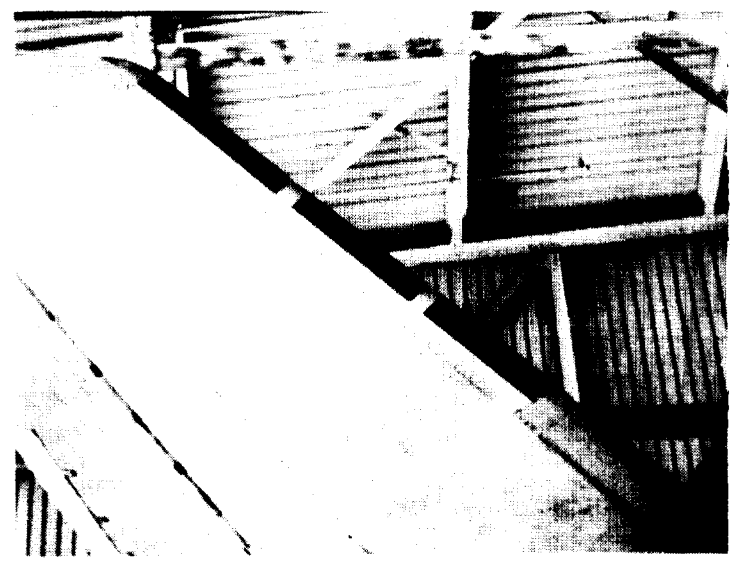

(d) Right Horizontal Tail Leading Edge (Control Part)

Figure 25. Condition of Coatings (2435 hr)

The control part was inspected at Guam after 3815 flight-hours (fig. 26a). Chemglaze, on the outboard panel, and CAAPCO, on the inboard panel, were in good condition. The Astrocoat center panel, (fig. 26b) had three small spots on the leading edge where the coating had eroded down to bare metal.

The flight service evaluation was concluded when the part was removed from N2475 in October 1981, at which time the coatings had accumulated 4873 flight-hours. Figures 27a through 27e show the condition of the coatings and an exposed leading edge between coated panels at the conclusion of the evaluation. The Chemglaze and CAAPCO panels remained in good condition and were only slightly eroded at the inboard end leading edges (figs. 27b and 27d). There was similar erosion at the inboard end of the Astrocoat panel and extensive damage along the leading edge (fig. 27c). There was evidence that touchup repair of the Astrocoat panel had been attempted in the field, however, the details were not reported.

Figure 27e shows the bare leading-edge section between the Chemglaze and Astrocoat panels. Incipient leading-edge erosion is evident in the photograph. (An example of severe leading-edge erosion is shown for comparison in fig. 28.) Because the control part was new when coated and installed on the airplane, this erosion took place during the 4873-hour evaluation period. The 1.27-cm (0.5-in) border around all coated panels is BMS 10-79 epoxy primer that was applied beyond the coated areas to prevent edge lifting of the coatings when masking tape was removed.

4.2.2 DELTA AIR LINES EVALUATION

A flight service evaluation on a Delta Air Lines (DL) 727 began in November 1979. Delta monitored condition of the coatings during the agreed-upon 1-year evaluation period and provided field inspection reports on approximately a monthly basis. The coatings remained on the airplane an additional year, during which time two inspections were made by Boeing personnel at commercial service stopovers.

The coating configuration and results of the evaluation are discussed in the following paragraphs.

4.2.2.1 Coating Configuration

Coatings were applied in a 10.16-cm (4-in) strip along wing slat leading edges and on the horizontal tail leading edge, back to the front spar (approximately 10% chord). Delta requested that gray coatings be applied to the wing slats to reduce color contrast with other areas of the wing and that a wash primer be used to facilitate coating removal at the conclusion of the evaluation. The latter request was modified to allow an epoxy primer over the wash primer on the left side of the airplane so that the merits of the two types of primer could be assessed. The resulting primer and coating configuration is shown in Figure 29.

Coatings were applied by DL maintenance personnel as described in Reference 2. Nominal coating thickness at the leading edge was 12 mil, which, on the horizontal tail, tapered to about 5 mil at the front spar. Gray Chemglaze M413 was substituted for black M313 on the wing slats; a gray CAAPCO B-274 was obtained from the manufacturer. The spanwise selection of coatings shown in Figure 29 was made to assess the variation in erosion severity with changes in leading-edge radius or with other factors associated with spanwise location.

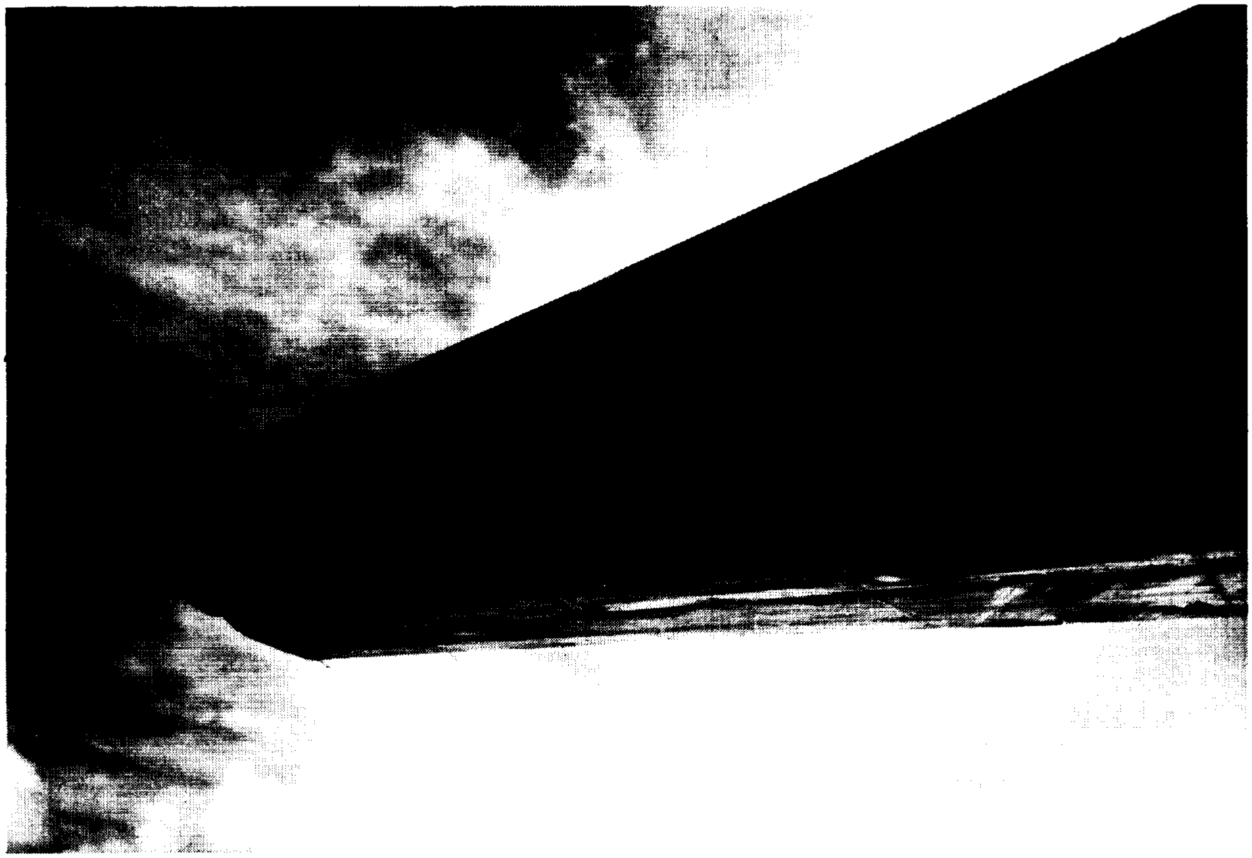

(a) Control Part Coating Panels

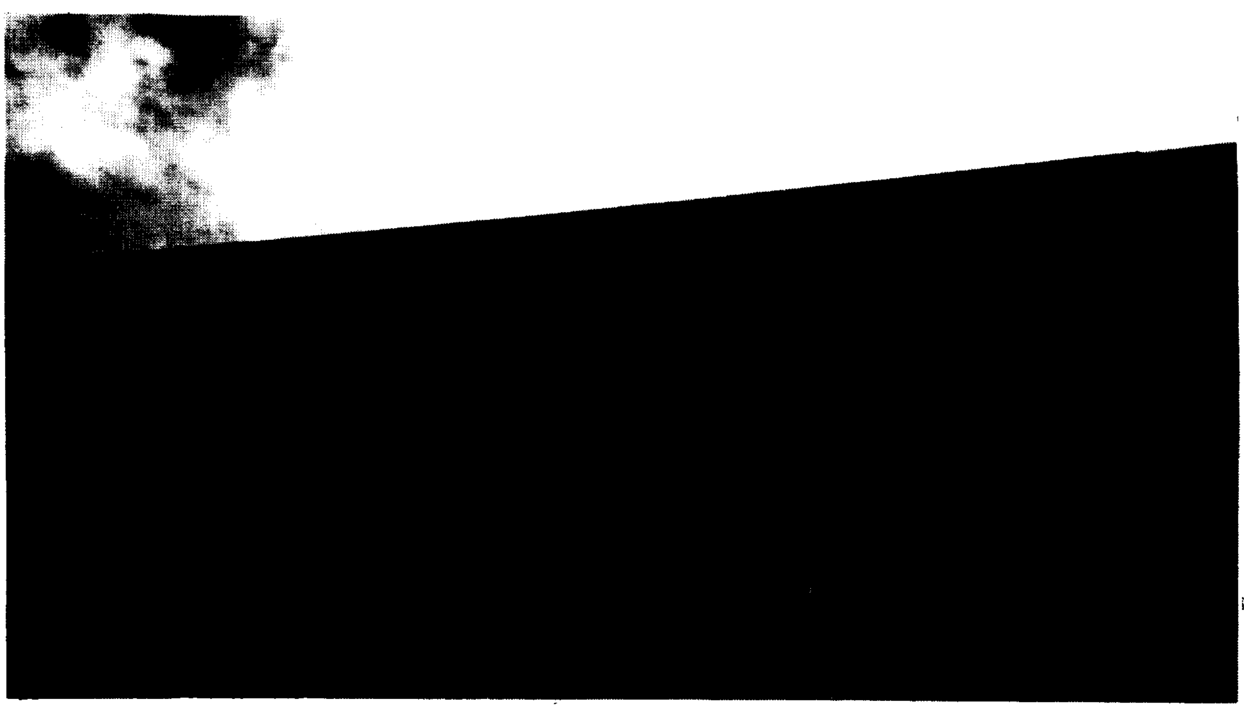

(b) Astrocoat Center Panel—Three Small Erosion Spots on Leading Edge

Figure 26. Laboratory-Applied Coatings on Control Part (3815 hr)

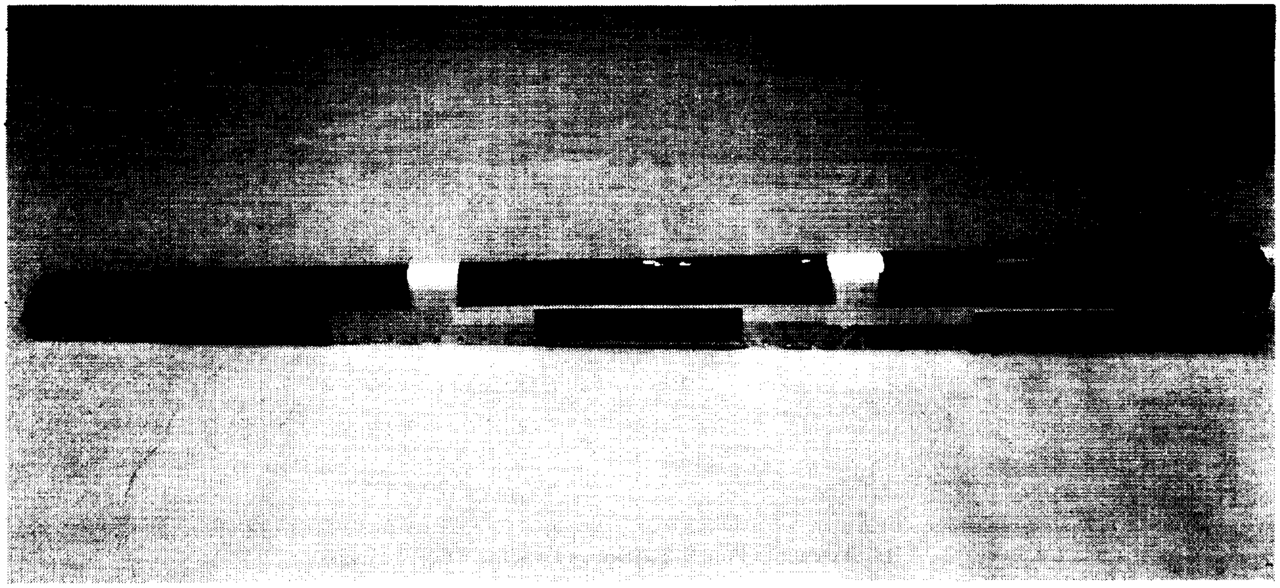

(a) Three Coated Panels on Control Part After Service Evaluation

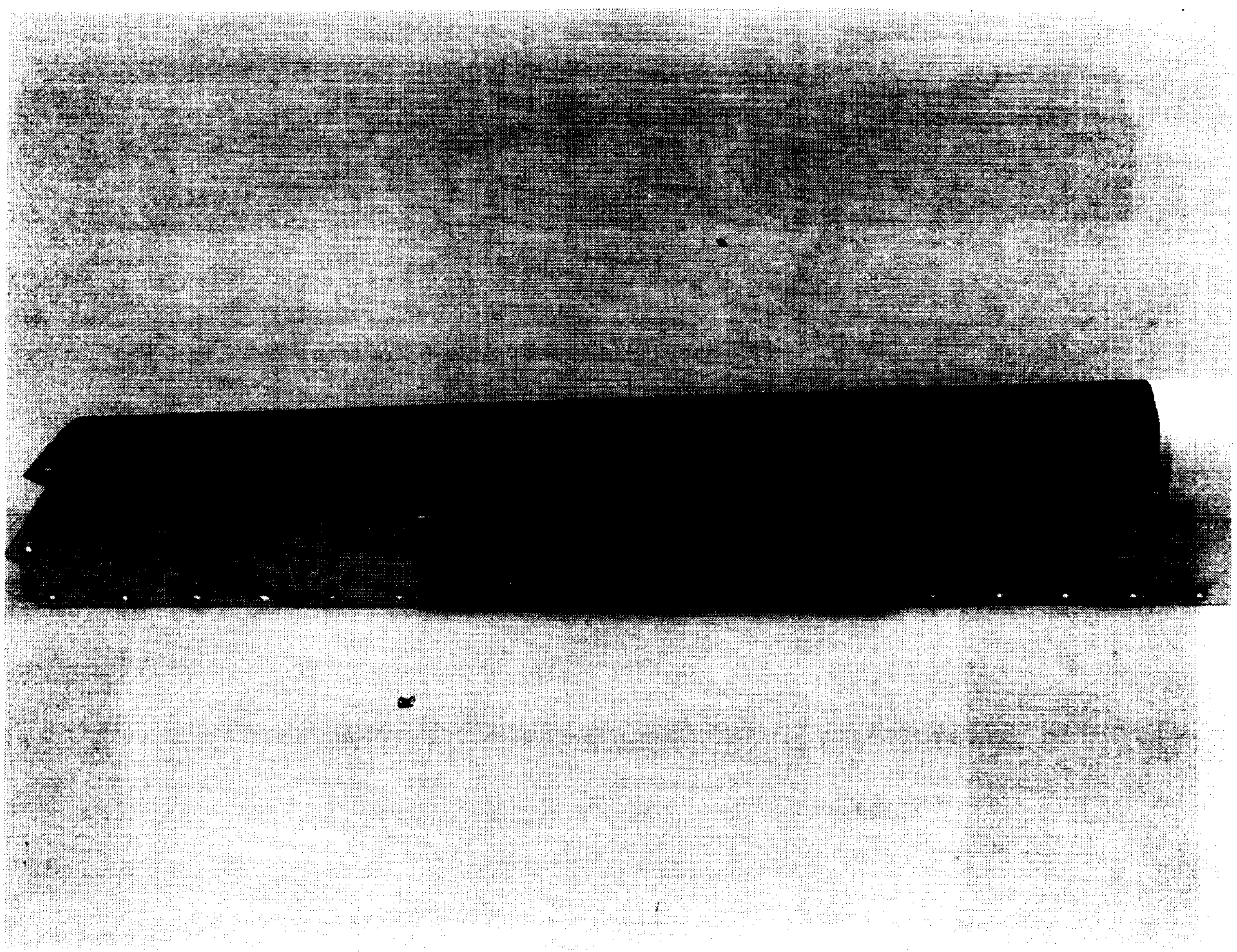

(b) Chemglaze Panel—Good Condition, Except Some Dulling

Figure 27. Laboratory-Applied Coatings on Control Part (4873 hr)

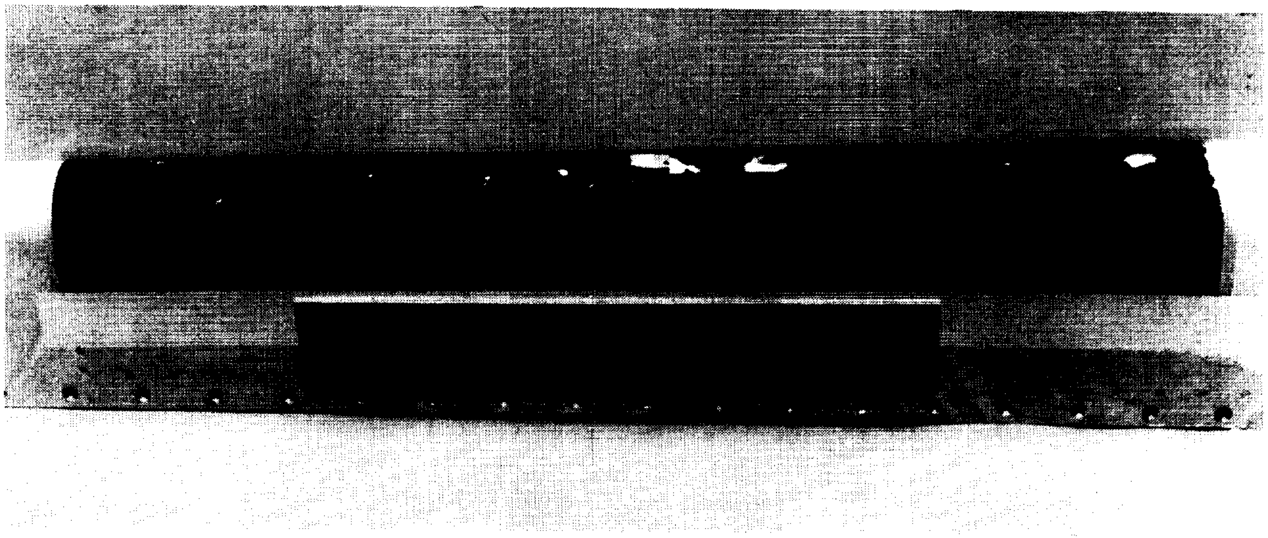

(c) Astrocoat Panel—Extensive Leading-Edge Damage

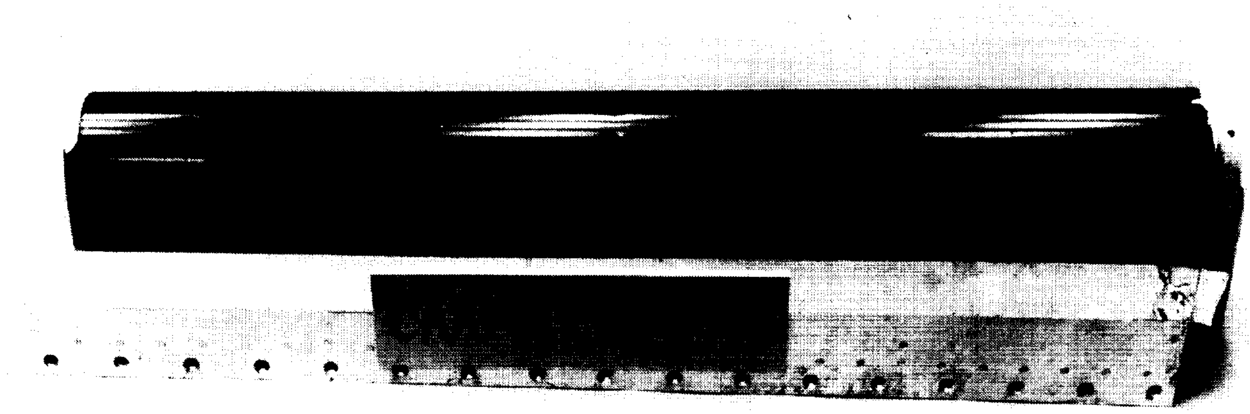

(d) CAAPCO Panel—Good Condition and Glossy

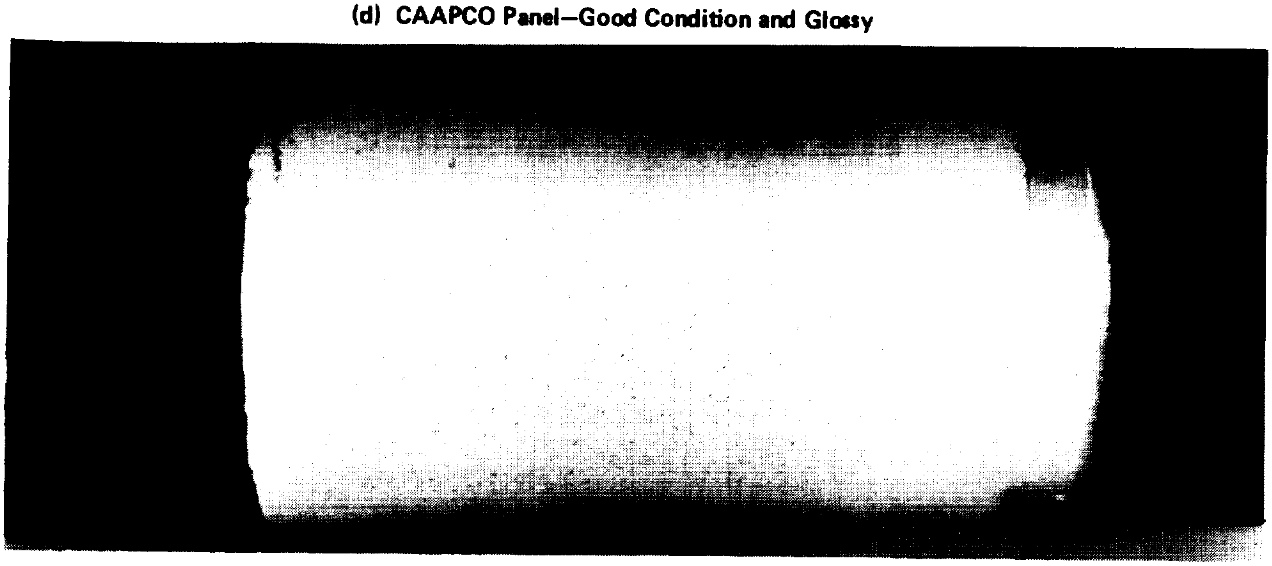

(e) Leading-Edge Erosion of Bare Metal

Figure 27. Laboratory-Applied Coatings on Control Part (4873 hr) (Concluded)

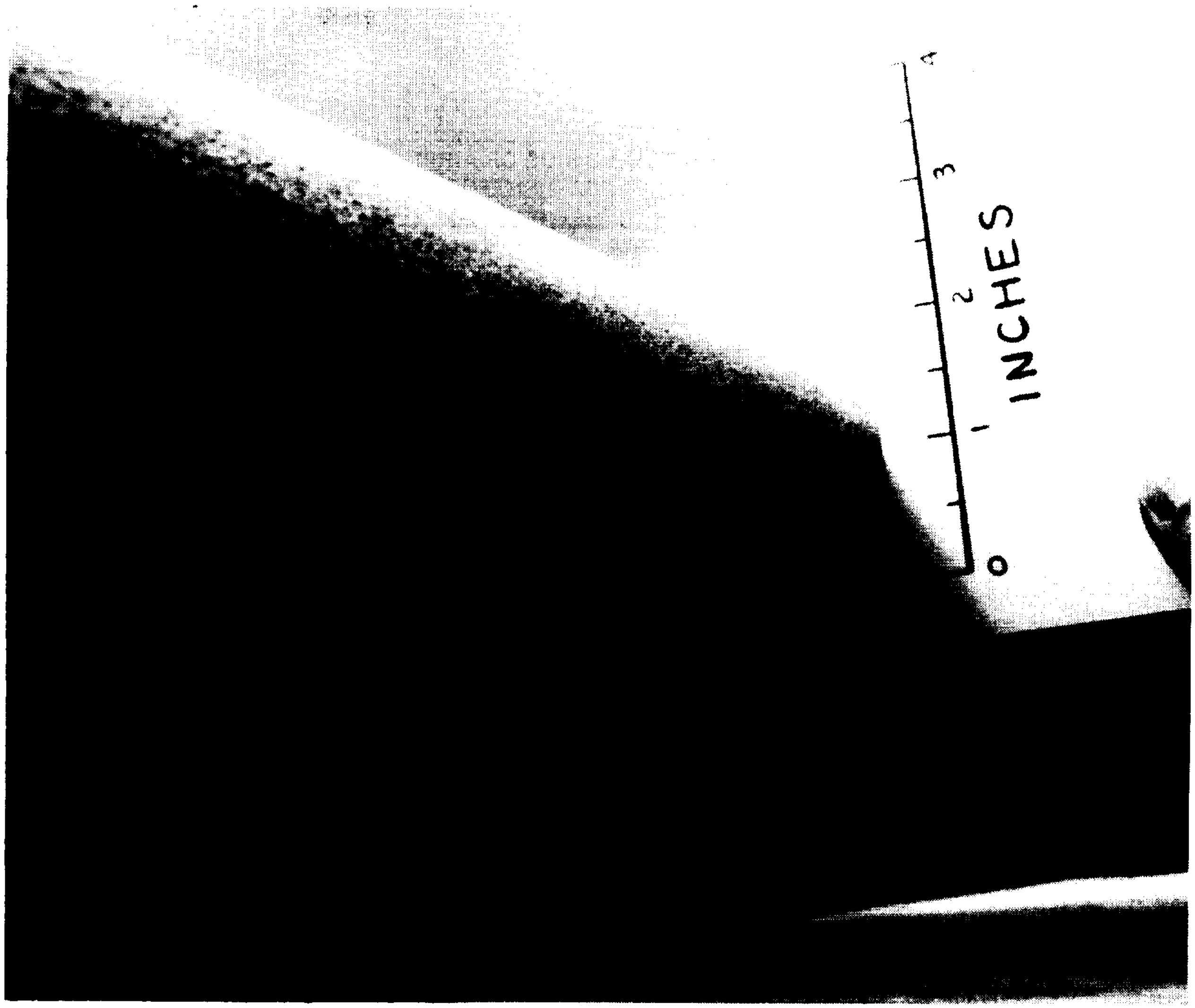

Figure 28. Example of Severe Leading-Edge Erosion

4.2.2.2 Evaluation Results

The coatings were evaluated over a 2-year period, during which they accumulated 6435 flight-hours on Delta U.S. domestic routes. Observations made during periodic inspections are summarized as a function of flight-hours in Table 2.

CAAPCO on slat 1 (fig. 30a) and slat 4 (fig. 30b) was in good condition at the end of the 2-year evaluation. Slat 1 had a peeled strip about 2.54 by 61 cm (1 by 24 in) along the lower inboard edge that was observed at 273 flight-hours and remained essentially unchanged throughout the remainder of the evaluation. Likewise, the slight lifting of the coating at the inboard end of slat 4 remained stable. There was no discoloration of the coatings or other indications of ultraviolet (UV) radiation effects.

Slats 2 and 3, coated with Chemglaze M413, began to lose gloss after about 600 flight-hours and began to yellow from UV exposure after about 2400 hours. At the 2901-hour inspection, erosion down to the primer had occurred on the slat 2 leading edge. Leading-edge erosion began on slat 3 shortly after that inspection. Slat 3 erosion at 4348 flight-hours is shown in Figures 31a and 31b. The dark patches along the leading edge are areas where primer is exposed.

RIGHT-HAND SIDE OF AIRPLANE			
ITEM	WASH PRIMER	COATING	COLOR
5	Hughson 9924	CAAPCO B-274	Gray
6	Hughson 9924	Chemglaze M413	Gray
7	Hughson 9924	Chemglaze M413	Gray
8	Hughson 9924	CAAPCO B-274	Gray
12	Hughson 9924	Chemglaze M313	Black
13	–	Uncoated	Black
14	Hughson 9924	CAAPCO B-274	Black

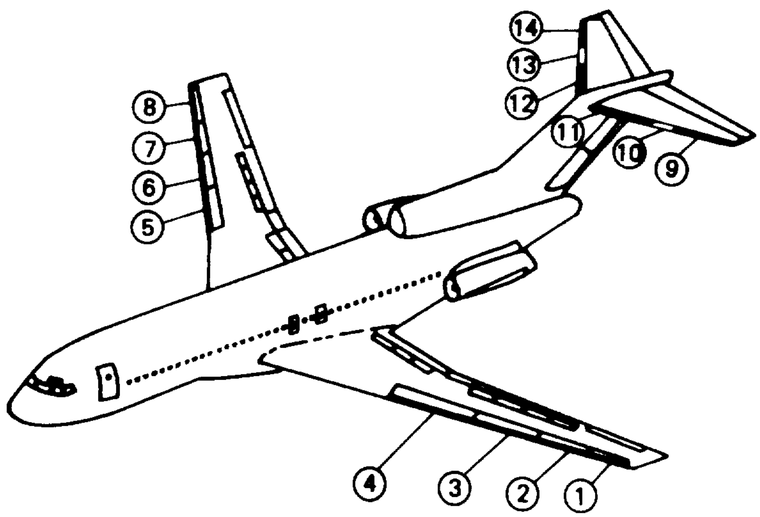

LEFT-HAND SIDE OF AIRPLANE			
ITEM	EPOXY PRIMER	COATING	COLOR
1	BMS 10-79	CAAPCO B-274	Gray
2	BMS 10-79	Chemglaze M413	Gray
3	BMS 10-79	Chemglaze M413	Gray
4	BMS 10-79	CAAPCO B-274	Gray
9	BMS 10-79	Chemglaze M313	Black
10	–	Uncoated	Black
11	BMS 10-79	CAAPCO B-274	Black

Figure 29. Delta Air Lines Surface Coatings Configuration

Table 2. Delta Air Lines Evaluation—Summary of Inspection Reports

		ITEM	COATING	FLIGHT-HOURS–CUMULATIVE 273	598	873	1413	1752	2052	2394	2901	3240[a]	4348[b]	6435[c]
Wing slats (gray coatings)	Epoxy primer over wash primer	1	CAAPCO B-274	Peeled strip lower inboard corner approximately 2.54 x 61 cm (1 x 24 in)	Slight peeling at inboard leading edge	No change	No change	Lower inboard end peeling at very slow rate	No change	Peeling continuing slowly at lower inboard end	No change	No change	No change	No leading-edge erosion No UV discoloration or tackiness (fig. 30a)
		2	Chemglaze M413	OK	Some loss of gloss	Additional loss of gloss (should have had UV topcoat)	No change	No change	Continuing loss of gloss	Yellowing from UV exposure	Leading edge eroded to primer some areas	Yellowing from UV Leading-edge erosion	Eroded to primer 25% of leading edge Inboard end eroded 1.27 cm (0.5 in)	Extensive leading-edge erosion exposing primer or bare metal No peeling (fig. 32a)
		3	Chemglaze M413	OK	Some loss of gloss	Additional loss of gloss	No change	No change	Continuing loss of gloss	Yellowing from UV exposure	No change	UV yellowing Leading-edge erosion	Leading edge eroded to primer, several places (fig. 31a, b)	Extensive leading-edge erosion to primer or bare metal No peeling (fig. 32b, c)
		4	CAAPCO B-274	Lifting and rollback at inboard end, 0.6 cm (0.25 in)	Slight edge peeling at inboard corners approximately 1.3 cm (0.5 in)	No change	No change	No change	No change	No change	No change	No change	No change	No leading-edge erosion No UV discoloration Inboard end eroded 1.27 cm (0.5 in) (fig. 30b)
	Wash primer only	5	CAAPCO B-274	Lifting and rollback at inboard end, 0.6 cm (0.25 in)	Edge peeling inboard end approximately 5 cm (2 in)	No change	Peeling continuing	Peeling at slow rate	No change	No change	No change	Approximately 10% of coated area peeled	Coating peeled 45.7 cm (18 in) inboard end and two places 20.3 cm (8 in) near fence 2.54 x 5.08 cm (1 x 2 in)	No change (fig. 33)
		6	Chemglaze M413	OK	Some loss of gloss	Additional loss of gloss	Slight erosion developing at inboard end	No change	Continuing loss of gloss	Yellowing from UV exposure	No change	UV yellowing Beginning of leading edge erosion	Lwr outbd corner eroded to primer 30.5 cm (12 in) Outbd LE lwr inbd corner peeled 5 x 10 cm (2 x 4 in)	No change
		7	Chemglaze M413	OK	Some loss of gloss	Additional loss of gloss	Slight erosion developing at inboard end	No change	Continuing loss of gloss	Yellowing from UV exposure	No change	Leading-edge erosion beginning UV yellowing continuing	Eroded to primer along outboard leading edge Slight erosion at inboard end	No change
		8	CAAPCO B-274	Lower inboard end peeled approximately 2.54 x 76.2 cm (1 x 30 in)	Inboard end peeling 15.2 cm (6 in)	No change	Peeling continuing	Peeling at slower rate	Peeling continuing	Large areas of coating peeled	Approximately 50% of coating peeled	Approximately 90% of coating peeled		
Horizontal tail (black coatings)	Epoxy primer over wash primer	9	Chemglaze M313	OK	OK	OK	OK	OK	OK	Losing gloss	No change	No change	Good condition	No leading-edge e or peeling Good condition (fig. 34a)
		10	Bare											Slight leading-edge erosion
		11	CAAPCO B-274	OK	OK	OK	OK	OK	OK	Two small blisters at fastener heads on leading edge	Apparent bird strike on leading edge No peeling	No change		Several peeled spots on leading-edge Dent from bird strike (fig. 34a, b)
	Wash primer only	12	Chemglaze M313	OK	OK	OK	Slight erosion developing at inboard end	No change	No change	Losing gloss	No change	No change		Two peeled spots on leading-edge approximately 2.54-cm (1-in) diameter Inboard end eroded 5.1 cm (2 in) (fig. 35)
		13	Bare											Slight leading-edge erosion
		14	CAAPCO B-274	OK	Coating removed at approximately 500 hr because of excessive peeling									

[a]Final Delta field report after 1-year evaluation. [b]Boeing inspection at 16 months. [c]Boeing inspection at 2 years

(a) Slat 1

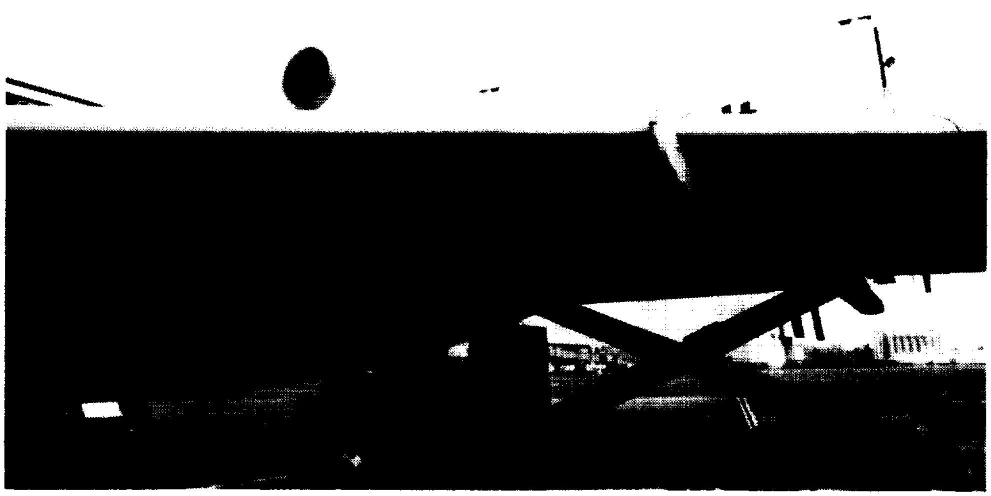

(b) Slat 4

Figure 30. CAAPCO Coating Over Epoxy Primer—Intact After 6435 hr

(a) Leading-Edge Erosion

(b) Exposed Primer, Inboard End of Slat

Figure 31. Slat 3 at 4348 hr—Chemglaze Over Epoxy Primer

Coating erosion on slat 2 (fig. 32a) and slat 3 (fig. 32b) had become quite prevalent at 6435 flight-hours. Bare metal was exposed over much of the leading-edge span, typical of that shown in Figure 32c. The Chemglaze adhered well to the epoxy primer. There was no peeling on either slats 2 or 3. A UV protective coating over Chemglaze M413 probably would have increased its erosion life significantly by delaying and/or reducing deterioration caused by UV radiation.

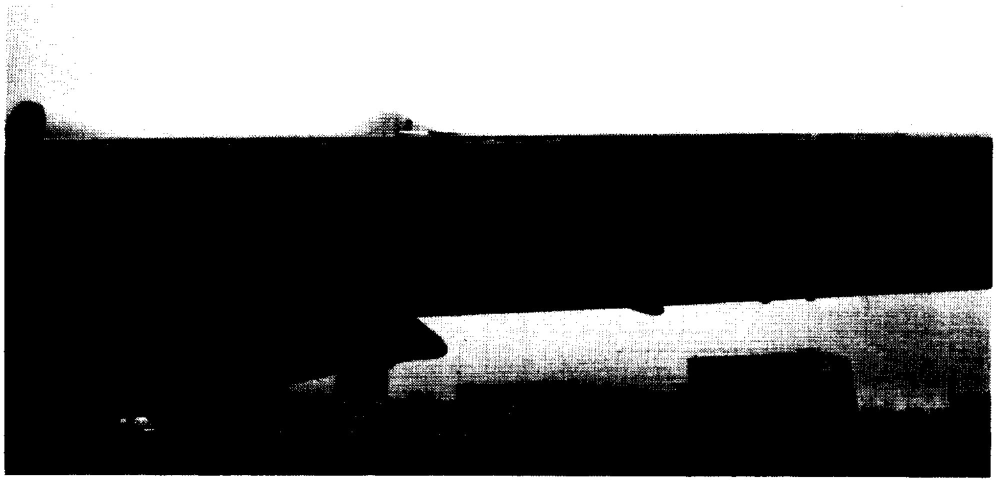

(a) Leading-Edge Erosion on Slat 2

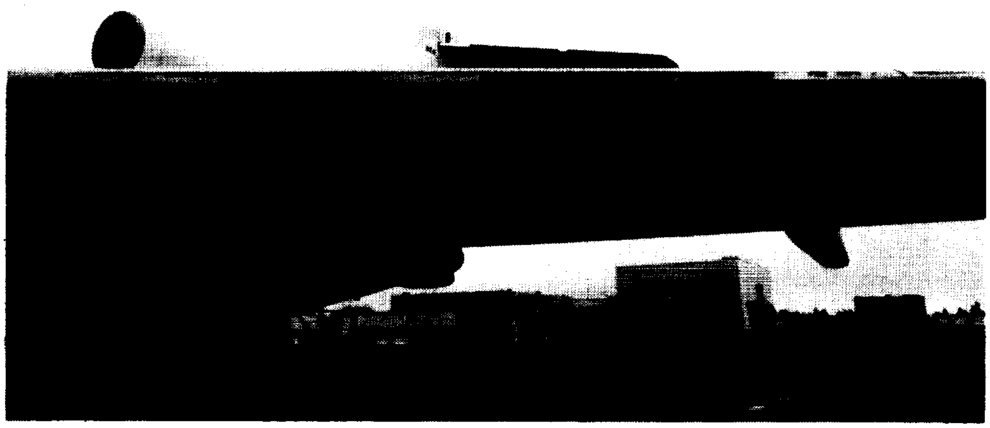

(b) Leading-Edge Erosion on Slat 3

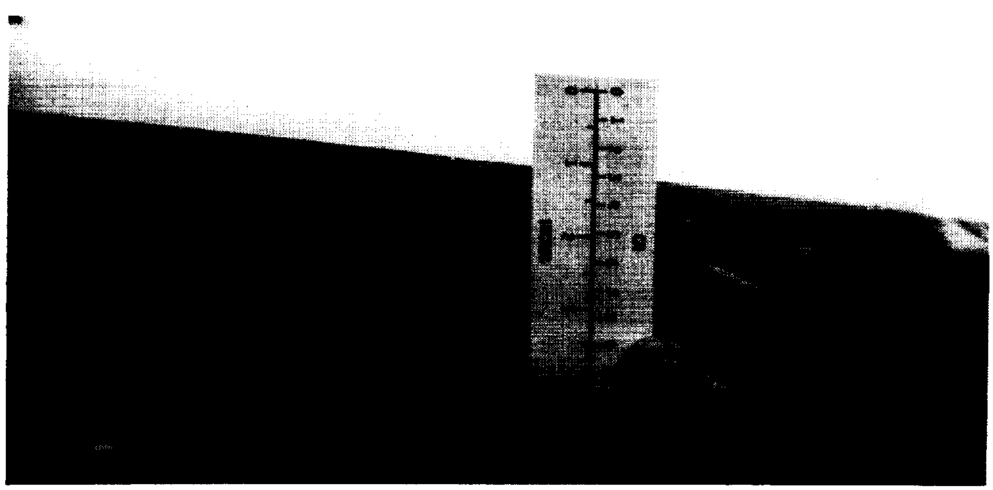

(c) Bare Metal Exposed on Slat 3 Leading Edge

Figure 32. Chemglaze Coating Over Epoxy Primer (6435 hr)

On the right wing, where only wash primer was applied as an undercoating, the CAAPCO coating on slats 5 and 8 peeled extensively. Peeling at the inboard end of slat 5 began early in the evaluation and grew to about 45.7 cm (18 in). In addition, two strips about 20.3 cm (8 in) wide had peeled down to the primer, as is visible in Figure 33. Slat 8 began peeling early in the evaluation and continued peeling until essentially all the coating was gone at 3240 flight-hours. This slat received damage repair before being coated, and surface preparation prior to coating possibly was not as thorough as it was for the other parts.

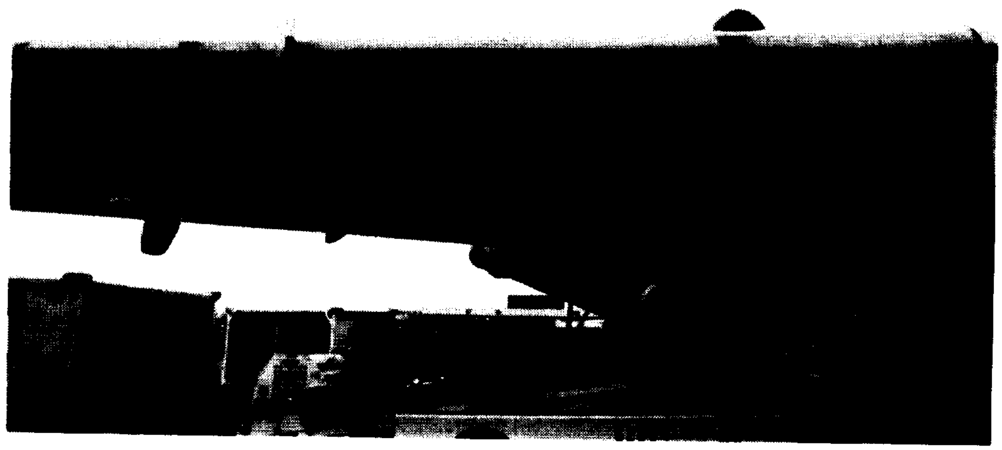

Figure 33. Slat 5 at 6435 hr—Primer Exposed in Two Peeled Areas

Slats 6 and 7 showed leading-edge erosion and UV discoloration similar to, but not as severe as, that on the Chemglaze-coated slats on the left side of the airplane (slats 2 and 3). Except for a small 5- by 10-cm (2- by 4-in) area at the lower inboard corner of slat 6, there was no peeling on either slat. This implies that the adhesive bond between Chemglaze and wash primer is satisfactory and that an epoxy primer is not necessary with Chemglaze.

Chemglaze M313, on the left outboard horizontal tail leading edge (fig. 34a), survived the evaluation in good condition. The coating began losing gloss after about 2400 flight-hours; however, at the end of the evaluation the coating showed no peeling or leading-edge erosion. The adjacent inboard section, coated with CAAPCO, had several peeled spots along the leading edge. Figure 34b is a closeup of the CAAPCO leading edge just inboard of midspan. The photo shows a dent in the vicinity of peeled spots, which is the result of a bird strike reported at the 2901-hour inspection. Peeling in that area began about 2000 flight-hours later.

The right horizontal tail leading edge is shown at 6435 hours in Figure 35. The inboard panel, coated with Chemglaze, had erosion at the inboard end that grew to about 5 cm (2 in) by the end of the evaluation. Also, there were two peeled spots on the leading edge about 2.54 cm (1 in) in diameter. The outboard panel began losing CAAPCO coating very early, and the coating had to be removed at about 500 hours.

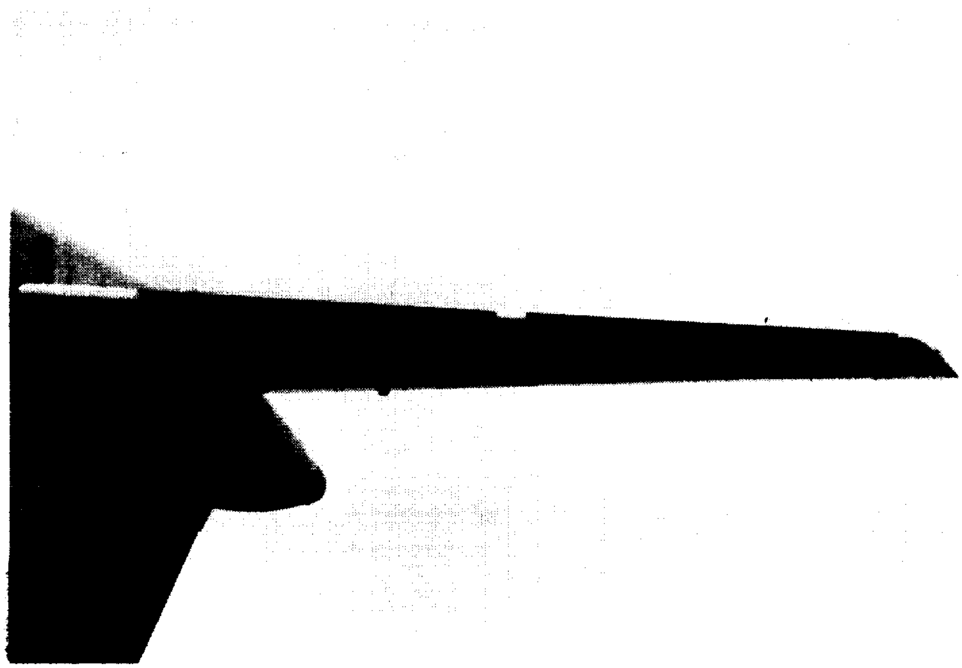

(a) Chemglaze Coating in Good Condition; CAAPCO Spotted

(b) Bird Strike on CAAPCO Panel

Figure 34. Left Horizontal Tail Leading Edge (6435 hr)

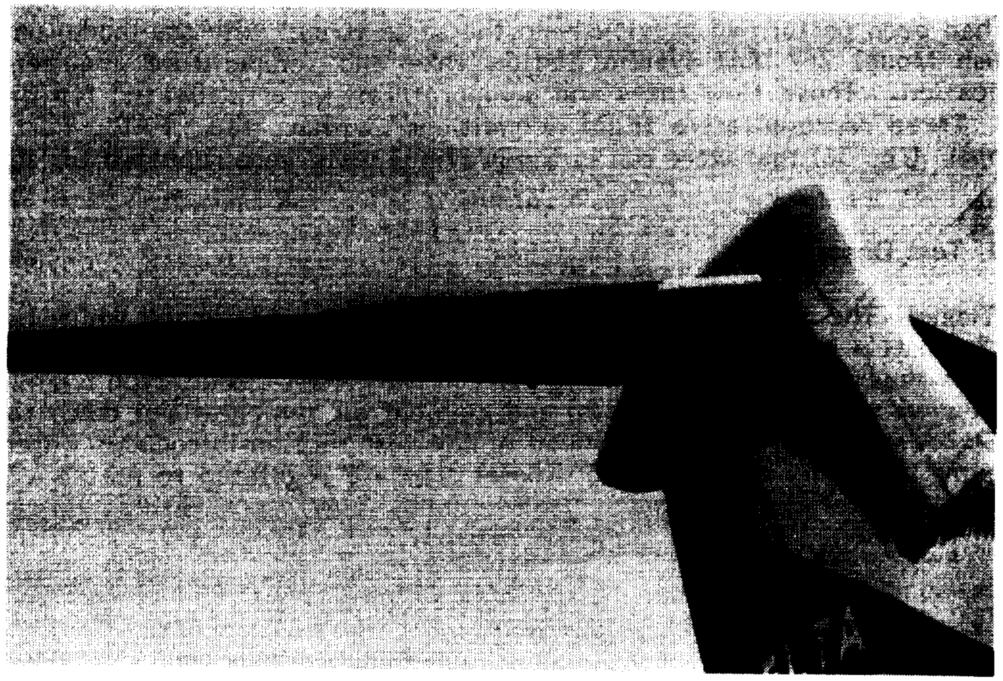

Figure 35. Inboard Panel at 6435 hr—Erosion at Inboard End

4.2.3 CONCLUSIONS

The following were concluded from the flight service evaluations:

- CAAPCO applied over an epoxy primer, such as BMS-10-79, is the most durable coating system, with a life in excess of 6500 flight-hours.
- The life of Chemglaze M413 would be increased significantly by adding a UV protective topcoat. Chemglaze M313 and M413 demonstrated good adhesion over either a wash primer or an epoxy primer.
- It is important that the substrate be thoroughly cleaned prior to application of either coating.
- The erosion life of either CAAPCO or Chemglaze is greater than that for Astrocoat.

4.3 ENVIRONMENTAL TESTS

Laboratory tests and analyses were conducted to determine the suitability of the candidate elastomeric polyurethane coatings to certain operational factors in the airline transport environment. The compatibility of coatings with thermal anti-icing systems, their effect on lightning strike and precipitation static, and their ability to protect the substrate from erosion and corrosion were investigated.

4.3.1 ICING TESTS

Icing tunnel tests were run on a wing leading-edge slat model to determine if CAAPCO and Chemglaze coatings were compatible with the operation of airplane thermal anti-icing (TAI) systems. The tests provided information on the effects of reduced thermal conductivity on ice prevention and elimination, the effects of elevated temperatures on coating adhesion and durability, and the ability of the coatings to shed ice without damaging the coatings.

Tests had been performed previously in the same tunnel with the model uncoated to establish Model 767 TAI system airflow rate and temperature requirements for certification. Those flow rates and temperatures were duplicated for the coating tests. Three representative flight conditions within the FAR Part 25 icing envelopes (fig. 36) that were run in the previous tests were repeated for the coating tests.

4.3.1.1 Test Description

Icing Tunnel—The tests were conducted in the Boeing icing tunnel, which has a 38.1- by 50.8-cm (15- by 20-in) test section. The icing tunnel and associated instrumentation are shown schematically in Figure 37. The closed-circuit-type tunnel produces velocities up to 87.2 m/s (195 mi/h) and ambient air temperatures down to -28.9°C (-20°F). A set of spray nozzles ahead of the test section introduces water into the airstream. Quantity of water and droplet size are regulated to match a predetermined liquid water content.

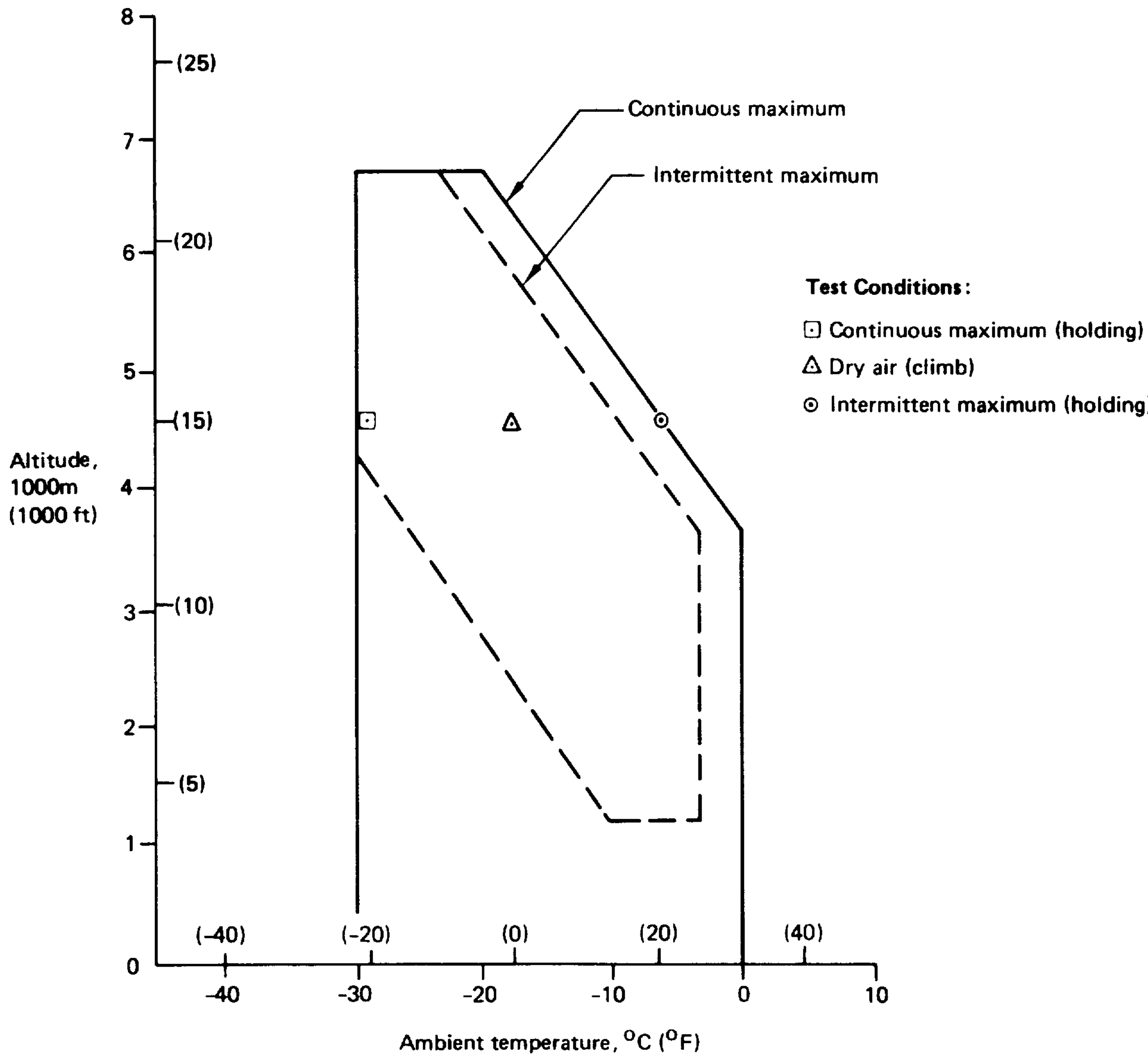

Figure 36. FAR Part 25 Icing Envelopes

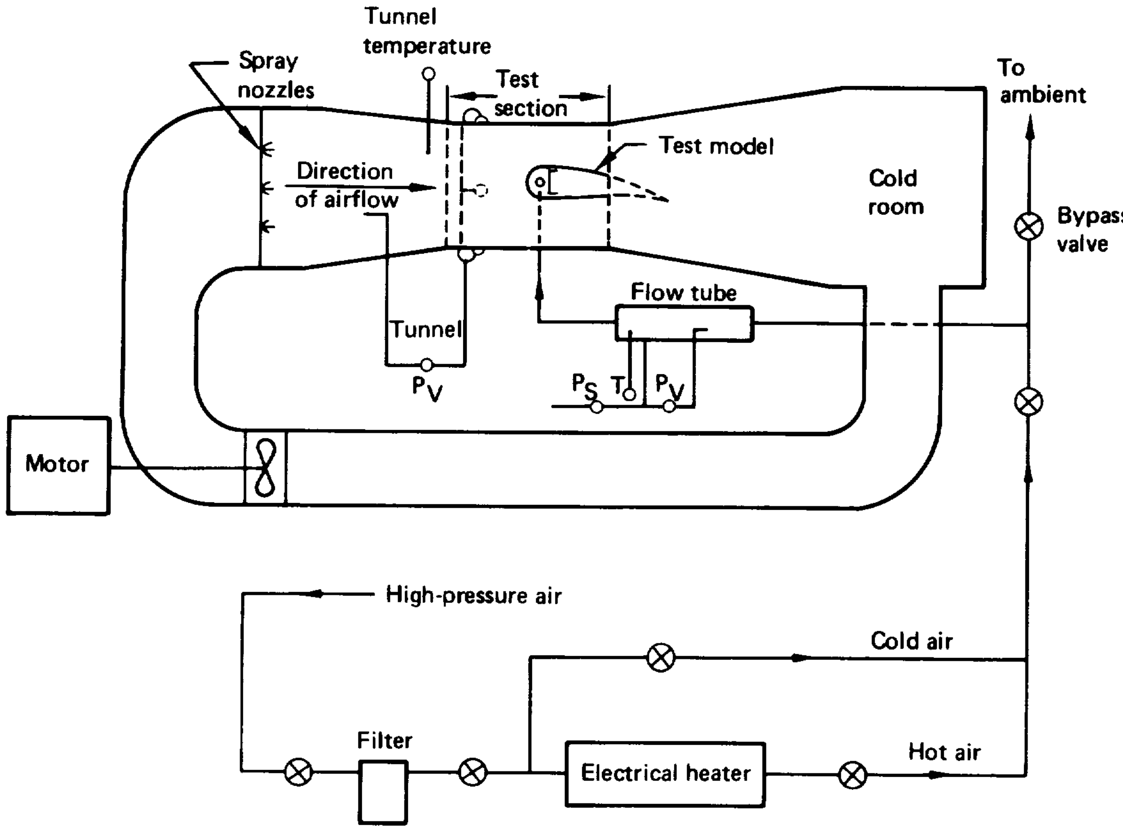

Figure 37. Schematic of Icing Tunnel

High-pressure air passes through a filter, a heater, and into an instrumented flow tube where temperature and pressures are measured to provide TAI system airmass flow data. TAI air temperature is measured by a thermocouple located within the spray tube in the model. Both temperature and flow rate are regulated by a system of valves, which are adjusted manually.

A viewing window in the side of the test section allows the model to be observed and photographed during runs.

Model Description—Figure 38 shows the icing test model. The forward 30.48 cm (12 in) of chord length is contoured to the dimensions of a 767 full-scale wing leading-edge slat. The aft section is a slab-sided closure panel containing no instrumentation. As shown in Figure 39, the nose section contains the TAI spray tube, which has 10 bleed holes directed toward the leading edge. The bleed holes are 3.81 cm (1.5 in) apart and have a 3.58-mm (0.141-in) diameter. Two rows of thermocouples (T/C) are installed in the exterior skin. The inboard row (T/C 1 through 10) is in line with a spray tube bleed hole; the outboard row (T/C 11 through 21) is located midway between bleed holes. TAI air passes into the vented D-duct, into the aft plenum area, and exhausts from the model through a hole in the lower surface skin, aft of the D-duct web.

The TAI spray tube, D-duct, and aft plenum contain temperature and pressure instrumentation. Temperatures from the skin and air T/Cs were recorded on tape by a Fluke Data Logger. Pressures were measured on manometers and recorded manually.

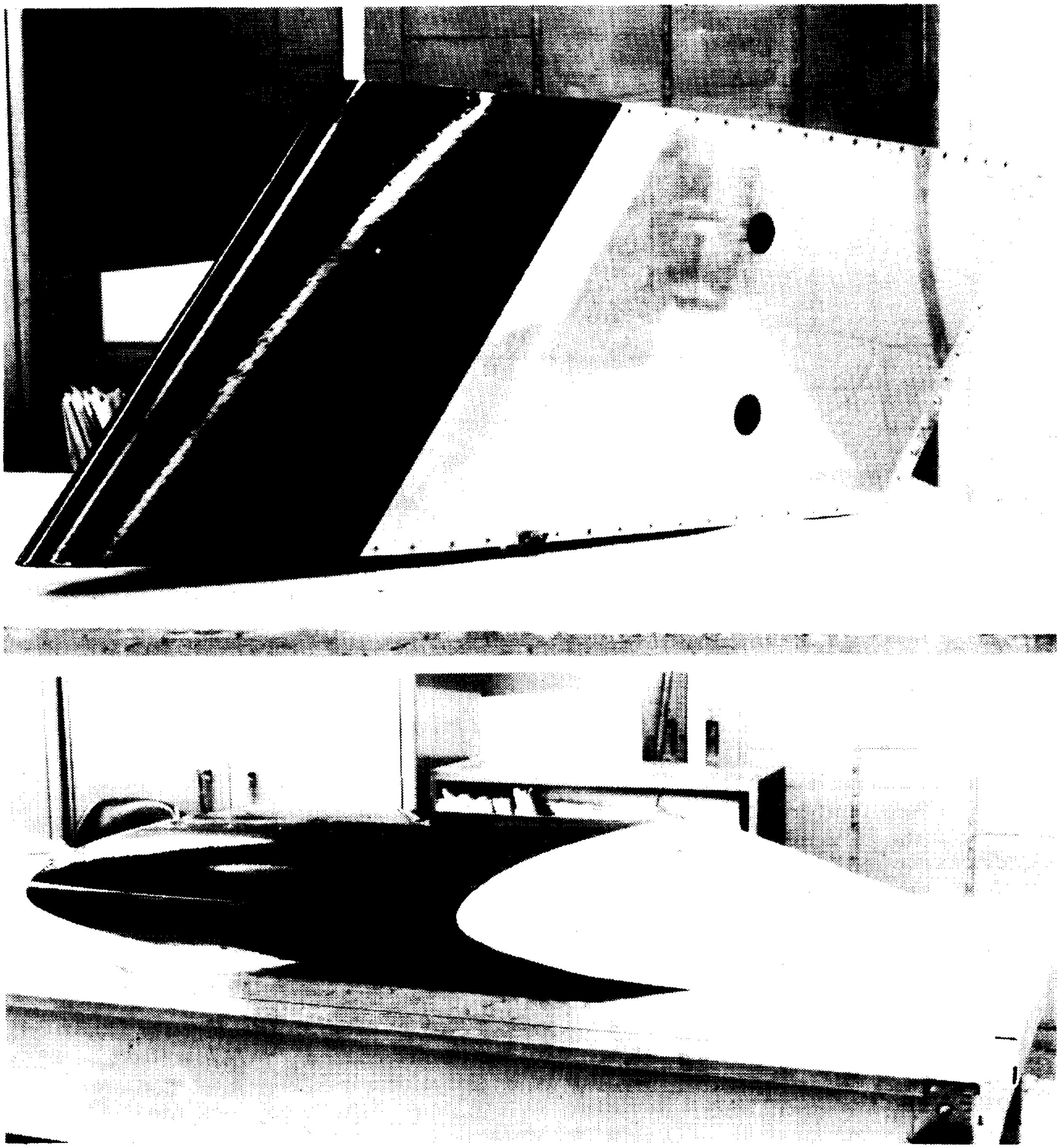

Figure 38. Icing Test Model

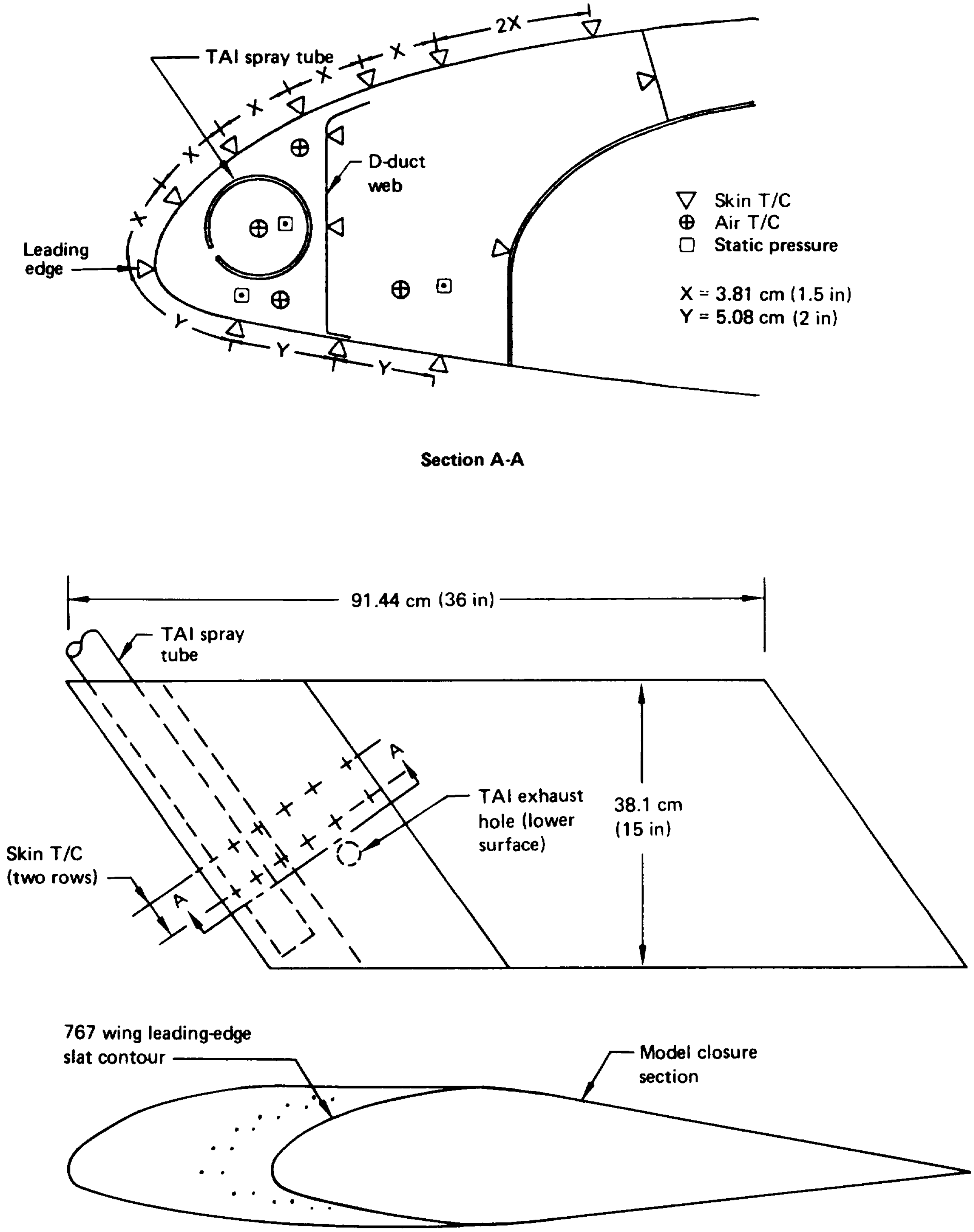

Figure 39. Icing Test Model Description

4.3.1.2 Test Procedure

The icing tests performed are summarized in Table 3. The first series of tests were run on the uncoated model to duplicate selected simulated flight conditions tested for the Model 767 ice protection certification program. Three icing conditions were tested with the system operating in the anti-icing mode: intermittent maximum icing (IMI) during holding at 4572m (15 000 ft), continuous maximum icing (CMI) for the same flight condition, and climb through dry air (DA) at 4572m (15 000 ft). The last condition produced the highest temperatures within the leading edge and is of interest because these temperatures represent the upper limits to which the D-duct, the leading-edge coatings, skin, and the internal structure were subjected.

Table 3. Summary of Icing Tests

RUN NO.	COATING	ICING CONDITION	TAI SYSTEM	
			FLOW, %	OPERATING MODE
1	Uncoated	Intermittent maximum	100	Anti-icing
2		Intermittent maximum	75	
3		Dry air	100	
4		Dry air	75	
5		Continuous maximum	100	
6		Continuous maximum	75	
7	CAAPCO B-274	Continuous maximum	100	
8		Continuous maximum	75	
9		Intermittent maximum	100	
10		Intermittent maximum	75	
11		Dry air	100	
12		Dry air	75	
16	Chemglaze M313	Continuous maximum	100	
17		Continuous maximum	75	
18		Intermittent maximum	100	
19		Intermittent maximum	75	
21		Dry air	75	
22		Dry air	100	Anti-icing
23	Chemglaze M313	Intermittent maximum	100	Deicing

The test method varied somewhat with the test condition. In all cases, tunnel velocity and temperatures and TAI flow rate and temperature were stabilized before the test began. Continuous maximum icing was simulated by introducing water at a controlled rate and drop size for a period of time equivalent to the airplane traveling 32.2 km (20 mi). During this time, thermocouple temperatures were continuously recorded. Intermittent maximum icing was simulated by the same method, except that the duration of the run was equivalent to traveling only 9.2 km (6 mi). No water was introduced into the tunnel during dry air tests. This condition represented TAI system operation in preparation for predicted icing conditions in the vicinity of the airplane flight path. Each of the three conditions was run with the TAI system operating at 100% airflow rate (the flow rate selected for Model 767 operation) and at 75% flow rate. The latter rate was included for interpolation of test data in case the Model 767 airplane flow rates were revised subsequent to the test.

The same test conditions were repeated with CAAPCO B-274 and Chemglaze M313 coatings on the model. In each case, the coatings were applied over the entire leading-edge section, back to the forward edge of the closure section (fig. 38). The coatings were approximately 12 mil thick at the leading edge, tapering to approximately 5 mil at the aft edges.

Following the anti-icing tests, a run was made in the deicing mode to observe ice buildup and shedding characteristics of Chemglaze coating. Prior to the test, the outboard half of the coated area was overcoated with a thin layer of icephobic silicone compound (G.E. 117-8441B), which was an experimental ice preventative used on U.S. Army helicopter blades. When the run was made, the tunnel was stabilized in the intermittent maximum icing condition. Visual observations were made and photographs were taken.

The model was mounted in the tunnel at a +4-deg angle of attack for all runs. This angle represented a best compromise between climb and cruise attitudes and was the setting used during Model 767 certification testing.

4.3.1.3 Test Results

Results of the icing tests are summarized below. More detailed supplementary data are contained in Appendix B.

Figure 40 compares slat skin temperatures of the coated and uncoated model

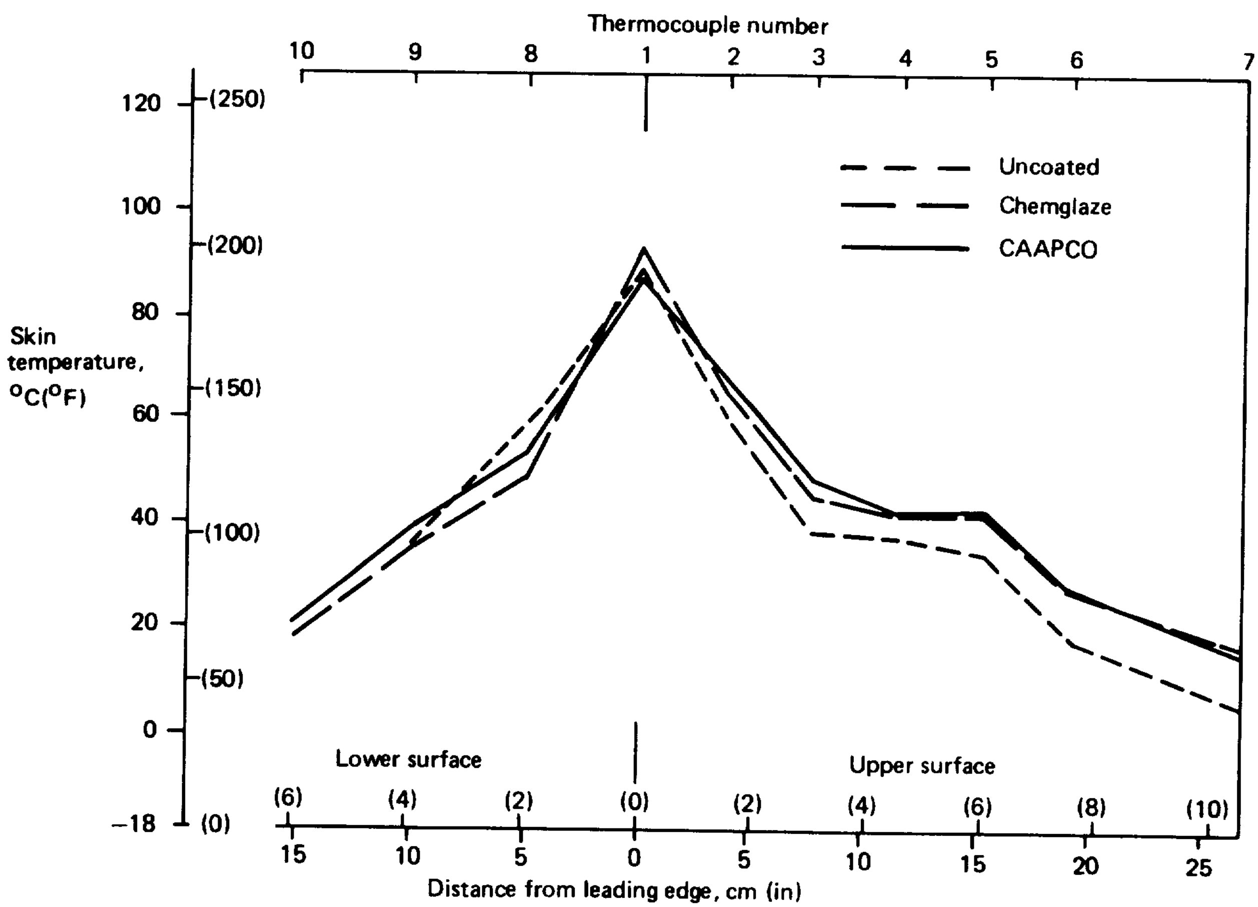

Figure 40. Skin Temperature Profile—Continuous Maximum Icing

configurations for the continuous maximum icing condition. Maximum temperatures of about 90°C (194°F) occurred at the leading edge for the three coating configurations. Aft of the leading edge, the uncoated upper surface stabilized at temperatures slightly below those of the coated surfaces. Figure 41 shows the coated model in the icing tunnel at the conclusion of continuous maximum icing runs. The upper photo (CAAPCO coating) shows an area of thin ice (about 1 mm thick) on the lower inboard surface, well aft of the leading edge. Although not evident in the photograph, most of the surface was wet and skim ice of a similar thickness was formed on the upper surface aft of the truncation line.

In general, the icing tendencies of CAAPCO and Chemglaze were similar. The Chemglaze coating (fig. 41b) accumulated a thin ice film near the inboard leading edge and, like CAAPCO, a trace of ice was formed well aft of the leading edge on the upper and lower surfaces. Excessive ice formation within about 5 cm (2 in) of either end of the model was discounted because of restricted TAI air circulation in those areas and heat absorption by the model endplates.

Figures 42a and 42b compare ice formation on the uncoated versus the CAAPCO-coated surface. These runs were made for the continuous maximum icing condition with TAI flow reduced to 75%. Runback on the uncoated surface formed a thin skim of ice just forward of the truncation line, whereas with the CAAPCO coating, the line of ice formation moved forward. On the lower surface, ice formation moved to approximately 7.5 cm (3 in) of the leading edge and built up to about 3 mm in spots. Figure 42 shows that there is a slight reduction in rate of heat transfer through the coating that, at the reduced rate of TAI airflow (75% of rated), results in marginal anti-icing performance.

Results of the intermittent maximum icing tests are shown in Figure 43. Skin temperatures with either CAAPCO or Chemglaze applied are nearly identical and are considerably higher than for the uncoated surface. The difference in temperatures is most pronounced at the leading edge, where the coating thickness is the greatest, i.e., 12 mil. Temperatures aft of the leading edge stabilized at values higher than those for the continuous maximum icing runs (fig. 40) because the intermittent icing runs were of shorter duration, simulating flight through 9.6 km (6 mi) of icing conditions. Figure 44 shows the model after the intermittent maximum icing runs. Both of the coatings picked up a thin skim of ice along the aft edges of the coated area. Ice on the lower surface extended far enough forward to be visible in the photographs. The uncoated model, under the same test conditions, accumulated a thin skim of ice aft of the truncation line, which is just aft of the heated nose section of the slat.

The dry air tests were performed to obtain maximum skin temperature profiles expected during normal TAI system operation. In these tests, the model does not benefit from the cooling effect of water in the airstream. As seen in Figure 45, skin temperatures at the leading edge are approximately 30°C (54°F) higher than for the continuous and intermittent maximum icing conditions. There is a negligible temperature difference between the two coatings; however, the uncoated upper surface exhibited slightly lower temperatures as the distance from the leading edge increased. The maximum temperatures of about 120°C (250°F) at the leading edge produced no evident effect on the coatings. There was no evidence of hardening, blistering, peeling, or discoloration.

At the conclusion of the anti-icing tests, the model with the Chemglaze coating was tested in the deicing mode of operation. The purpose of this test was to determine if

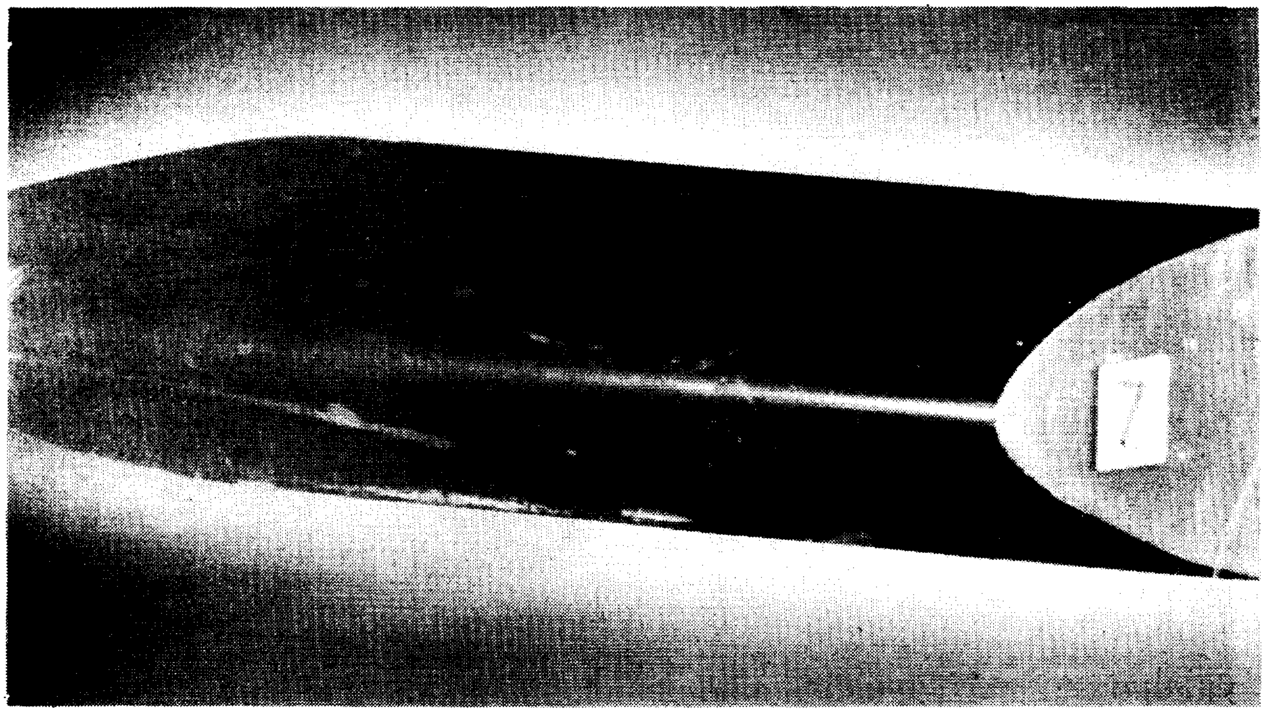

(a) CAAPCO Coating

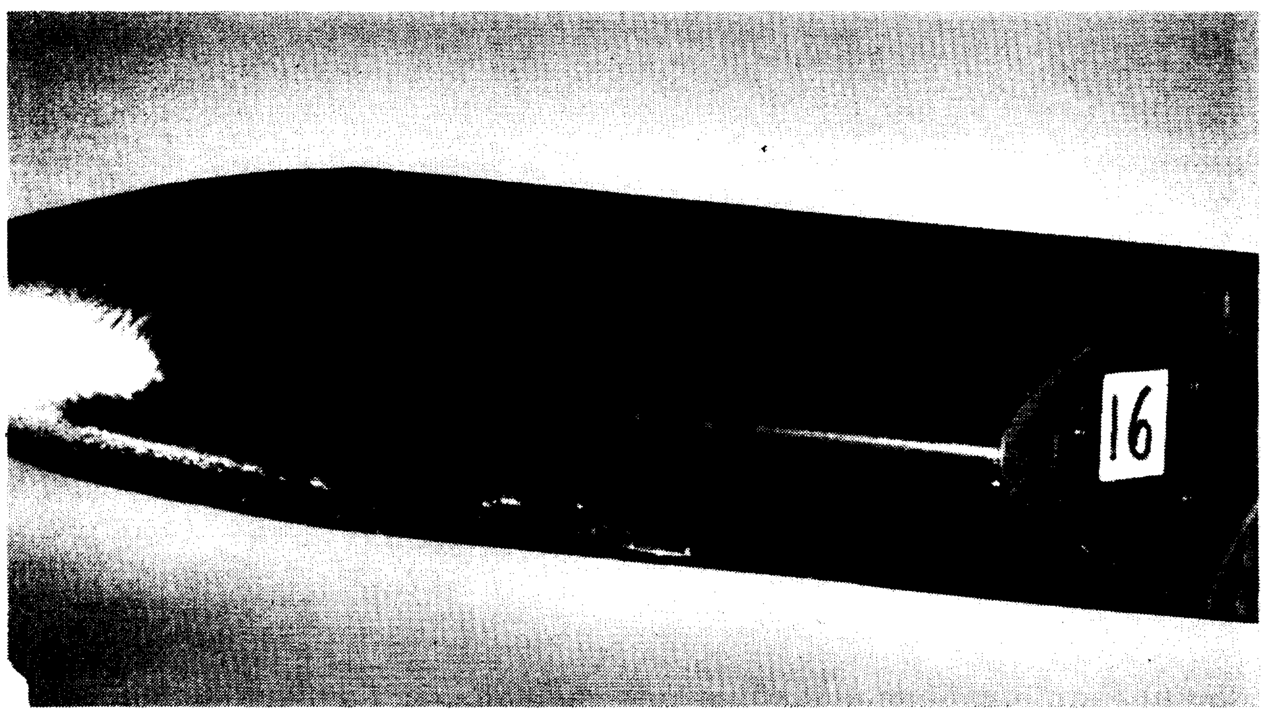

(b) Chemglaze Coating

Figure 41. Coated Model After CMI Runs at 100% TAI Flow Rate

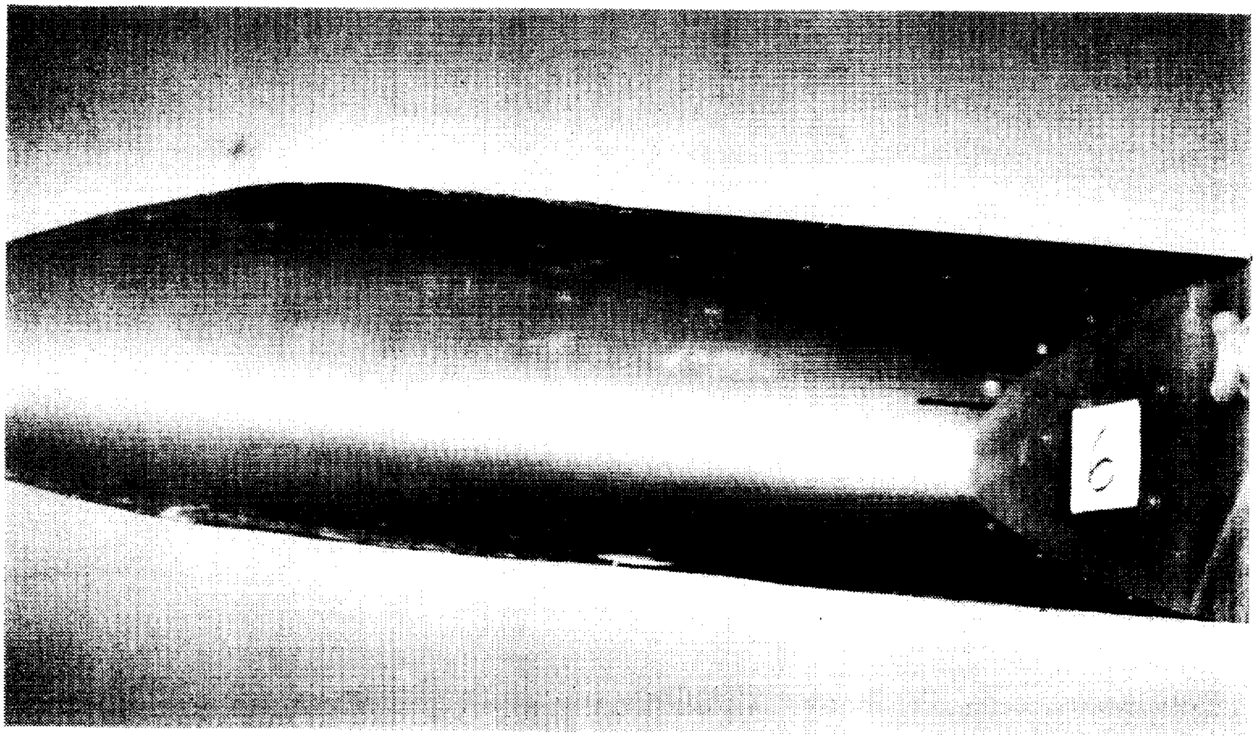

(a) Uncoated

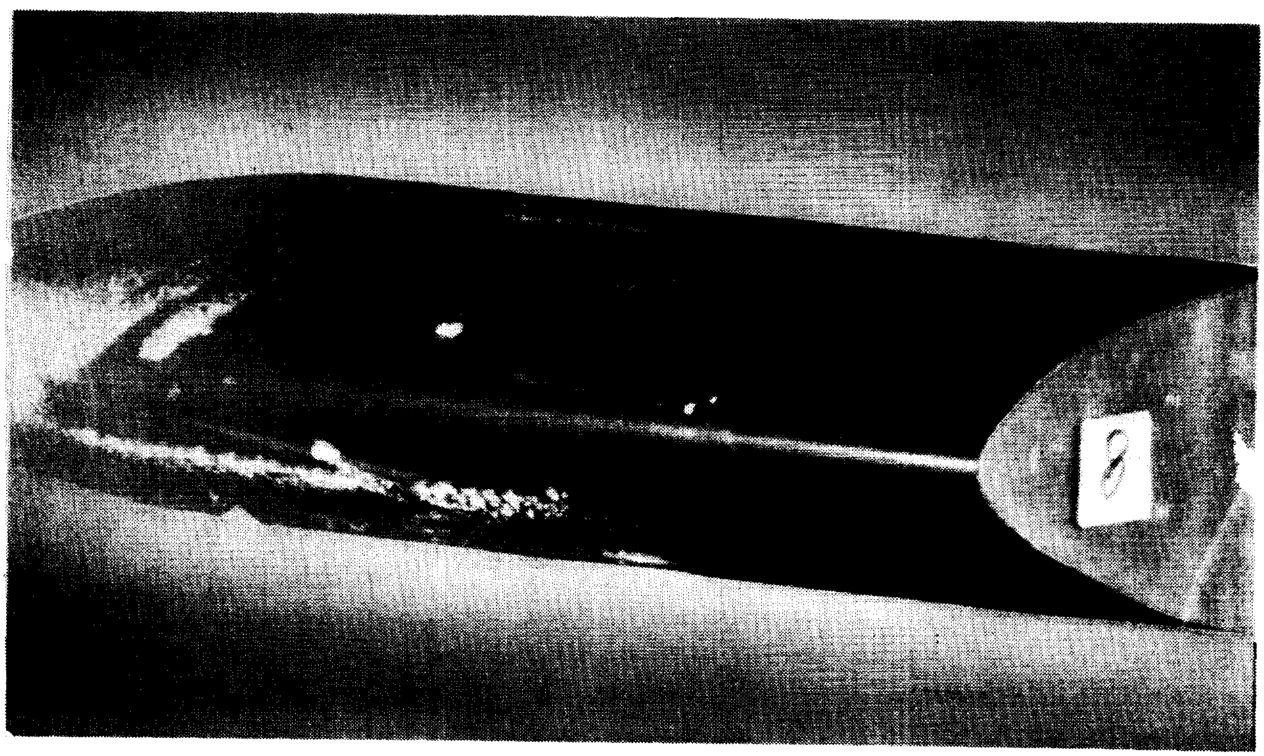

(b) CAAPCO Coating

Figure 42. Comparison of Coated and Uncoated Model After CMI Runs at 75% TAI Flow Rate

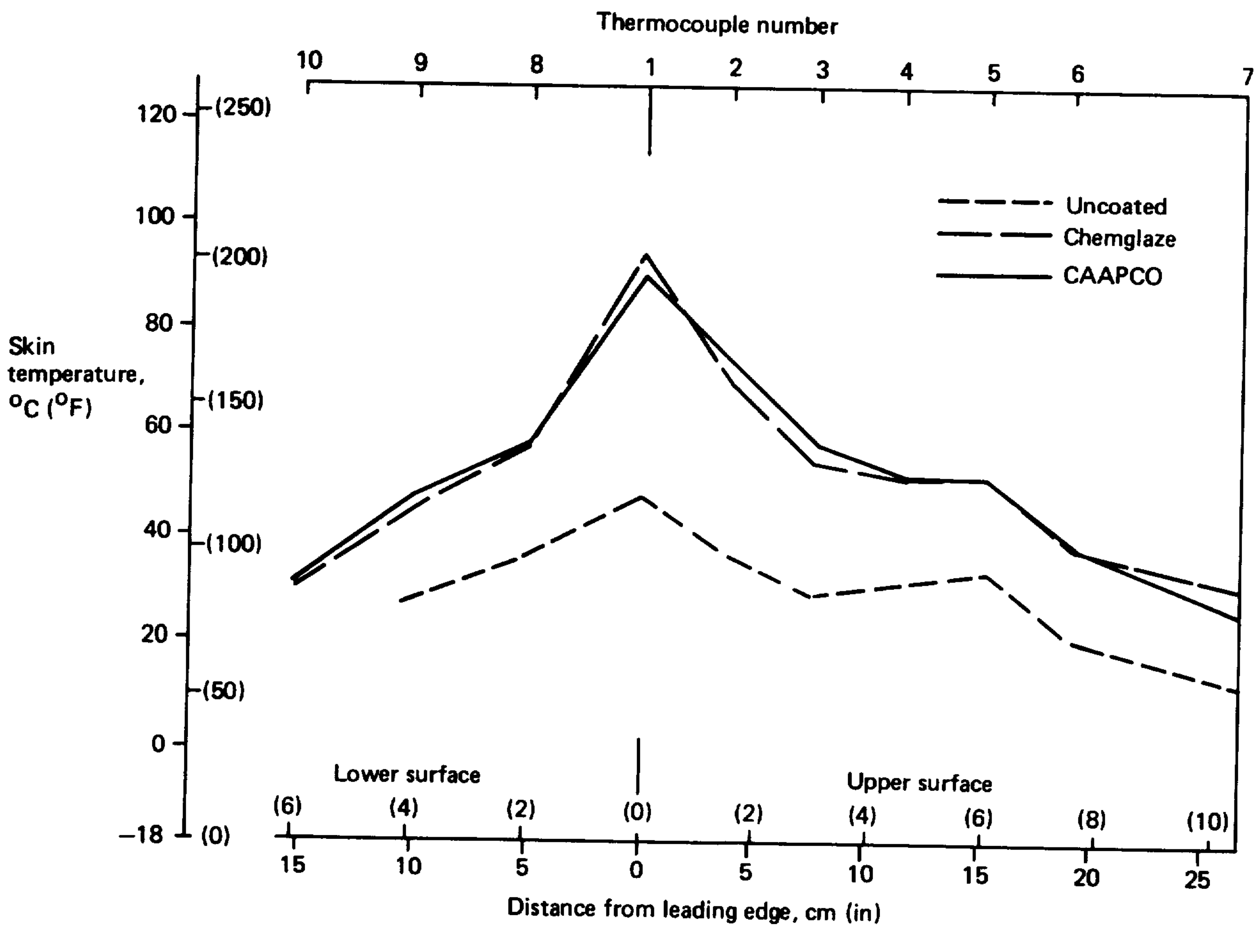

Figure 43. Skin Temperature Profile—Intermittent Maximum Icing

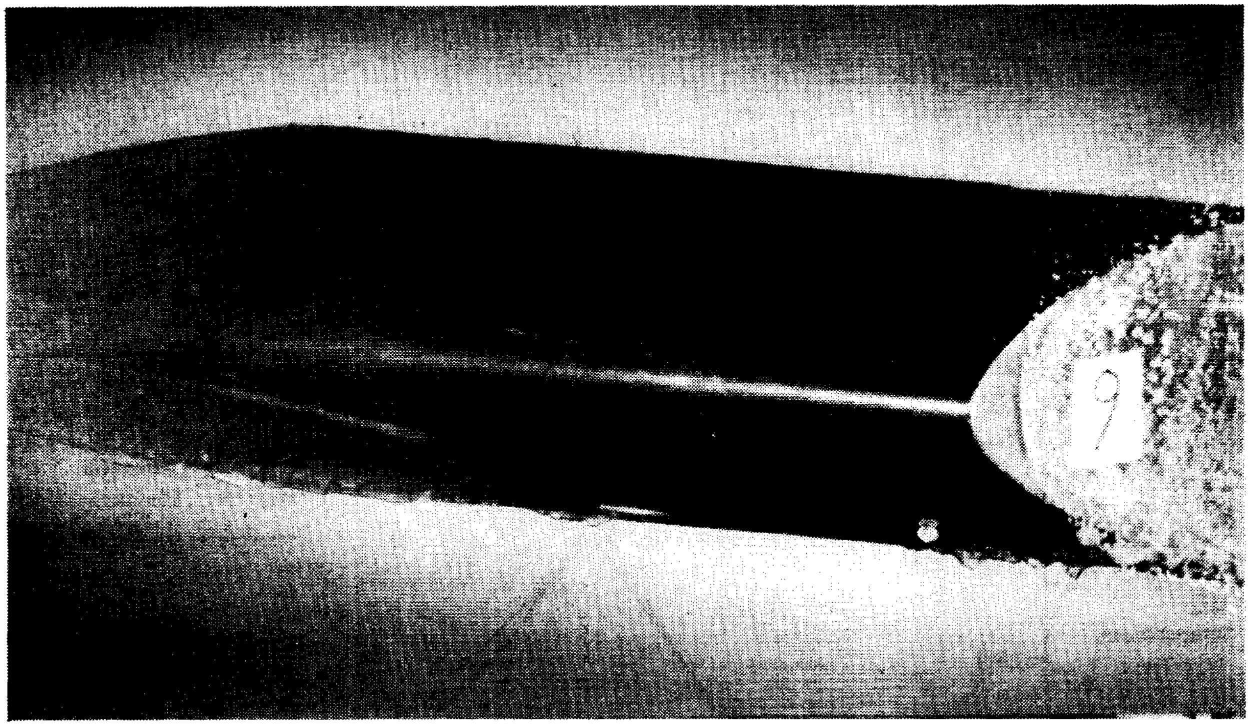

(a) CAAPCO Coating

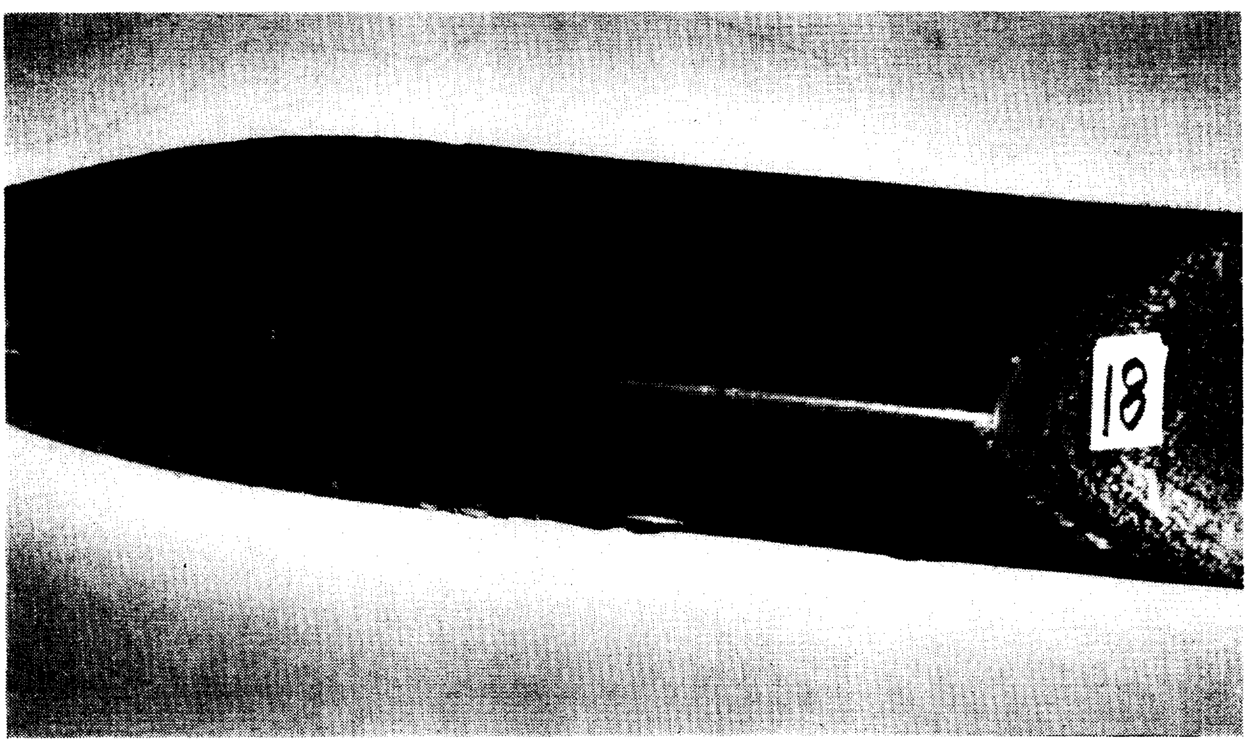

(b) Chemglaze Coating

Figure 44. Coated Model After IMI Runs at 100% TAI Flow Rate

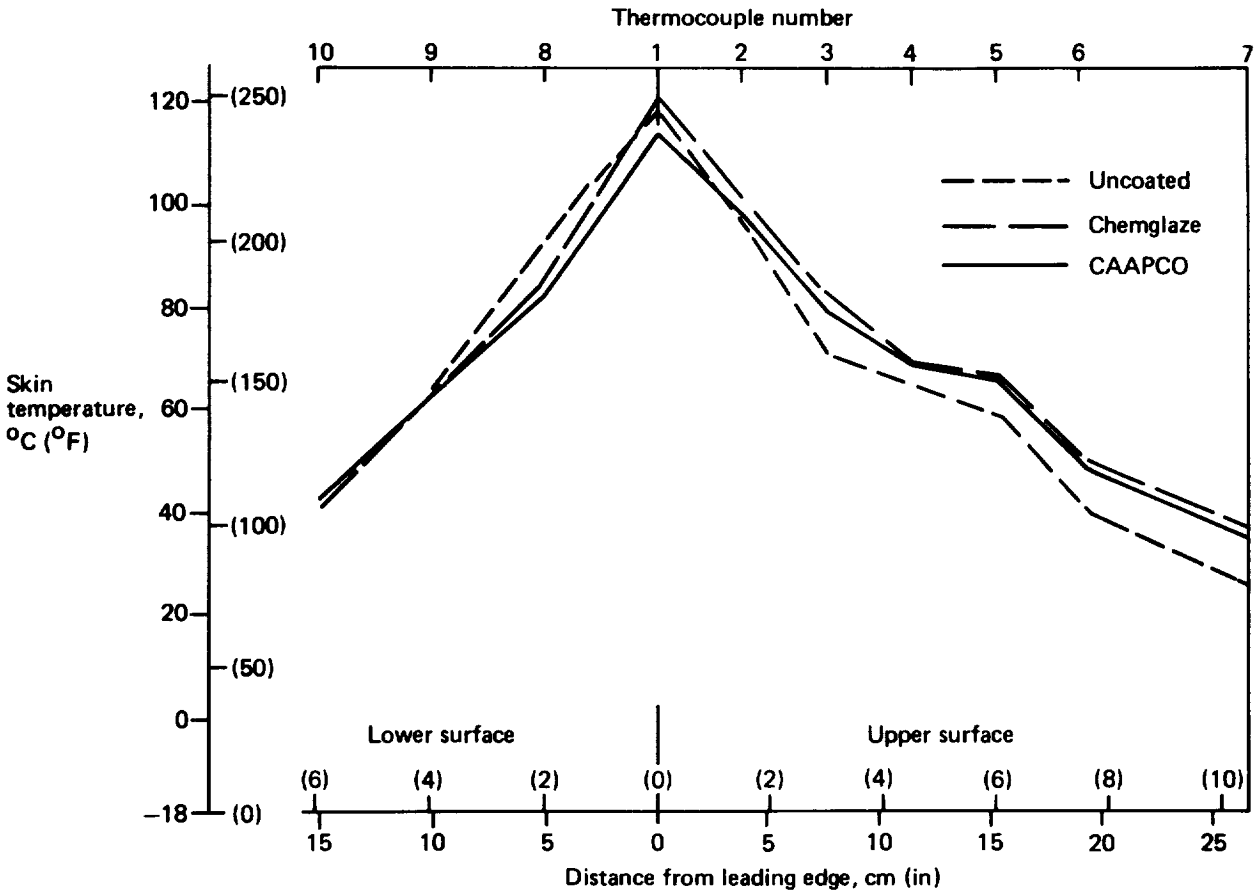

Figure 45. Skin Temperature Profile—Dry Air

ice being shed from the surface would tend to pit, tear, or otherwise degrade the coating. As an adjunct to the test, an icephobic silicone compound was applied to the outboard half of the model over the Chemglaze. Figure 46 shows the model installed in the tunnel, prior to the deicing test. The area to the right of the midspan line has the silicone material applied over the Chemglaze.

Five deicing cycles were run during the test. In each cycle, ice was allowed to build up along the leading edge (fig. 47a) and then the TAI system was activated until all leading-edge ice was dissipated. Figures 47b and 47c show progressive stages of ice dissipation. Ice was removed from the silicone-coated portion in 30 to 45 seconds of TAI operation, whereas the remaining area required 2 to 2.5 minutes. Water runback from the melted leading-edge ice resolidified near the aft end of the Chemglaze area and through the five cycles built up to in excess of 13 mm (0.5 in) before being dislodged by the airstream. No ice reformed near the aft end of the silicone-treated area. The contrast between the two areas is apparent in Figure 47c.

At the end of the deicing test, which totaled about 25 minutes of tunnel operation, neither the Chemglaze coating nor the silicone overcoat showed loss or degradation. Comments by the manufacturer material indicate that its erosion life is relatively short. Frequent reapplication probably would be required if the silicone were used as a jet transport leading-edge icephobic material.

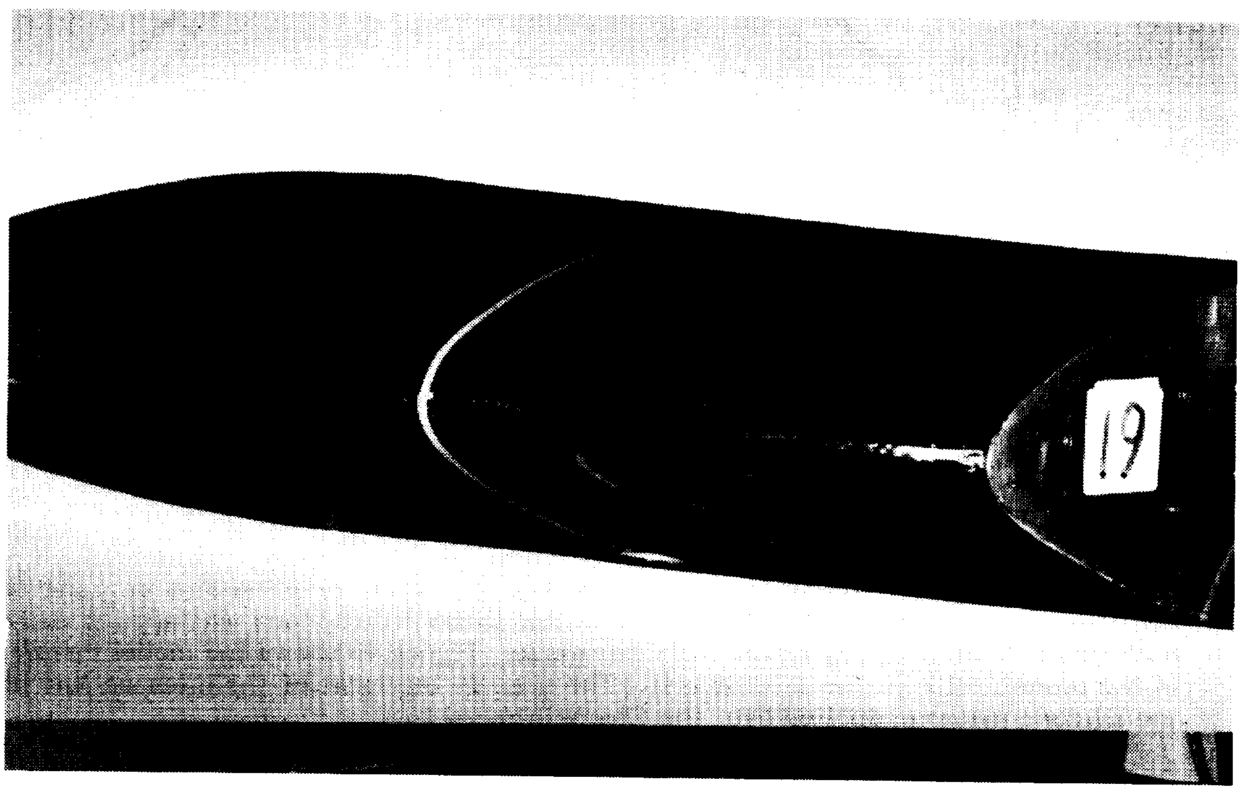

Figure 46. Coating Configuration for Deicing Test

(a) Leading-Edge Ice Prior to TAI-System Operation

(b) Ice Partially Dissipated by TAI Heat

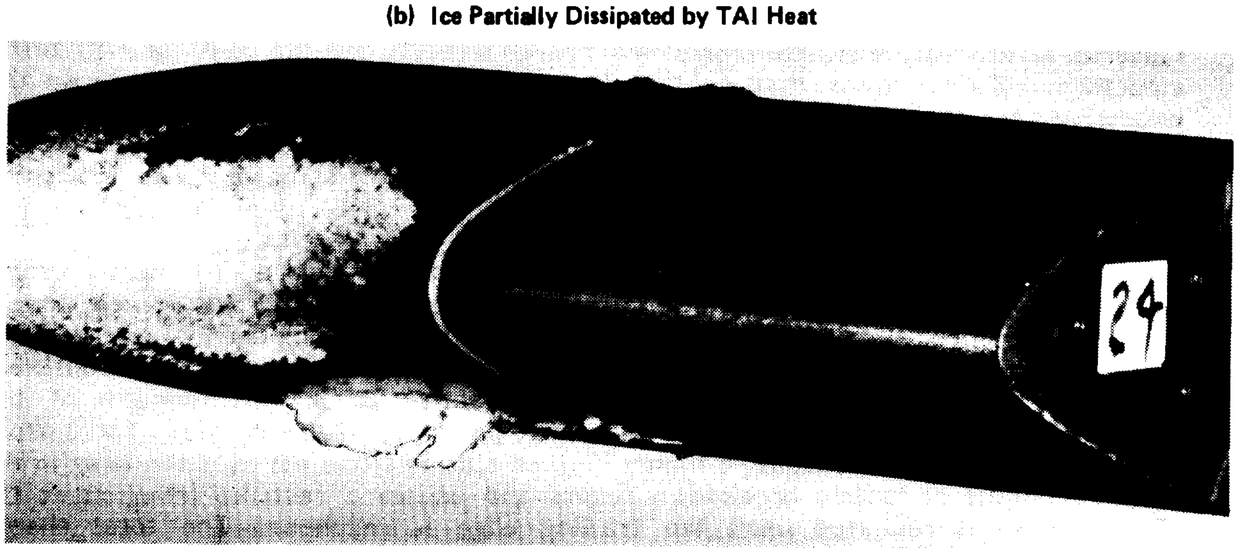

(c) Ice Gone From Silicone-Overcoated Area

Figure 47. Deicing Tests—Chemglaze Coating With Silicone on Right Half

4.3.1.4 Conclusions

The limited icing tests performed with CAAPCO and Chemglaze coatings indicated that:

- Thermal anti-icing systems, at normal temperature and airflow settings, would function satisfactorily in either the anti-icing or deicing mode with coated surfaces.

- The coatings showed no effects from exposure to the elevated temperatures of the TAI system.

- Ice shed from the model did not remove or otherwise degrade the coatings.

4.3.2 LIGHTNING AND PRECIPITATION STATIC ANALYSES

Investigations were made to evaluate the effects of coatings on atmospheric electrical charge dissipation. The lightning-strike investigation was limited to analysis of a typical transport (B737) to illustrate the method used to assess configuration-oriented areas of concern. The precipitation static (P-static) investigation included both test and analysis. P-static results were not configuration sensitive.

4.3.2.1 Lightning Analysis

Various areas of a jet transport are classified in three zones for lightning analyses (fig. 48). Zone 1 areas are those most susceptible to initial strike attachment. They include the tips of wing and tail surfaces, the body nose radome, and the inlet cowls of nacelles. Zone 2 areas are aft of zone 1 areas and have a high probability of swept stroke reattachment. The fuselage, nacelles aft of the nose cowl, and wing areas adjacent to wing-mounted nacelles are in zone 2. The remaining areas are in zone 3 and have a low probability of lightning arc attachment.

Zone 2 areas contain primary structure and are the focus of lightning hazard analyses. The objective of the analyses is to determine if there is enough conducting material to dissipate a typical worst case charge without causing melt-through in the structure. Zone 2 areas that contain fuel are of particular interest because the excessive heat accompanying melt-through could ignite fuel vapors. If the wing area immediately behind the wing-mounted engines contains fuel, it becomes critical for a hazard analysis. None of the zone 1 areas contain primary structure and, therefore, are not areas of special concern.

The lightning phenomena that take place are illustrated in Figure 49. The waveform is divided into four components. The initial stroke (component A) occurs in a zone 1 area, such as a nacelle nose cowl. The terminus of the lightning channel continues to move aft into zone 2 until a dielectric surface (coated wing surface) is encountered. When the potential gradient exceeds the dielectric breakdown strength of the coating, the channel attaches to the aluminum substrate where it dwells for a short period. During the dwell time, a highly ionized plasma flows aft over the wing in the airstream until dielectric breakdown recurs and causes a restrike (component D). This process is repeated until the trailing edge is reached. The total charge transferred during the restrike phenomenon is the sum of the charges in components B, C, and D:

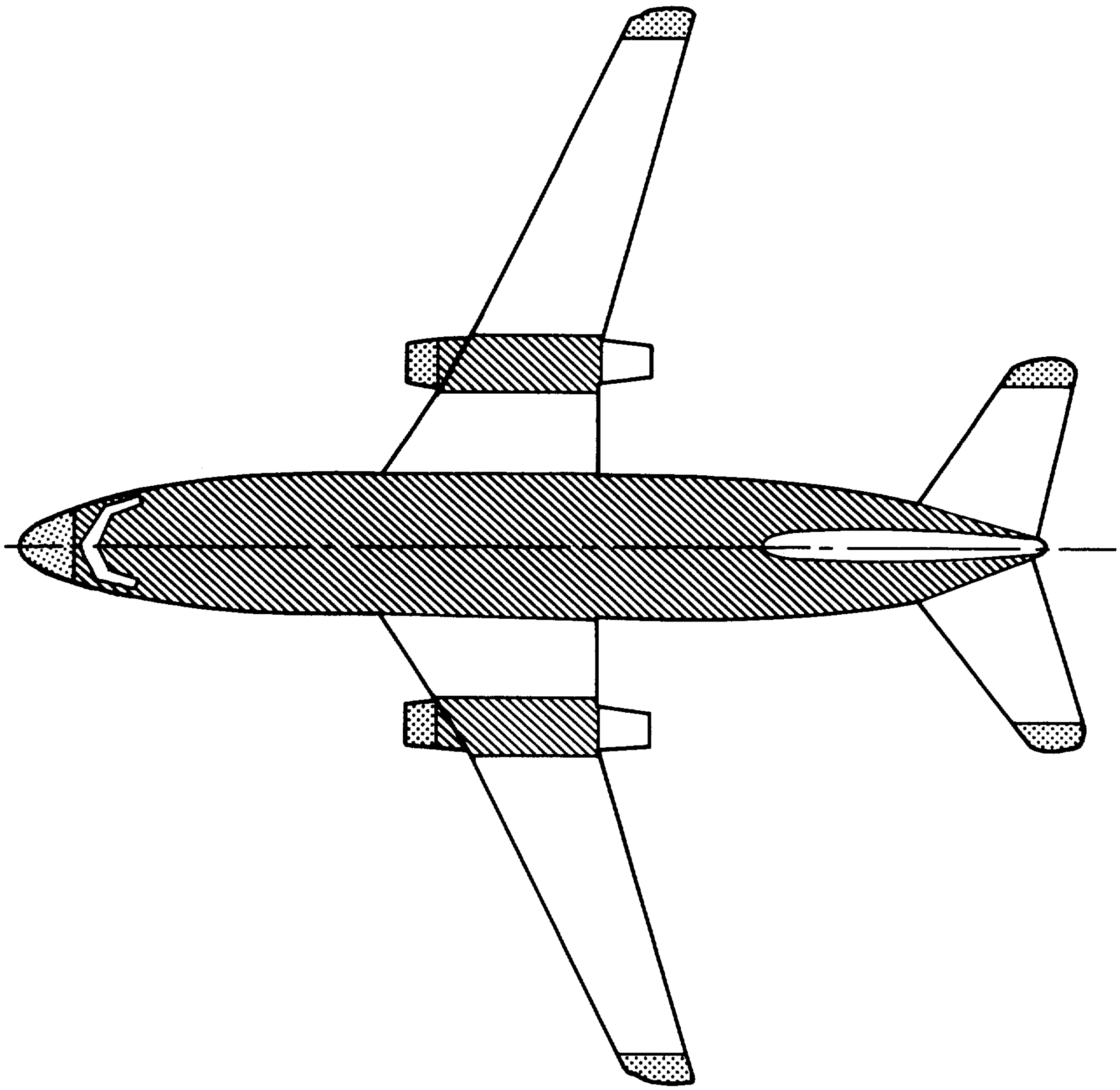

	Zone 1	Initial attachment point with probability of flash hang-on.
	Zone 2	High probability of swept stroke reattachment from zone 1.
	Zone 3	Low probability of lightning arc attachment.

Figure 48. Lightning Zones on Aircraft

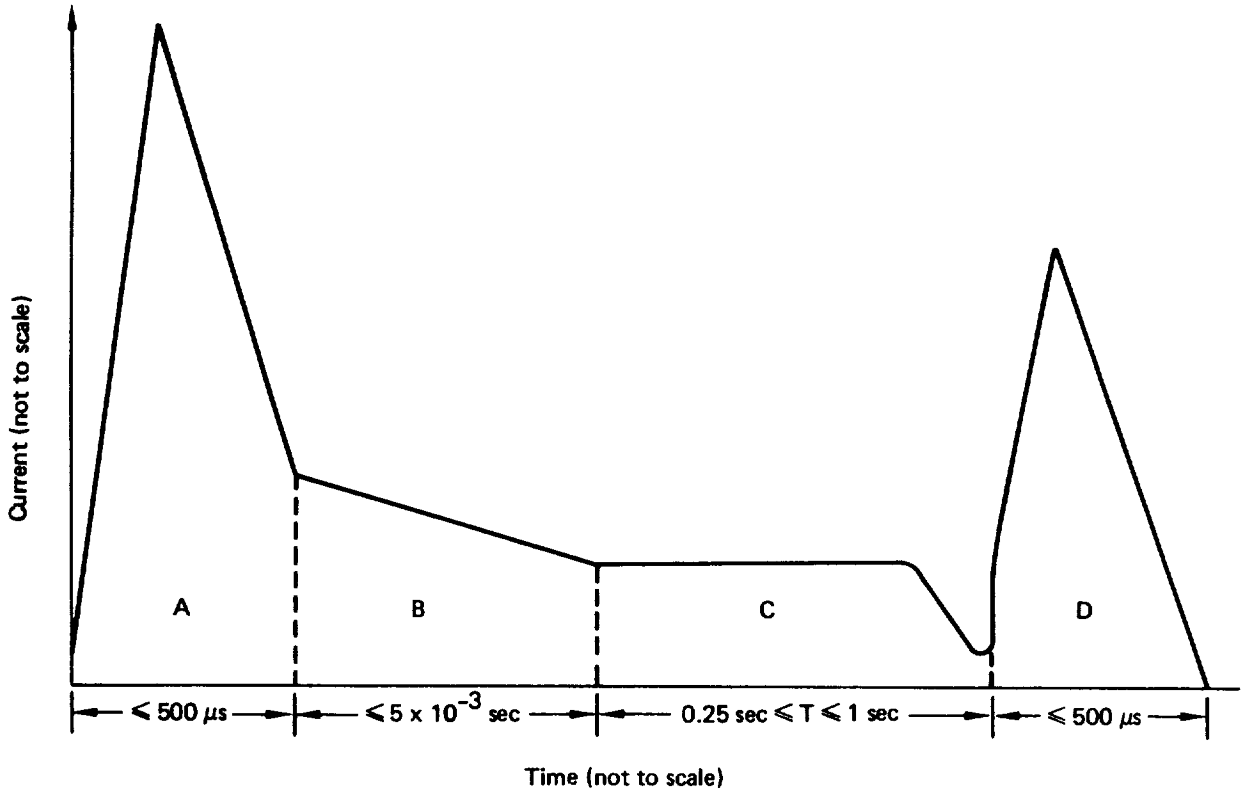

Component	Current
A (initial stroke)	200 kA ±10% peak
B (intermediate current)	2 kA ±10% average
C (continuing current)	0.2 to 0.8 kA
D (restrike)	100 kA ±10% peak

Figure 49. Lightning Simulation Test Waveform

$$Q_T = Q_B + Q_C + Q_D$$

Where Q_T = total charge in coulombs

Q_B = (average current) x time (ref. fig. 49)

Q_C = (maximum current) x T_D

Where T_D = dwell time = $\frac{S_D}{V_A}$

and S_D = distance between spars (m)

V = aircraft velocity (m/s)

$$Q_D = \frac{2\text{ (action integral)}}{\text{peak current}}$$

Using the B737 as an example in a worst case situation, the total restrike charge transfer at the nacelle wing station would be:

$$Q_B = 2\text{ kA} \times 0.5 \text{ s} = 10C$$

$$Q_C = 800A \times \frac{2.11m}{62.34 \text{ m/s}} = 27C$$

$$Q_D = \frac{2\,(0.25 \times 10^6 A^2 s)}{100 \text{ k A}} = 5C$$

$$Q_T = Q_B + Q_C + Q_D = 10 + 27 + 5 = 42C$$

Figure 50 shows the minimum charge transfer for melt-through versus skin thickness. The B737 example previously discussed falls in the questionable region, and

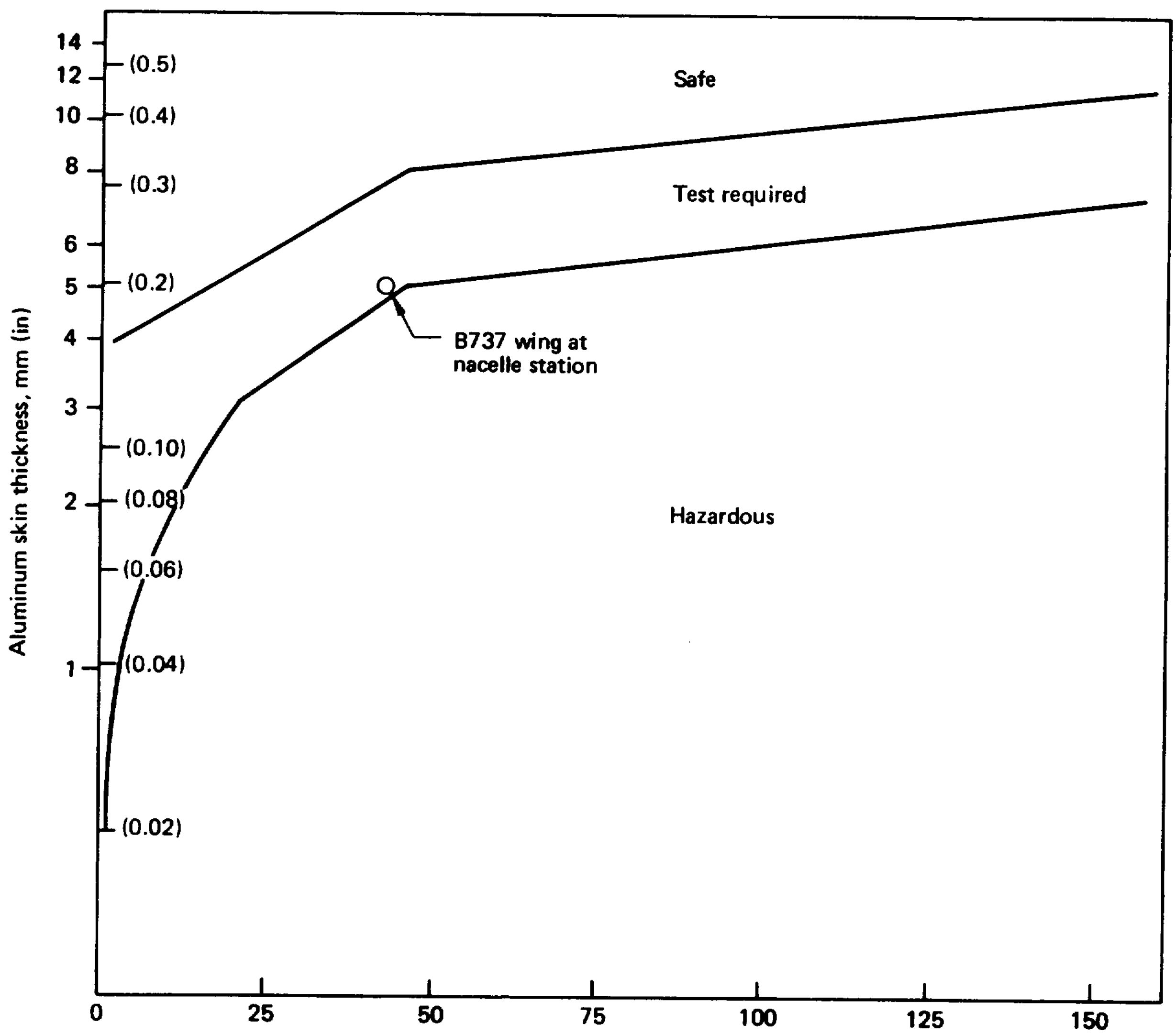

Figure 50. Minimum Charge Transfer for Melt-Through

simulated lightning tests should be performed on a full-scale model before applying a dielectric coating to the inspar surface above the nacelle. If tests show that a potentially hazardous condition would be created, then the coating should be omitted from the inspar area adjacent to the nacelle or, if possible, a conductive material should be added to the coating in that area to reduce its dielectric strength.

4.3.2.2 P-Static Analyses

P-static tests were conducted during the first phase of the surface coatings program, prior to the first flight service evaluation of CAAPCO and Chemglaze. The purpose of the tests was to clear the materials for P-static interference when applied to wing and horizontal tail leading edges only. Test results are reported in Reference 1.

Test results were reviewed relative to an extension of the coating applications back to the rear spar of wing and tail surfaces. The coating configuration analyzed consisted of a 12-mil application of CAAPCO, Chemglaze, or Astrocoat at the leading edge, tapering to 5 mil at the front spar; the surface between front and rear spars was dual-coated with 3 to 4 mil of the elastomer and a 1- to 2-mil topcoat of polyurethane enamel for Skydrol protection. The analysis showed that coating configuration would produce no P-static interference with communication or navigation equipment aboard an airplane.

4.3.2.3 Conclusions

The following conclusions were reached as a result of the lightning and P-static analyses:

- Airplanes with wing fuel in the immediate vicinity of wing-mounted engines should be analyzed for lightning-strike effects when a dielectric coating is applied.

- The example analysis of a B737 wing at the nacelle station showed that a dielectric coating in that area would produce marginally safe conditions when exposed to lightning strike. Lightning tests should be performed on a full-scale model to determine if safety would be compromised.

- If an unsafe area is identified, the coating should be omitted from that immediate area or a conductive material should be added to the coating.

- CAAPCO, Chemglaze, or Astrocoat applied from the leading edge to rear spar of wing and tail surfaces will not cause P-static interference with communication and navigation equipment.

4.3.3 EROSION RESISTANCE

Two series of tests were conducted to investigate: (1) coating durability as a function of coating thickness and (2) the erosion protection afforded to nonmetallic leading edges by coatings.

Both test series included rain erosion testing in the AFML whirling-arm facility at Wright-Patterson Air Force Base, Ohio. Test velocity was 224 m/s (500 mi/h), rainfall rate was 2.54 cm/h (1 in/h), and drop size was 1.8 mm (0.071 in). The second test series, on nonmetallic substrates, included coating-adhesion and peel tests.

4.3.3.1 Optimum Coating Thickness

Much of the rain erosion testing conducted in this study and elsewhere was done on 12-mil-thick coatings. Because coating thickness affects airplane weight and application costs, it was of interest to determine the minimum coating thickness that could be applied without sacrificing durability.

Test Description—To find optimum coating thickness, tests were run on aluminum substrate specimens with coatings of CAAPCO, Chemglaze, and Astrocoat ranging in thickness from 4 mil to 21 mil. Prior to coating, the specimens were grit blasted, alodined, and primed with 0.7 to 1.0 mil of BMS 10-79 epoxy primer. After coating, the specimens were allowed to cure a minimum of 7 days at room temperature.

Specimens were run in pairs, with a specimen mounted at either end of the whirling arm. Runs generally were terminated when deterioration of one of the specimens was observed through the closed-circuit TV monitor. There were a few exceptions to this rule, however, as can be seen in Table 4. If neither specimen showed deterioration within 180 minutes run time, the test was terminated and the coatings were considered very durable.

Test Results—Table 4 summarizes test results. Test time to initial coating failure, percentage of the coated surface affected (percentage of area failed), and mode of failure are noted. The results observed for each coating are discussed below.

CAAPCO B-274. All specimens had a smooth, glossy surface. Typical mode of failure was a single pit in the coating, exposing the primer or substrate, as shown in Figure 51a. The 5-mil coating lost one 5-mm (0.2-in) piece, exposing the substrate, and two smaller pits, exposing the primer. Scuffing or loss of coating, visible at the ends of most specimens, was due to end clamps that held the specimens in the test fixture.

The two 9-mil specimens shown in Figure 51a ran the full 180 minutes without apparent damage. One of the two 20-mil specimens lost a 5-mm (0.2-in) piece after 115 minutes of testing. The other specimen of the pair remained in good condition.

CAAPCO coatings also were tested at thicknesses of 12, 17, and 18 mil. One of the 12-mil specimens lost a single piece about 3 by 5 mm (0.12 by 0.20 in) after 127 minutes of testing; the other remained in good condition. The single 17-mil specimen (tested with the 5-mil Astrocoat specimen) had minor damage after 90 minutes testing. The 18-mil specimens each had a single piece removed after 79 minutes testing, exposing the primer or substrate.

Chemglaze M313. All specimens had a smooth, glossy surface. The most prevalent mode of failure was loss of patches of coating that did not expose either the primer or substrate. The only exceptions were the 4-mil specimens and one of the 17-mil specimens, which were each pitted down to the primer in one place.

Results of the 4-, 9-, and 20-mil tests are shown in Figure 51b. The 4-mil test was terminated at 131 minutes when several small patches of coating were lost. The 9-mil coatings were in generally good condition after 180 minutes, except for one area of partial coating loss about 2 by 4 mm (0.08 by 0.16 in) on one of the specimens. When the 20-mil tests were terminated at 180 minutes, both specimens had lost sizable patches of coating.

Table 4. Rain Erosion Test Results (Aluminum Substrate)

COATING	THICKNESS, mil	TEST TIME, min	AREA FAILED, %	FAILURE MODE
CAAPCO	5	43	10	Coating smooth and glossy Single piece removed to primer
		105	25	Coating smooth and glossy Several pieces removed to primer or substrate (fig. 51a)
	9	180	0	No damage
		180	0	No damage (fig. 51a)
	12	127	0	No damage
		127	5	Single piece removed to substrate
	17	90	5	Several minute pits Primer not exposed
	18	79	10	Single piece removed to substrate
		79	10	Single piece removed to primer
	20	115	15	Single piece removed to primer
		115	0	No damage (fig. 51a)
Chemglaze	4	131	25	Coating smooth and glossy Several pits One pit to primer
		131	10	Coating smooth and glossy Several pits One pit to primer (fig. 51b)
	7	180	10	Several pieces removed–no primer showing
		180	15	Several pieces removed–no primer showing
	9	180	5	Single small pit–no primer showing
		180	0	No damage (fig. 51b)
	17	150	0	No damage
		150	10	Single piece removed to primer
	20	180	10	Two pieces removed–no primer showing
		180	30	Several pieces removed–no primer showing (fig. 51b)
Astrocoat	5	90	5	Surface pitting Single small pit removed to primer (fig. 51c)
	8	186	25	Erosion failure–pieces removed to primer
		186	25	Erosion failure–pieces removed to primer (fig. 51c)
	17	150	0	No damage
		150	10	Coating peeled through delamination beyond normal erosion area Primer not exposed Origin of peeling probably from single pit down to primer
	21	150	40	Coating peeled through delamination beyond normal erosion area Primer not exposed Several pits in erosion area down to primer
		95	40	Same as above (fig. 51c)

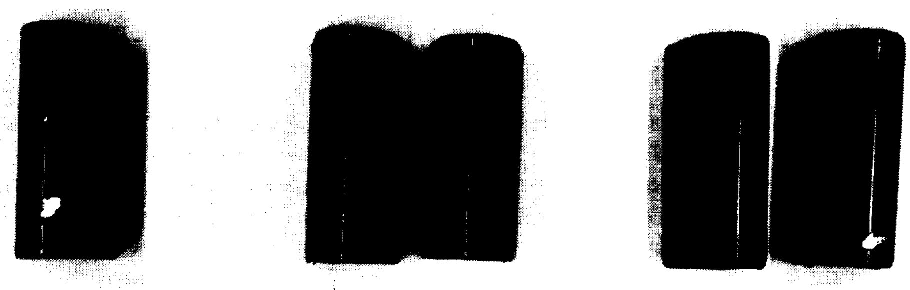

5 mil
105 min

9 mil
180 min

20 mil
115 min

CM
0 1 2 3 4 5 6 7 8 9 10

(a) CAAPCO B-274

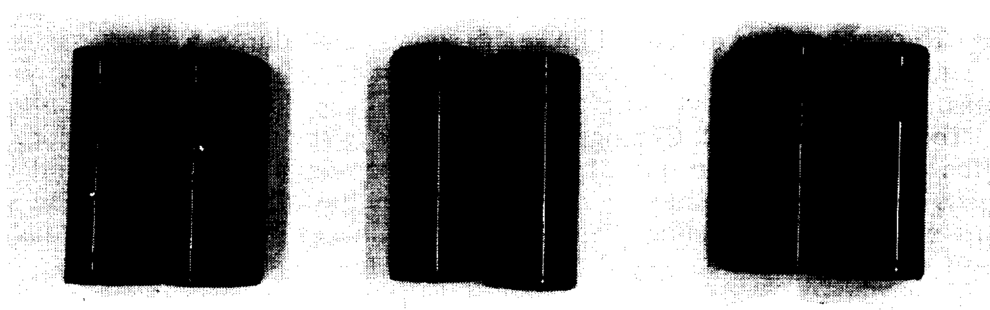

4 mil
131 min

9 mil
180 min

20 mil
180 min

CM
0 1 2 3 4 5 6 7 8 9 10

(b) Chemglaze M313

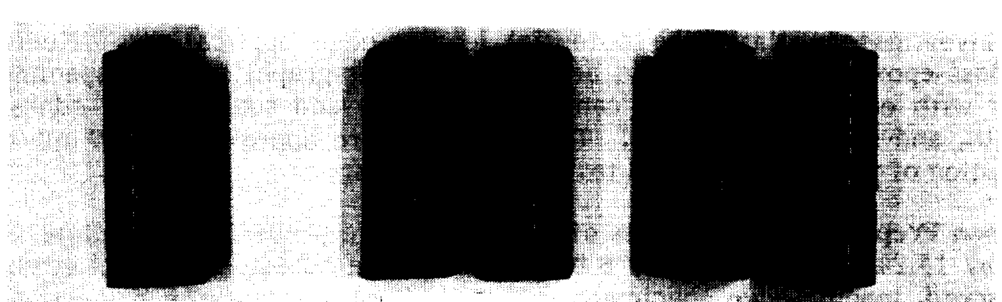

5 mil
90 min

8 mil
186 min

21 mil
150 min

CM
0 1 2 3 4 5 6 7 8 9 10

(c) Astrocoat Type I

Figure 51. Rain Erosion Specimens Tested at Various Coating Thicknesses (Aluminum Substrate)

The 7-mil specimens had several patches of coating missing after 180 minutes, and one specimen had several very small pits. In no place was the primer exposed. Testing of 17-mil specimens was terminated at 150 minutes when a large patch of coating was lost from one of the two specimens. The other specimen was in good condition.

Astrocoat Type I. All specimens had a glossy, orange peel surface. Four thicknesses of coatings were tested, three of which are shown in Figure 51c. The 5-mil specimen had a single pit that exposed the primer after 90 minutes and several minute surface pits visible under a magnifying glass. The 8-mil specimens were allowed to run 186 minutes, at which time they had several small coating pits; the primer was exposed in two places on each specimen. The 21-mil specimens had several pitted areas along the leading edge, the deepest of which exposed the primer and appeared to be the origin of large coating delamination patches that extended nearly to the trailing edge.

A pair of 17-mil specimens was tested 150 minutes before a leading-edge pit occurred in one specimen, causing a narrow strip of the coating outer layer to peel back to the trailing edge. The other specimen was in good condition.

Coating Thickness, Conclusions—Figure 52 shows test duration to time of coating initial failure as a function of coating thickness. Coatings tested in the 7- to 9-mil thickness range were in the best condition after the full 180-minute allotted test time. The CAAPCO and Chemglaze specimens were in good condition, with the exception of a single pit in one of the Chemglaze specimens. The 8-mil Astrocoat specimens were the only ones to run longer than the allotted time. The specimens were pitted along the leading edge after 186 minutes testing, and it can only be presumed that they were damaged during the last few minutes of testing.

Coatings of 9-mil thickness in lieu of the previously recommended 12 mil for areas of high erosion would reduce airplane weight by a few kilograms and would reduce application time and cost.

4.3.3.2 Nonmetallic Leading Edges

Several fiber-epoxy materials have been developed for aircraft application to reduce weight and, eventually, to reduce cost. The characteristics of four of these materials were investigated relative to potential leading-edge applications. Kevlar-epoxy, fiberglass-epoxy, graphite-epoxy, and hybrid Kevlar-graphite-epoxy specimens were coated with each of the three candidate coatings and subjected to adhesion, peel strength, and rain erosion tests. The coatings were approximately 9 mil thick. A description of the specimens and test results follows.

Specimen Preparation—Two types of specimens were prepared: flat plate specimens 10.16 by 15.24 by 0.32 cm (4 by 6 by 1/8 in) for the adhesion and peel strength tests and curved, leading-edge specimens 6.1 cm (2.4 in) long for the rain erosion tests. Figure 53 shows curved specimens of each of the four substrates. The materials used were:

Graphite	Specification	BMS 8-212 Type II, class 1 Grade 190 (0.0074) Prepreg tape

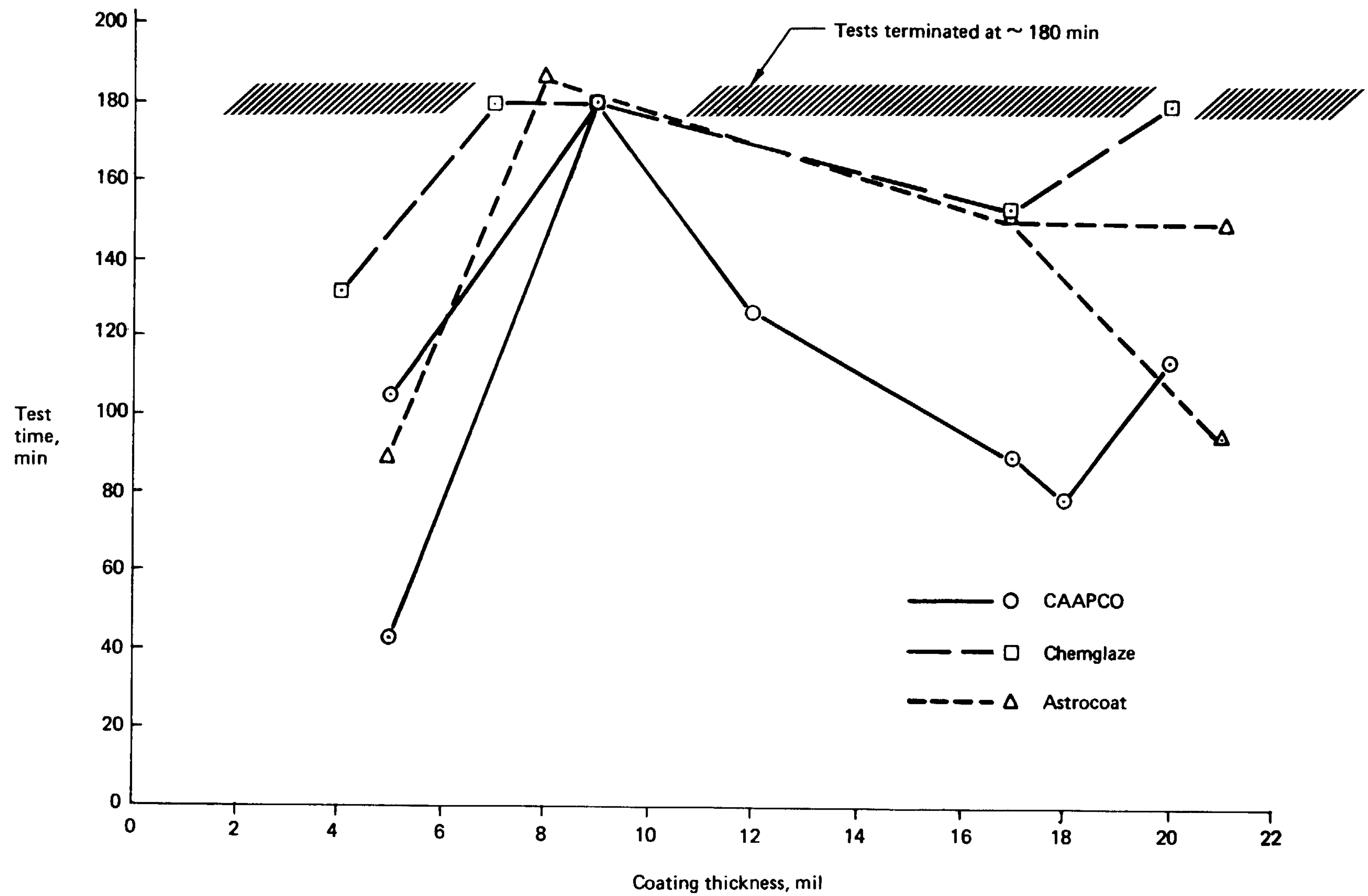

Figure 52. Effect of Coating Thickness on Erosion Durability

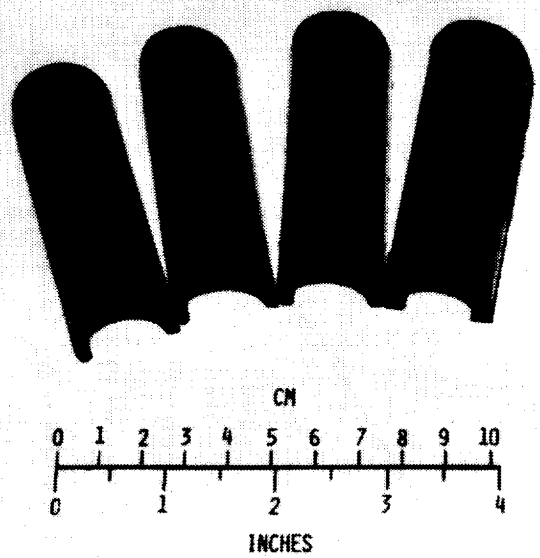

Figure 53. Rain Erosion Tests—Nonmetallic Leading-Edge Specimens

Fiberglass	Specification	BMS 8-139A Type 181 Style 1581 (0.008 to 0.012) Fabric
Kevlar	Specification	BMS 8-218 Style 285 Crowfoot weave 1140 denier Fabric

Specimens were fabricated of multiple layers of fabric (or tape) with alternating ± 45-deg orientation. The hybrid specimens were built up of alternating layers of graphite and Kevlar, with a top layer of Kevlar. Following layup, all specimens were cured in an autoclave at 177°C (350°F) and 586 kPa (85 lbf/in^2). After curing, the specimens were prepared for coating by the following procedure:

1. Clean with Toluene, MEK, or MIBK solvent.
2. Abrade manually with 150 or finer grit abrasive.
3. Repeat step 1.
4. Apply static conditioner filler (pinhole filler).
5. Apply laminar surfacer.
6. Apply BMS 10-21 type I conductive coating.
7. Apply BMS 10-79 type II epoxy primer.
8. Apply 9-mil elastomeric polyurethane coating (CAAPCO B-274, Chemglaze M313, or Astrocoat Type I).
9. Cure a minimum of 7 days.

Adhesion Tests—Dry and wet adhesion tests were performed on coated flat plate specimens per FTMS 141, method 6301. In both tests, a series of parallel lines are

Table 5. Adhesion Test Results

SUBSTRATE	ADHESION TEST	COATING: CAAPCO B-274	COATING: CHEMGLAZE M313	COATING: ASTROCOAT TYPE II
Graphite	Dry Wet	Pass Pass (few blisters)	Pass Pass	One pass[a], one fail[b] Fail[a]
Fiberglass	Dry Wet	Pass Pass (few blisters)	Pass Pass	Pass Fail (blisters)[b]
Kevlar	Dry Wet	Pass Pass (few blisters)	Pass Pass	Pass Fail
Kevlar-graphite (hybrid)	Dry Wet	Pass Pass (few blisters)	Pass Pass	Pass Fail

[a]Adhesion failure at coating-primer surface.
[b]Few small blisters.

scribed down to the substrate through the coating. A second series of lines are then scribed diagonally to the first series to form a grid of diamond-shaped coating patches. (In the wet adhesion tests, this is done after the specimens have been immersed in distilled water at room temperature for 7 days.) A strip of 2.54-cm (1-in) 3M 250 tape is applied to the coated surface with a minimum pressure of 34.5 kPa (5 lbf/in^2) and removed within 5 minutes with an abrupt motion 90 deg to the surface. If coating patches adhere to the tape, the coating fails the adhesion test.

Results of the adhesion tests are presented in Table 5. CAAPCO and Chemglaze coatings passed both dry and wet adhesion tests on the four substrate materials. A few small blisters were observed in the CAAPCO wet adhesion specimens, however, they did not cause adhesion failure. The Astrocoat exhibited poor wet adhesion and all of the four substrate specimens failed this test. Adhesion of Astrocoat to graphite in the dry tests also was marginal, and one of the two specimens failed.

Adhesion of the coatings to these fiber-epoxy substrates might be improved with modified surface preparation procedures, however, the scope of work in this instance did not permit such experimentation to take place.

Peel Tests—Tests were performed on flat plate specimens to determine the peel strength of the coatings on the four substrate materials. Parallel cuts to the substrate were scribed through the coatings 2.54 cm (1 in) apart per ASTM D903. The edge of the scribed strip was clamped in jaws that pulled 90 deg to the surface at a rate of 5.08 cm/min (2 in/min). A scale attached to the jaws measured pull force.

Test results are shown in Table 6. Adhesion of the CAAPCO coatings was so great that a free tab to initiate the test could not be produced. The peel strength of Chemglaze averaged about 1.11 kg/cm (6.25 lb/in) for all specimens, with only a $\pm$4% variation between substrates. The average peel strength of Astrocoat specimens was 0.65 kg/cm (3.64 lb/in), with about $\pm$5% variation between substrates. In all cases, the release face was between the coating and primer.

Early in the Surface Coatings program, a peel strength goal of 1.85 kg/cm (10 lb/in) was set for coatings in areas of high erosion and 0.56 kg/cm (3 lb/in) for coatings in

Table 6. Peel Test Results

SUBSTRATE	COATING		
	CAAPCO B-274	CHEMGLAZE M313, kg/cm (lb/in)	ASTROCOAT TYPE I, kg/cm (lb/in)
Graphite	Unable to start peel	1.05 (5.9) 1.07 (6.0)	0.62 (3.5) 0.75 (4.2)
Fiberglass	Unable to start peel	1.16 (6.5)	0.68 (3.8)
Kevlar	Unable to start peel	1.09 (6.1) 1.07 (6.0)	0.48 (2.7) 0.77 (4.3)
Kevlar-graphite (hybrid)	Unable to start peel	1.00 (5.6) 1.32 (7.4)	0.61 (3.4) 0.64 (3.6)

low erosion areas (ref. 1). Subsequent testing with aluminum substrates indicated that coatings with about 0.89 kg/cm (5 lb/in) peel strength would be satisfactory in areas of high erosion.

Rain Erosion Tests—Specimens were tested in pairs and run until failure of either one or both specimens occurred. Each of the substrate materials is discussed individually with the effect of coating systems. Test results are summarized in Table 7. Figure 54 compares bare specimens before and after testing and shows the best coating (after test) with each substrate material.

Graphite. Graphite performed the best of the uncoated specimens, enduring 12.8 minutes of rain erosion testing. The next best uncoated specimen (fiberglass) lasted only 8.9 minutes. Even at the failure point, the extent of damage was not as serious as with the other uncoated specimens.

Each of the coated graphite specimens endured for approximately the same length of time (about 40 minutes), but both CAAPCO and Chemglaze failed because of adhesion loss and Astrocoat failed because of erosion.

Fiberglass. The uncoated fiberglass specimens eroded through the outer ply in 8.9 minutes. With the CAAPCO coating, erosion life was increased tenfold to 90.2 minutes. This combination exceeded the durability of any of the other coated specimens by a factor greater than two. The failure mode was loss of adhesion.

The Chemglaze coating failed in adhesion after 38.4 minutes of testing, and Astrocoat failed through erosion after 35.6 minutes.

Kevlar. Uncoated Kevlar had virtually no rain erosion resistance, and it began to fail immediately upon exposure. Within 1.4 minutes, serious failure occurred: Individual strands were severed, destroying the cross-weaved structure of the outer ply. Kevlar coated with CAAPCO increased rain erosion resistance from 1.4 minutes to 16.8 minutes. The coating did not adhere very well to the substrate, causing failure by loss of adhesion (blistering), followed by intercoat adhesion failure between layers of the CAAPCO coating. Failure of the Chemglaze and Astrocoat specimens was initiated by failure of the substrate, which was shattered by rain impingement, followed by blistering and peeling of the coating. The Chemglaze and Astrocoat specimens lasted 32.4 and 24.5 minutes, respectively.

Table 7. Rain Erosion Test Results (Nonmetallic Substrate)

SUB-STRATE	COATING	AREA ERODED, %	TEST TIME, min	FAILURE MODE
Graphite	Uncoated	10 0	12.8 12.8	First ply eroded First ply damaged
	CAAPCO	5 0	39.5 39.5	Erosion-adhesion failure Adhesion damage: blistered over 5% of area
	Chemglaze	10 0	38.7 38.7	Adhesion failure: blistered over 60% of area Adhesion damage: blistered over 40% of area
	Astrocoat	10 10	43.1 43.1	Rain erosion failure Rain erosion failure
Fiberglass	Uncoated	90 95	8.9 8.9	Erosion failure First ply removed Erosion failure First ply removed
	CAAPCO	1 5	90.2 90.2	Adhesion failure: blistered over 10% of area Single, small rain-erosion pit through to substrate Adhesion failure: blistered over 15% of area Blister removed to primer in one small area (5%)
	Chemglaze	10 0	38.4 38.4	Adhesion failure: blister broken through to substrate Adhesion damage: blistered over 10% of area
	Astrocoat	15 15	35.6 35.6	Erosion failure: pitted through coating to substrate Erosion failure: pitted
Kevlar	Uncoated	100 100	1.4 1.4	Erosion failure: cut through first ply Failure began immediately Same as above
	CAAPCO	0 25	16.8 16.8	Adhesion damage: blistered over 25% of area Adhesion failure and intercoat-adhesion failure Blistered over 90% of area
	Chemglaze	1 5	32.4 32.4	Adhesion failure: blistered over 25% of area; one small pit through blister to substrate Substrate-adhesion failure: blistered over 75% of area
	Astrocoat	10 0	24.5 24.5	Substrate failure followed by adhesion failure Cut through blister and damaged first ply No damage
Kevlar-graphite (hybrid)	Uncoated	100 100	1.4 1.4	Cut through layer of Kevlar to layer of graphite Same as above
	CAAPCO	0 5	17.5 17.5	No damage Adhesion failure: blistered over 75% of area
	Chemglaze	0 5	34.4 34.4	No damage Substrate failure: blistered over 90% of area Kevlar punctured to graphite layer in small pit
	Astrocoat	0 10	32.1 32.1	Undamaged Adhesion-substrate failure: eroded through Kevlar layer to graphite layer; blistered over 55% of area

Test Conditions:

Velocity 224 m/s (500 mi/h)
Rain rate 2.54 cm/h (1 in/h)
Drop size 1.8 mm (0.056 in)

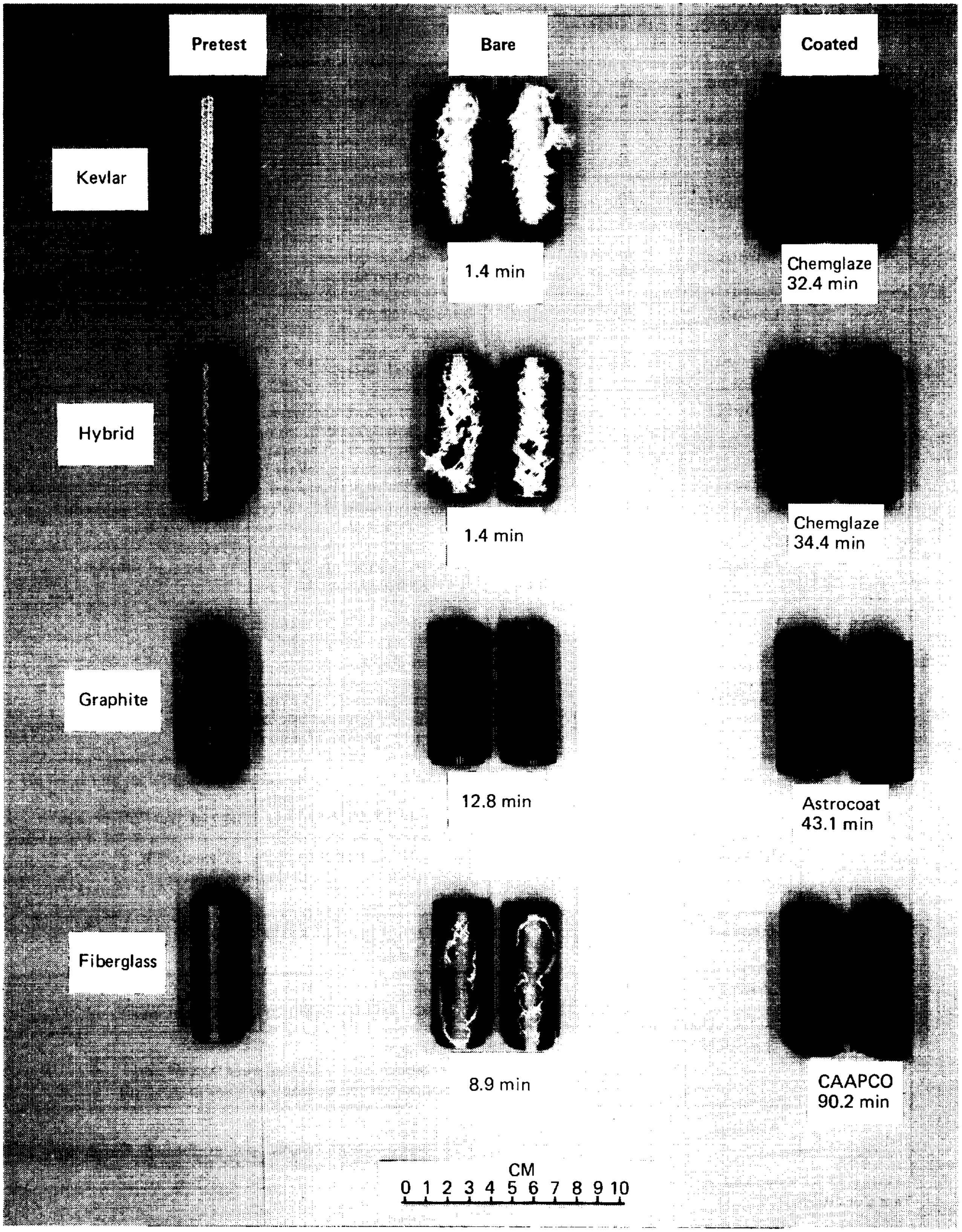

Figure 54. Comparison of Nonmetallic Rain Erosion Test Specimens

Hybrid. The hybrid composite tested was composed of alternating layers of graphite and Kevlar, with an outer layer of Kevlar. Because the outer layer was Kevlar, the net effect was to perform almost identically with the Kevlar specimens. Modes of failure and endurance times for each of these were similar to those for Kevlar; the only notable exception was an increase of about 8 minutes in the failure time for Astrocoat.

Nonmetallic Leading Edges, Conclusions—Neither Kevlar nor hybrid substrates are suitable for areas exposed to high-impact rain erosion. The structure of the coated and uncoated Kevlar and hybrid specimens is subject to rapid destruction in rain erosion environments. Although the coated graphite and fiberglass substrates are more durable, only the CAAPCO-fiberglass combination can be considered marginally acceptable for commercial jet transport leading-edge application. Perhaps modified application procedures, including use of a different primer, might eliminate the adhesion mode of failure and thereby greatly increase the durability of coated graphite or fiberglass leading edges.

4.3.4 CORROSION PROTECTION

The primary function of paint or coating systems applied to aircraft structure is to protect the structure from corrosion. Various paint and primer systems are in current usage on the load-bearing skins of the wing and empennage, between front and rear spars (inspar area). These systems provide good corrosion protection, except that they tend to fail at fastener heads or skin joints where there is some relative movement under stress cycling. It was thought that the elastomeric qualities of elastomeric polyurethanes could overcome this deficiency. If so, these materials could be used on inspar areas and the potential drag benefits discussed in Section 4.1 could be realized.

Salt-spray, filiform, and dynamic tests were conducted on coated 7075-T6 aluminum-alloy specimens (fig. 55) to obtain an initial evaluation of the corrosion protection capabilities of elastomeric polyurethanes. Test methods are described in Appendix C. Six coating systems were evaluated: Three elastomeric test coatings were compared to three control coatings that currently are used on commercial transports. The test coatings included CAAPCO, Chemglaze, and Astrocoat, each with an undercoat of epoxy primer and a topcoat of polyurethane enamel for protection from synthetic-type hydraulic fluid. The three control coatings included polyurethane enamel over a polysulfide primer, polyurethane enamel over an epoxy primer, and Corogard paint over an epoxy primer. The coating systems and test specimens are described in Appendix C.

After each test series, the specimens were visually examined and rated for corrosion density and distance of migration, according to the following system:

0 = no corrosion
1 = trace corrosion
2 = moderate corrosion
3 = medium corrosion
4 = excessive corrosion
5 = extremely heavy corrosion

4.3.4.1 Salt-Spray Tests

After the coatings on the salt-spray (and filiform) test specimens had cured for 7

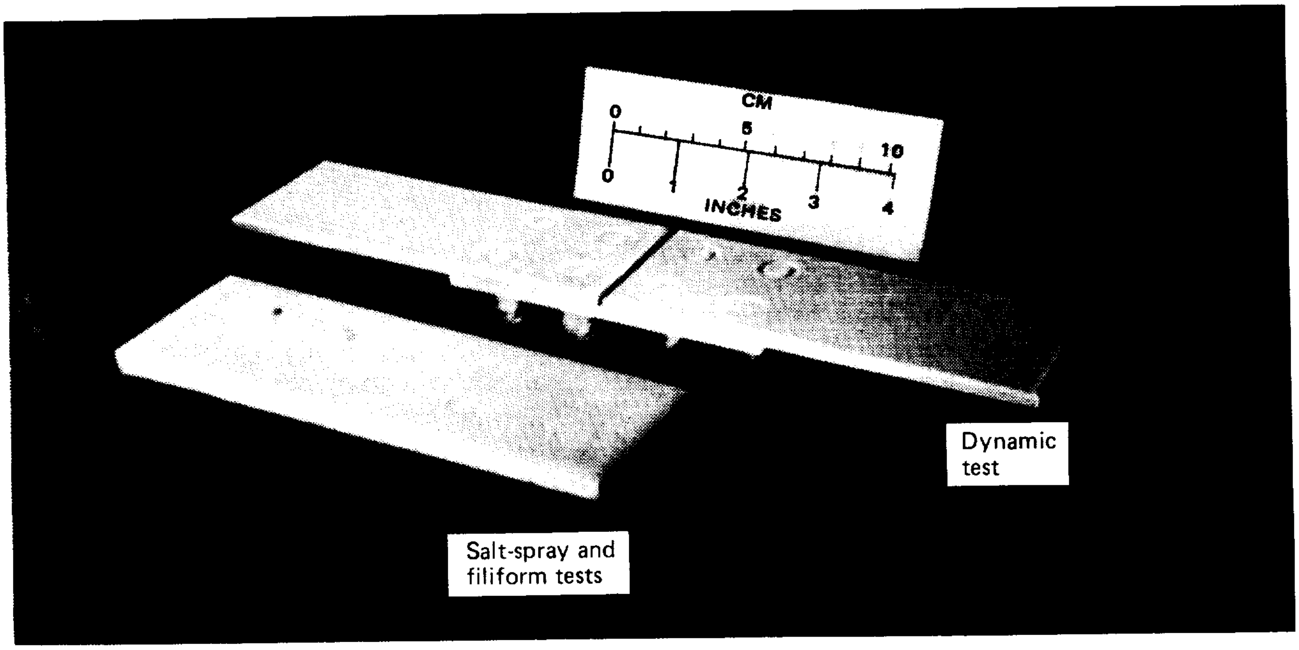

Figure 55. Corrosion Test Specimens

days, collars on the titanium fasteners were loosened and the fasteners were rotated to break the coating seal. The collars were then retightened. This prerequisite for testing was done to artificially create a corrosion path and to evaluate the behavior of coatings under this condition.

The salt-spray tests were conducted on three sets of test coatings and one set of control coatings. The specimens were exposed to salt spray for 90 days, per ASTM B117, then were lightly brushed in water to remove loose corrosion and salt deposits, and allowed to dry. Fasteners were carefuly removed and the areas around the holes, in the countersink, and in the holes were examined for evidence of corrosion (chalky, white deposits).

None of the specimens showed evidence of exfoliation corrosion around the fastener heads. Conditions in the countersink areas and in the fastener holes were rated as shown in Table 8.

4.3.4.2 Filiform Tests

The filiform specimens were identical to those used in the salt-spray tests. As on the salt-spray specimens, fasteners were rotated to break the coating seal prior to testing. Three sets of test-coated and one set of control-coated specimens were exposed to hydrochloric acid vapor for 1 hour, as described in Appendix C, and were immediately transferred to an elevated-temperature, high-humidity environment, where they remained for 90 days. At the end of that time, the specimens were washed and examined.

None of the specimens showed filiform corosion migrating from the edges of fastener heads. Overall appearance varied, however, because the tougher, more elastic test coatings were frayed around fastener heads where the coatings were broken prior to test. Fasteners were carefully removed, and countersink areas and fastener holes were examined for corrosion deposits and were rated as shown in Table 9.

Table 8. Rating of Exfoliation Corrosion

COATING	COUNTERSINK	HOLES
Control		
Enamel/epoxy primer (BMS 10-60/BMS 10-79)	Trace	None
Enamel/polysulfide primer (BMS 10-60/PR 1432)	Trace	None
Corogard/epoxy primer (EC 843/BMS 10-79)	Trace	Trace
Test		
Enamel/CAAPCO/epoxy primer (BMS 10-60/B-274/BMS 10-79)	Trace Moderate Trace	None None None
Enamel/Chemglaze/epoxy primer (BMS 10-60/M313/BMS 10-79)	Trace Trace Trace	None Trace Trace
Enamel/Astrocoat/epoxy primer (BMS 10-60/Type I/BMS 10-79)	Trace None Trace	None None None

Table 9. Rating of Corrosion Deposits

COATINGS	COUNTERSINK	HOLES
Control		
Enamel/epoxy primer (BMS 10-60/BMS 10-79)	Trace	None
Enamel/polysulfide primer (BMS 10-60/PR 1432)	Trace	None
Corogard/epoxy primer (EC 843/BMS 10-79)	Trace	None
Test		
Enamel/CAAPCO/epoxy primer (BMS 10-60/B-274/BMS 10-79)	Trace Moderate Moderate	Medium Trace Trace
Enamel/Chemglaze/epoxy primer (BMS 10-60/M313/BMS 10-79)	Moderate Moderate Moderate	Medium None None
Enamel/Astrocoat/epoxy primer (BMS 10-60/Type I/BMS 10-79)	Moderate Moderate Trace	Trace Moderate None

The test coatings present tough nonporous barriers to corrosion and depend on their elastomeric characteristics to prevent coating fracture. When the coatings are deliberately fractured, as in this test, they do not contain a corrosion inhibitor, as does Corogard. Therefore, a corrosion concentration cell develops at the interface of the coating and substrate, and greater corrosion deposits are produced than with Corogard. Table 9 shows more deposits for the test coatings than for the control coatings.

4.3.4.3 Dynamic Tests

Dynamic tests were devised to evaluate the coatings after exposure to the simulated operational conditions to which a wing upper surface skin would be subjected. Corrosion-inducing factors were combined with cyclic stress loading of the specimens to cause movement of fasteners and create a corrosion path if the coatings failed. The test consisted of a series of five parts conducted in sequence:

1.	Condensing humidity	2 weeks
2.	Weatherometer	1 week
3.	Cyclic loading	250 cycles
4.	Salt spray	1 week
5.	Potentiostat	measure current flow (corrosion penetration)

The test series was repeated three times, using the same specimens. During each series, the tension stress level was increased during cyclic loading. Appendix C contains a description of the specimens, coating systems, and test procedures. Tables of potentiostat test data are also included.

The potentiostat test apparatus, shown schematically in Appendix C, provided a constant potential between the coating surface over a fastener head and the corresponding aluminum plate in the specimen. The amount of current flowing through this circuit, measured at 2-minute intervals for 10 minutes, was proportional to the degree of corrosion penetration or coating failure.

Average current flow for each of the three control coatings is shown in Figure 56 for the three potentiostat tests. The three control coatings registered a current flow in each of the potentiostat tests. Enamel over polysulfide primer (coating A) had a current of 1 mA at the end of the first test, which increased to 5.3 mA in the second test, and to 7.2 mA in the third test. Enamel over epoxy primer (coating B) was slightly lower in the first test, 0.6 mA, but increased to 7.4 mA in the second test, and to 11.7 mA at the end of the third test. Corogard (coating C) registered a current of only 0.04 mA in the first test, but increased an order of magnitude to 0.76 mA in the second test, and again doubled to 1.7 mA in the third test. The three test coatings (coatings I, II, and III) showed essentially zero current in all of the tests, the exception being a very slight current in the order of 1 A on all of the four fastener heads.

At the conclusion of the dynamic tests, the specimens were inspected for visual evidence of corrosion. It was noted that the cyclic loading had caused some fracturing at the coating surface at fastener heads of all specimens. On the test coating specimens, only the enamel topcoat was broken, and the elastomeric polyurethane basecoat remained intact. Fasteners were removed and the holes and countersink areas evaluated for exfoliation corrosion. No corrosion was observed on the test coating specimens. The control coating specimens showed trace corrosion.

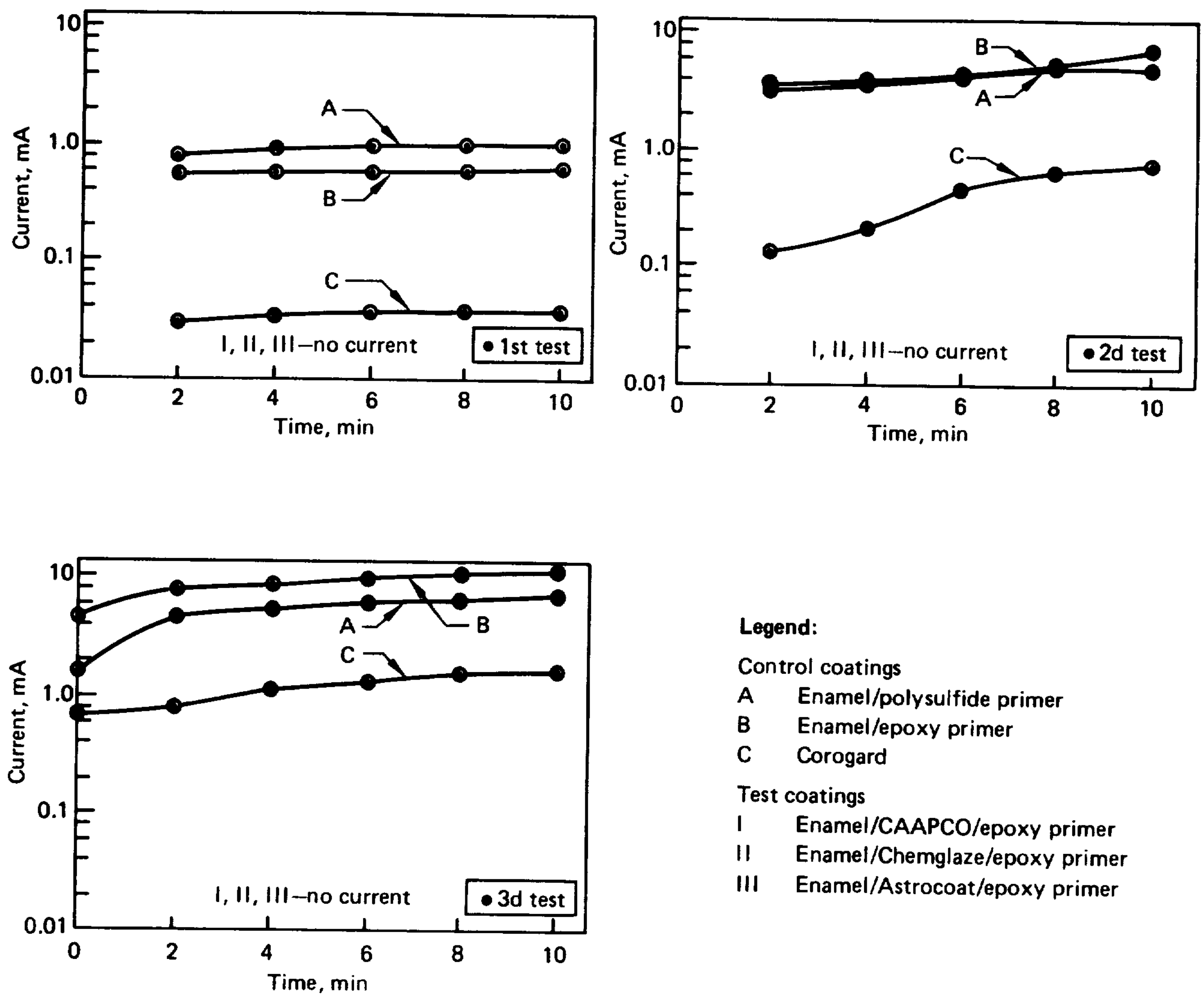

Figure 56. Potentiostat Test Results

Following the visual inspection, the specimens were subjected to metallographic examination of the countersink areas. Evidence of corrosion revealed in macrophotographs corrolated well with potentiostat test data. A typical fastener countersink, with fastener removed, was photographed at 8.1X enlargement. The specimens were bisected through the center of the holes and photographs were taken at 100X, showing a section at the top of the countersink wall. Figures 57 and 58 show these photos of the control coating specimens and test coating specimens, respectively.

Control coating A (refer to fig. 56 for description) is shown in Figure 57a. The left photo shows discoloration that was common, in various degrees, on all specimens. The right photo, however, reveals an area of corrosion undercutting the countersink face. The dotted line was added to indicate the area missing. Coating A showed a high current in the potentiostat tests.

Control coating B (fig. 57b) shows a larger area of corrosion at the top edge of the countersink. This coating had the highest potentiostat current flow. Control coating C, Corogard, is shown in Figure 57c. Although this coating had a low potentiostat current, there is no evidence of corrosion on the countersink face. It is believed that aluminum particles in the Corogard contributed to a current path.

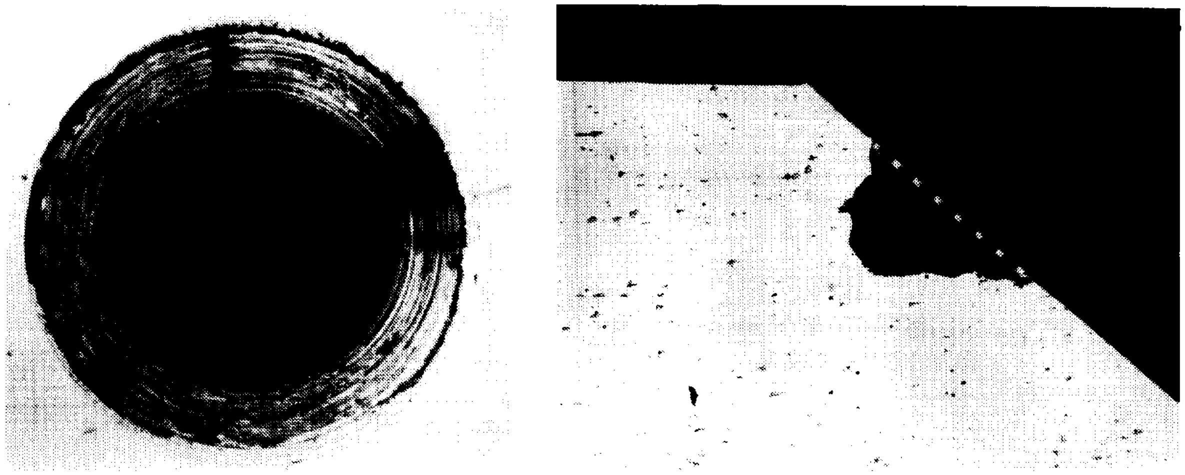

X8.1 (a) Control Coating A X100

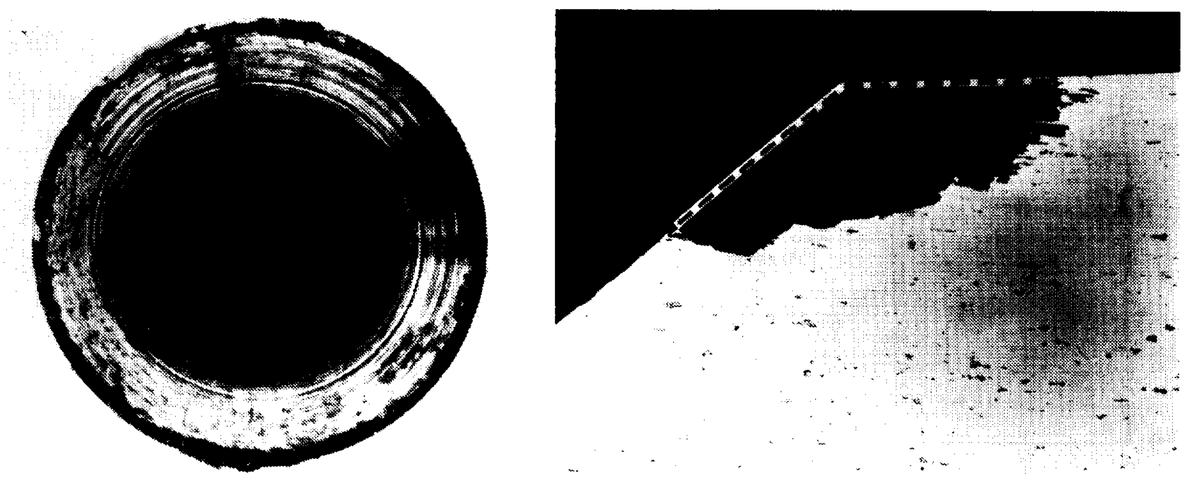

X8.1 (b) Control Coating B X100

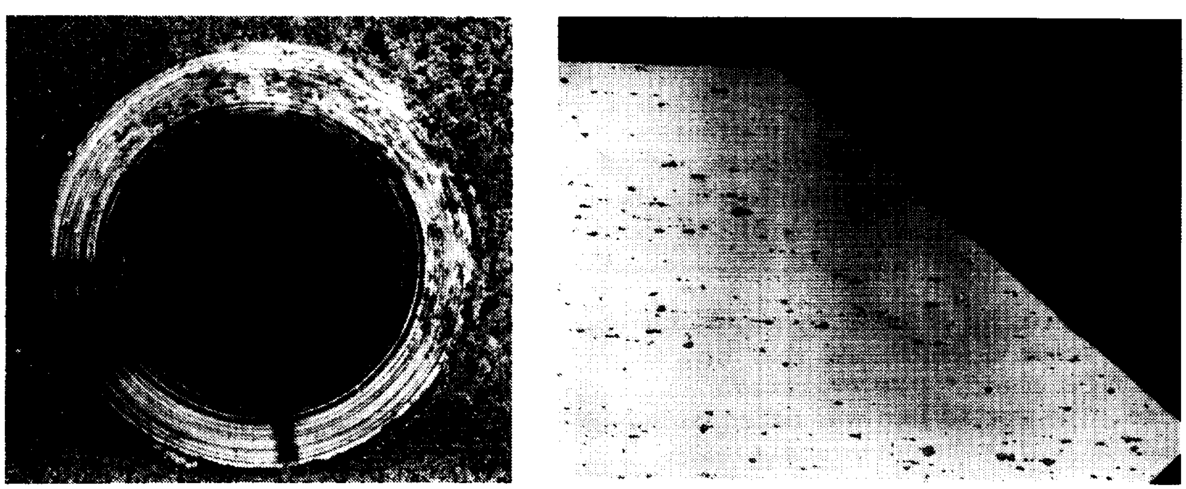

X8.1 (c) Control Coating C (Corogard) X100

Figure 57. Macrophotographs of Fasterner Countersinks in Control Coating Specimens—Dynamic Tests

The test coatings in Figure 58 show no corrosion in the countersink area. The barrier provided by the elastomeric polyurethane basecoats (CAAPCO, Chemglaze, Astrocoat) did not break down, as confirmed by the potentiostat tests, which showed zero current flow.

4.3.4.4 Conclusions

The following conclusions were reached as a result of testing for corrosion:

- Test-coating specimens showed slightly more corrosion than control-coating specimens when the coatings were fractured by turning the fasteners prior to exposing the specimens to a corrosive environment. The test coatings are tough and superior in their ability to resist fracture; but when deliberately fractured, the frayed surface presents a larger area of potential corrosion attack.

- Corogard, which has displayed outstanding corrosion protection in field experience, performed the best of the three control coatings in the dynamic tests. The enamel/epoxy primer (BMS 10-60/BMS10-79) and enamel/polysulfide primer (BMS 10-60/PR1432) control coating offered much less corrosion protection.

- None of the test coatings showed corrosion penetration at fastener heads during the dynamic tests.

The cyclic loads and temperatures used in the dynamic tests were more severe than those designed for in service. Tension stress levels during cyclic loading tests were approximately 155, 193, and 241 MPa (22 550, 28 000, and 35 000 lbf/in^2) as compared to a service design stress level of about 124 MPa (18 000 lbf/in^2). Temperatures during cyclic loading were -54^{0}C (-65^{0}F). Although the enamel topcoat over the test coatings fractured under these conditions, it is anticipated that the topcoat would remain intact under normal service conditions. Extended service evaluation of the test coatings is recommended to determine if aging in an airline environment has an effect on their corrosion-protection performance.

4.4 COST/BENEFIT ASSESSMENT

The cost/benefit analysis of Reference 2 was updated to reflect changes in material, labor, and fuel costs and to reflect results from the airline service evaluations and drag measurement flight tests. The example airplane used in this assessment was the 737 because the drag measurements were obtained on the NASA 737 test airplane. Fleet operating assumptions are listed below:

Airplane	737-200
Fleet size	30
Utilization	2400 and 2700 flight-hours per year
Average flight segment	556 km (300 nmi)

Costs of materials were based on quantity purchases for a fleet of 30 airplanes. The two annual utilization rates represent an average experienced by the entire fleet of 737s and higher utilization experienced by airlines whose route structures permit more efficient usage.

Two cases were examined, as shown in Figure 59. Case I evaluated the benefits from coatings applied to leading edges for erosion protection. Although the drag tests discussed in Section 4.1 identified a drag penalty due to rough leading edges, airlines

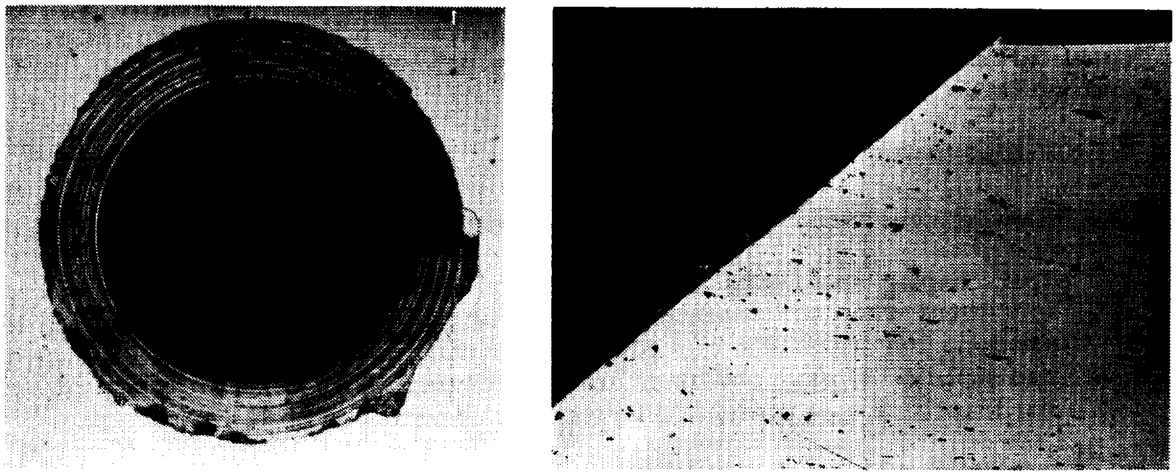

X8.1 (a) Test Coating I (CAAPCO) X100

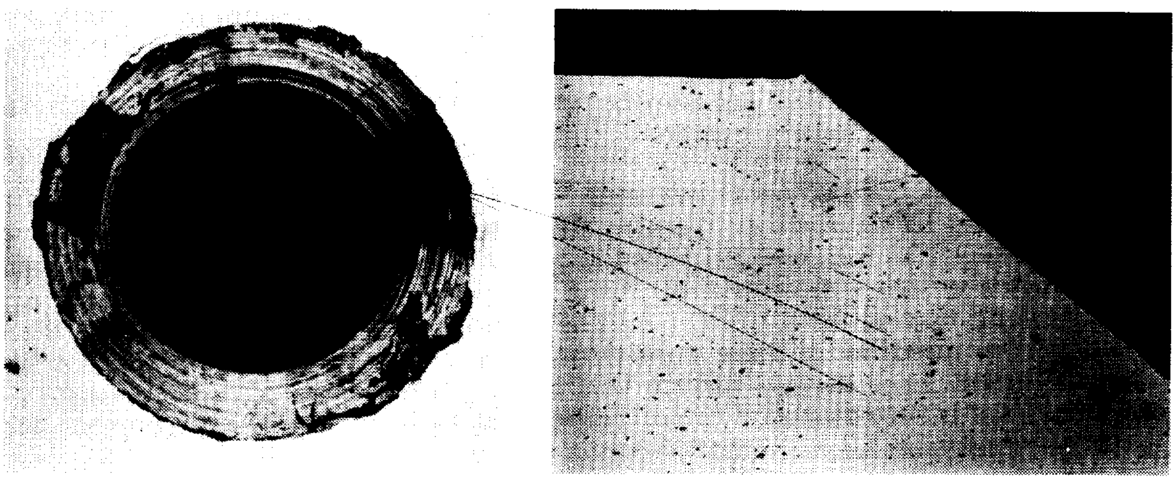

X8.1 (b) Test Coating II (Chemglaze) X100

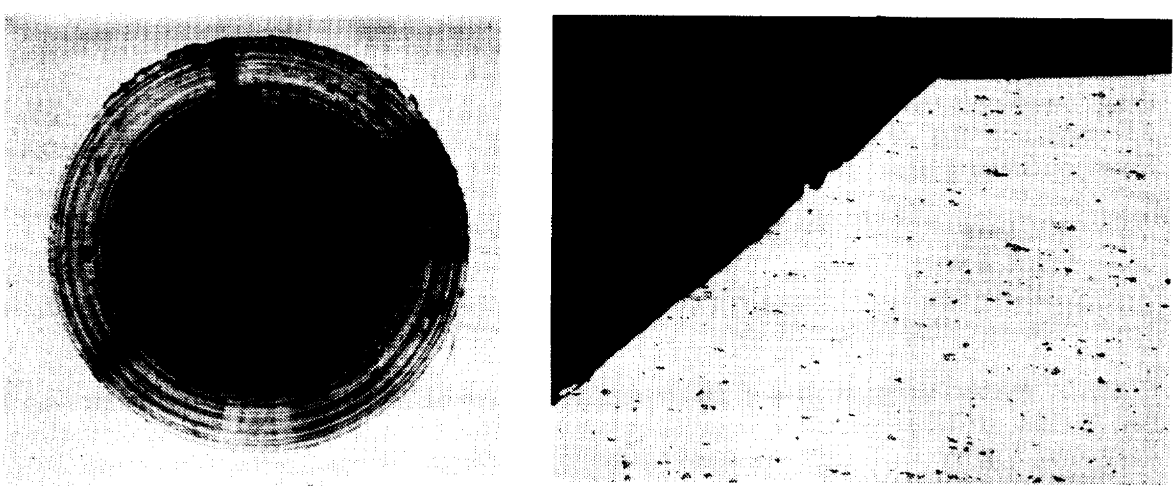

X8.1 (c) Test Coating III (Astrocoat) X100

Figure 58. Macrophotographs of Fastener Countersinks in Test Coating Specimens—Dynamic Tests

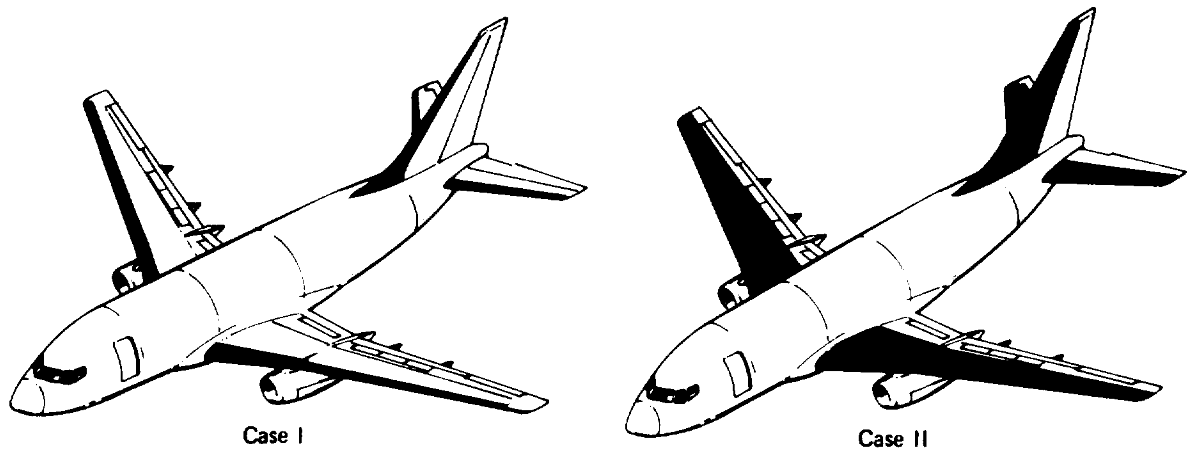

Figure 59. 737 Coating Application Areas

with severe erosion problems consider this secondary to reducing leading-edge maintenance. In extreme cases, leading edges become pitted after 1000 to 1200 hours, depending on the routes flown, rainfall and contaminants in the air, and to some extent, airplane geometry. Repeated buffings reduce the leading-edge skin thickness to a limit (e.g., 25% reduction on B737) that eventually requires replacement of parts.

The case I analysis was based on a 9-mil coating of CAAPCO or Chemglaze applied from leading edge to front spar. The 0.3% drag penalty identified in Section 4.1 was assessed to a rough wing leading edge; no additional penalty was assumed for rough empennage leading edges. The analysis also assumed one buffing per year was required for uncoated leading edges; however, no charge was included for replacement of parts.

Case II extends the coating coverage to the rear spar. The area between spars (inspar area) had a 4.5-mil CAAPCO or Chemglaze basecoat, covered with a 2-mil topcoat of polyurethane enamel. This coating provided good corrosion protection for the inspar area and produced a drag reduction. In case II, a drag benefit of 0.85% was used, based on the findings of Section 4.1. This benefit came from replacing wing upper surface Corogard with the coating system (0.4% drag reduction), smooth wing leading edge (0.3%), and the coating system applied to both sides of empennage surfaces in place of paint (0.15%). No drag credit was assumed for coating the wing lower surface because of the many access panels in that area and exposure to foreign object damage (FOD).

4.4.1 COST ANALYSIS

All costs were calculated in 1981 dollars. Changes in costs from the analysis of Reference 2 resulted from changes in labor and material costs and from a re-evaluation of coating life based on results of the flight service evaluations by Delta and Continental. It was concluded from these evaluations that the projected life of CAAPCO in a rain erosion environment should be increased from 6000 to 6500 flight-hours and that Chemglaze should be reduced from 6000 to 5000 flight-hours.

Table 10 shows the number of applications of paint, CAAPCO, or Chemglaze over a 24 000-hr cycle and the total time (flow-hours) and labor-hours involved per

Table 10. 24 000-hr Cycle Requirements for Painting and Coating Applications

APPLICATIONS	STANDARD PAINT		CAAPCO COATING		CHEMGLAZE COATING	
	CASE I	CASE II	CASE I	CASE II	CASE I	CASE II
Factory						
Number of applications	–	1	1	1	1	1
Flow-hours per application	–	64	84.5	94.5	76	86
Labor-hours per application	–	56	99	218	74	176
Field leading-edge recoat	a	a				
Number of applications	5	4	3	2	4	3
Flow-hours per application	–	–	84.5	84.5	76	76
Labor-hours per application	4	4	132	132	98	98
Field total recoat	b	b				
Number of applications	–	1	–	1	–	1
Flow-hours per application	–	64	–	94.5	–	86
Labor-hours per application	–	102	–	327	–	264

[a]Field leading-edge buffing.
[b]Field total repaint.

application. The factory application was at time of airplane production using standard paint spray facilities in a paint hangar. The field applications were assumed to have been accomplished in airline maintenance hangars by skilled painters. The labor-hours for field applications were arbitrarily increased 33% over factory labor-hours for case I and 50% for case II because of the different facilities available and a lower frequency of field application (learning curve effect).

Table 11 contains a summary of the areas covered and the weights of each element of the standard paint system and the coating systems when applied to a 737 airplane. The weight increase in each coating system over the standard paint system results in a fuel-burn penalty that is shown in Figure 60. Table 12 shows the cost of materials involved in each application of paint or coating.

The total cost increments of coating systems over those of the standard paint configuration ranged between \$6 000 and \$10 000 prorated on an annual basis, depending on airplane utilization, coating system applied, and extent of application (case I or case II). The greatest cost increment was in flow time, or greater airplane downtime, to allow for proper curing of the coatings. The second most important cost factor was labor; the least significant factor was materials costs. No credit was taken for any possible offsetting benefits from reduced maintenance to leading edges and inspar structure, other than an annual buffing (4 labor-hours) of uncoated leading edges.

4.4.2 BENEFIT ANALYSIS

Results of the analysis performed on a 737-200 airplane are presented in Figure 61. Coating the wing and empennage leading edges only (case I, shown in fig. 61a), would not return a net benefit to the operator until the price of fuel increased above present levels. The breakeven fuel price is about 36¢/L (\$1.37/gal) for CAAPCO and

Table 11. Painting and Coating Areas and Weights of Applied Materials

	CASE I			CASE II		
Painting	AREA, m^2 (ft^2)	WEIGHT, kg (lb)		AREA, m^2 (ft^2)	WEIGHT, kg (lb)	
Primer	–	–		86.3 (929)	2.36 (5.2)	
Corogard	–	–		40.4 (435)	3.45 (7.61)	
Polyurethane enamel	–	–		45.9 (494)	3.13 (6.91)	
Total	–	–			8.94 (19.72)	
Coating		CAAPCO	CHEMGLAZE		CAAPCO	CHEMGLAZE
Primer	45.8 (493)	1.25 (2.76)	1.25 (2.76)	127.1 (1368)	3.47 (7.66)	3.47 (7.66)
Coating	45.8 (493)	12.07 (26.62)	14.09 (31.06)	127.1 (1368)	22.79 (50.25)	26.59 (58.62)
Polyurethane enamel	0 (0)	0 (0)	0 (0)	81.3 (875)	5.56 (12.25)	5.56 (12.25)
Total		13.32 (29.38)	15.34 (33.82)		31.82 (70.16)	35.62 (78.47)
Weight differential (coating-painting)		13.32 (29.38)	15.34 (33.82)		22.88 (50.94)	26.68 (58.75)

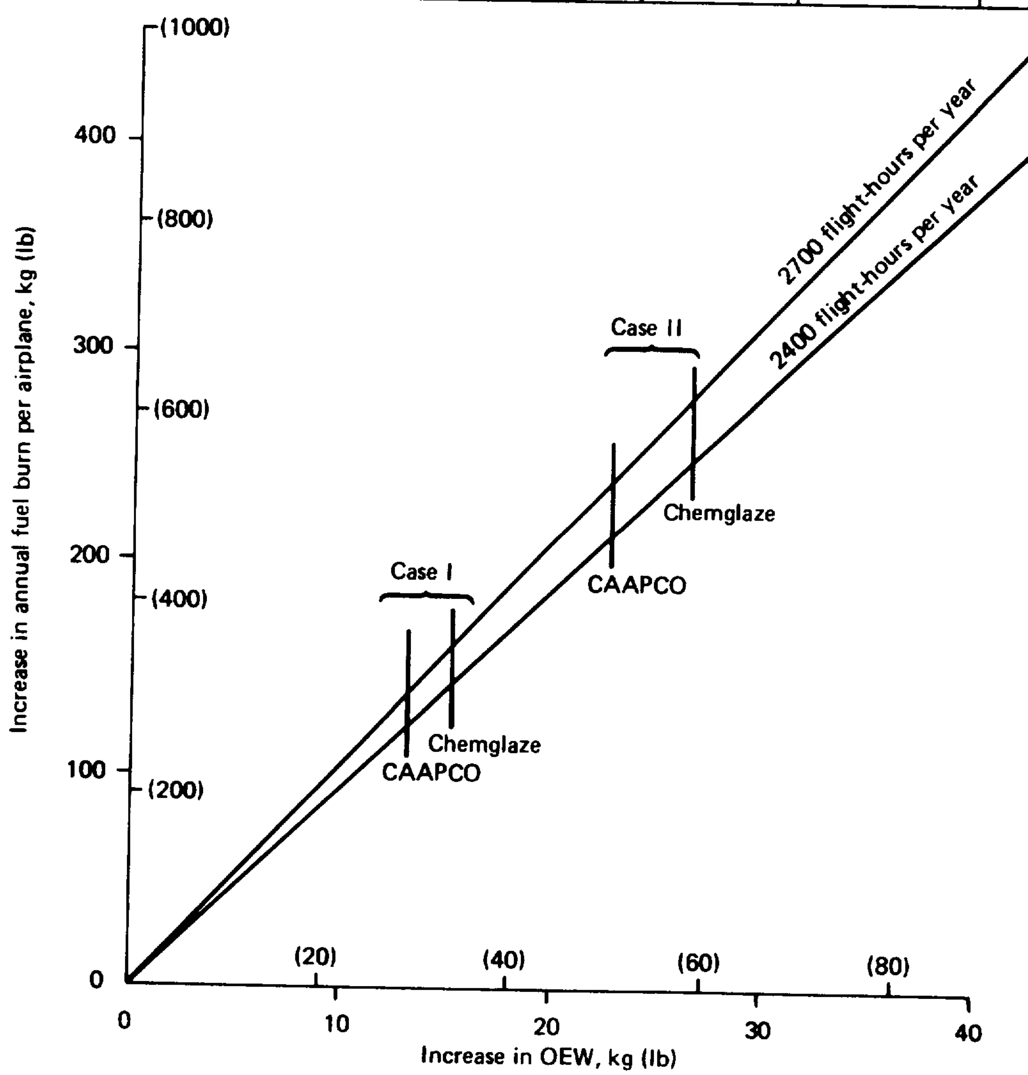

Figure 60. 737-200 Fuel-Burn Sensitivity to Increase in Weight

Table 12. Material Costs

	CASE I			CASE II		
	COMPONENT COST, $	TOTAL COST, $	MATERIAL COST DIFFERENCE COAT-PAINT, $	COMPONENT COST, $	TOTAL COST, $	MATERIAL COST DIFFERENCE COAT-PAINT, $
Painting						
Primer	–	–	–	33	–	–
Corogard	–	–	–	248	–	–
Polyurethane enamel	–	–	–	53	334	
Coating						
Primer	18	–	–	49	–	–
Polyurethane enamel	–	–	–	93	–	–
CAAPCO	489	507	507	941	1083	749
Chemglaze	265	283	283	518	660	326

40¢/L ($1.51/gal) for Chemglaze. These results were based on a 0.3% drag reduction benefit from preserving a smooth wing leading edge in contrast to flying with a severely eroded wing leading edge. Because the effects of empennage leading-edge erosion were not measured during the drag tests described in Section 4.1, no additional drag benefits were assumed from these surfaces. Some airlines, flying in extreme erosion environments, must replace leading edges after several buffings. No credit was included in the analysis for reduced costs for parts replacement.

Case II results are shown in Figure 61b. Significant benefits came from extending the CAAPCO or Chemglaze coating systems back to the rear spar of wing and empennage. The combined effects of smooth leading edges, replacing Corogard on wing upper surfaces with coating and replacing empennage paint with coating—for an estimated drag reduction of 0.85%—produced net savings of $10 000 to $20 000 per airplane per year, depending on utilization and the price of fuel.

As stated earlier in this document, the drag increment from Corogard found in the flight tests discussed in Section 4.1 was for an application that was somewhat rougher than the average for the existing fleet (160 μin versus 150 μin average), and recent application techniques now produce Corogard surfaces of about a 90 to 100 μin roughness. To compensate for this difference in roughness, no penalty was included in the analysis for the rapid increase in Corogard drag with increase in Reynolds number found in the drag measurement flight tests. Therefore, only the Corogard drag penalty during high-altitude cruise was included.

Benefits from using the coatings on other types of aircraft are beyond the scope of this assessment. Many factors influence the cost/benefit results that are peculiar to airplane geometry and airplane usage. It is speculated that the 737 assessment would apply, in general, to other jet transports: coatings applied to leading edges only for a reduction in fuel burn produce marginal benefits; coatings applied from the leading edge to rear spar produce significant savings. In some cases, however, it might be desirable to apply coatings to the leading edges to preserve low-speed handling qualities or to reduce costs of parts replacement, aside from fuel-burn considerations.

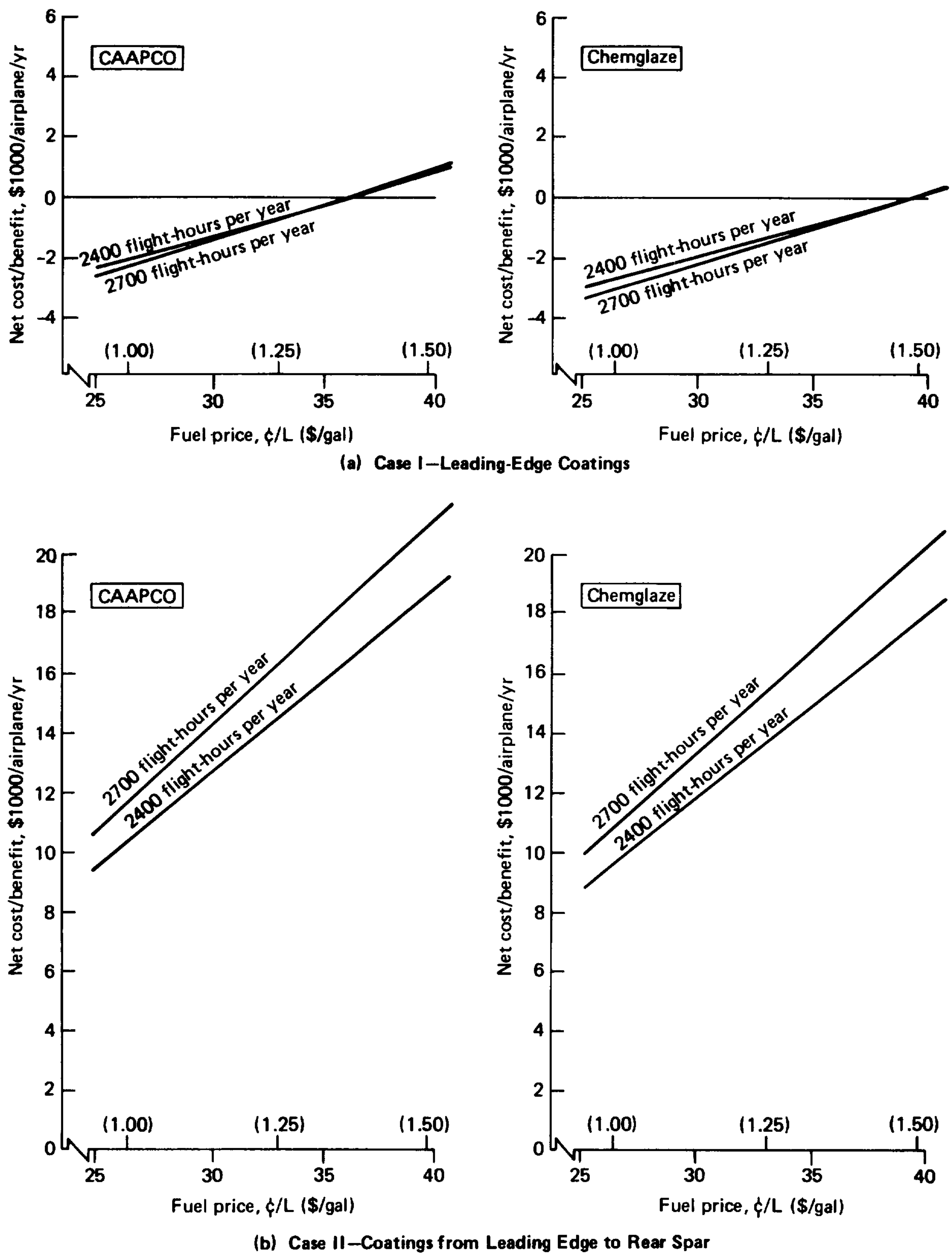

Figure 61. Estimated Cost/Benefit of Coatings on 737-200

5.0 CONCLUSIONS AND RECOMMENDATIONS

The test and analyses of surface coatings conducted under Contracts NAS1-14742 and NAS1-15325 showed two elastomeric polyurethane spray-on products, CAAPCO B-274 and Chemglaze M313, to be effective erosion deterrents when applied to leading edges. These materials, when applied to inspar areas with a polyurethane enamel topcoat, provide good protection from corrosion and from attack by synthetic-type hydraulic fluid (e.g., Skydrol or Hyjet IV). These coatings tend to mask small excrescences in the substrate surface and present a smooth surface that results in a reduction in airplane drag.

The following conclusions and recommendations are derived from results of a drag measurement test, airline service evaluations, laboratory environmental tests, and a cost/benefit assessment described in this document.

5.1 CONCLUSIONS

5.1.1 DRAG MEASUREMENT TEST

The effects of coatings on wing boundary layer were measured on a 737 in flight tests. The effects on drag were also estimated, based on the boundary layer data. The results shown below are wing upper surface effects during cruise. Greater effects would be expected if coated areas had included the empennage surfaces.

- CAAPCO B-274 applied to the 737 wing upper surface showed a section profile drag reduction of 0.75% to 1.5% relative to the bare metal surface, depending on Reynolds number. This is equivalent to about 0.2% reduction in total airplane drag at a cruise unit Reynolds number of 6.5 million per meter (2.0 million per foot).

- Corogard paint applied to the wing upper surface inspar area (average measured roughness of 160 in) increased section profile drag 0.5% to 3.5%, depending on Reynolds number. This increase is equivalent to an increase in total airplane drag of about 0.2% at cruise unit Reynolds number (6.5 million per meter). The drag increment increases rapidly with increase in Reynolds number.

- At a typical cruise condition ($C_L = 0.45$), a simulated badly eroded wing leading edge increased the section profile drag 1.6%, which is equivalent to about 0.3% airplane drag for erosion along the entire span. The drag increment becomes greater at higher lift coefficients.

- The masking characteristics and surface smoothness of Chemglaze M313 are similar to CAAPCO B-274, therefore, it can be assumed that Chemglaze would produce equal drag benefits.

5.1.2 FLIGHT SERVICE EVALUATIONS

Airline evaluations of CAAPCO and Chemglaze coatings (and to a limited degree, Astrocoat) applied to leading edges for erosion prevention led to the following conclusions:

- CAAPCO B-274 is the most durable of the three coatings tested. When properly applied over an epoxy primer (BMS 10-79 or equivalent), it has a leading-edge life in excess of 6500 flight-hours in normal airline service.

- Chemglaze M313 has a leading-edge life in excess of 5000 flight-hours. It demonstrated good adhesion when applied over either a wash primer or epoxy primer.

- It is essential that the substrate be thoroughly cleaned prior to application of either type of primer.

- Spot repair of the coatings in the field can best be accomplished during layup for scheduled maintenance to allow sufficient time for proper reapplication and curing. Major repair can be completed in 48 hours with the aid of heat lamps to accelerate curing.

- The erosion life of CAAPCO and Chemglaze is greater than that for Astrocoat.

5.1.3 ENVIRONMENTAL TESTS

Laboratory tests to evaluate the compatibility of coatings with the jet transport operating environment showed that:

- Coatings can be used on leading edges equipped with thermal anti-icing (TAI). The coatings will withstand TAI elevated temperatures and will not significantly degrade TAI system performance.

- If an airplane has wing-mounted nacelles and fuel contained in the wing in that immediate area, a lightning strike analysis should be performed before applying coatings to that area.

- Coatings will not cause precipitation static interference with communication and navigation equipment.

- Dual coatings of CAAPCO, Chemglaze, or Astrocoat with a polyurethane enamel topcoat provide good corrosion protection when applied to inspar areas. The elastomeric properties of the basecoat prevent coating fracture at fastener heads. In dynamic tests, the dual coatings compared favorably with Corogard for corrosion protection.

- Rain erosion tests indicated that a 9-mil coating is as durable as thicker coatings in a high erosion environment. (Note: At this coating thickness, none of the three materials failed within the 180-minute time limit for testing at AFML. Therefore, the comparative erosion life of the three materials was not determined from this particular test. Previous erosion tests and flight service evaluation results led to the conclusions regarding their relative durability.)

- Because of their poor resistance to rain erosion, composite materials, such as graphite-epoxy, fiberglass-epoxy, Kevlar-epoxy or a hybrid of Kevlar-graphite-epoxy, are unsuitable as leading edges in high- speed transport aircraft. A 9-mil protective coating of elastomeric polyurethane increased the erosion life three- to tenfold; however, even with the coating, the most durable specimen tested (CAAPCO over fiberglass) had an erosion life roughly equivalent to 1 year in airline service. This is less than half the erosion life of CAAPCO over an aluminum substrate.

5.1.4 COST/BENEFIT ASSESSMENT

- A cost/benefit assessment of coatings applied to the 737-200 showed that coatings applied only to leading-edge areas for erosion protection produce marginal benefits at fuel prices less than 36¢/L ($1.37/gal). This did not include any possible additional benefits from reduction of costs of replacing leading edges if coatings are not used.

- Coatings on the 737-200 from leading edge to rear spar show a potential annual benefit of $10,000 to $20,000 per airplane, depending on utilization rate and the price of fuel.

5.2 RECOMMENDATIONS

The two elastomeric polyurethane coatings (CAAPCO B-274 and Chemglaze M313) investigated under Contracts NAS1-14742 and NAS1-15325 were found to provide good protection against leading-edge erosion and a potential reduction in airplane drag. Corrosion protection to structural skins was evaluated in laboratory tests and tentatively found to be superior to that of currently used protective systems. The long-term corrosion protection characteristics of these coatings must be thoroughly investigated, however, before they can replace current coating systems on structural skins. The effects of environmental factors such as ozone, ultraviolet radiation, temperature and pressure cycling, exposure to aircraft fluids and stress cycling must also be evaluated over long-term inflight service to ensure that the corrosion protection demonstrated in the laboratory endures.

It is recommended that industry pursue necessary and sufficient additional corrosion protection investigations of these coatings to fully qualify them for application to the jet transport fleet.

6.0 REFERENCES

1. Boeing Commerical Airplane Company (BCAC). Aircraft Surface Coatings Study, NASA CR 158954, January 1979.

2. BCAC. Aircraft Surface Coatings Study—Verification of Selected Materials, NASA CR 159288, September 1980.

3. BCAC. Flight Test Evaluation of Drag Effects of Surface Coatings on the NASA Boeing 737 TCV Airplane, NASA CR 165767, June 1981.

4. Nash, J. F. and Bradshaw, P. "The Magnification of Roughness Drag by Pressure Gradients," Journal of the Royal Aeronautical Society, Vol. 1, January 1967.

APPENDIX A
DRAG TEST DATA ANALYSIS

Analysis Method

The test analysis method is described in Reference 3; following is a discussion of the principal steps. First, the boundary layer velocity profiles were determined from the measured total pressure loss within the boundary layer. Then, the momentum loss profile was calculated and was integrated to obtain the momentum thickness. These calculations were performed by an existing Boeing computer program, A-55, "Turbulent Boundary Layer Profile Analysis."

Measurements were taken at the 73% chord location. Therefore, the increments in momentum thickness had to be extrapolated to the trailing edge to express the results in terms of section profile drag. This was done by calculating boundary layer growth along the test section from measured surface static pressure distributions and deriving a magnification factor that translates a given increment in momentum thickness, measured at the rake location, into a corresponding increment in section profile drag coefficient:

$$\Delta c_d = m \frac{\Delta \theta}{c}$$

where $\Delta\theta = \theta_{left} - \theta_{right}$ is the momentum thickness difference between the left and right wing test sections, and m is the magnification factor.

The boundary layer growth calculations were performed by another existing Boeing computer program, TEM 139, "A Finite Difference Method To Calculate the Boundary Layer Development on an Infinite Yawed Wing." The magnification factor was calculated following a method given by Nash and Bradshaw (ref. 4).

This calculation yields incremental drag coefficients based on the chord of the test section. The ultimate objective—to determine effects of the various surface configurations on total airplane drag—is complicated by a number of factors that must be taken into consideration, e.g., the chordwise extent of the coated area along the entire span and local flow conditions that also vary along the span. Assuming that similar conditions and effects exist at all spanwise stations, conversion factors for airplane drag can be calculated.

Data Processing

The data processing and test analysis were accomplished in six steps, as shown in Figure A-1. NASA provided raw data tapes that contained time histories of 16 variables, including boundary layer rake pressures, reference total, static and dynamic pressures, total temperature, remaining fuel weight, airspeed, altitude, and angle of attack. Each measured quantity was recorded at the rate of 40 readings per second. Because the data-taking interval during each of the 15 test conditions lasted about 2 minutes (two scanning cycles), the basic tapes contained a large volume of data (some 1.2 million readouts per flight).

The first step of the data-reduction process was to filter, average, and reformat the data contained in the raw data tapes. An auxiliary computer program was written to accomplish this task and provided an interface between the recorded data and the computer programs used to analyze the data. Data that were unreasonably out of range (stray points) were deleted, and the mean and standard deviations were

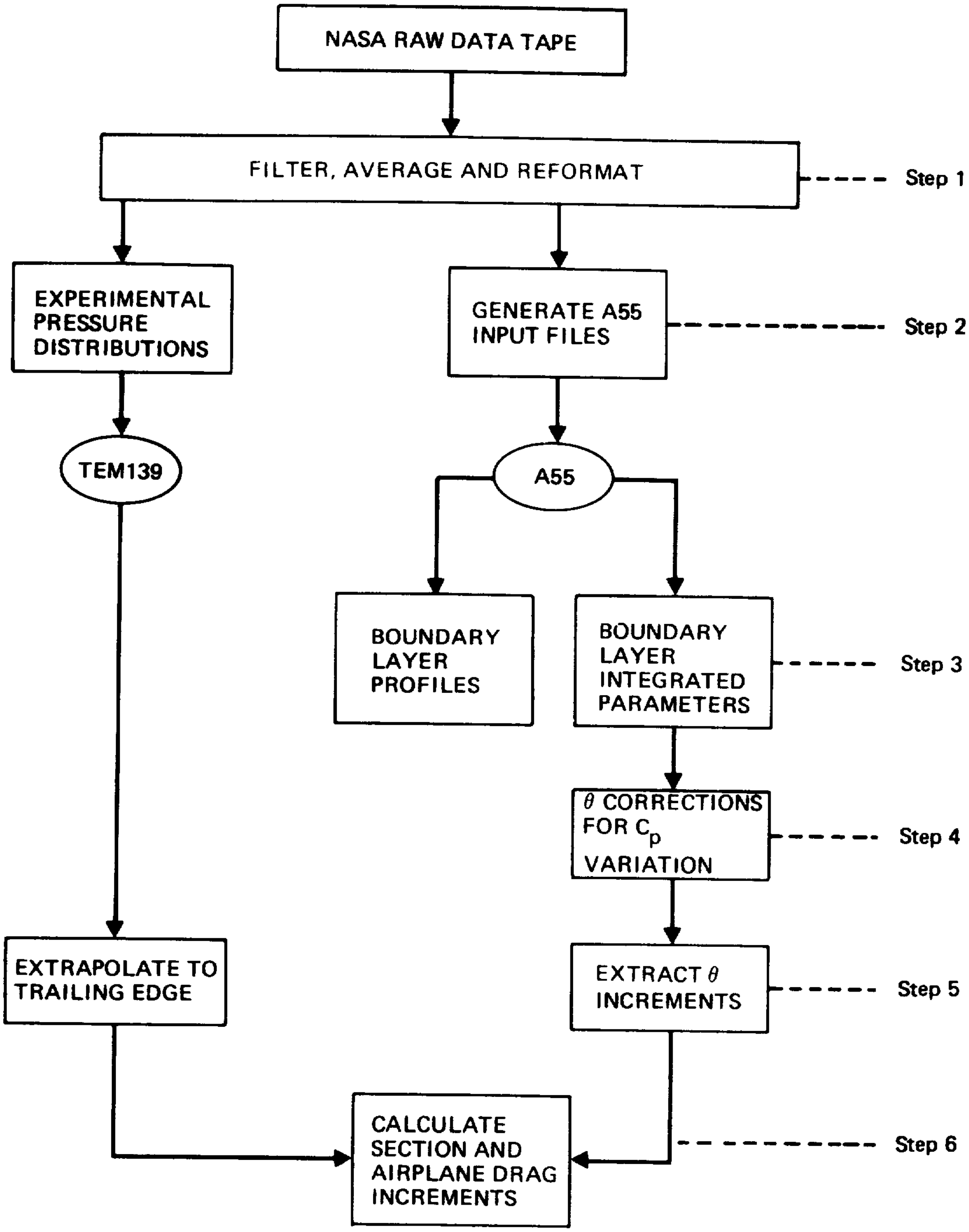

Figure A-1. Data Processing Sequence

computed for each remaining data point. Based on the standard deviation, if the scatter in a set of data was too large, these data were deleted. Most of the data, however, fell within very narrow scatter bands (±0.1%), thus only very few data points were actually deleted. Another main function of the interface program was to generate average values of the test variables. The boundary layer rake data and the reference pressure data were averaged for each scan position. Those variables that were essentially constant during a given test condition (such as airspeed, altitude, and temperature) were averaged for the entire scanning cycle. The averaged data then were adjusted for such small-scale perturbations as zero shift, amplifier sensitivity drift, or slight variations in airspeed during a scanning cycle.

In the second step of the data-reduction process, input files were generated for the two principal computer programs used in the test analysis: the boundary layer profile analysis program (A-55) and the boundary layer growth analysis program (TEM 139).

The third step constituted processing the test data by the A-55 and TEM 139 computer programs. Data from flights 1, 3, 4, and 5 (i.e., the boundary layer survey data) were processed by A-55, and the surface pressure survey data from flight 2 were processed by TEM 139. From the output of A-55, two plot files were generated, which allowed machine plotting of the test results. One file included the boundary layer profile parameters (i.e., those variables that are dependent on height), and the other contained the global or integrated parameters.

In the fourth step of data processing, a correction was applied to the boundary layer momentum thickness data to compensate for slight differences in the local static pressures, c_p, between the left and right wing test sections.

During the fifth step, momentum thickness increments between the left and right wing test sections were extracted from the data. In parallel with this task, the applicable magnification factors were determined for each test condition based on results of the boundary layer calculations made by TEM 139.

The sixth step of the data reduction process consisted of translating the local momentum thickness increments measured at the rake location (73% test section chord) into section profile drag increments and, ultimately, extrapolation of the section profile drag increments in terms of total airplane drag increments.

The section pressure distributions from flight 2 were used, according to the method described in Reference 3, to convert boundary layer momentum losses measured at 73% chord of the upper surface to full-chord section profile drag increments at the measurement station. Boundary layer data from flight 3 (both test panels bare metal) were compared and a correction factor was applied to the right wing reference panel data. This permitted boundary layer changes due to coatings or paint (flights 1, 2, 4, and 5) to be evaluated from data taken simultaneously on left and right wing panels.

APPENDIX B
ICING TEST DATA

This appendix contains data from icing and thermal conductivity tests to support Section 4.3.1. It contains comparisons of temperature profiles obtained from the two parallel rows of slat skin thermocouples, comparisons of skin temperatures produced by 100% versus 75% thermal anti-icing (TAI) system flow rate, and a reproduction of temperatures recorded during the tests.

Three series of tests were conducted in the anti-icing mode. Runs 1 to 6 were made with the model uncoated, runs 7 to 12 with CAAPCO coating, and runs 16 to 22 with Chemglaze coating. Runs 13 to 15 and 20 were not recorded because of inadvertent errors in setting up test conditions in the icing tunnel. Each series contained six runs: Each condition—dry air, intermittent maximum icing, and continuous maximum icing—was run at 100% and 75% rated flow of the TAI system.

Following the anti-icing tests, a test (run 23) was conducted in the deicing mode with the Chemglaze coating and an overcoat of silicone compound (G.E. 117-8441B) on the outboard half of the model. Tunnel conditions of run 18 were duplicated, and five cycles of ice buildup and dissipation were observed and photographed (figs. 46 and 47). Thermocouple temperatures were not recorded.

Thermocouple (T/C) locations and numbers are shown in Figure B-1 and in the tabulation below the figure. These numbers correspond to the T/C numbers in Tables B-1 through B-6. The two rows of leading-edge skin T/Cs are numbered 1 through 10 and 11 through 21, respectively. T/Cs 1 through 10 are directly in line with a TAI spray tube orifice (10 orifices, 3.81 cm [1.50 in] apart, 3.58-mm [0.141-in] diameter); T/Cs 11 through 21 are midway between two orifices.

Figures B-2, B-3, and B-4 show temperature comparisons from the two rows of skin T/Cs for each of the three coating configurations. There was very little difference in temperatures, and T/Cs 1 through 10 generally were higher where differences existed. For this reason and for clarity, data from T/Cs 1 through 10 only are shown in Section 4.3.1.

Figures B-5, B-6, and B-7 show temperature comparisons from 100% TAI rated flow and 75% TAI rated flow. As expected, temperatures produced by 100% flow (the flow rate selected for Model 767 slat anti-icing from previous tests of the model) were appreciably higher than those recorded during 75% TAI flow testing. Again for clarity, data from the 100% TAI flow runs only are shown in Section 4.3.1.

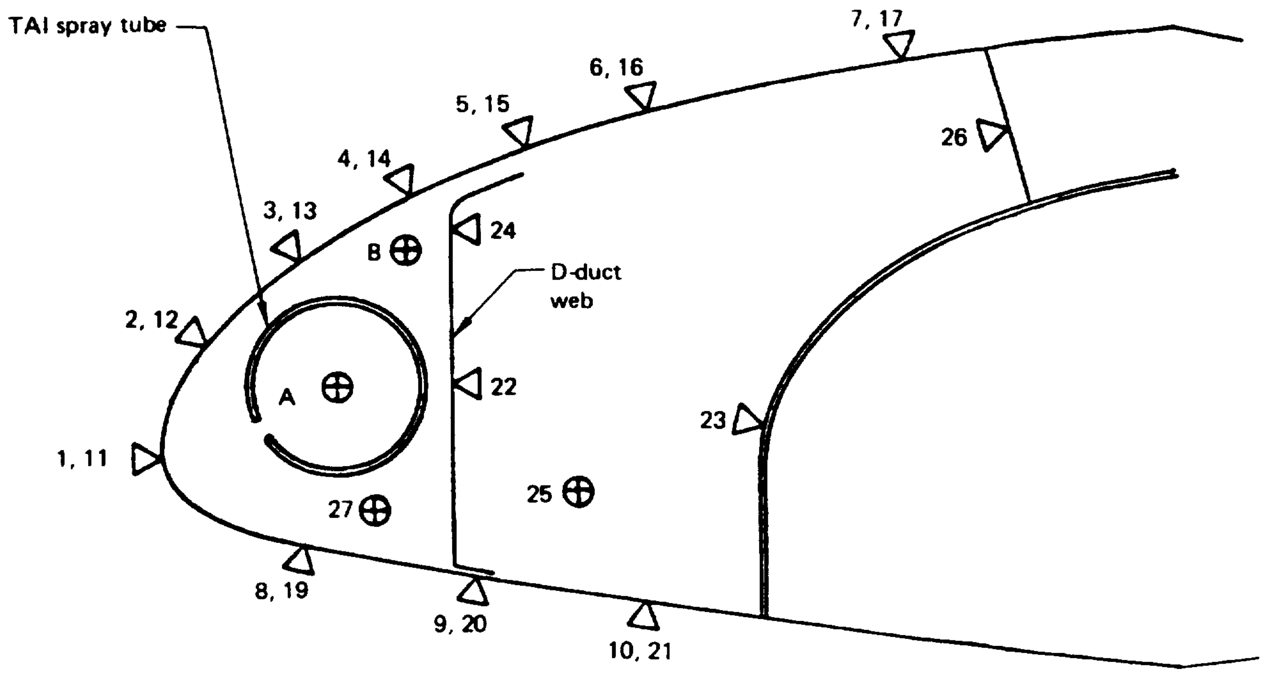

	THERMOCOUPLE NUMBERS, VARIABLE			
RUN SERIES	A (SPRAY TUBE)	B (UPPER D-DUCT)	TUNNEL (NOT SHOWN)	FLOW TUBE (NOT SHOWN)
1 to 6	29	28	30	18
7 to 12	30	28	31	29
16 to 22	29	18	31	28

Figure B-1. Thermocouple Numbers and Locations

Table B-1. Test Conditions Summary: Uncoated

DATE 10/28/80	ICING CONDITION	DRY AIR		INTERMITTENT MAX.		CONTINUOUS MAX.	
	RUN NO.	3	4	1	2	5	6
	TAI FLOW RATE	100%	75%	100%	75%	100%	75%
FLIGHT:	Condition	Climb		Holding		Holding	
	Altitude, m	4,572		4,572		4,572	
	, (ft)	(15,000)		(15,000)		(15,000)	
	Velocity, m/s	190		138		131	
	, (knots)	(370)		(268)		(255)	
	Temperature, ^oC	-17.8		- 6.1		- 28.9	
	, (^oF)	(0)		(21)		(-20)	
	Horiz. Ext., km	----		9.6		32.2	
	, (nm)	----		(5.2)		(17.4)	
TUNNEL:	Altitude, m	-0-	-0-	-0-	-0-	-0-	-0-
	Velocity, m/s	70.2	70.2	67.1	67.1	85.8	85.8
	Equiv Temp, ^oC	-17.8	-17.8	-17.8	-17.8	-28.9	-28.9
(T/C 30)	Actual Temp, ^oC	-18.2	-17.7	-18.4	-18.4	-29.0	-28.1
	Drop Diam, microns	----	----	27.8	27.8	20.6	20.6
	LWC, g/m^3	----	----	2.10	2.10	0.29	0.29
	P_V , cm H_2O	34.8	35.1	32.0	32.0	54.6	54.6
	Time, seconds						
FLOW TUBE:	P_S, cm Hg	117.9	86.9	75.2	51.6	95.3	51.6
	P_V, cm H_2O	23.6	19.1	17.5	12.2	20.8	13.0
(T/C 18)	Air Temp., ^oC	205.7	215.1	208.1	222.2	204.2	208.4
	Air Flow, kg/min	1.90	1.55	1.43	1.09	1.67	1.13
TAI SPRAY TUBE:	P_S, cm Hg	114.3	84.8	72.6	49.3	94.2	49.0
(T/C 29)	Air Temp., ^oC	188.2	192.9	184.3	191.4	184.0	178.9
COMMENTS:							

Table B-2. Temperature Printout: Uncoated

RUN 1 DATE 10/28/80

T/C NO.	T/C TEMPERATURES DURING RUN, °F								AVG TEMPS °F	AVG TEMPS °C	T/C NO.
32	*****	*****	*****	*****	*****	*****	*****	*****	*****	*****	32
31	379.4	385.1	385.6	381.4	387.6	380.4	385.5	381.6	384.1	195.8	31
30	-1.6	-1.7	-1.7	-1.6	-1.0	-0.4	-0.4	-0.6	-1.1	-18.4	30
29	367.5	367.0	365.0	363.6	363.9	362.1	362.4	363.3	363.4	184.3	29
28	273.1	255.3	235.7	236.5	231.2	229.3	232.8	258.0	233.1	111.8	28
27	269.8	259.7	236.4	235.1	231.7	228.1	228.6	251.6	232.0	111.2	27
26	186.0	184.0	169.0	163.8	161.8	157.8	156.3	166.6	161.7	72.1	26
25	180.8	176.1	163.1	159.3	157.0	152.6	151.7	161.8	156.7	69.3	25
24	227.2	225.6	207.9	198.1	195.8	190.5	187.9	197.9	196.0	91.2	24
23	140.1	139.9	136.0	131.1	127.4	124.0	121.0	120.7	127.9	53.3	23
22	239.9	238.8	220.6	211.2	208.3	203.4	201.0	210.8	208.9	98.4	22
21	106.3	106.6	86.8	81.9	80.5	73.9	69.3	82.6	78.5	25.9	21
20	130.8	131.4	87.9	92.1	86.0	78.1	74.8	106.5	83.8	28.8	20
19	172.8	171.5	93.4	99.8	92.9	89.7	86.3	144.6	92.4	33.6	19
18	407.9	408.1	406.5	407.7	406.5	404.4	406.6	404.4	406.3	208.1	18
17	64.2	63.9	58.3	52.5	52.6	50.7	50.0	51.4	52.8	11.6	17
16	82.7	87.1	75.9	69.3	70.8	66.5	65.0	70.4	69.5	20.9	16
15	115.2	114.9	94.6	88.9	92.2	83.0	80.3	93.2	87.8	31.0	15
14	127.7	129.1	93.1	91.6	96.2	82.1	77.8	102.5	88.2	31.2	14
13	137.9	142.3	84.1	87.3	92.2	77.1	74.9	107.0	83.1	28.4	13
12	*****	*****	*****	*****	*****	*****	*****	*****	*****	*****	12
11	*****	*****	*****	*****	*****	*****	*****	*****	*****	*****	11
10	*****	*****	*****	*****	*****	*****	*****	*****	*****	*****	10
9	134.6	136.9	86.9	85.3	92.4	75.7	75.0	99.2	83.1	28.4	9
8	186.5	189.0	99.9	101.9	107.0	93.0	91.1	142.8	98.6	37.0	8
7	65.3	65.0	61.7	54.1	53.3	52.3	51.1	51.4	54.5	12.5	7
6	88.7	88.3	80.7	69.8	71.4	67.8	66.0	67.6	71.1	21.7	6
5	119.9	119.9	102.0	91.8	97.2	87.5	85.6	91.5	92.8	33.8	5
4	132.0	133.6	96.8	89.5	101.6	80.9	79.8	95.6	89.7	32.1	4
3	146.6	148.3	88.3	86.0	100.2	77.3	77.8	99.9	85.9	30.0	3
2	187.1	184.6	95.8	101.2	114.6	90.6	92.5	132.1	98.9	37.2	2
1	226.3	226.3	116.8	120.9	128.6	112.0	115.1	183.3	118.7	48.2	1
0	*****	*****	*****	*****	*****	*****	*****	*****	*****	*****	0

Table B-2. Temperature Printout: Uncoated (Continued)

RUN 2 DATE 10/28/80

T/C NO.	T/C TEMPERATURES DURING RUN, °F								AVG TEMPS °F	AVG TEMPS °C	T/C NO.
32	*****	*****	*****	*****	*****	*****	*****	*****	*****	*****	32
31	443.5	439.2	434.5	440.4	439.3	447.1	442.6	439.8	440.8	227.3	31
30	0.1	0.1	-0.4	-1.0	-1.3	-1.3	-1.3	-1.6	-1.1	-18.4	30
29	379.9	378.9	376.6	377.1	375.9	376.1	375.8	376.8	376.3	191.4	29
28	266.5	244.5	229.4	227.1	222.1	221.4	230.6	250.1	226.1	107.9	28
27	262.0	250.7	229.2	226.8	221.9	219.9	224.2	243.6	224.4	107.0	27
26	174.9	173.0	158.1	153.1	149.8	147.8	146.5	155.8	151.1	66.2	26
25	173.3	169.4	156.4	152.2	148.2	147.4	148.2	159.0	150.5	65.9	25
24	213.2	212.4	195.9	186.8	181.7	177.7	176.3	186.2	183.7	84.3	24
23	124.1	124.1	121.3	117.5	113.8	110.7	108.2	108.2	114.3	45.8	23
22	224.8	224.2	208.1	199.4	194.2	190.4	188.6	198.3	196.1	91.2	22
21	95.8	96.9		72.9	67.4	63.2	62.0	73.9	66.4	19.1	21
20	120.6	121.6		78.4	71.1	68.7	68.1	96.2	71.6	22.0	20
19	162.7	158.9		89.8	84.1	81.4	81.3	134.4	84.2	29.0	19
18	431.9	430.6		431.7	430.2	432.3	432.5	431.6	431.7	222.2	18
17	56.6	57.0		46.4	44.7	43.6	42.9	44.2	44.4	6.9	17
16	78.8	79.4		61.9	59.9	57.5	56.9	62.1	59.9	15.5	16
15	105.3	106.3		80.7	76.6	72.3	71.5	84.5	75.3	24.1	15
14	117.8	121.0		81.9	76.1	70.4	69.9	93.8	74.6	23.7	14
13	128.1	133.7		77.9	71.8	67.8	67.4	98.0	71.2	21.8	13
12	*****	*****		*****	*****	*****	*****	*****	*****	*****	12
11	*****	*****		*****	*****	*****	*****	*****	*****	*****	11
10	*****	*****		*****	*****	*****	*****	*****	*****	*****	10
9	124.3	128.5		76.5	71.4	67.8	67.2	91.2	70.7	21.5	9
8	176.1	180.5		94.2	87.0	83.8	82.6	134.3	86.9	30.5	8
7	57.0	57.4		48.4	46.1	45.3	44.3	43.7	46.0	7.8	7
6	78.3	79.0		61.8	60.5	58.5	56.6	58.9	59.4	15.2	6
5	108.5	110.5		83.1	81.3	76.4	74.1	83.3	78.7	26.0	5
4	122.3	127.9		81.3	77.1	69.5	67.6	88.2	73.9	23.3	4
3	136.4	144.6		79.8	74.7	68.4	67.7	93.3	72.7	22.6	3
2	175.3	179.3		95.7	87.6	81.2	81.6	126.3	86.5	30.3	2
1	213.8	212.5		114.8	108.2	104.5	102.5	175.7	107.5	42.0	1
0	*****	*****		*****	*****	*****	*****	*****	*****	*****	0

Table B-2. Temperature Printout: Uncoated (Continued)

RUN 3 DATE 10/28/80

T/C NO.	T/C TEMPERATURES DURING RUN, °F								AVG TEMPS °F	AVG TEMPS °C	T/C NO.
32	*****	*****	*****	*****	*****	*****	*****	*****	*****	*****	32
31	439.6	426.1	424.1	431.2	430.1	439.2	421.0	437.8	431.1	221.9	31
30	-1.0	-1.1	-1.2	-1.0	-0.9	-0.6	-0.4	-0.4	-0.8	-18.2	30
29	368.8	369.3	369.1	370.2	370.6	372.0	371.2	372.8	370.5	188.2	29
28	286.6	287.6	287.2	288.2	288.6	289.5	288.9	290.1	288.3	142.5	28
27	287.7	288.1	288.1	288.9	289.3	290.0	289.9	290.8	289.1	142.9	27
26	204.5	203.9	204.7	205.0	205.8	206.0	206.0	206.2	205.3	96.4	26
25	202.1	202.5	201.9	203.8	202.7	204.9	202.4	204.9	203.2	95.2	25
24	246.3	246.8	247.0	247.3	247.8	248.3	248.6	249.2	247.7	119.9	24
23	158.4	158.8	159.0	159.1	159.8	160.1	160.2	160.5	159.5	70.9	23
22	258.6	259.0	259.5	259.7	260.4	260.5	261.1	261.5	260.0	126.8	22
21	116.1	116.1	116.5	116.6	117.0	117.6	117.8	117.8	116.9	47.2	21
20	144.6	144.6	145.0	145.3	145.7	146.0	146.7	147.0	145.6	63.2	20
19	189.5	189.7	190.5	190.2	191.1	191.1	192.2	192.5	190.9	88.3	19
18	400.9	399.4	401.7	402.2	402.9	402.6	401.9	404.3	402.0	205.7	18
17	77.8	78.0	77.8	78.1	78.3	78.7	79.0	79.2	78.4	25.8	17
16	103.3	103.5	103.5	103.6	104.0	104.3	104.8	105.0	104.0	40.0	16
15	132.0	132.3	132.3	132.4	132.9	133.1	133.7	134.0	132.8	56.0	15
14	143.2	143.6	143.8	143.9	144.5	144.6	145.3	145.6	144.3	62.4	14
13	150.4	151.0	150.9	151.1	151.6	152.0	152.9	152.9	151.6	66.5	13
12	*****	*****	*****	*****	*****	*****	*****	*****	*****	*****	12
11	*****	*****	*****	*****	*****	*****	*****	*****	*****	*****	11
10	*****	*****	*****	*****	*****	*****	*****	*****	*****	*****	10
9	146.6	146.9	147.0	147.3	147.7	148.1	148.6	148.7	147.6	64.3	9
8	200.8	201.3	201.4	201.6	202.2	202.7	203.4	203.4	202.1	94.6	8
7	76.7	76.9	76.9	77.0	77.5	77.7	78.1	78.4	77.4	25.2	7
6	103.4	103.6	103.7	103.8	104.1	104.5	104.9	105.1	104.1	40.1	6
5	136.3	136.7	136.8	136.9	137.5	137.7	138.1	138.5	137.3	58.5	5
4	148.0	148.1	148.2	148.5	149.2	149.4	149.8	150.1	148.9	65.0	4
3	159.7	159.9	159.8	160.3	161.2	161.1	161.8	161.8	160.7	71.6	3
2	204.1	204.3	204.6	204.9	205.8	206.0	206.7	206.6	205.4	96.4	2
1	243.7	244.6	244.8	245.0	245.8	245.8	246.7	246.8	245.4	118.7	1
0	*****	*****	*****	*****	*****	*****	*****	*****	*****	*****	0

Table B-2. Temperature Printout: Uncoated (Continued)

RUN 4 DATE 10/28/80

T/C NO.	T/C TEMPERATURES DURING RUN, °F								AVG TEMPS °F	AVG TEMPS °C	T/C NO.
32	*****	*****	*****	*****	*****	*****	*****	*****	*****	*****	32
31	439.4	454.0	445.1	454.8	452.1	451.8	454.5	450.1	450.2	232.5	31
30	0.6	0.5	0.3	0.2	-0.1	-0.2	-0.2	-0.3	0.1	-17.7	30
29	377.9	379.0	378.5	378.8	378.8	378.8	379.6	379.6	378.9	192.9	29
28	284.8	285.7	285.3	285.5	286.3	285.2	286.0	285.6	285.6	141.0	28
27	283.5	283.9	283.5	284.1	284.2	283.5	284.3	284.4	283.9	140.1	27
26	198.9	199.3	198.9	199.4	199.3	199.2	198.8	198.8	199.1	92.9	26
25	189.2	189.0	189.9	190.4	188.7	189.1	189.9	191.3	189.7	87.7	25
24	238.6	239.0	238.9	239.2	239.1	239.1	239.4	239.4	239.1	115.1	24
23	149.7	149.7	149.7	150.0	149.6	149.8	150.1	149.9	149.8	65.5	23
22	251.7	251.9	251.8	252.1	252.1	252.0	252.5	252.4	252.1	122.4	22
21	111.5	111.7	111.8	111.5	111.6	111.1	111.3	111.6	111.5	44.2	21
20	138.1	138.3	138.0	138.1	138.1	137.7	138.2	138.0	138.1	59.0	20
19	183.8	183.9	183.7	184.1	184.6	183.3	183.7	183.3	183.8	84.4	19
18	418.4	418.9	417.0	420.3	418.9	419.1	419.4	418.9	418.9	215.1	18
17	72.0	72.1	71.9	72.0	71.8	71.6	71.9	71.7	71.9	22.2	17
16	96.9	96.9	96.7	96.9	96.9	96.6	96.8	96.7	96.8	36.0	16
15	125.4	125.4	125.2	125.4	125.4	125.1	125.4	125.2	125.3	51.9	15
14	137.1	137.2	137.1	137.2	137.4	137.1	137.3	137.1	137.2	58.5	14
13	144.5	144.6	144.5	144.4	144.6	144.1	144.0	144.4	144.5	62.6	13
12	*****	*****	*****	*****	*****	*****	*****	*****	*****	*****	12
11	*****	*****	*****	*****	*****	*****	*****	*****	*****	*****	11
10	*****	*****	*****	*****	*****	*****	*****	*****	*****	*****	10
9	140.5	140.5	140.6	140.3	140.5	140.2	140.7	140.3	140.5	60.3	9
8	195.0	194.8	195.0	194.7	194.9	194.4	195.2	194.8	194.9	90.6	8
7	70.9	70.8	70.9	70.7	70.7	70.7	70.7	71.4	70.9	21.6	7
6	96.3	96.4	96.5	96.3	96.2	96.2	96.1	96.3	96.3	35.8	6
5	129.7	129.8	129.9	128.6	128.6	128.8	128.8	128.8	128.8	53.8	5
4	140.5	140.6	141.0	140.5	140.7	140.5	140.8	140.9	140.7	60.4	4
3	153.5	153.4	153.9	153.2	153.7	153.1	153.5	153.7	153.5	67.6	3
2	197.1	197.2	197.8	196.9	197.6	197.1	197.5	197.6	197.5	92.0	2
1	237.9	237.0	238.5	238.1	238.0	238.1	238.5	238.5	238.2	114.6	1
0	*****	*****	*****	*****	*****	*****	*****	*****	*****	*****	0

Table B-2. Temperature Printout: Uncoated (Continued)

RUN 5 (SHEET 1 OF 3) DATE 10/28/80

T/C NO.	T/C TEMPERATURES DURING RUN, °F								AVG TEMPS °F	AVG TEMPS °C	T/C NO.
32	*****	*****	*****	*****	*****	*****	*****	*****			32
31	425.8	420.8	425.7	426.0	413.9	433.8	419.6	422.5			31
30	- 22.1	- 21.8	- 21.7	- 21.6	- 21.3	- 21.3	- 21.0	- 20.7			30
29	363.3	362.7	362.8	362.5	362.3	363.8	362.9	363.1			29
28	258.6	259.0	244.0	245.3	253.9	256.5	256.4	257.4			28
27	256.1	258.2	248.1	243.7	251.9	255.5	255.3	255.9			27
26	174.7	174.1	171.8	164.6	168.4	171.0	172.2	172.9			26
25	169.0	169.6	165.9	159.0	163.7	164.7	165.5	167.2			25
24	73.9	74.5	74.5	74.7	74.9	75.0	74.1	*****			24
23	122.6	122.6	122.6	119.3	118.5	118.9	119.6	120.4			23
22	224.7	224.4	223.4	211.1	215.7	219.4	220.9	221.9			22
21	83.1	63.3	83.7	75.0	78.6	81.1	82.2	83.1			21
20	100.7	100.8	101.0	83.9	95.2	98.8	99.6	100.2			20
19	137.1	137.6	134.1	101.1	129.5	134.3	135.1	136.0			19
18	398.9	399.0	400.5	398.3	399.7	399.6	398.9	398.8			18
17	43.1	43.2	43.9	37.1	39.4	41.8	43.2	43.6			17
16	64.7	64.9	65.4	56.1	60.0	63.3	64.5	65.1			16
15	93.2	93.4	93.7	81.0	87.5	91.2	92.6	93.3			15
14	101.5	101.6	102.4	84.8	95.1	99.6	100.8	101.6			14
13	101.1	101.0	102.1	75.6	93.0	98.6	99.6	100.6			13
12	*****	*****	*****	*****	*****	*****	*****	*****			12
11	*****	*****	*****	*****	*****	*****	*****	*****			11
10	*****	*****	*****	*****	*****	*****	*****	*****			10
9	100.3	100.5	101.3	74.9	91.3	97.2	98.2	98.6			9
8	146.1	146.2	147.9	87.7	133.1	140.8	141.9	142.3			8
7	42.8	42.6	43.3	38.2	38.7	41.0	42.4	43.1			7
6	65.9	66.0	66.8	58.7	59.9	63.8	65.6	66.0			6
5	96.2	96.2	97.4	82.3	88.3	93.2	95.2	95.8			5
4	102.8	102.8	103.4	80.1	93.1	99.3	101.5	101.9			4
3	106.2	106.2	107.4	73.3	93.1	101.8	104.0	104.1			3
2	150.1	149.9	152.8	86.7	133.3	143.5	146.2	146.4			2
1	206.1	206.0	207.3	116.0	192.1	200.0	202.2	201.9			1
0	*****	*****	*****	*****	*****	*****	*****	*****			0

▲ H_2O ON

Table B-2. Temperature Printout: Uncoated (Continued)

RUN 5 (SHEET 2 OF 3) DATE 10/28/80

T/C NO.	T/C TEMPERATURES DURING RUN, °F								AVG TEMPS °F	AVG TEMPS °C	T/C NO.
32	*****	*****	*****	*****	*****	*****	*****	*****			32
31	416.6	426.3	417.6	424.8	417.5	428.2	424.1	414.7			31
30	-20.5	-20.6	-20.2	-20.1	-19.8	-19.8	-19.4	-19.3			30
29	363.1	363.2	363.3	363.2	363.0	363.5	362.6	362.4			29
28	256.0	255.9	255.2	255.6	254.5	254.3	253.9	253.0			28
27	255.3	254.9	254.7	254.8	253.3	252.9	252.7	251.8			27
26	172.8	173.2	173.3	173.4	172.8	172.8	172.0	172.1			26
25	167.8	166.6	164.9	165.4	165.0	163.2	163.8	162.7			25
24	*****	*****	*****	*****	*****	*****	*****	*****			24
23	120.9	120.9	121.2	121.2	121.2	120.9	120.7	120.5			23
22	222.2	221.2	221.1	220.9	220.7	219.5	219.3	219.0			22
21	83.3	83.0	83.0	83.3	83.5	83.2	83.2	83.2			21
20	100.1	99.0	99.2	99.3	99.5	99.2	99.5	99.6			20
19	135.7	132.9	133.6	133.4	132.5	132.1	132.5	132.4			19
18	400.0	398.7	400.9	398.3	398.8	399.0	399.3	400.1			18
17	44.1	43.9	43.8	44.0	44.2	44.0	43.9	44.0			17
16	65.4	65.1	65.3	65.1	65.3	64.9	64.7	64.9			16
15	93.4	93.1	93.3	93.1	93.3	92.8	92.5	92.5			15
14	101.8	101.3	101.4	101.2	101.4	100.8	100.5	100.2			14
13	100.9	100.6	100.2	100.0	100.2	99.2	99.0	98.5			13
12	*****	*****	*****	*****	*****	*****	*****	*****			12
11	*****	*****	*****	*****	*****	*****	*****	*****			11
10	*****	*****	*****	*****	*****	*****	*****	*****			10
9	99.1	97.1	97.0	97.1	97.2	96.5	97.4	97.7			9
8	142.8	137.6	138.1	137.6	137.7	135.7	137.7	137.3			8
7	43.6	43.4	43.6	43.4	43.9	43.4	43.5	43.1			7
6	66.7	66.4	66.3	66.2	66.5	66.0	66.0	66.0			6
5	96.5	96.1	96.1	95.8	96.1	95.2	95.1	94.9			5
4	102.3	102.0	101.9	101.5	101.9	101.0	100.9	100.4			4
3	104.5	104.1	103.2	103.2	103.3	101.8	101.7	100.7			3
2	146.7	145.1	143.7	143.7	143.4	139.2	140.0	139.0			2
1	201.8	196.1	196.3	195.3	195.6	186.7	189.8	188.5			1
0	*****	*****	*****	*****	*****	*****	*****	*****			0

Table B-2. Temperature Printout: Uncoated (Continued)

RUN 5 (SHEET 3 OF 3) DATE 10/28/80

T/C NO.	T/C TEMPERATURES DURING RUN, °F				AVG TEMPS °F	AVG TEMPS °C	T/C NO.
32	*****	*****	*****	*****	*****	*****	32
31	427.6	422.3	426.7	424.5	422.7	217.2	31
30	-19.0	-19.0	-18.5	-18.4	-20.1	-29.0	30
29	363.4	361.7	362.8	363.1	363.0	184.0	29
28	253.3	250.8	244.1	249.4	254.8	123.9	28
27	251.7	249.4	243.6	247.0	253.9	123.4	27
26	172.1	170.7	168.0	167.3	172.4	78.1	26
25	162.2	161.5	157.2	159.6	164.7	73.8	25
24	*****	*****	*****	*****	*****	*****	24
23	120.2	119.9	119.0	117.9	120.5	49.2	23
22	218.3	217.4	213.5	211.4	220.1	104.6	22
21	82.9	82.8	81.2	79.8	82.9	28.3	21
20	99.4	98.6	95.2	93.7	99.4	37.5	20
19	132.0	130.0	118.9	117.7	133.3	56.3	19
18	399.0	398.7	400.3	398.3	399.2	204.2	18
17	43.7	43.4	42.4	41.5	43.7	6.5	17
16	64.2	63.6	62.2	60.2	64.7	18.2	16
15	91.3	91.0	88.8	86.7	92.6	33.7	15
14	98.8	98.2	95.8	93.1	100.6	38.1	14
13	97.9	96.5	92.6	89.3	99.4	37.5	13
12	*****	*****	*****	*****	*****	*****	12
11	*****	*****	*****	*****	*****	*****	11
10	*****	*****	*****	*****	*****	*****	10
9	97.1	96.3	93.0	90.3	97.4	36.4	9
8	136.3	134.0	122.1	116.9	138.4	59.2	8
7	42.7	42.7	41.8	40.6	43.1	6.2	7
6	65.5	65.3	63.5	62.2	66.0	18.9	6
5	94.3	93.9	91.4	89.5	95.2	35.1	5
4	99.6	98.6	95.9	93.0	101.0	38.4	4
3	99.9	98.1	94.2	90.2	102.3	39.1	3
2	137.5	133.9	119.9	114.6	142.2	61.3	2
1	185.5	180.1	147.8	145.5	193.8	90.0	1
0	*****	*****	*****	*****	*****	*****	0

▲ H_2O OFF

Table B-2. Temperature Printout: Uncoated (Continued)

RUN 6 (SHEET 1 OF 3) DATE 10/28/80

T/C NO.	T/C TEMPERATURES DURING RUN, °F								AVG TEMPS °F	AVG TEMPS °C	T/C NO.
32	****.*	****.*	****.*	****.*	****.*	****.*	****.*	****.*			32
31	394.2	395.6	389.4	387.0	393.5	389.3	386.4	387.9			31
30	-20.5	-20.3	-20.1	-20.1	-19.8	-19.7	-19.6	-19.4			30
29	360.2	358.6	357.5	357.7	357.8	356.5	355.1	355.5			29
28	232.6	210.8	224.3	227.4	222.9	222.9	221.2	220.6			28
27	228.5	209.3	218.0	222.2	219.6	219.1	216.8	216.8			27
26	143.3	134.8	135.1	138.1	137.7	138.1	137.6	136.2			26
25	147.4	135.0	139.8	141.7	140.8	139.8	138.7	139.1			25
24	75.9	79.3	76.1	76.1	76.4	76.7	75.9	76.1			24
23	93.2	92.1	90.3	89.8	89.7	89.4	89.1	88.9			23
22	190.1	182.3	178.9	182.4	183.3	181.5	181.1	180.4			22
21	61.1	54.3	54.4	56.6	57.9	57.7	57.7	57.3			21
20	77.9	59.1	67.5	73.7	74.6	73.2	73.3	72.7			20
19	113.1	67.3	94.0	106.2	103.7	100.5	99.4	98.8			19
18	412.2	411.2	410.4	409.8	410.5	409.3	409.0	408.7			18
17	25.6	25.3	17.9	18.4	19.9	19.8	20.0	20.3			17
16	43.3	40.6	37.1	39.5	41.0	40.3	40.4	40.5			16
15	69.0	62.4	60.4	64.5	66.4	65.5	65.4	65.1			15
14	77.4	64.1	66.0	72.8	74.9	73.1	73.1	72.9			14
13	79.0	61.5	63.9	73.8	75.3	72.4	72.5	72.1			13
12	****.*	****.*	****.*	****.*	****.*	****.*	****.*	****.*			12
11	****.*	****.*	****.*	****.*	****.*	****.*	****.*	****.*			11
10	****.*	****.*	****.*	****.*	****.*	****.*	****.*	****.*			10
9	78.9	69.3	62.6	72.7	75.1	72.4	73.0	72.1			9
8	121.9	85.7	91.6	112.5	111.6	104.7	106.7	104.5			8
7	26.9	28.6	20.7	18.6	20.2	20.4	20.2	20.0			7
6	45.0	42.9	37.8	39.9	42.0	41.5	41.3	41.4			6
5	72.3	69.5	61.6	67.0	69.2	68.2	67.9	67.8			5
4	78.3	73.9	62.7	72.0	75.1	73.3	73.0	72.5			4
3	83.1	73.5	60.1	75.3	79.0	74.8	75.0	73.9			3
2	124.5	88.0	84.1	113.5	115.0	102.0	105.4	103.4			2
1	175.2	106.2	127.7	164.7	158.6	134.7	141.2	141.4			1
0	****.*	****.*	****.*	****.*	****.*	****.*	****.*	****.*			0

H_2O ON

Table B-2. Temperature Printout: Uncoated (Continued)

RUN 6 (SHEET 2 OF 3) DATE 10/28/80

T/C NO.	T/C TEMPERATURES DURING RUN, °F								AVG TEMPS °F	AVG TEMPS °C	T/C NO.
32	*****	*****	*****	*****	*****	*****	*****	*****			32
31	384.9	387.6	381.3	391.4	389.1	384.0	381.0	382.1			31
30	- 19.3	- 18.9	- 18.8	- 18.4	- 18.4	- 18.1	- 18.0	- 17.8			30
29	354.5	354.5	354.2	354.6	353.9	352.7	352.4	352.2			29
28	219.6	218.6	216.4	216.2	216.8	216.7	218.1	218.9			28
27	215.3	214.5	211.9	211.4	211.6	211.8	212.6	214.0			27
26	135.7	132.0	129.5	132.3	130.8	133.6	133.0	131.9			26
25	137.7	136.5	135.2	135.4	135.0	135.3	134.9	135.8			25
24	76.9	76.8	76.9	77.4	77.1	77.1	76.4	76.4			24
23	88.5	88.3	88.0	87.5	87.3	86.8	86.8	86.8			23
22	179.4	178.9	177.3	175.9	175.8	175.6	175.8	177.1			22
21	57.0	56.9	56.1	55.5	55.4	55.3	55.3	56.1			21
20	72.4	72.1	70.1	69.6	69.6	70.0	70.3	71.5			20
19	97.4	96.5	91.8	91.0	92.3	93.1	94.4	98.4			19
18	407.2	408.1	406.7	406.9	407.5	405.5	405.3	405.3			18
17	20.7	20.8	20.6	20.2	21.0	20.6	20.5	21.3			17
16	40.0	40.5	39.8	38.9	39.6	38.9	38.5	38.0			16
15	64.8	64.6	63.7	63.0	63.0	62.7	62.1	61.9			15
14	72.5	72.2	71.1	69.9	69.8	69.6	68.9	68.6			14
13	71.6	70.9	69.6	68.3	68.6	68.6	68.4	69.0			13
12	*****	*****	*****	*****	*****	*****	*****	*****			12
11	*****	*****	*****	*****	*****	*****	*****	*****			11
10	*****	*****	*****	*****	*****	*****	*****	*****			10
9	71.5	70.7	69.1	67.4	67.4	67.5	67.9	69.0			9
8	104.0	101.9	96.3	92.8	94.5	94.8	95.4	99.7			8
7	20.6	20.4	20.3	19.9	20.0	20.2	20.0	20.5			7
6	41.1	40.7	40.5	39.6	39.4	39.3	39.7	39.7			6
5	67.2	66.6	66.0	65.0	64.8	64.6	64.5	64.8			5
4	72.4	71.6	70.9	69.4	68.9	69.0	68.4	68.2			4
3	73.9	72.4	71.2	68.9	68.3	68.7	68.0	67.9			3
2	103.2	100.6	97.2	92.4	93.5	94.4	93.8	97.4			2
1	138.9	135.5	129.1	123.3	128.0	128.7	130.4	144.3			1
0	*****	*****	*****	*****	*****	*****	*****	*****			0

Table B-2. *Temperature Printout: Uncoated (Concluded)*

RUN 6 (SHEET 3 OF 3) DATE 10/28/80

T/C NO.	T/C TEMPERATURES DURING RUN, °F				AVG TEMPS °F	AVG TEMPS °C	T/C NO.
32	*****	*****	*****		*****	*****	32
31	386.5	391.8	381.7		386.4	197.0	31
30	-17.6	-17.4	-17.3		-18.6	-28.1	30
29	352.0	350.6	350.9		353.7	178.9	29
28	215.8	216.9	223.1		218.4	103.6	28
27	211.1	212.1	216.9		213.8	101.1	27
26	130.1	129.4	135.7		133.1	56.2	26
25	134.8	135.3	138.6		136.4	58.0	25
24	76.8	76.8	76.6		76.7	24.9	24
23	87.0	86.8	87.0		87.8	31.0	23
22	176.3	175.8	177.7		177.8	81.1	22
21	56.0	55.9	56.1		56.3	13.5	21
20	70.4	70.6	72.2		71.2	21.8	20
19	93.3	94.5	100.1	105.7	95.5	35.3	19
18	405.2	404.6	405.2	404.8	406.9	208.4	18
17	21.2	21.2	20.6	22.3	20.6	-6.3	17
16	38.9	39.2	39.6	42.1	39.5	4.2	16
15	62.4	62.6	63.4	66.4	63.6	17.6	15
14	69.2	69.4	70.9	74.5	70.8	21.6	14
13	69.2	69.0	71.0	75.6	70.0	21.1	13
12	*****	*****	*****	*****	*****	*****	12
11	*****	*****	*****	*****	*****	*****	11
10	*****	*****	*****	*****	*****	*****	10
9	68.7	67.8	69.7	74.2	69.6	20.9	9
8	95.3	95.1	102.5	112.8	98.9	37.2	8
7	20.6	20.6	19.8	20.2	20.3	-6.5	7
6	40.2	39.9	39.9	42.0	40.3	4.6	6
5	64.9	64.7	64.8	67.9	65.9	18.8	5
4	68.3	68.0	68.6	73.4	70.3	21.3	4
3	67.8	66.8	68.8	76.8	70.6	21.5	3
2	93.2	91.9	98.2	113.7	97.6	36.4	2
1	124.3	130.6	146.7	165.9	133.1	56.2	1
0	*****	*****	*****	*****	*****	*****	0

H_2O OFF

Table B-3. Test Conditions Summary: CAAPCO B-274

DATE 11/24-25/80	ICING CONDITION	DRY AIR		INTERMITTENT MAX.		CONTINUOUS MAX.	
	RUN NO.	11	12	9	10	7	8
	TAI FLOW RATE	100%	75%	100%	75%	100%	75%
FLIGHT:	**Condition**	Climb		Holding		Holding	
	Altitude, m	4,572		4,572		4,572	
	, (ft)	(15,000)		(15,000)		(15,000)	
	Velocity, m/s	190		138		131	
	, (knots)	(370)		(268)		(255)	
	Temperature, ^{o}C	-17.8		-6.1		-28.9	
	, (^{o}F)	(0)		(21)		(-20)	
	Horiz. Ext., km	-----		9.6		32.2	
	, (nm)	-----		(5.2)		(17.4)	
TUNNEL:	**Altitude, m**	-0-	-0-	-0-	-0-	-0-	-0-
	Velocity, m/s	70.2	70.2	67.1	67.1	85.8	85.8
	Equiv Temp, ^{o}C	-17.8	-17.8	-17.8	-17.8	-28.9	-28.9
(T/C 31)	**Actual Temp, ^{o}C**	-17.6	-17.6	-17.8	-17.9	-28.9	-29.2
	Drop Diam, microns	-----	-----	27.8	27.8	20.6	20.6
	LWC, g/m^3	-----	-----	2.10	2.10	0.29	0.29
	P_V, cm H_2O	34.5	34.8	31.8	31.8	54.6	54.6
	Time, seconds	-----	-----	70	70	245	245
FLOW TUBE:	**P_S, cm Hg**	90.7	62.2	64.8	36.8	77.0	37.3
	P_V, cm H_2O	24.1	18.0	18.8	12.2	20.8	12.7
(T/C 29)	Air Temp., ^{o}C	192.1	194.0	195.3	194.7	192.6	195.2
	Air Flow, kg/min	1.79	1.41	1.45	1.05	1.59	1.07
TAI SPRAY TUBE:	P_S, cm Hg	87.6	59.7	72.1	49.0	74.2	36.3
(T/C 30)	Air Temp., ^{o}C	187.2	187.3	188.8	185.9	186.7	186.3
COMMENTS:				Runs 9 and 10 Running wet coated surface. Ice 2 mm thick formed aft of coated area (aft of anti-iced area).		Run 7 Runback ice 1-2 mm thick on 2.5 cm upr surface on aft 7.5 cm lwr-surface(Figure 41). Run 8 Runback ice 1-2 mm thick to within 5 cm of l.e. on upr surface; to within 7.5 cm of l.e. on lwr surface (Figure 42).	

Table B-4. Temperature Printout: CAAPCO B-274

RUN 7 (SHEET 1 of 3) DATE 11/24/80

T/C NO.	T/C TEMPERATURES DURING RUN, °F								AVG TEMPS °F	AVG TEMPS °C	T/C NO.
32	3099	3195	3092	3187	3057	3188	3176	3094			32
31	- 215	- 214	- 214	- 213	- 211	- 209	- 207	- 207			31
30	3688	3703	3686	3696	3679	3695	3696	3682			30
29	3788	3813	3798	3809	3783	3808	3807	3779			29
28	2539	2549	2489	2497	2498	2515	2508	2495			28
27	2430	2435	2385	2378	2380	2388	2392	2375			27
26	1749	1752	1739	1719	1714	1718	1722	1723			26
25	1716	1730	1710	1694	1667	1679	1674	1720			25
24	*****	*****	*****	624	2029	638	640	645			24
23	1277	1281	1281	1272	1263	1260	1258	1257			23
22	2152	2156	2144	2113	2105	2106	2111	2105			22
21	841	845	839	823	815	816	815	817			21
20	1123	1125	1108	1072	1078	1082	1084	1083			20
19	1428	1440	1351	1285	1333	1346	1349	1340			19
18	*****	*****	*****	*****	*****	*****	*****	*****			18
17	547	548	550	516	503	504	510	513			17
16	892	894	894	869	869	874	877	878			16
15	1181	1180	1178	1146	1151	1158	1162	1164			15
14	1219	1219	1215	1163	1179	1190	1195	1195			14
13	1396	1398	1384	1281	1330	1347	1354	1353			13
12	1778	1779	1739	1583	1683	1699	1707	1701			12
11	2058	2055	1993	1885	1976	1986	1989	1966			11
10	746	745	750	723	718	714	714	713			10
9	1092	1095	1099	1032	1032	1033	1034	1034			9
8	1452	1452	1462	1269	1323	1329	1333	1329			8
7	647	646	652	625	611	613	616	623			7
6	885	886	889	861	860	861	865	867			6
5	1143	1144	1146	1106	1108	1109	1115	1116			5
4	1166	1167	1171	1109	1112	1120	1128	1130			4
3	1322	1324	1336	1189	1226	1246	1253	1254			3
2	1754	1753	1769	1489	1626	1648	1652	1655			2
1	2039	2097	2099	1835	1977	1982	1988	1982			1
0	*****	*****	*****	*****	*****	*****	*****	*****			0

▲ H_2O ON

Table B-4. *Temperature Printout: CAAPCO B-274 (Continued)*

RUN 7 (SHEET 2 of 3) DATE 11/24/80

T/C NO.	T/C TEMPERATURES DURING RUN, °F								AVG TEMPS °F	AVG TEMPS °C	T/C NO.
32	313.9	311.5	309.4	313.0	318.5	317.1	308.2	311.4			32
31	-20.5	-20.3	-20.0	-19.9	-19.8	-19.7	-19.4	-19.4			31
30	368.8	368.1	367.5	367.8	368.6	368.1	367.3	367.8			30
29	379.6	378.2	377.5	377.5	379.1	379.2	377.3	378.4			29
28	248.6	247.8	248.3	249.3	249.0	248.8	247.5	246.2			28
27	236.5	235.7	235.6	236.2	236.5	236.6	235.8	233.9			27
26	171.3	170.3	170.1	169.8	170.1	170.2	170.1	169.2			26
25	168.0	165.1	166.5	164.8	162.3	166.8	166.9	166.3			25
24	64.1	64.0	64.1	64.2	64.3	64.4	64.2	97.0			24
23	125.4	124.7	124.6	124.0	124.3	124.3	124.0	124.1			23
22	209.5	208.6	207.9	207.9	208.2	208.2	208.4	208.0			22
21	81.5	81.3	81.4	81.4	81.5	81.8	82.0	81.3			21
20	107.4	107.2	107.1	107.7	108.1	108.5	108.5	107.2			20
19	131.0	129.8	130.5	132.4	133.3	133.7	133.6	128.2			19
18	****.*	****.*	****.*	****.*	****.*	****.*	****.*	****.*			18
17	51.4	51.0	51.0	51.1	51.1	51.4	51.5	51.6			17
16	87.4	86.7	86.4	86.2	86.2	86.4	86.2	85.7			16
15	115.7	115.0	114.6	114.3	114.4	114.5	114.4	113.5			15
14	118.8	117.8	117.3	117.0	117.1	117.6	117.3	116.3			14
13	133.4	131.9	131.6	131.7	132.3	132.7	132.3	130.8			13
12	165.9	163.9	164.6	165.4	166.9	167.0	166.6	162.9			12
11	190.7	189.0	191.2	193.0	195.4	194.8	195.5	190.4			11
10	70.9	70.5	70.3	70.1	70.2	70.1	70.1	69.7			10
9	102.5	101.8	101.4	102.0	102.4	102.7	102.8	102.3			9
8	127.5	120.9	121.8	128.6	130.2	130.9	130.2	128.7			8
7	61.5	60.6	60.2	59.8	59.7	59.7	59.7	59.9			7
6	85.9	85.1	84.6	84.3	84.3	84.4	84.5	84.1			6
5	110.7	109.7	108.9	108.6	108.8	108.9	108.9	108.3			5
4	112.0	110.3	109.6	108.9	109.0	109.3	109.2	108.2			4
3	122.5	120.1	119.2	119.1	119.6	120.2	120.1	118.3			3
2	157.9	154.2	153.8	155.0	157.0	157.7	157.1	153.8			2
1	189.5	187.0	166.8	189.5	192.2	192.6	192.9	189.5			1
0	****.*	****.*	****.*	****.*	****.*	****.*	****.*	****.*			0

Table B-4. Temperature Printout: CAAPCO B-274 (Continued)

RUN 7 (SHEET 3 of 3) DATE 11/24/80

T/C NO.	T/C TEMPERATURES DURING RUN, °F					AVG TEMPS °F	AVG TEMPS °C	T/C NO.
32	311.1	313.0	311.2	310.8	315.2	312.8	156.0	32
31	-19.1	-19.1	-18.9	-18.6	-18.4	-20.1	-28.9	31
30	367.2	367.9	367.0	366.9	367.9	368.2	186.7	30
29	377.6	379.2	377.9	376.7	378.7	378.8	192.6	29
28	246.5	246.3	246.7	250.0	251.2	248.5	120.3	28
27	233.7	234.1	234.2	237.0	239.0	236.4	113.6	27
26	169.1	169.0	168.7	170.5	171.6	170.7	77.0	26
25	163.3	166.3	165.2	171.4	168.4	166.8	74.9	25
24	90.6	144.7	65.0	*****	64.3	81.5	27.5	24
23	123.8	123.7	123.3	123.8	124.2	125.0	51.7	23
22	207.1	206.5	206.3	208.0	209.9	209.1	98.4	22
21	81.0	80.7	80.7	81.4	82.1	81.6	27.6	21
20	106.5	106.1	106.1	107.5	108.9	107.7	42.0	20
19	127.0	127.4	127.8	132.5	135.8	131.5	55.3	19
18	*****	*****	*****	*****	*****	*****	*****	18
17	50.6	49.9	49.7	49.7	50.8	51.2	10.7	17
16	84.5	83.5	83.3	84.8	86.3	86.4	30.2	16
15	112.3	111.6	111.4	113.7	115.3	114.6	45.9	15
14	114.6	113.9	114.0	116.5	118.6	117.4	47.4	14
13	127.9	127.5	128.1	131.3	134.3	132.0	55.6	13
12	158.6	158.6	159.9	165.5	169.4	165.4	74.1	12
11	185.0	185.6	187.4	196.9	200.1	192.8	89.3	11
10	68.8	68.3	68.0	68.0	69.0	70.6	21.4	10
9	100.7	100.3	100.2	101.5	104.2	102.7	39.3	9
8	122.8	122.7	123.3	129.5	135.9	128.9	53.8	8
7	59.4	58.7	58.5	57.9	58.2	60.7	15.9	7
6	83.2	82.6	82.5	83.4	85.5	85.0	29.4	6
5	106.9	106.1	106.1	107.5	109.6	109.5	43.0	5
4	106.4	105.6	105.5	106.8	110.1	110.0	43.3	4
3	115.4	114.6	114.8	117.9	123.7	120.8	49.3	3
2	147.5	147.3	148.4	156.7	165.7	157.2	69.6	2
1	182.9	182.8	184.1	195.9	203.6	191.5	88.6	1
0	*****	*****	*****	*****	*****	*****	*****	0

H_2O OFF

Table B-4. Temperature Printout: CAAPCO B-274 (Continued)

RUN 8 (SHEET 1 of 3) DATE 11/24/80

T/C NO.	T/C TEMPERATURES DURING RUN, °F								AVG TEMPS °F	AVG TEMPS °C	T/C NO.
32	2806	2796	2770	2843	2763	2829	2815	2792			32
31	-221	-221	-217	-217	-215	-213	-213	-211			31
30	3680	3679	3675	3681	3671	3677	3677	3672			30
29	3845	3840	3834	3848	3825	3838	3838	3837			29
28	2234	2237	2201	2202	2202	2202	2199	2177			28
27	2111	2117	2082	2092	2076	2078	2066	2060			27
26	1409	1412	1403	1395	1387	1388	1389	1391			26
25	1439	1436	1409	1413	1413	1391	1402	1387			25
24	1709	1711	1701	1687	1680	1672	1666	1660			24
23	911	912	911	907	907	903	901	897			23
22	1764	1767	1760	1745	1736	1728	1723	1716			22
21	609	611	611	595	590	587	588	588			21
20	839	843	830	819	811	806	805	804			20
19	1140	1157	1074	1101	1090	1090	1085	1055			19
18	*****	*****	*****	*****	*****	*****	*****	*****			18
17	310	311	313	306	306	306	307	306			17
16	588	587	588	563	568	570	571	571			16
15	867	868	865	852	855	855	854	853			15
14	923	924	921	903	910	910	909	905			14
13	1078	1087	1068	1041	1054	1061	1055	1044			13
12	1435	1448	1397	1372	1397	1405	1392	1366			12
11	1717	1721	1648	1658	1672	1676	1659	1612			11
10	553	557	559	539	533	526	523	520			10
9	829	833	834	803	790	775	765	760			9
8	1153	1174	1155	1084	1067	1047	1030	1007			8
7	391	395	397	389	383	383	383	383			7
6	603	606	607	583	578	578	578	577			6
5	841	842	846	827	823	821	817	813			5
4	883	886	889	860	859	856	853	845			4
3	1020	1032	1029	961	973	967	960	944			3
2	1398	1411	1405	1294	1330	1321	1305	1268			2
1	1723	1725	1704	1617	1633	1625	1602	1566			1
0	*****	*****	*****	*****	*****	*****	*****	*****			0

H_2O ON

Table B-4. Temperature Printout: CAAPCO B-274 (Continued)

RUN 8 (SHEET 2 of 3) DATE 11/24/80

T/C NO.	T/C TEMPERATURES DURING RUN, °F								AVG TEMPS °F	AVG TEMPS °C	T/C NO.
32	279,5	278,7	279,9	276,3	281,2	279,5	279,1	277,9			32
31	- 20,9	- 20,7	- 20,4	- 20,3	- 20,2	- 19,9	- 19,7	- 19,5			31
30	367,1	367,3	367,0	367,0	367,4	367,2	367,0	366,9			30
29	383,3	383,3	383,0	383,2	383,9	383,1	382,8	382,5			29
28	217,4	215,7	216,6	214,6	214,6	213,9	213,8	214,7			28
27	204,4	203,4	203,2	202,8	201,6	201,4	201,4	201,5			27
26	137,3	137,0	136,4	136,1	136,0	135,7	135,2	135,2			26
25	138,5	138,2	137,7	136,8	136,2	136,4	137,1	136,6			25
24	164,8	163,9	163,3	163,1	162,4	162,2	161,9	161,8			24
23	89,5	89,2	89,1	88,8	88,4	88,2	88,1	88,0			23
22	170,6	169,7	169,1	168,9	168,2	168,0	167,9	167,7			22
21	58,7	58,4	58,2	57,9	57,3	57,0	56,7	56,6			21
20	79,4	78,7	78,3	77,8	76,5	76,7	76,3	76,4			20
19	102,3	100,9	99,9	98,6	95,1	96,4	96,5	98,5			19
18	*****	*****	*****	*****	*****	*****	*****	*****			18
17	30,6	30,4	30,3	30,0	29,7	29,5	29,4	29,0			17
16	56,9	56,5	56,2	55,9	55,2	54,9	54,5	54,1			16
15	84,7	84,1	83,5	82,9	81,9	81,4	80,5	80,1			15
14	89,6	88,9	88,1	87,0	85,7	85,2	84,1	83,9			14
13	102,0	100,6	99,6	98,6	96,3	96,5	95,4	95,9			13
12	132,3	130,2	128,6	126,7	121,9	123,3	122,5	125,0			12
11	157,8	155,7	155,2	153,2	148,4	150,2	149,5	152,8			11
10	51,7	51,3	51,0	50,7	50,2	49,8	49,6	49,4			10
9	74,8	73,7	73,3	72,5	71,7	71,3	70,7	70,4			9
8	97,0	95,1	94,4	93,3	91,2	91,3	91,0	91,8			8
7	38,0	37,6	37,6	37,5	37,4	37,1	37,1	37,0			7
6	56,9	56,1	55,9	55,6	55,5	55,2	54,8	54,7			6
5	80,0	78,9	78,4	77,7	77,3	76,8	76,1	75,9			5
4	83,1	81,7	81,0	79,8	79,0	78,5	77,2	77,0			4
3	91,5	89,6	88,9	87,7	86,2	85,5	84,7	84,4			3
2	119,2	116,8	115,7	115,0	112,6	113,3	113,0	114,1			2
1	150,7	148,6	148,0	147,5	145,0	146,2	146,1	147,7			1
0	*****	*****	*****	*****	*****	*****	*****	*****			0

Table B-4. Temperature Printout: CAAPCO B-274 (Continued)

RUN 8 (SHEET 3 of 3) DATE 11/24/80

T/C NO.	T/C TEMPERATURES DURING RUN, °F				AVG TEMPS °F	AVG TEMPS °C	T/C NO.
32	281.4	278.0	282.7	279.1	279.7	137.6	32
31	-19.5	-19.2	-19.0	-19.0	-20.5	-29.2	31
30	367.0	366.9	367.2	367.1	367.4	186.3	30
29	383.4	382.6	383.2	383.1	383.3	195.2	29
28	213.7	213.4	216.1	217.8	216.4	102.4	28
27	201.5	201.3	203.1	205.4	204.0	95.6	27
26	135.2	135.2	135.5	136.2	136.9	58.3	26
25	136.9	137.0	136.9	137.7	138.1	58.9	25
24	161.7	65.9	66.0	163.0	157.8	69.9	24
23	87.9	87.9	87.7	88.0	89.1	31.7	23
22	167.6	167.6	167.5	168.9	170.0	76.7	22
21	56.5	56.3	56.2	56.8	57.9	14.4	21
20	76.6	76.3	76.6	78.3	78.5	25.8	20
19	97.9	98.2	101.2	106.3	101.8	38.8	19
18	*****	*****	*****	*****	*****	*****	18
17	29.0	28.7	28.5	28.8	30.0	-1.1	17
16	53.7	53.1	52.6	53.9	55.7	13.2	16
15	79.3	78.3	77.3	79.3	82.9	28.3	15
14	83.1	82.0	80.7	83.1	87.4	30.8	14
13	95.6	95.1	95.5	99.1	100.1	37.8	13
12	123.7	124.2	126.5	133.3	130.1	54.5	12
11	151.3	152.9	157.5	164.6	157.0	69.4	11
10	49.1	48.8	48.8	49.2	51.0	10.6	10
9	70.3	69.9	69.6	70.8	73.9	23.3	9
8	91.6	91.6	91.6	96.1	96.8	36.0	8
7	36.7	36.7	36.7	36.8	37.7	3.2	7
6	54.3	54.2	53.8	54.0	56.2	13.4	6
5	75.3	74.9	74.2	74.5	78.8	26.0	5
4	76.3	75.3	74.3	75.8	81.1	27.3	4
3	84.2	83.9	83.6	86.3	89.8	32.1	3
2	113.7	113.8	113.7	126.9	119.9	48.8	2
1	146.8	147.7	147.8	163.1	151.9	66.6	1
0	*****	*****	*****	*****	*****	*****	0

H_2O OFF

Table B-4. Temperature Printout: CAAPCO B-274 (Continued)

RUN 9 DATE 11/25/80

T/C NO.	T/C TEMPERATURES DURING RUN, °F									AVG TEMPS °F	AVG TEMPS °C	T/C NO.
32	365.3	364.4	373.2	366.0	370.8	371.6	362.4	371.6	367.6	368.1	186.7	32
31	-0.4	-0.5	-0.6	-1.0	-0.7	-0.1	0.6	1.0	1.0	-.055	-17.8	31
30	371.5	371.4	372.4	371.3	372.1	372.4	371.5	372.4	371.7	371.9	188.8	30
29	382.8	382.4	384.8	382.1	385.0	384.3	382.6	384.0	383.3	383.5	195.3	29
28	264.7	264.7	265.0	252.2	248.9	246.4	244.5	249.4	259.2	254.9	123.8	28
27	253.1	253.1	254.3	239.9	235.4	233.0	231.4	234.3	244.4	242.10	116.7	27
26	189.4	189.2	189.8	183.9	179.4	177.0	176.2	176.5	181.8	182.6	83.7	26
25	178.6	177.5	183.3	171.1	171.5	166.9	165.9	169.8	174.2	173.2	78.4	25
24	*****	*****	*****	*****	*****	*****	*****	*****	*****	*****	*****	24
23	144.0	144.3	144.8	143.8	141.2	138.0	135.0	132.9	133.4	139.7	59.8	23
22	229.2	229.2	229.9	225.1	218.5	214.7	213.1	212.6	217.9	221.1	105.0	22
21	105.7	105.7	106.1	97.9	93.7	88.8	86.3	86.9	93.7	96.1	35.6	21
20	136.7	137.0	139.8	120.9	113.6	108.6	106.8	103.6	123.0	121.7	49.8	20
19	162.6	169.7	173.7	135.5	123.7	119.3	118.0	120.6	152.0	142.5	61.4	19
18	*****	*****	*****	*****	*****	*****	*****	*****	*****	*****	*****	18
17	76.3	76.4	76.3	73.3	69.0	67.0	66.1	65.7	68.4	70.9	21.6	17
16	108.5	108.5	108.6	103.1	98.6	96.4	95.2	94.8	99.4	101.5	38.6	16
15	137.7	137.7	139.7	128.9	124.0	121.4	119.9	119.9	126.9	128.3	53.5	15
14	146.1	146.0	148.8	132.6	124.0	121.2	119.7	119.9	132.5	132.3	55.7	14
13	167.0	167.1	171.5	144.2	130.5	127.4	125.9	125.0	149.5	145.5	63.0	13
12	198.4	198.7	201.3	166.7	152.9	149.4	148.4	148.0	180.7	171.6	77.6	12
11	219.0	219.5	220.3	186.8	176.9	172.8	172.0	171.2	205.1	193.7	89.8	11
10	97.8	97.9	98.1		87.1	84.0	82.6	82.3	38.1	89.7	32.1	10
9	135.0	134.9	137.3		111.4	106.3	104.2	103.4	116.8	118.7	48.2	9
8	170.6	170.7	173.6	147.0	97.9	121.8	116.4	92.2	145.3	137.3	58.5	8
7	79.8	86.1	85.9	84.0	78.6	75.8	74.5	74.1	76.2	79.4	26.3	7
6	109.3	103.3	109.5	106.6	99.6	97.1	95.8	95.1	98.3	102.3	39.0	6
5	135.6	135.6	136.4	130.4	121.7	118.6	116.7	116.0	121.3	125.8	52.1	5
4	142.7	142.6	145.0	135.8	119.3	115.7	113.6	112.9	122.8	127.8	53.2	4
3	161.6	161.4	165.8	147.4	122.0	117.8	116.1	115.7	135.1	138.1	58.9	3
2	195.8	195.8	197.9	172.8	146.0	141.8	139.8	139.3	167.8	166.3	74.6	2
1	221.6	221.7	222.0	195.3	177.5	173.5	171.9	171.2	200.7	195.0	90.6	1
0	*****	*****	*****	*****	*****	*****	*****	*****	*****	*****	*****	0

H_2O ON H_2O OFF

Table B-4. Temperature Printout: CAAPCO B-274 (Continued)

RUN 10 DATE 11/25/80

T/C NO.	T/C TEMPERATURES DURING RUN, °F									AVG TEMPS °F	AVG TEMPS °C	T/C NO.
32	277.9	275.5	273.7	276.3	274.3	275.6	274.7	275.1	277.0	275.6	135.3	32
31	-0.4	-0.6	-0.8	-1.0	-0.8	-0.3	0.1	0.4	0.6	-0.3	-17.9	31
30	367.6	367.0	367.0	367.0	366.3	367.0	366.0	366.2	366.5	366.7	185.9	30
29	383.1	382.0	383.0	383.2	381.6	383.1	381.0	381.6	382.7	382.4	194.7	29
28	238.8	238.6	236.5	227.7	222.7	221.1	221.1	223.5	230.6	229.0	109.4	28
27	227.7	227.8	226.8	216.1	211.2	208.9	207.7	210.0	218.1	217.1	102.8	27
26	161.4	161.0	161.8	157.3	152.9	150.8	149.4	149.1	152.3	155.1	68.4	26
25	165.3	166.5	165.2	160.1	155.8	153.6	149.7	152.8	157.7	158.5	70.3	25
24	192.3	191.8	192.2	187.5	181.7	178.1	175.7	175.6	179.3	183.8	84.3	24
23	119.5	118.4	118.2	117.3	115.2	113.4	111.7	110.8	110.9	114.9	46.0	23
22	197.9	197.5	197.7	193.8	188.6	185.1	162.8	182.6	185.6	190.2	87.9	22
21	88.6	88.4	88.6	83.4	79.7	77.3	75.6	75.5	78.4	81.7	27.6	21
20	114.4	114.0	116.1	101.7	94.7	92.1	90.3	92.1	101.3	101.9	38.8	20
19	146.2	146.0	149.1	115.4	105.5	102.8	101.5	105.7	128.8	122.3	50.2	19
18	*****	*****	*****	*****	*****	*****	*****	*****	*****	*****	*****	18
17	58.6	58.3	58.0	56.7	54.0	52.5	51.5	51.4	52.6	54.8	12.7	17
16	86.4	85.1	86.2	83.2	79.2	77.4	75.9	76.0	78.7	81.0	27.2	16
15	113.4	113.0	114.4	108.0	102.8	100.5	98.6	98.9	103.1	105.9	41.1	15
14	122.8	122.6	125.8	112.7	104.7	102.0	100.0	100.7	109.2	111.2	44.0	14
13	140.8	140.4	144.9	121.1	109.6	106.8	104.8	106.1	123.3	122.0	50.0	13
12	171.5	171.1	173.3	141.4	130.2	127.4	125.7	127.1	152.9	146.7	63.7	12
11	192.8	192.4	192.5	161.2	152.9	150.7	148.8	151.1	177.4	168.9	76.1	11
10	82.3	82.6	82.8	78.7	74.6	71.6	69.7	69.0	71.5	75.9	24.4	10
9	114.1	113.8	116.1	104.1	94.4	90.6	88.6	88.1	97.0	100.8	38.2	9
8	147.2	146.9	149.2	123.3	107.6	103.5	101.8	101.7	123.3	122.7	50.4	8
7	67.8	67.1	67.2	66.0	62.4	60.3	59.1	58.8	60.1	63.2	17.3	7
6	88.1	87.9	88.2	86.2	81.6	78.6	77.0	76.5	78.6	82.5	28.1	6
5	111.8	111.7	112.5	108.2	101.8	97.9	95.9	95.3	98.7	103.8	39.9	5
4	120.3	120.3	122.1	113.7	102.8	97.9	95.8	95.3	102.0	107.8	42.1	4
3	137.7	137.6	141.2	122.7	104.7	99.5	97.5	97.3	112.4	116.7	47.1	3
2	169.9	169.8	170.9	144.8	124.9	120.3	118.3	118.2	142.1	142.1	61.2	2
1	193.6	193.2	193.4	164.9	151.5	148.4	146.2	146.4	172.1	167.7	75.4	1
0	*****	*****	*****	*****	*****	*****	*****	*****	*****	*****	*****	0

H_2O ON (between 3rd and 4th readings) H_2O OFF (between 7th and 8th readings)

Table B-4. Temperature Printout: CAAPCO B-274 (Continued)

RUN 11 (SHEET 1 of 2) DATE 11/25/80

T/C NO.	T/C TEMPERATURES DURING RUN, °F								AVG TEMPS °F	AVG TEMPS °C	T/C NO.
32	2998	2962	2988	2919	2953	2981	2968	2926			32
31	03	02	03	03	05	03	03	03			31
30	3700	3696	3699	3688	3692	3688	3690	3684			30
29	3791	3783	3787	3776	3775	3779	3786	3771			29
28	2748	2747	2745	2742	2740	2740	2740	2739			28
27	2662	2658	2660	2655	2655	2654	2654	2652			27
26	2037	2036	2036	2034	2036	2035	2034	2033			26
25	2017	2034	2021	2017	2011	2031	2031	1977			25
24	740	2385	2383	2385	2383	2381	2381	2379			24
23	1598	1598	1597	1597	1597	1596	1597	1595			23
22	2456	2455	2454	2455	2454	2450	2451	2449			22
21	1153	1151	1151	1151	1150	1151	1148	1148			21
20	1466	1463	1462	1462	1460	1461	1460	1460			20
19	1800	1799	1799	1799	1738	1797	1797	1794			19
18	*****	*****	*****	*****	*****	*****	*****	*****			18
17	860	860	859	859	859	857	857	858			17
16	1201	1200	1199	1199	1199	1197	1197	1197			16
15	1495	1494	1494	1494	1493	1492	1491	1489			15
14	1572	1570	1570	1572	1571	1569	1569	1568			14
13	1772	1771	1770	1772	1772	1768	1768	1765			13
12	2103	2103	2100	2104	2101	2099	2098	2096			12
11	2321	2323	2319	2322	2320	2316	2316	2315			11
10	1084	1084	1083	1087	1084	1083	1083	1082			10
9	1461	1460	1460	1460	1462	1457	1457	1457			9
8	1820	1818	1818	1819	1820	1815	1816	1814			8
7	896	949	947	947	949	947	945	946			7
6	1212	1212	1211	1211	1211	1209	1208	1208			6
5	1510	1510	1509	1509	1509	1508	1508	1506			5
4	1560	1560	1559	1558	1560	1557	1558	1556			4
3	1746	1744	1744	1746	1746	1742	1743	1741			3
2	2103	2102	2099	2101	2100	2099	2097	2096			2
1	2382	2383	2377	2382	2378	2376	2374	2373			1
0	*****	*****	*****	*****	*****	*****	*****	*****			0

Table B-4. Temperature Printout: CAAPCO B-274 (Continued)

RUN 11 (SHEET 2 of 2) DATE 11/25/80

T/C NO.	T/C TEMPERATURES DURING RUN, °F			AVG TEMPS °F	AVG TEMPS °C	T/C NO.
32	296.3	305.0	296.2	297.3	147.4	32
31	0.2	0.3	0.2	0.3	-17.6	31
30	368.1	369.3	367.9	369.0	187.2	30
29	376.9	377.9	376.4	377.8	192.1	29
28	274.0	274.0	273.7	274.2	134.6	28
27	265.0	265.2	265.0	265.5	129.7	27
26	202.8	202.9	202.8	203.3	95.2	26
25	201.5	201.6	201.1	201.6	94.2	25
24	237.7	237.8	237.8	223.2	106.2	24
23	159.3	159.1	159.2	159.6	70.9	23
22	244.8	244.8	244.9	245.2	118.4	22
21	114.8	114.8	114.6	115.0	46.1	21
20	146.0	146.0	146.0	146.1	63.4	20
19	179.3	179.6	179.6	179.7	82.1	19
18	****.*	****.*	****.*	*****	*****	18
17	85.5	85.8	85.7	85.8	29.9	17
16	119.4	119.6	119.6	119.8	48.8	16
15	148.8	149.0	149.0	149.2	65.1	15
14	156.7	156.8	156.9	157.0	69.4	14
13	176.5	176.6	176.8	126.9	80.5	13
12	209.4	209.5	209.7	209.9	98.8	12
11	231.3	231.2	231.6	231.8	111.0	11
10	107.9	108.2	108.3	108.3	42.4	10
9	145.5	145.6	145.7	145.8	63.2	9
8	181.1	181.2	191.4	181.6	83.1	8
7	94.4	94.4	94.4	94.2	34.6	7
6	120.6	120.6	120.7	120.9	49.4	6
5	150.4	150.3	150.4	150.7	65.9	5
4	155.3	155.4	155.6	155.7	68.7	4
3	173.8	174.0	174.2	174.3	79.1	3
2	209.2	209.3	209.5	209.8	98.8	2
1	237.0	237.0	237.3	237.6	114.2	1
0	****.*	****.*	****.*	*****	*****	0

Table B-4. Temperature Printout: CAAPCO B-274 (Continued)

RUN 12 (SHEET 1 of 2) DATE 11/25/80

T/C NO.	T/C TEMPERATURES DURING RUN, °F								AVG TEMPS °F	AVG TEMPS °C	T/C NO.
32	316.2	317.6	317.2	322.1	324.7	328.6	327.8	327.4			32
31	0.4	0.3	0.3	0.3	0.3	0.4	0.4	0.3			31
30	368.9	368.4	368.5	369.3	368.8	369.9	369.0	369.8			30
29	380.7	379.5	380.1	382.4	380.2	382.7	380.4	382.2			29
28	259.9	259.3	260.1	260.4	259.8	260.1	260.0	260.6			28
27	243.6	249.1	248.7	249.3	248.9	249.5	249.3	249.3			27
26	185.3	185.0	185.0	185.2	184.9	185.2	195.0	185.3			26
25	179.0	180.3	177.4	175.8	177.8	176.2	179.3	176.2			25
24	217.7	217.6	217.7	217.9	217.7	217.9	217.7	218.1			24
23	141.9	141.8	141.9	141.9	142.1	142.0	141.8	142.0			23
22	224.3	224.2	224.3	224.5	224.4	224.7	224.4	224.6			22
21	102.4	102.3	102.4	102.3	102.4	102.4	102.4	102.4			21
20	131.4	131.4	131.3	131.3	131.1	131.4	131.3	131.6			20
19	164.2	164.2	164.2	164.2	164.2	164.5	164.2	164.4			19
18	*****	*****	*****	*****	*****	*****	*****	*****			18
17	73.7	73.8	73.7	73.9	73.8	74.0	73.8	73.9			17
16	105.7	105.8	105.6	105.9	105.7	105.9	105.6	105.7			16
15	133.7	133.6	133.6	133.7	133.6	133.7	133.6	133.7			15
14	141.5	141.3	141.4	141.5	141.2	141.4	141.3	141.4			14
13	160.8	160.6	160.8	160.9	160.6	160.8	160.6	161.1			13
12	193.4	193.0	193.2	193.2	193.2	193.3	193.4	193.6			12
11	215.0	214.5	214.7	214.8	214.7	215.0	215.1	215.3			11
10	93.4	93.5	93.5	93.6	93.4	93.6	93.6	93.6			10
9	129.9	130.1	130.2	130.1	130.2	130.0	130.2	130.1			9
8	165.1	165.2	165.2	165.0	165.2	164.9	165.2	165.2			8
7	83.1	83.2	83.2	83.1	83.2	83.2	83.3	83.2			7
6	105.9	105.7	105.8	105.8	105.9	105.8	106.0	106.0			6
5	133.6	133.5	133.4	133.5	133.6	133.6	133.6	133.6			5
4	137.9	138.0	137.9	137.8	138.1	137.7	138.1	137.9			4
3	156.5	156.6	156.6	156.5	156.8	156.3	156.8	156.6			3
2	191.6	191.7	191.7	191.6	191.7	191.5	191.9	191.8			2
1	217.8	217.7	217.7	217.5	217.8	217.7	218.0	219.1			1
0	*****	*****	*****	*****	*****	*****	*****	*****			0

Table B-4. Temperature Printout: CAAPCO B-274 (Concluded)

RUN 12 (SHEET 2 of 2) DATE 11/25/80

T/C NO.	T/C TEMPERATURES DURING RUN, °F		AVG TEMPS °F	AVG TEMPS °C	T/C NO.
32	326.7	321.0	323.9	162.2	32
31	0.4	0.3	0.34	-17.6	31
30	369.6	369.7	369.2	187.3	30
29	381.3	382.2	381.2	194.0	29
28	260.4	260.3	260.1	126.7	28
27	249.6	249.6	249.2	120.7	27
26	185.6	185.3	185.2	85.1	26
25	178.5	175.6	177.6	80.9	25
24	218.1	218.2	217.9	103.3	24
23	142.1	142.1	142.0	61.1	23
22	224.8	224.8	225.0	107.2	22
21	102.5	102.7	102.4	39.1	21
20	131.7	131.8	131.4	55.2	20
19	164.7	164.7	164.4	73.6	19
18	****.*	****.*	*****	*****	18
17	74.0	73.9	73.9	23.3	17
16	106.1	105.9	105.8	41.0	16
15	134.0	133.8	133.7	56.5	15
14	141.8	141.7	141.5	60.8	14
13	161.1	161.1	160.8	71.6	13
12	193.7	193.7	193.4	89.7	12
11	215.3	215.2	215.0	101.7	11
10	93.5	93.6	93.5	34.2	10
9	130.2	130.4	130.1	54.5	9
8	165.2	165.5	165.2	74.0	8
7	83.2	83.3	83.2	28.4	7
6	106.0	106.1	105.9	41.1	6
5	133.7	133.7	133.6	56.4	5
4	138.2	138.4	138.0	58.9	4
3	156.6	157.1	156.6	69.2	3
2	191.7	192.3	191.8	88.8	2
1	218.2	218.3	217.9	103.3	1
0	****.*	****.*	*****	*****	0

Table B-5. Test Conditions Summary: Chemglaze M313

DATE 1/27/81	ICING CONDITION	DRY AIR		INTERMITTENT MAX.		CONTINUOUS MAX.	
	RUN NO.	22	21	18	19	16	17
	TAI FLOW RATE	100%	75%	100%	75%	100%	75%
FLIGHT:	Condition	Climb		Holding		Holding	
	Altitude, m	4,572		4,572		4,572	
	, (ft)	(15,000)		(15,000)		(15,000)	
	Velocity, m/s	190		138		131	
	, (knots)	(370)		(268)		(255)	
	Temperature, ^{o}C	-17.8		-6.1		-28.9	
	, (^{o}F)	(0)		(21)		(-20)	
	Horiz. Ext., km	-----		9.6		32.2	
	, (nm)	-----		(5.2)		(17.4)	
TUNNEL:	Altitude, m	- 0 -	- 0 -	- 0 -	- 0 -	- 0 -	- 0 -
	Velocity, m/s	70.2	70.2	67.1	67.1	85.8	85.8
	Equiv Temp, ^{o}C	-17.8	-17.8	-17.8	-17.8	-28.9	-28.9
(T/C 31)	Actual Temp, ^{o}C	-17.5	-17.8	-18.2	-18.0	-29.1	-29.2
	Drop Diam, microns	-----	-----	27.8	27.8	20.6	20.6
	LWC, g/m^3	-----	-----	2.10	2.10	0.29	0.29
	P_V , cm H_2O	35.1	35.1	31.5	32.0	55.1	54.6
	Time, seconds						
FLOW TUBE:	P_S, cm Hg	91.4	62.2	64.8	38.1	77.0	41.9
	P_V, cm H_2O	24.4	18.3	18.3	12.4	21.3	13.5
(T/C 29)	Air Temp., ^{o}C	198.0	192.6	194.3	193.5	191.9	191.9
	Air Flow, kg/min	1.79	1.41	1.42	1.06	1.60	1.12
TAI SPRAY TUBE:	P_S, cm Hg	88.9	60.2	62.0	36.1	73.7	40.6
(T/C 30)	Air Temp., ^{o}C	193.0	------	-----	-----	-----	-----
COMMENTS:							

Table B-6. *Temperature Printout: Chemglaze M313*

RUN 16 (SHEET 1 OF 3) DATE 1/27/81

T/C NO.	T/C TEMPERATURES DURING RUN, °F								AVG TEMPS °F	AVG TEMPS °C	T/C NO.
32	388.1	393.5	396.9	397.9	395.7	394.4	404.3	394.4			32
31	-22.0	-21.8	-21.7	21.5	-21.3	21.0	20.9	20.7			31
30	*****	*****	*****	*****	*****	*****	*****	*****			30
29	376.2	376.5	376.5	376.7	377.0	376.7	377.2	377.3			29
28	387.3	388.0	387.8	389.1	388.5	388.0	388.6	389.0			28
27	251.7	246.4	244.2	245.2	244.5	240.6	243.5	243.9			27
26	177.1	175.2	174.2	172.8	172.7	171.0	170.7	171.4			26
25	184.7	182.4	180.2	179.8	179.1	176.1	178.6	178.4			25
24	59.1	191.5	214.1	213.0	212.1	210.5	209.9	210.6			24
23	132.2	131.5	129.9	128.8	127.9	127.1	126.3	126.3			23
22	222.2	221.1	218.5	217.0	216.3	214.8	214.1	214.7			22
21	80.5	75.4	76.9	77.1	77.2	74.9	74.6	75.0			21
20	103.0	97.2	96.1	97.2	97.8	93.1	94.0	96.5			20
19	[illegible]	125.4	121.3	126.1	124.7	117.4	121.8	127.7			19
18	264.9	259.9	258.7	258.9	257.7	254.5	256.2	258.7			18
17	53.4	53.1	50.3	48.5	48.9	49.5	47.0	47.4			17
16	84.1	81.6	81.4	81.2	81.6	80.5	79.6	80.9			16
15	111.0	106.5	107.5	107.3	107.9	106.4	105.4	106.9			15
14	113.1	107.3	107.3	107.4	108.4	106.5	104.4	107.3			14
13	128.9	119.5	117.2	117.2	117.9	114.7	112.5	119.8			13
12	173.5	154.9	150.8	155.2	152.9	145.6	148.9	159.0			12
11	207.1	194.1	189.0	187.9	185.5	182.9	185.4	192.4			11
10	70.6	68.8	67.6	67.1	67.1	66.2	64.1	64.4			10
9	102.9	100.0	97.7	96.0	96.7	94.3	90.8	93.7			9
8	140.5	134.3	126.0	121.2	120.5	116.9	112.5	119.7			8
7	64.3	65.1	63.9	63.2	61.4	60.8	57.9	60.8			7
6	86.9	86.7	84.8	84.1	84.4	83.8	81.4	83.1			5
5	115.1	114.4	112.3	110.9	111.3	110.6	107.6	109.6			5
4	114.5	114.3	109.9	108.2	108.9	108.1	103.9	106.9			4
3	111.1	129.5	119.8	115.7	117.1	113.7	108.6	115.9			3
2	175.2	173.2	161.1	151.2	150.0	149.4	138.7	153.6			2
1	220.3	219.5	211.4	197.5	197.7	197.6	190.6	201.0			1
0	*****	*****	*****	*****	*****	*****	*****	*****			0

Table B-6. *Temperature Printout: Chemglaze M313 (Continued)*

RUN 16 (SHEET 2 OF 3) DATE 1/27/81

T/C NO.	T/C TEMPERATURES DURING RUN, °F								AVG TEMPS °F	AVG TEMPS °C	T/C NO.
32	394.6	395.1	395.3	402.2	398.9	391.0	398.2	395.3			32
31	- 20.3	- 20.0	20.1	20.0	19.8	19.5	19.5	19.3			31
30	*****	*****	*****	*****	*****	*****	*****	*****			30
29	377.2	377.3	377.5	377.9	377.9	377.7	378.0	377.9			29
28	388.7	388.9	389.0	399.4	389.3	389.0	389.6	389.3			28
27	244.6	242.7	242.9	243.3	242.8	243.3	243.9	244.1			27
26	171.4	171.0	171.1	170.9	171.0	170.8	171.5	171.9			26
25	177.6	178.5	177.9	178.4	178.1	177.5	178.1	179.4			25
24	210.8	210.5	210.0	210.2	209.8	210.3	210.4	210.7			24
23	126.4	126.1	126.1	126.2	126.1	126.0	125.8	126.2			23
22	214.6	214.4	214.1	214.4	214.0	214.4	214.8	214.9			22
21	75.5	75.0	75.2	75.2	75.4	75.5	75.8	76.1			21
20	97.2	95.9	96.7	97.1	97.1	98.0	97.5	97.7			20
19	128.8	123.0	125.8	126.1	126.8	123.4	129.1	129.1			19
18	258.4	256.5	255.7	257.2	256.9	257.3	259.2	258.6			18
17	48.1	48.5	48.0	48.7	48.3	48.4	48.6	48.7			17
16	81.4	80.8	90.7	90.6	80.1	80.1	73.6	80.0			16
15	107.4	107.0	106.8	106.7	106.0	106.0	105.4	105.9			15
14	107.8	107.4	106.8	106.6	105.5	105.8	105.4	105.9			14
13	119.3	118.2	117.3	117.7	115.9	117.2	117.1	117.8			13
12	159.1	153.3	155.2	156.3	154.2	157.3	156.7	158.1			12
11	192.9	188.0	188.5	191.1	189.2	193.2	193.9	194.3			11
10	65.0	64.7	64.2	64.3	63.7	64.2	64.1	64.0			10
9	93.8	93.1	93.1	94.1	92.8	94.1	93.7	93.6			9
8	118.9	117.1	116.4	118.9	116.4	119.4	118.5	118.2			8
7	61.0	60.8	59.7	59.7	60.3	59.9	60.0	59.8			7
6	83.6	83.2	82.5	82.6	81.8	82.2	82.3	82.4			6
5	110.3	109.7	109.1	109.1	108.0	108.4	108.6	108.7			5
4	107.5	107.0	106.0	106.0	104.6	105.3	105.3	105.2			4
3	115.8	114.8	112.8	113.0	111.2	112.3	112.3	112.0			3
2	151.5	148.9	145.5	147.0	143.7	147.2	147.0	146.7			2
1	199.6	197.6	195.6	196.9	193.0	199.0	198.4	199.4			1
0	*****	*****	*****	*****	*****	*****	*****	*****			0

Table B-6. Temperature Printout: Chemglaze M313 (Continued)

RUN 16 (SHEET 3 OF 3) DATE 1/27/81

T/C NO.	T/C TEMPERATURES DURING RUN, °F		AVG TEMPS °F	AVG TEMPS °C	T/C NO.
32	398.0	393.4	396.0	202.2	32
31	19.2	19.0	-20.4	-29.1	31
30	*****	*****	*****	*****	30
29	378.4	378.3	377.3	191.9	29
28	390.0	389.7	388.8	198.2	28
27	244.6	243.9	244.2	117.9	27
26	171.9	171.8	172.1	77.9	26
25	179.1	178.6	179.0	81.7	25
24	211.0	211.1	201.4	94.1	24
23	126.6	126.9	126.4	52.4	23
22	215.1	215.2	215.8	102.1	22
21	76.5	76.3	76.0	24.2	21
20	98.0	97.9	97.1	36.2	20
19	129.6	129.2	126.8	52.7	19
18	259.0	258.6	257.9	125.5	18
17	48.9	49.4	49.1	9.5	17
16	80.0	80.4	80.8	27.1	16
15	105.7	106.2	106.8	41.5	15
14	105.4	106.0	106.9	41.6	14
13	116.8	117.3	117.9	47.7	13
12	157.4	157.0	155.9	68.8	12
11	195.2	193.7	191.4	88.5	11
10	64.4	64.5	65.5	18.6	10
9	94.1	94.5	94.9	35.0	9
8	113.1	119.6	120.8	49.3	8
7	60.3	60.6	61.1	16.1	7
6	82.8	83.5	83.5	28.6	6
5	108.9	109.6	110.1	43.4	5
4	105.3	105.6	107.4	41.9	4
3	112.2	112.6	114.6	45.9	3
2	146.5	147.3	151.3	66.3	2
1	198.8	199.7	200.8	93.8	1
0	*****	*****			0

Table B-6. Temperature Printout: Chemglaze M313 (Continued)

RUN 17 (SHEET 1 OF 3) DATE 1/27/81

T/C NO.	T/C TEMPERATURES DURING RUN, °F								AVG TEMPS °F	AVG TEMPS °C	T/C NO.
32	412.8	417.5	411.8	417.0	411.9	418.2	415.7	415.7			32
31	-21.8	-21.7	-21.5	-21.5	-21.2	-21.1	-21.0	-20.9			31
30	****.*	****.*	****.*	****.*	****.*	****.*	****.*	****.*			30
29	376.9	377.0	377.1	377.0	377.1	377.1	377.1	377.1			29
28	392.9	393.2	393.2	393.2	393.3	393.5	393.4	393.4			28
27	228.0	223.6	221.8	223.5	223.5	222.2	221.2	218.4			27
26	143.2	142.9	140.3	140.9	141.2	141.1	140.2	139.6			26
25	156.3	154.2	151.5	151.7	151.4	151.5	151.1	149.2			25
24	62.8	184.8	191.6	181.7	182.0	180.9	61.9	179.3			24
23	101.4	101.3	100.4	100.0	99.9	99.4	99.3	99.0			23
22	188.5	187.6	194.8	184.6	164.7	183.9	183.3	182.2			22
21	61.1	60.3	57.3	57.0	57.7	57.5	57.5	56.9			21
20	80.5	78.9	74.9	75.8	77.8	76.8	76.8	73.4			20
19	117.5	107.4	102.7	113.2	111.1	107.8	108.1	98.0			19
18	242.2	237.0	234.7	237.6	239.7	236.4	236.7	234.5			18
17	35.7	35.9	34.2	32.9	33.5	33.6	33.8	33.8			17
16	61.2	61.0	58.1	57.3	58.3	58.5	59.0	58.3			16
15	86.8	86.5	83.7	84.1	85.3	84.9	85.3	83.9			15
14	90.3	89.4	84.6	86.6	88.3	87.3	87.5	85.5			14
13	107.7	104.7	95.0	102.4	104.7	100.6	101.5	96.5			13
12	147.7	138.0	126.2	141.2	143.2	135.4	138.1	124.5			12
11	179.7	169.0	159.7	173.5	172.9	166.0	167.7	159.3			11
10	53.4	53.2	50.9	48.8	49.4	49.2	49.3	48.9			10
9	80.5	80.5	74.1	75.7	77.0	75.7	75.2	73.0			9
8	116.4	113.7	95.3	107.1	109.8	100.4	101.2	95.1			8
7	****.*	****.*	****.*	****.*	****.*	****.*	****.*	****.*			7
6	64.5	64.9	62.5	60.8	61.5	61.5	61.4	60.5			6
5	89.1	90.0	86.2	86.0	86.8	86.7	86.3	85.1			5
4	91.2	91.2	86.1	86.2	88.1	87.5	86.9	85.4			4
3	104.5	103.8	91.1	96.1	100.0	95.2	93.2	91.9			3
2	147.3	145.6	117.8	136.1	141.3	127.4	130.6	122.9			2
1	199.1	187.2	163.1	178.5	182.3	169.4	172.0	167.6			1
0	****.*	****.*	****.*	****.*	****.*	****.*	****.*	****.*			0

Table B-6. Temperature Printout: Chemglaze M313 (Continued)

RUN 17 (SHEET 2 OF 3) DATE 1/27/81

T/C NO.	T/C TEMPERATURES DURING RUN, °F								AVG TEMPS °F	AVG TEMPS °C	T/C NO.
32	4185	4086	4147	4163	4184	4127	4194	4118			32
31	-207	-204	-203	-202	-200	-198	-198	-195			31
30	*****	*****	*****	*****	*****	*****	*****	*****			30
29	3773	3773	3775	3776	3779	3776	3778	3779			29
28	3935	3937	3936	3933	3941	3938	3940	3943			29
27	2171	2160	2161	2161	2157	2152	2169	2176			27
26	1383	1374	1375	1377	1372	1367	1379	1377			26
25	1484	1477	1473	1474	1481	1471	1480	1477			25
24	1777	1768	1763	1764	1762	1760	1761	1765			24
23	983	980	973	972	967	966	967	967			23
22	1809	1800	1796	1795	1793	1790	1792	1734			22
21	551	537	524	528	526	525	520	521			21
20	714	696	696	695	691	683	687	695			20
19	940	924	942	942	943	934	966	1004			19
18	2330	2307	2307	2315	2313	2301	2330	2325			18
17	334	330	328	327	329	328	329	330			17
16	559	550	539	538	537	534	530	534			16
15	522	807	805	804	793	793	793	799			15
14	829	814	814	914	810	805	807	818			14
13	917	899	903	907	904	900	910	932			13
12	1176	1157	1177	1180	1178	1173	1215	1270			12
11	1533	1517	1527	1523	1531	1527	1556	1609			11
10	475	465	458	456	454	452	449	446			10
9	703	690	683	681	675	673	669	670			9
8	901	889	865	890	891	889	890	908			8
7	*****	*****	*****	*****	*****	*****	*****	*****			7
6	586	575	563	563	561	561	559	559			6
5	831	623	815	815	814	814	812	815			5
4	827	815	803	812	808	808	806	813			4
3	872	853	851	856	854	854	852	863			3
2	1141	1122	1120	1131	1130	1131	1139	1166			2
1	1607	1596	1535	1602	1690	1603	1606	1632			1
0	*****	*****	*****	*****	*****	*****	*****	*****			0

Table B-6. Temperature Printout: Chemglaze M313 (Continued)

RUN 17 (SHEET 3 OF 3) DATE 1/27/81

T/C NO.	T/C TEMPERATURES DURING RUN, °F		AVG TEMPS °F	AVG TEMPS °C	T/C NO.
32	416.3	413.4	415.0	212.8	32
31	-19.3	-19.2	-20.6	-29.2	31
30	****.*	****.*	*****	*****	30
29	378.1	378.1	377.4	191.9	29
28	394.4	394.4	393.7	200.9	28
27	217.4	216.6	219.3	104.1	27
26	137.9	137.4	139.2	59.6	26
25	149.0	147.5	149.7	65.4	25
24	****.*	****.*	164.2	73.4	24
23	96.3	96.9	98.4	36.9	23
22	179.4	179.3	182.0	83.3	22
21	52.4	52.1	55.2	12.9	21
20	69.7	69.7	72.8	22.7	20
19	99.6	95.3	101.1	38.4	19
18	232.6	231.7	234.2	112.3	18
17	33.0	33.0	33.5	0.8	17
16	53.7	54.1	56.2	13.4	16
15	79.7	79.5	82.3	28.0	15
14	81.6	81.0	84.1	28.9	14
13	93.1	91.5	95.8	35.5	13
12	125.6	120.0	127.4	53.0	12
11	153.6	155.6	160.9	71.6	11
10	44.4	44.3	47.6	8.7	10
9	66.5	66.3	71.6	22.0	9
8	90.6	89.9	96.3	35.7	8
7	****.*	****.*	*****	*****	7
6	56.0	56.2	59.1	15.0	6
5	81.3	81.4	84.0	28.9	5
4	81.2	80.9	84.1	28.9	4
3	86.5	85.9	89.8	32.1	3
2	116.1	115.2	122.7	50.4	2
1	162.4	162.5	167.7	75.4	1
0	****.*	****.*	*****	*****	0

Table B-6. Temperature Printout: Chemglaze M313 (Continued)

RUN 18 DATE 1/27/81

T/C NO.	T/C TEMPERATURES DURING RUN, °F						AVG TEMPS °F	AVG TEMPS °C	T/C NO.
32	396.3	399.6	395.5	396.9	395.0	391.2	395.8	202.1	32
31	-0.4	-0.9	-1.2	-1.0	-0.6	-0.4	-0.8	-18.2	31
30	****.*	****.*	****.*	****.*	****.*	****.*	*****	*****	30
29	381.7	381.8	381.5	381.8	381.6	381.6	381.7	194.3	29
28	393.7	393.8	393.5	393.9	393.7	393.7	393.7	201.0	28
27	266.3	255.2	246.2	244.0	241.8	241.4	249.2	120.6	27
26	194.3	191.2	185.2	182.3	180.2	179.1	185.4	85.2	26
25	199.0	193.6	186.2	183.1	181.9	182.4	187.7	86.5	25
24	232.6	230.7	221.1	216.4	213.4	212.1	221.1	105.0	24
23	149.4	148.1	145.7	143.1	140.8	139.3	144.2	62.4	23
22	238.1	236.5	229.4	223.8	220.9	219.2	227.8	108.8	22
21	104.1	100.1	93.0	90.1	87.6	86.1	93.5	34.2	21
20	133.9	123.9	108.6	105.3	102.0	100.3	112.3	44.6	20
19	175.0	152.1	125.9	122.8	119.7	118.0	135.6	57.5	19
18	276.8	271.6	261.4	259.6	258.2	256.6	264.0	128.9	18
17	77.8	77.4	72.0	69.0	67.5	66.8	71.8	22.1	17
16	107.9	106.8	98.1	95.1	93.4	92.8	99.0	37.2	16
15	135.7	134.5	121.7	118.0	116.1	115.4	123.6	50.9	15
14	144.0	141.7	119.5	115.3	113.3	113.0	124.5	51.4	14
13	165.4	158.7	122.6	119.0	116.5	115.5	133.1	56.2	13
12	199.9	184.2	144.9	142.8	140.0	139.4	158.5	70.3	12
11	224.2	207.2	180.4	178.4	175.5	174.5	190.0	87.8	11
10	95.6	96.0	86.1	82.2	80.0	78.1	86.3	30.2	10
9	133.0	134.2	106.9	103.1	101.0	99.0	113.2	45.1	9
8	172.8	171.5	123.9	117.3	115.4	113.4	135.7	57.6	8
7	94.5	94.3	88.0	85.4	83.2	82.6	88.0	31.1	7
6	110.8	111.6	101.5	97.4	95.8	94.7	*****	*****	6
5	139.8	141.0	126.4	121.4	119.6	118.5	*****	*****	5
4	144.2	147.4	121.9	115.2	114.0	112.6	125.9	52.2	4
3	162.3	168.5	122.5	114.7	114.4	112.6	132.5	55.8	3
2	200.5	203.1	145.8	139.5	138.4	136.5	160.6	71.5	2
1	235.2	233.5	192.4	188.2	186.5	184.7	203.4	95.2	1
0	****.*	****.*	****.*	****.*	****.*	****.*			0

Table B-6. *Temperature Printout: Chemglaze M313 (Continued)*

RUN 19 DATE 1/27/81

T/C NO.	T/C TEMPERATURES DURING RUN, °F							AVG TEMPS °F	AVG TEMPS °C	T/C NO.
32	443.6	442.6	440.1	443.4	443.2	450.2	442.7	444.5	229.2	32
31	-0.4	-0.7	-0.4	-0.4	-0.4	-0.3	-0.4	-0.4	-18.0	31
30	*****	*****	*****	*****	*****	*****	*****	*****	*****	30
29	379.9	379.9	379.9	380.2	380.4	380.7	380.8	380.3	193.5	29
28	397.5	397.3	397.5	397.6	397.7	398.2	398.1	397.7	203.2	28
27	243.7	236.5	228.0	225.2	222.9	222.0	229.3	229.5	109.7	27
26	162.4	161.1	157.0	155.1	153.3	152.2	153.5	156.4	69.1	26
25	173.0	168.4	164.3	161.8	151.2	159.4	159.1	163.7	73.2	25
24	63.9	202.1	195.5	131.6	188.7	187.2	187.9	173.9	78.8	24
23	122.5	122.3	121.5	120.0	116.2	116.9	116.1	119.6	48.7	23
22	205.0	204.9	199.5	196.0	193.2	191.6	192.1	197.5	91.9	22
21	85.8	83.2	79.3	75.9	74.2	72.7	74.1	77.9	25.5	21
20	110.2	104.1	94.2	89.3	86.5	85.1	89.9	94.2	13.5	20
19	148.9	134.3	112.0	105.6	103.3	102.2	117.1	117.6	47.6	19
18	255.9	252.7	242.8	238.4	237.0	237.7	242.7	243.9	117.7	18
17	60.1	60.5	57.7	55.7	54.6	53.9	53.6	56.6	13.7	17
16	86.0	86.1	81.4	78.7	76.9	76.3	76.7	80.3	26.8	16
15	111.7	111.9	104.9	101.0	99.8	97.8	99.8	103.6	39.8	15
14	119.7	120.1	105.8	101.3	93.4	97.1	99.8	106.0	41.1	14
13	138.3	137.0	110.9	106.1	101.3	100.2	108.2	114.6	45.9	13
12	173.5	167.1	134.0	128.1	123.5	122.9	138.8	141.1	60.6	12
11	197.9	191.9	163.0	157.8	154.7	153.9	168.9	169.7	24.2	11
10	78.5	79.4	73.6	70.5	69.0	67.5	56.9	72.2	22.3	10
9	110.4	113.5	96.1	89.7	86.7	85.0	86.7	95.4	35.2	9
8	148.6	151.6	113.4	104.0	100.3	98.8	106.4	117.6	47.5	8
7	84.6	74.1	71.0	58.8	67.3	55.9	43.2	68.7	20.4	7
6	89.6	90.9	85.9	82.2	80.5	79.3	78.7	83.9	28.8	6
5	116.5	118.5	111.1	106.7	103.8	102.1	102.0	108.7	42.6	5
4	120.8	124.7	109.2	103.2	99.6	97.5	97.6	107.5	42.0	4
3	137.7	143.5	114.1	103.2	102.4	99.9	101.7	115.4	46.3	3
2	174.2	177.1	135.0	127.4	121.1	119.3	124.3	139.8	59.9	2
1	207.2	207.5	173.3	167.2	162.9	161.8	166.0	178.0	81.1	1
0	*****	*****	*****	*****	*****	*****	*****	*****	*****	0

Table B-6. Temperature Printout: Chemglaze M313 (Continued)

RUN 21 DATE 1/27/81

T/C NO.	T/C TEMPERATURES DURING RUN, °F						AVG TEMPS °F	AVG TEMPS °C	T/C NO.
32	411.7	418.9	419.1	414.7	416.7	422.1	417.2	214.0	32
31	0.0	0.1	0.0	0.0	0.1	0.0	-3.333	-17.8	31
30	*****	*****	*****	*****	*****	*****	*****	*****	30
29	378.1	378.7	379.7	378.4	378.8	379.0	378.6	192.6	29
28	390.2	390.9	390.8	390.3	391.3	391.5	390.8	199.4	28
27	260.4	260.3	260.4	260.4	260.4	260.1	260.3	126.9	27
26	189.5	198.9	189.6	189.1	199.2	189.1	188.9	87.2	26
25	189.8	190.4	191.2	193.4	193.3	192.2	191.7	88.7	25
24	69.6	227.1	227.3	227.3	227.4	227.3	201.0	93.9	24
23	144.2	144.0	144.4	144.1	144.4	144.4	144.3	62.4	23
22	231.4	231.5	231.8	231.9	232.0	231.9	231.8	111.0	22
21	100.3	100.5	100.5	100.5	100.6	100.6	100.5	38.1	21
20	126.9	127.2	127.3	127.4	127.5	127.7	127.3	53.0	20
19	167.4	167.6	167.9	167.8	168.0	168.0	167.8	75.4	19
18	272.2	271.2	272.9	272.5	273.0	272.1	272.3	133.5	18
17	74.4	74.6	74.5	74.5	74.7	74.7	74.6	23.6	17
16	104.1	104.4	104.4	104.5	104.5	104.7	104.4	40.2	16
15	130.2	130.4	130.4	130.3	130.6	130.8	130.5	54.7	15
14	137.3	137.5	137.6	137.6	137.7	137.7	137.6	58.6	14
13	157.5	157.7	158.0	157.8	158.2	157.9	157.9	69.9	13
12	194.9	193.0	195.3	195.2	195.6	195.3	195.2	90.7	12
11	219.3	219.5	213.7	219.7	220.0	220.0	219.7	104.3	11
10	92.2	92.1	92.2	92.0	92.1	92.3	92.2	33.4	10
9	128.0	128.1	127.9	128.0	128.1	128.0	128.0	53.3	9
8	167.4	167.4	167.5	167.7	167.6	167.8	167.6	75.3	8
7	25.0	90.0	84.2	79.6	67.9	79.1	71.0	21.6	7
6	106.3	106.3	106.4	106.5	106.6	106.6	106.5	41.4	6
5	134.5	134.4	134.5	134.6	134.8	134.6	134.6	57.0	5
4	138.6	138.6	139.6	139.7	138.8	138.7	138.7	59.3	4
3	43.1	159.0	158.8	158.9	159.0	159.1	139.7	59.8	3
2	194.7	194.8	194.9	194.9	195.0	195.1	194.9	90.5	2
1	229.4	229.4	229.6	229.8	229.9	229.9	229.7	109.8	1
0	*****	*****	*****	*****	*****	*****	*****	*****	0

Table B-6. Temperature Printout: Chemglaze M313 (Concluded)

RUN 22 DATE 1/27/81

T/C NO.	T/C TEMPERATURES DURING RUN, °F						AVG TEMPS °F	AVG TEMPS °C	T/C NO.
32	367.2	363.7	369.7	366.9	364.1	367.1	411.0	210.5	32
31	0.6	0.3	0.7	0.5	0.2	0.0	.5	-17.5	31
30	*****	*****	*****	*****	*****	*****	*****	*****	30
29	380.2	379.7	379.5	379.3	378.8	378.4	379.3	193.0	29
28	389.6	388.7	388.8	388.3	387.7	387.1	388.4	198.0	28
27	278.7	278.8	278.2	277.3	277.9	277.9	278.1	136.7	27
26	207.9	208.6	208.5	208.6	208.0	208.1	208.3	97.9	26
25	212.6	214.4	212.8	214.9	213.1	215.1	213.8	101.0	25
24	68.7	248.0	247.9	247.8	247.7	247.3	217.9	103.3	24
23	162.0	162.2	162.5	162.6	162.6	162.5	162.4	72.4	23
22	253.9	254.0	253.7	253.8	253.5	253.3	253.7	123.2	22
21	113.3	113.6	113.5	113.4	113.2	113.1	113.35	45.2	21
20	142.6	142.6	142.6	142.3	142.2	141.9	142.37	61.3	20
19	184.8	184.7	184.6	184.2	184.1	183.4	184.3	84.6	19
18	288.8	288.5	287.6	287.7	287.0	288.0	288.1	142.3	18
17	87.3	87.5	87.6	87.4	87.1	86.9	87.3	30.7	17
16	118.8	119.0	119.0	118.7	118.6	118.3	118.7	48.2	16
15	146.2	146.4	146.3	146.1	145.9	145.5	146.1	63.4	15
14	154.0	154.2	154.2	153.8	153.6	153.2	153.8	67.7	14
13	176.0	176.4	176.1	175.6	175.6	175.0	175.8	79.9	13
12	213.3	213.7	213.2	212.9	212.7	212.3	213.0	100.6	12
11	237.5	237.8	237.5	237.3	236.9	236.5	237.3	114.0	11
10	105.5	105.6	106.0	105.4	105.4	105.4	105.6	40.9	10
9	145.3	145.7	145.4	145.4	145.0	144.9	145.3	62.9	9
8	185.9	186.5	186.2	185.9	185.9	185.3	186.0	85.5	8
7	71.9	101.3	103.0	102.7	102.5	102.7	97.4	36.3	7
6	121.9	122.2	122.1	122.1	121.9	121.4	121.9	50.0	6
5	152.2	152.5	152.4	152.3	151.9	151.8	152.2	66.8	5
4	156.6	156.9	156.8	156.6	156.3	156.2	156.6	69.2	4
3	180.5	179.4	179.4	174.2	165.6	213.1	182.0	83.3	3
2	214.4	214.9	214.5	214.3	214.0	213.7	214.3	101.3	2
1	251.6	251.9	251.6	251.5	250.9	250.7	251.4	121.9	1
0	*****	*****	*****	*****	*****	*****	*****	*****	0

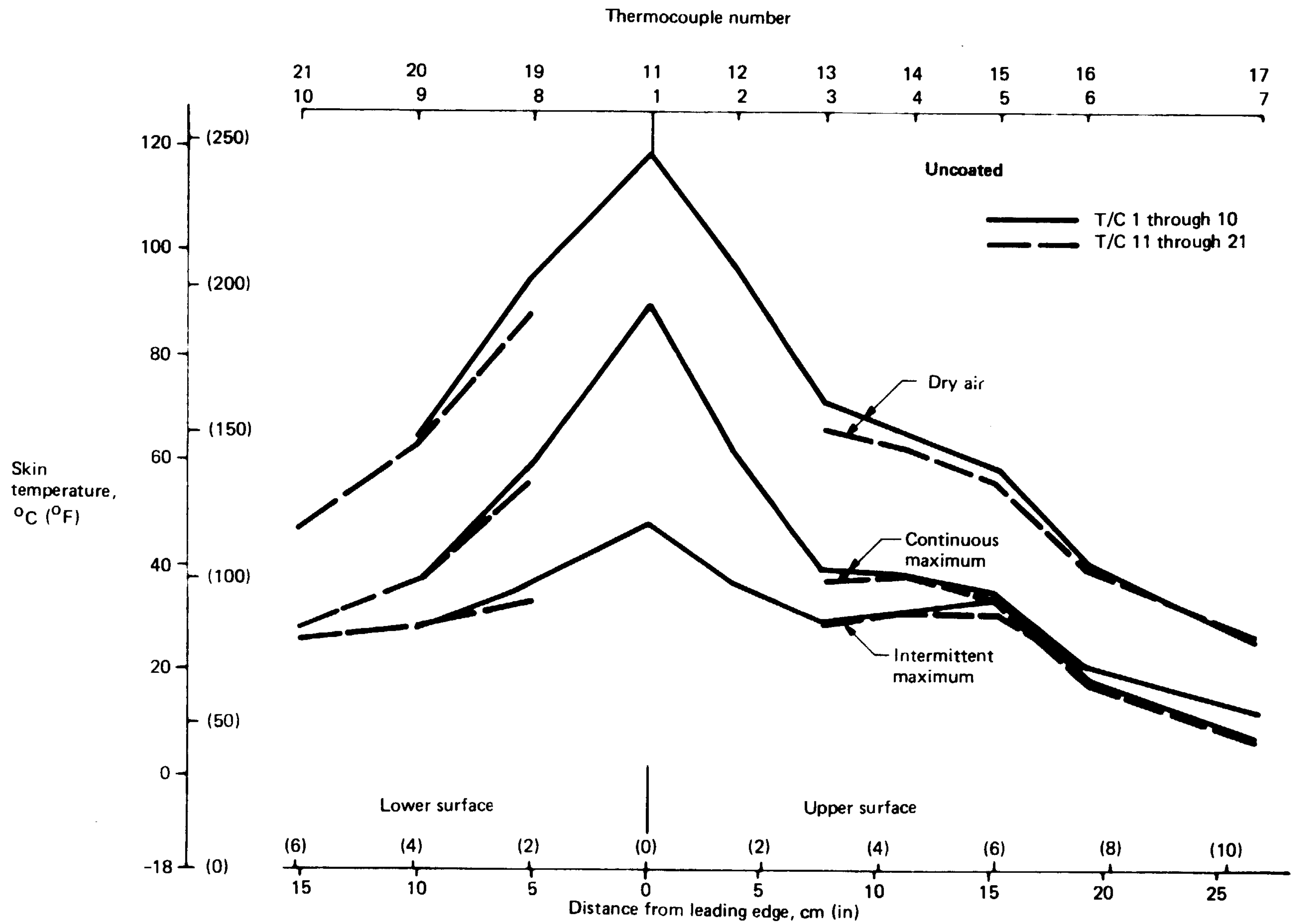

Figure B-2. Temperature Comparison Between Thermocouple Rows—Uncoated

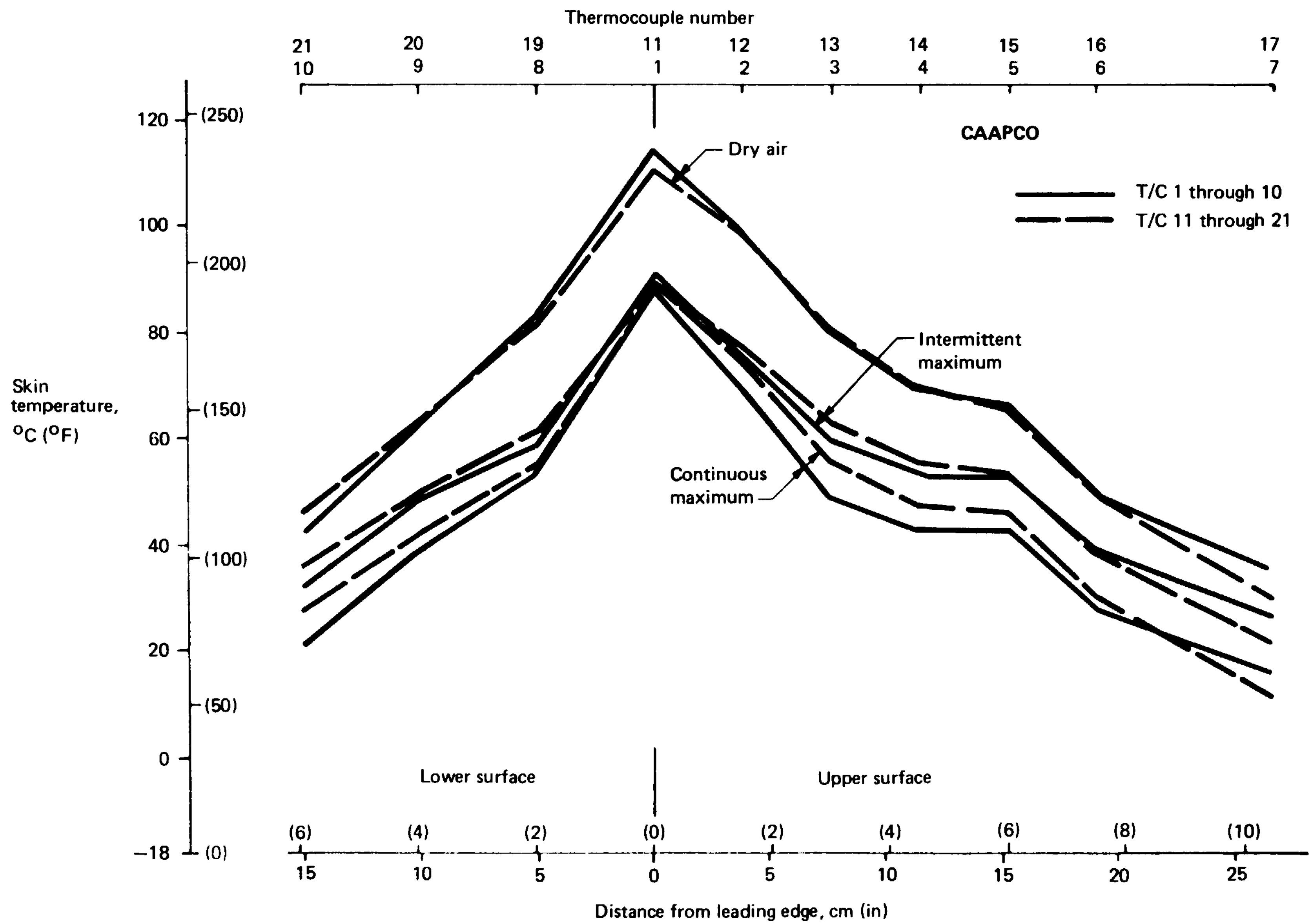

Figure B-3. Temperature Comparison Between Thermocouple Rows—CAAPCO Coating

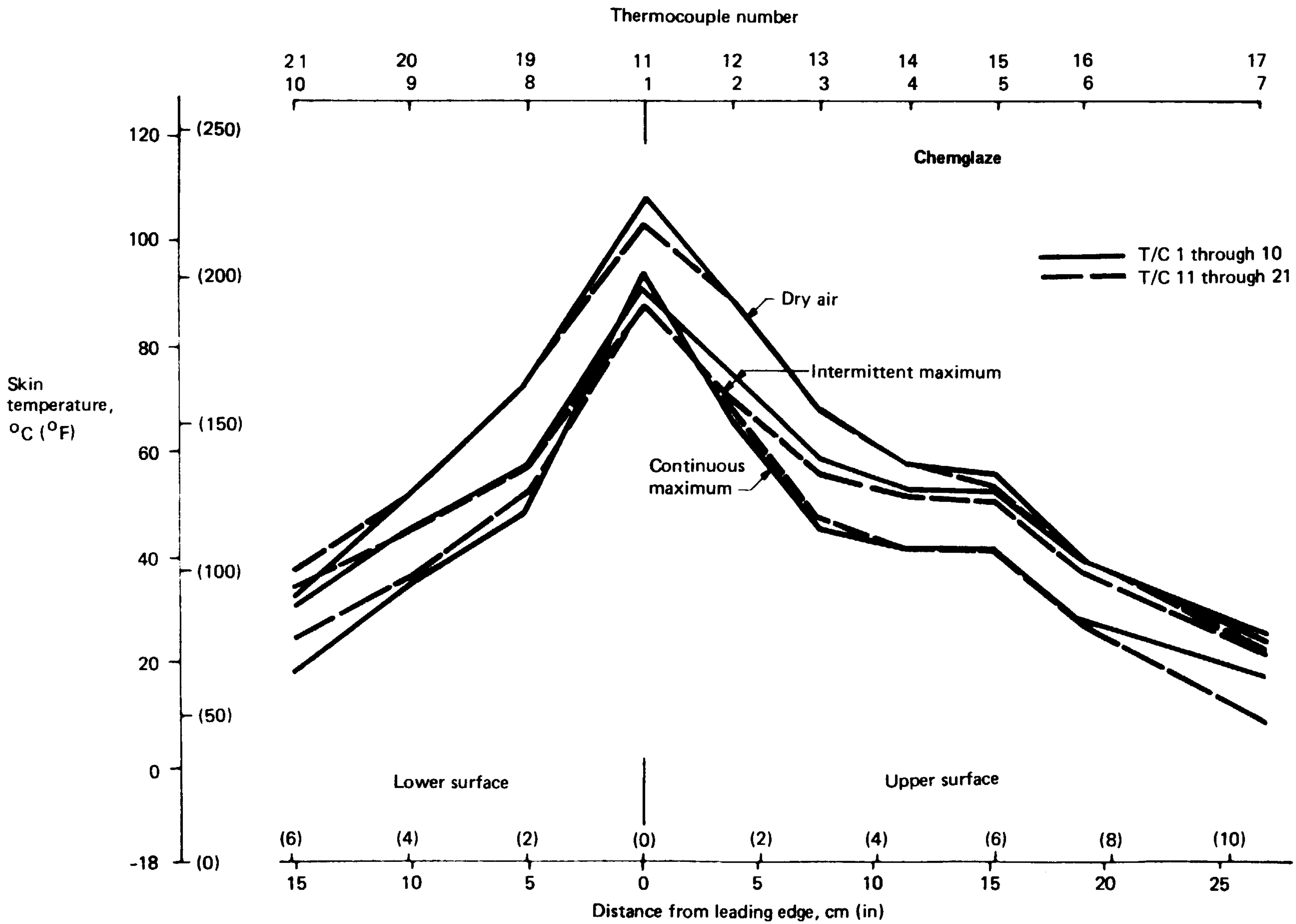

Figure B-4. Temperature Comparison Between Thermocouple Rows—Chemglaze Coating

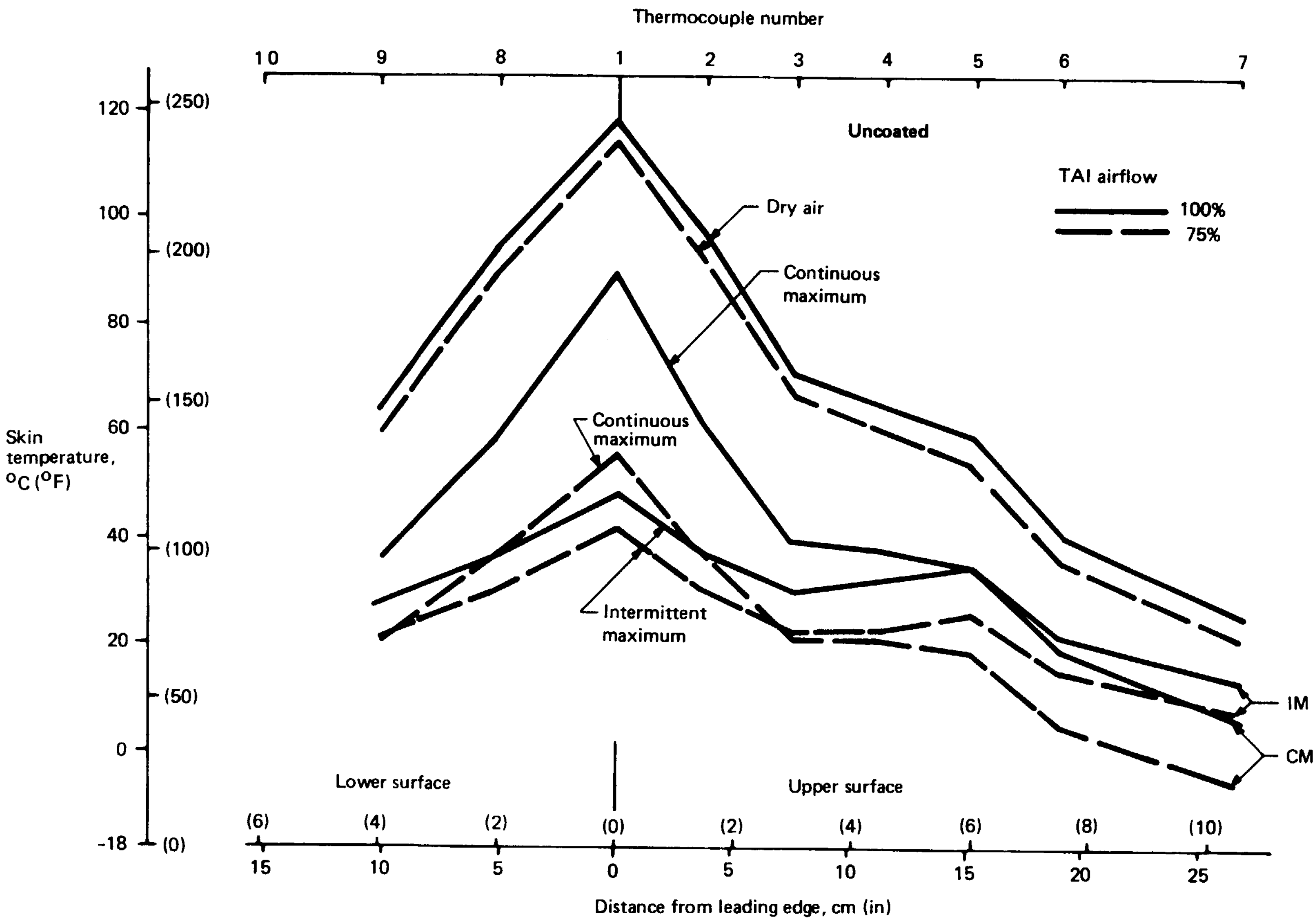

Figure B-5. Skin Temperature Versus TAI Flow Rate—Uncoated

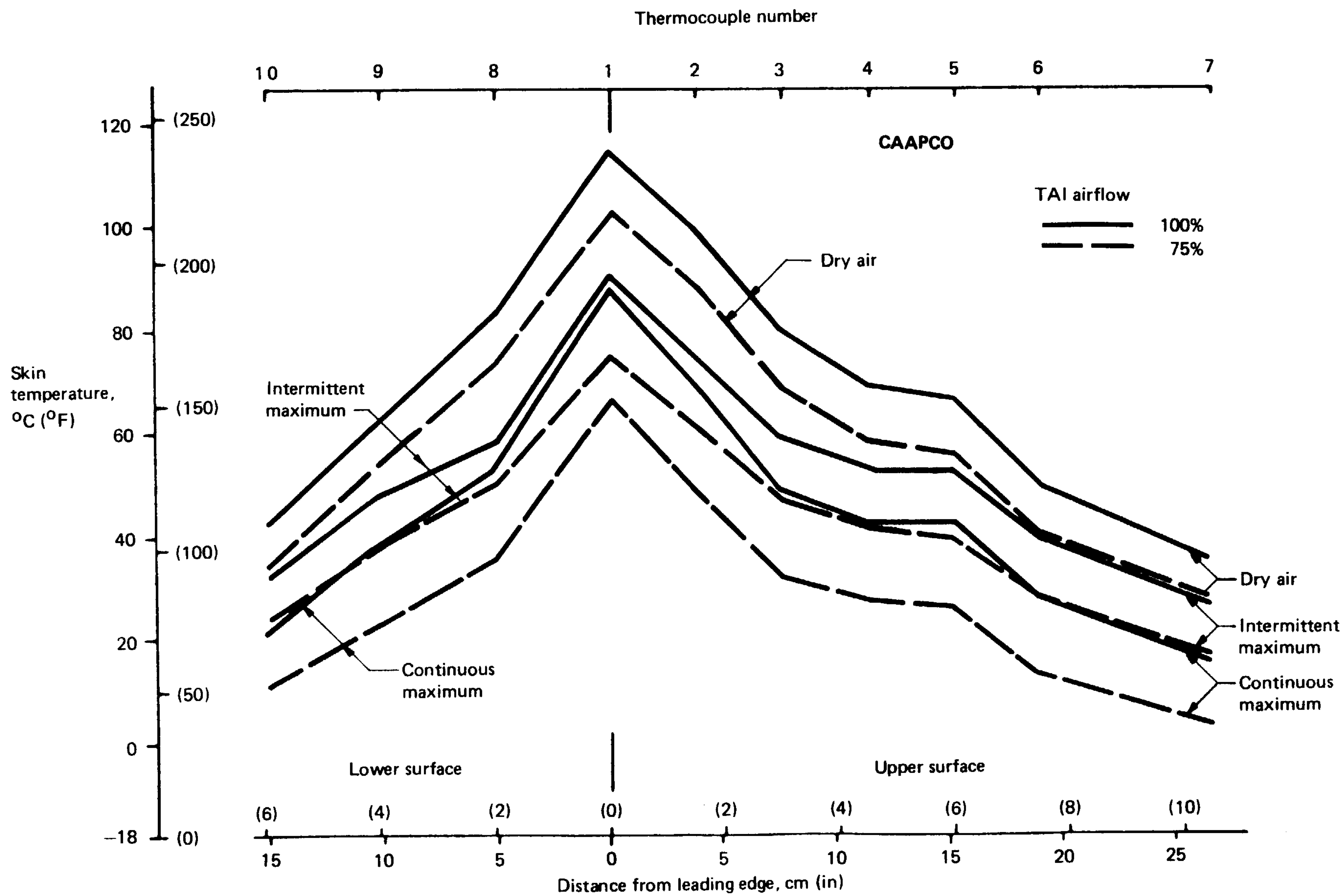

Figure B-6. Skin Temperature Versus TAI Flow Rate—CAAPCO Coating

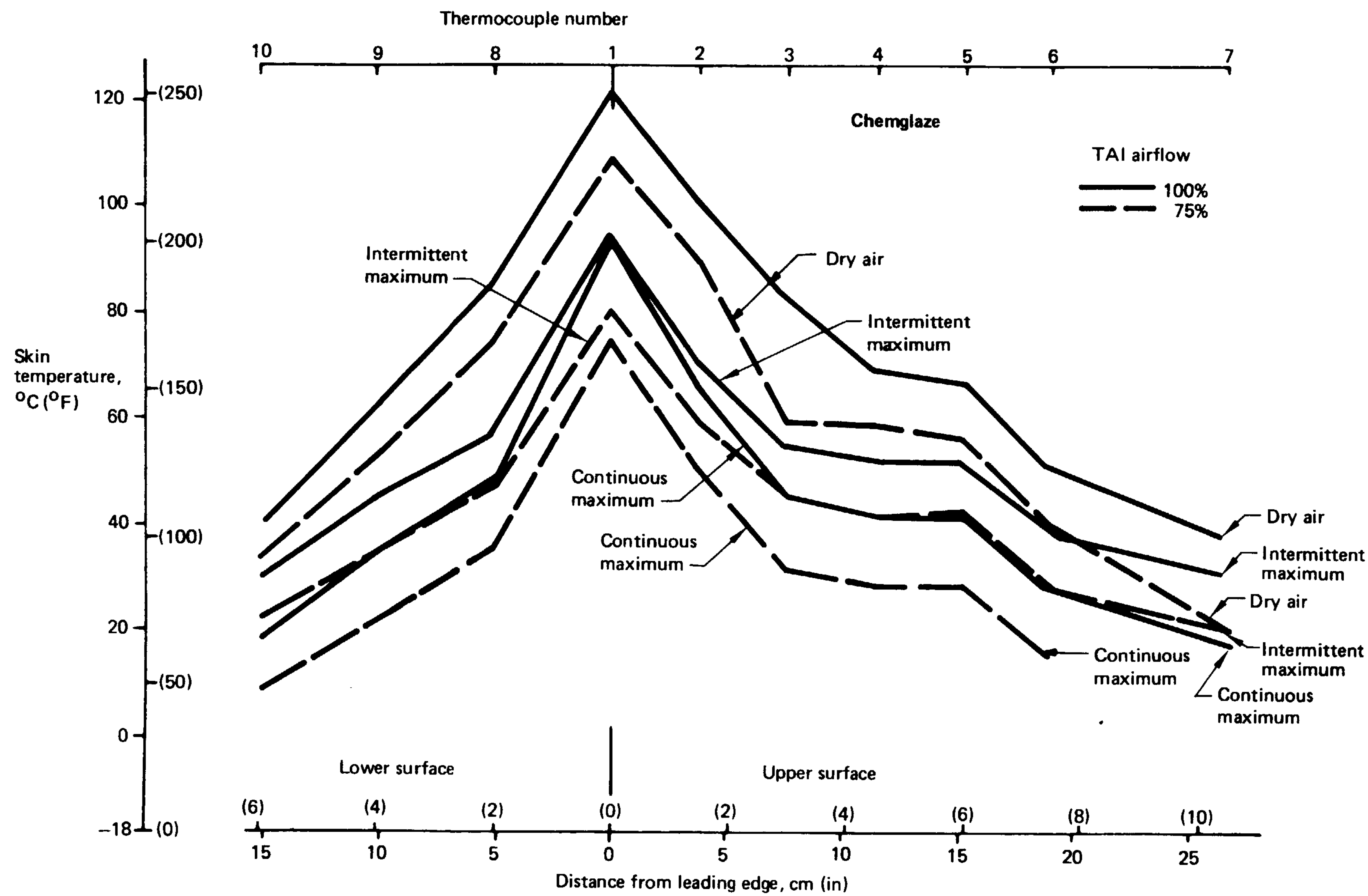

Figure B-7. Skin Temperature Versus TAI Flow Rate—Chemglaze Coating

APPENDIX C
CORROSION TEST METHODS

Three types of corrosion tests were performed: salt spray, filiform, and dynamic. Specimens were prepared with six different coating configurations—three were control coatings, currently used on commercial transports, and three were test coatings that had an elastomeric polyurethane basecoat and a polyurethane enamel topcoat. The enamel topcoat, added for protection of the basecoat against hydraulic fluid, was included in the tests to evaluate its reaction to the strains induced during dynamic test cyclic loading. It was found (sec. 4.3.4.3) that although there was some fracturing of the enamel topcoat, the elastomeric basecoat remained an intact corrosion barrier.

Specimen preparation, a description of test procedures, and potentiostat data from the dynamic tests are contained in this appendix. Corrosion test results are presented in Section 4.3.4.

Specimen Preparation

All specimens were made of 7075-T6 aluminum alloy with B30NW-8K4 Hi-Lok titanium fasteners installed. The salt-spray and filiform specimens and the top plates of the dynamic specimens were milled from plate stock, as shown in Figure C-1a, to expose end grain and promote corrosion. Dimensions of assembled specimens are shown in Figures C-1b and C-1c.

The number of test specimens prepared and the various coating configurations used are shown in Table C-1. The steps followed in specimen preparation were:

1. Anodize each aluminum part. Seal in deionized water to 10% $\pm$2% hydration. Apply BMS 10-20 Type II to all surfaces.

2. Drill and countersink holes to provide a clearance fit of 0.0254 to 0.127 mm (0.001 to 0.005 in). Install Hi-Lok B30NW-8K4 titanium fasteners and BACC30M aluminum collars. (Note: Strip aluminum-pigmented coating from fasteners to be used in salt-spray and filiform specimens prior to installation.)

3. Clean specimens with BMS 11-7 solvent or MEK.

4. Apply coatings as shown in Table C-1. Allow to cure at room temperature for 7 days.

5. Loosen fastener collars on only salt-spray and filiform specimens, rotate fasteners to break topcoat, and retighten collars.

6. Apply fillet seals, using BMS 5-26 sealant, as shown in Figure C-1b.

Test Procedures

Salt Spray Tests—Specimens were placed in a salt-spray environment for 90 days, per ASTM B117. The panels were inclined 15 deg from vertical, with coated surfaces up. At the end of the 90-day period, loose corrosion and salt deposits were removed by lightly brushing in water. Specimens were allowed to dry, then were examined and rated for corrosion density and distance of corrosion migration using the following qualitative scale:

0 = no corrosion
1 = trace
2 = moderate
3 = medium
4 = excessive
5 = extremely heavy

Filiform Tests—The test consisted of two parts. The specimens were exposed to hydrochloric acid (HCl) vapor for 1 hour, then were placed in a high-humidity environment for 90 days. The test setup for HCl exposure is shown in Figure C-2. Specimens were suspended vertically in a glass container above a solution of 12N HCl. Low-pressure air, at 23.89 $\pm$2.8°C (75 $\pm$5°F), was passed through the solution for 1 hour, exposing the specimens to HCl vapor. The specimens were then placed immediately in an environment of 35 $\pm$2.8°C (95 $\pm$5°F) and 80°C $\pm$5% relative humidity, where they remained for 90 days.

At the end of the 90-day period, specimens were cleaned, examined, and rated for corrosion penetration in the same manner as were the salt-spray specimens.

Dynamic Tests—The dynamic test specimens shown in Figure C-1c were subjected to a series of five tests performed in the following sequence:

1. Condensing humidity—specimens were placed in an environment of 48.89°C (120°F) and 100% relative humidity for 2 weeks.

2. Weatherometer—one-week exposure per FTMS 131, method 6152. (Test description in ref. 1.)

3. Cyclic loading—250 cycles in a tension loading machine at -53.89°C (-65°F).

4. Salt spray—1-week exposure per ASTM B117.

5. Potentiostat—determine degree of corrosion penetration by measuring current flow between the cathode and specimen plate. The test apparatus and method are described in the following paragraphs. Test data are included in Table C-2.

The above series of tests were repeated three times, with the cyclic-load stress level increasing progressively. Stress levels during the three cyclic load tests were:

Series 1	155 138 kPa	(22 500 lbf/in^2)
Series 2	193 060 kPa	(28 000 lbf/in^2)
Series 3	241 325 kPa	(35 000 lbf/in^2)

Potentiostat Test Apparatus: Figure C-3 is a schematic diagram of the potentiostat test apparatus. The principal elements include an electrochemical cell installed over a fastener head in the specimen, a potentiostat and recorder, and an electrometer (not shown). The equipment had the following characteristics:

1. Electrochemical cell—The cell consists of a 1.27 cm (0.5 in) inside diameter glass or plastic tube, with a rubber gasket that seals the tube to the specimen and exposes a 3/8-inch-diameter circle of the specimen to the solution. The

cathode is a platinum wire, and the reference electrode is a saturated calomel electrode.

2. Potentiostat—The potentiostat must provide a constant potential within ±1 mV of a present value with a current output of up to 1A.

3. Recorder—The recorder must have an accuracy of 1% of the absolute value of the reading.

4. Electrometer—The electrometer must have a high input impedance (10^{11} to $10^{14}\Omega$). A Keithley model 610C electrometer meets this requirement.

Potentiostat Test Method: The test provides a controlled environment for the measurement of corrosion current versus time on aluminum skin with titanium fasteners installed.

Under a constant potential, a protective film remains effective as long as there is no discontinuity or break in the film and, therefore, no current flow. When a crack or discontinuity appears, a measurable current flow occurs and is recorded as a function of time.

The test procedure is as follows:

1. Provide a test electrolyte of 5 wt % NaCl solution, adjusted to a pH of 3.0 with HCl.

2. Test temperature is 23.9 ±2.8°C (75 ±5°F)

3. Adjust the applied potential between the test specimen (aluminum top plate) and the reference electrode to -0.500V. Periodically check the applied potential on the potentiostat using the electrometer. Remove the electrometer from the test circuit before conducting the actual test.

4. Place specimen on jack table and apply pressure to seal the specimen with the gasket. Transfer 10 ml of the electrolyte into the test cell and place the reference electrode.

5. Connect the three electrodes to the potentiostat. The working electrode is the test specimen. The platinum electrode is the auxiliary electrode, and the reference electrode is the saturated calomel electrode.

6. Select an appropriate current sensitivity and connect the recorder to the potentiostat. Measure the corrosion current as a function of time for 10 minutes.

Further information on the theory and procedures for potentiostatic testing is contained in References C-1 and C-2.

References

C-1. Stone, J.; Tuttle, H. A.; and Bogard, H. N. "The Ford Anodized Aluminum Corrosion Test—FACT," Plating, 53:877, 1966.

C-2. ASTM G5. A standard reference method for taking potentiostatic and potentiodynamic measurements.

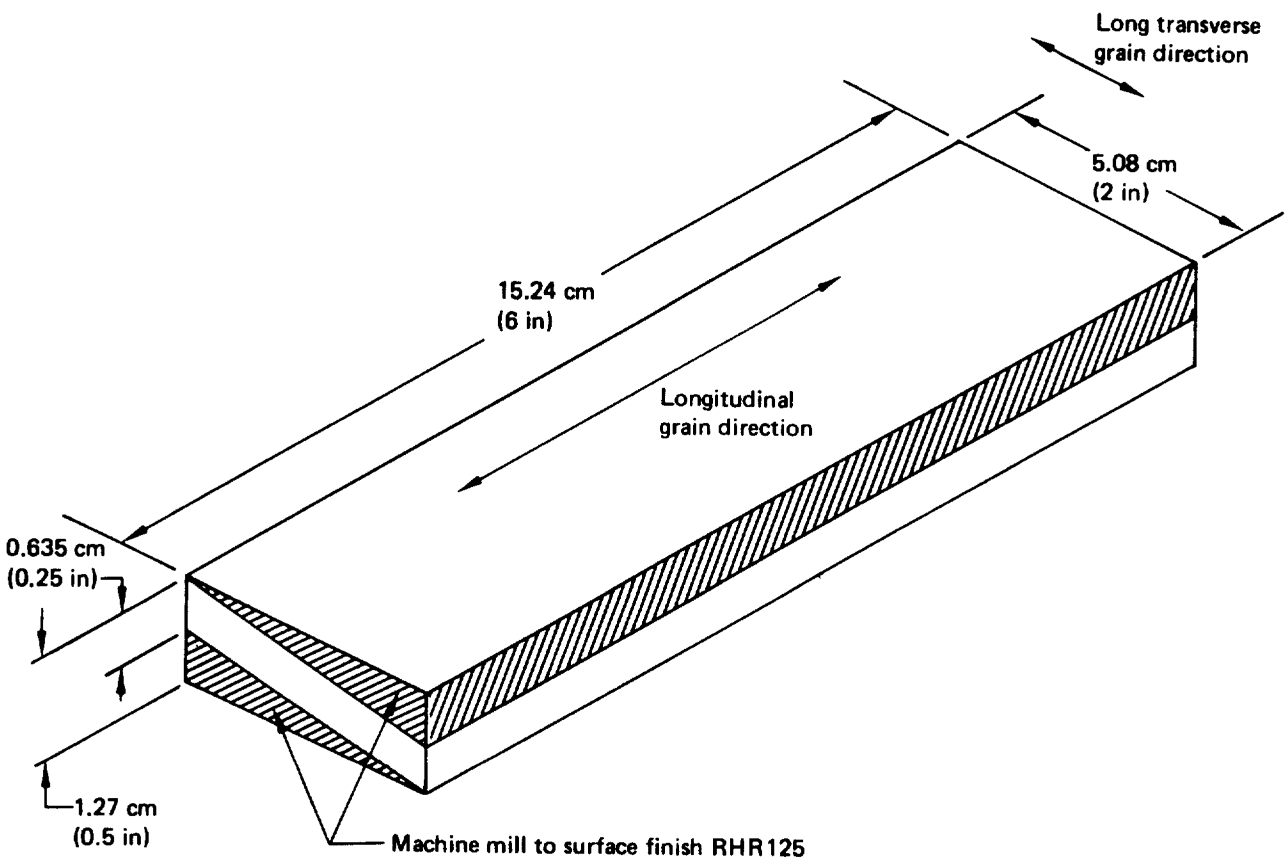

(a) Method of Milling 7075-T6 Plate To Expose Transverse Grain Ends

Figure C-1. Corrosion Test Specimen Fabrication

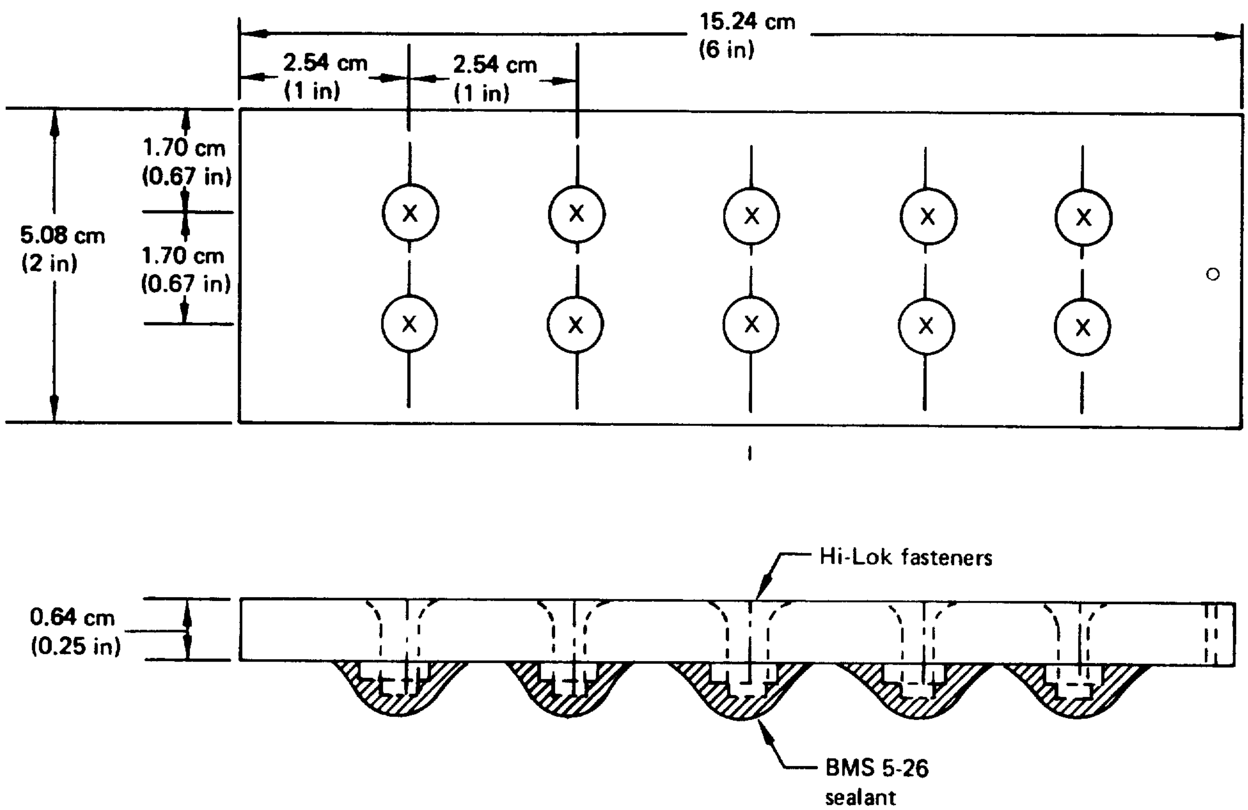

(b) Salt-Spray and Filiform Test Specimen

Figure C-1. Corrosion Test Specimen Fabrication (Continued)

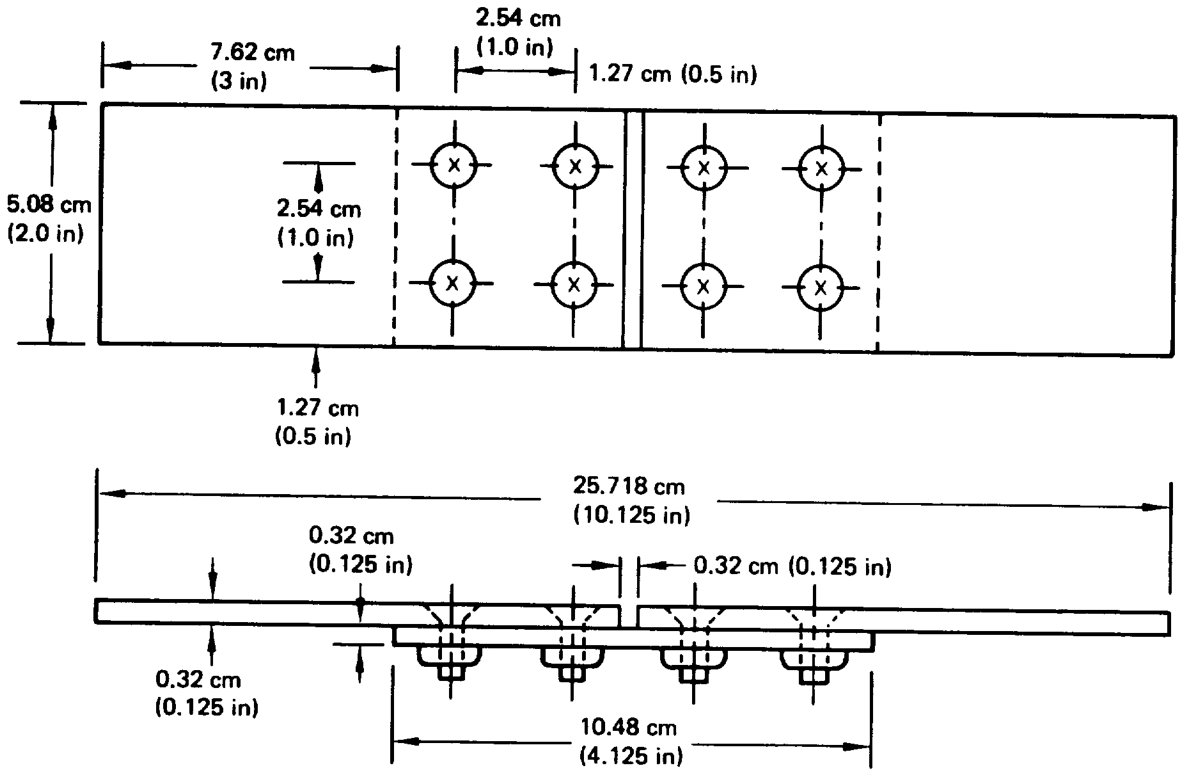

(c) Dynamic Test Specimen

Figure C-1. Corrosion Test Specimen Fabrication (Concluded)

Table C-1. Corrosion Test Specimens

	NUMBER OF SPECIMENS			COATING CONFIGURATION		
	FILI FORM	SALT SPRAY	DYNA-MIC	PRIMER	BASECOAT	TOPCOAT
Control coatings	1	1	1	Epoxy BMS 10-79 0.7 to 1.0 mil	–	Corogard 2 to 3 mil
	1	1	1	Polysulfide BMS 5-95 class F 0.7 to 1.0 mil	–	Polyurethane enamel BMS 10-60 1.4 to 1.8 mil
	1	1	1	Epoxy BMS 10-79 0.7 to 1.0 mil	–	Polyurethane enamel BMS 10-60 1.4 to 1.8 mil
Test coatings	3	3	1	Epoxy BMS 10-79 0.7 to 1.0 mil	Elastomeric polyurethane CAAPCO B-274 4.0 to 5.0 mil	Polyurethane enamel BMS 10-60 1.4 to 1.8 mil
	3	3	1	Epoxy BMS 10-79 0.7 to 1.0 mil	Elastomeric polyurethane Chemglaze M313 4.0 to 5.0 mil	Polyurethane enamel BMS 10-60 1.4 to 1.8 mil
	3	3	1	Epoxy BMS 10-79 0.7 to 1.0 mil	Elastomeric polyurethane Astrocoat Type I 4.0 to 5.0 mil	Polyurethane enamel BMS 10-60 1.4 to 1.8 mil

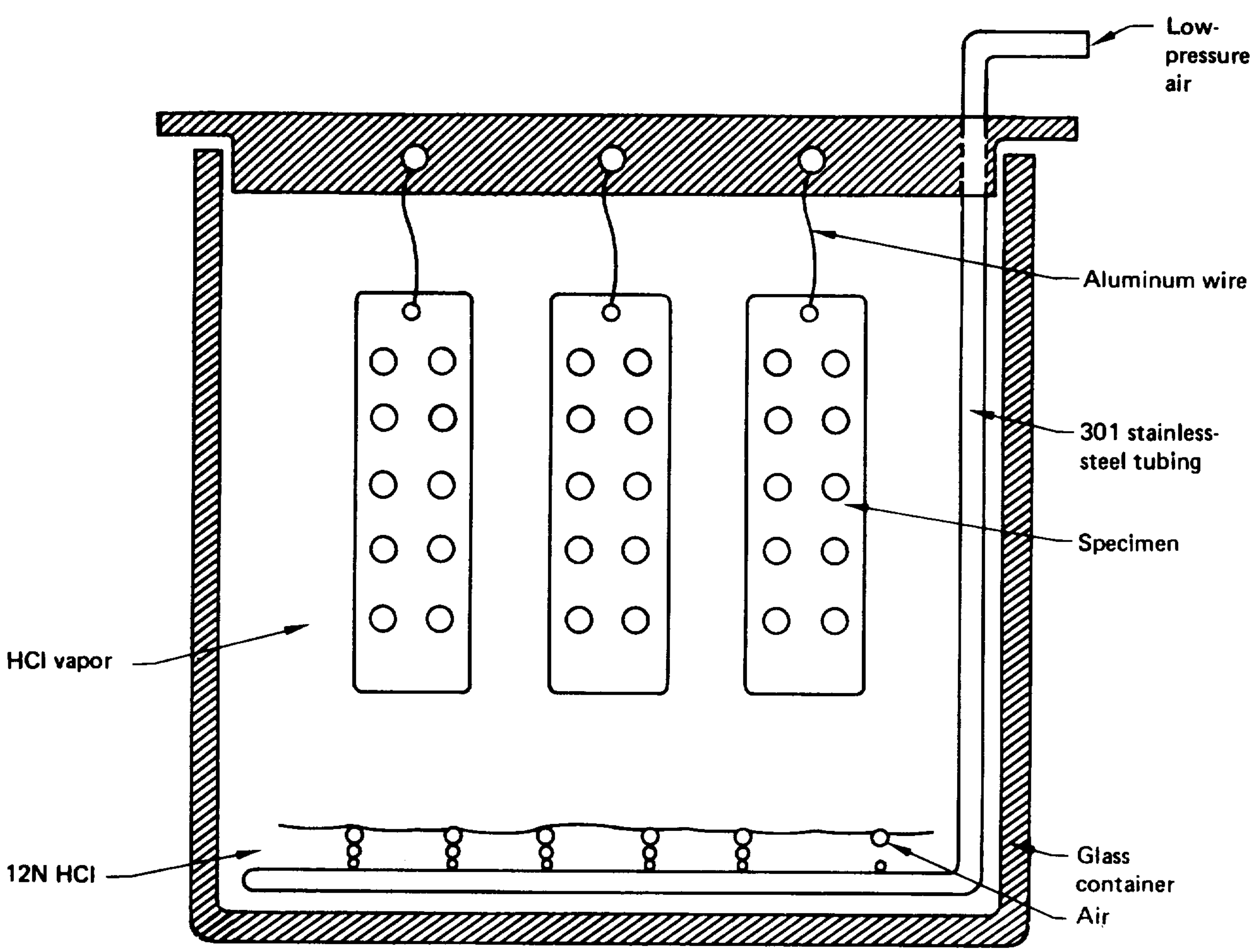

Figure C-2. HCl Vapor Exposure Test Setup

Table C-2. Potentiostat Test Data (First Test)

	COATING	FASTENER	CURRENT, mA, AT TIME, min					
			0	2	4	6	8	10
Control coatings	Polyurethane enamel (BMS 10-60) over polysulfide primer (PR 1432GP)	1		1.660	1.700	1.740	1.740	1.740
		2		0.617	0.617	0.759	0.759	0.759
		3		0.251	0.550	0.708	0.759	0.759
		4		0.646	0.646	0.759	0.794	1.050
		5						
		Average		0.794	0.878	0.992	1.010	1.080
		Log i		-3.100	-3.060	-3.000	-2.990	-2.970
	Polyurethane enamel (BMS 10-60) over epoxy primer (BMS 10-79)	1		0.398	0.437	0.468	0.525	0.479
		2		0.427	0.468	0.479	0.479	0.501
		3		0.955	0.955	0.933	0.933	0.955
		4		0.363	0.479	0.575	0.676	0.776
		5		0.490	0.447	0.427	0.417	0.457
		Average		0.527	0.557	0.576	0.606	0.634
		Log i		-3.280	-3.250	-3.240	-3.220	-3.200

Table C-2. Potentiostat Test Data (Third Test)

	COATING	FASTENER	CURRENT, mA, AT TIME, min					
			0	2	4	6	8	10
Control coatings	Polyurethane enamel (BMS 10-60) over polysulfide primer (PR 1432GP)	1	0.60	9.00	9.40	9.00	9.40	9.00
		2	0.80	4.80	6.10	7.40	7.80	8.30
		3	5.20	5.60	6.60	6.80	7.20	7.60
		4	0.12	1.00	2.30	3.50	5.00	6.40
		5	1.40	2.40	3.40	4.00	4.20	4.90
		Average	1.62	4.56	5.56	6.14	6.72	7.24
		Log i	-2.79	-2.34	-2.25	-2.21	-2.17	-2.14
	Polyurethane enamel (BMS 10-60) over epoxy primer	1	2.20	2.40	2.40	3.00	3.60	3.80
		2	—	6.30	8.00	9.60	9.60	10.00
		3	—	10.20	12.00	13.20	14.40	16.40
		4	3.00	6.00	6.50	7.50	8.20	8.70
		5	8.20	14.40	14.50	16.60	18.50	19.80
		Average	4.50	7.86	8.68	9.98	10.86	11.74
		Log i	-2.35	-2.10	-2.06	-2.00	-1.96	-1.93
	Corogard (EC-843) over epoxy primer (BMS 10-79)	1	—	0.47	0.87	0.94	1.22	1.56
		2	0.04	0.22	0.44	0.46	0.62	0.67
		3	0.01	0.10	0.12	0.16	0.20	0.25
		4	—	0.16	0.27	0.40	0.51	0.56
		5	2.00	3.00	3.80	4.50	5.50	5.60
		Average	0.68	0.79	1.10	1.29	1.61	1.73
		Log i	-3.17	-3.10	-2.96	-2.89	-2.79	-2.76
	CAAPCO B-274 elastomeric polyurethane over epoxy primer (BMS 10-79)	1	On fastener 2, a small current of 0.27 μA, otherwise, never a positive current					
		2						
		3						
		4						
		5						
		Average						
		Log i						
gs	Chemglaze M313 elastomeric	1						
		2						

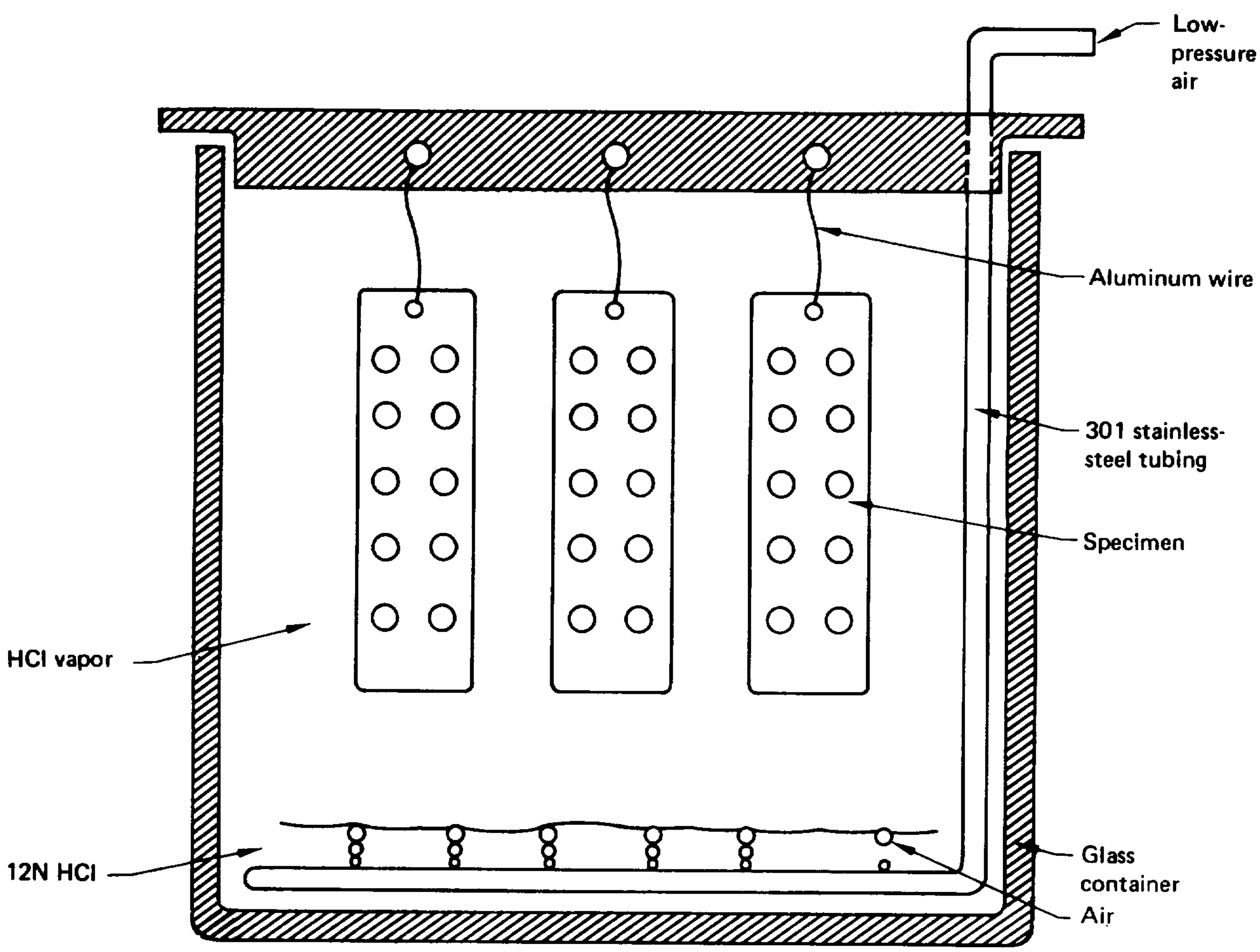

Figure C-2. HCl Vapor Exposure Test Setup

Table C-2. Potentiostat Test Data (First Test)

	COATING	FASTENER	CURRENT, mA, AT TIME, min					
			0	2	4	6	8	10
Control coatings	Polyurethane enamel (BMS 10-60) over polysulfide primer (PR 1432GP)	1		1.660	1.700	1.740	1.740	1.740
		2		0.617	0.617	0.759	0.759	0.759
		3		0.251	0.550	0.708	0.759	0.759
		4		0.646	0.646	0.759	0.794	1.050
		5						
		Average		0.794	0.878	0.992	1.010	1.080
		Log i		-3.100	-3.060	-3.000	-2.990	-2.970
	Polyurethane enamel (BMS 10-60) over epoxy primer (BMS 10-79)	1		0.398	0.437	0.468	0.525	0.479
		2		0.427	0.468	0.479	0.479	0.501
		3		0.955	0.955	0.933	0.933	0.955
		4		0.363	0.479	0.575	0.676	0.776
		5		0.490	0.447	0.427	0.417	0.457
		Average		0.527	0.557	0.576	0.606	0.634
		Log i		-3.280	-3.250	-3.240	-3.220	-3.200
	Corogard (EC-843) over epoxy primer (BMS 10-79)	1		0.014	0.013	0.020	0.021	0.016
		2		0.006	0.008	0.009	0.009	0.008
		3		0.050	0.055	0.062	0.065	0.068
		4		0.006	0.004	0.006	0.006	0.008
		5		0.074	0.087	0.091	0.093	0.093
		Average		0.030	0.033	0.038	0.039	0.038
		Log i		-4.52	-4.48	-4.43	-4.41	-4.42
Test coatings	CAAPCO B-274 elastomeric polyurethane over epoxy primer (BMS 10-79)	1, 2, 3, 4, 5, Average, Log i	No corrosion current					
	Chemglaze M313 elastomeric polyurethane over epoxy primer (BMS 10-79)	1, 2, 3, 4, 5, Average, Log i	No corrosion current					
	Astrocoat Type I elastomeric polyurethane over epoxy primer (BMS 10-79)	1, 2, 3, 4, 5, Average, Log i	No corrosion current					

Table C-2. Potentiostat Test Data (Second Test)

	COATING	FASTENER	CURRENT, mA, AT TIME, min					
			0	2	4	6	8	10
Control coatings	Polyurethane enamel (BMS 10-60) over polysulfide primer (PR 1432GP)	1		4.30	4.20	4.80	6.80	7.60
		2		3.30	4.40	4.50	5.10	5.00
		3		2.30	3.50	3.60	5.00	5.20
		4		4.00	4.40	4.50	4.90	4.40
		5		1.60	1.50	3.10	3.70	4.30
		Average		3.10	3.60	4.10	5.10	5.30
		Log i		-2.51	-2.44	-2.34	-2.29	-2.28
	Polyurethane enamel (BMS 10-60) over epoxy primer (BMS 10-79)	1		2.00	2.20	2.80	3.10	4.25
		2		8.20	9.60	9.40	9.60	10.50
		3		3.10	3.30	4.00	4.70	7.00
		4		2.10	2.50	3.30	6.10	7.50
		5		2.20	2.30	2.60	4.50	7.80
		Average		3.52	3.98	4.42	5.60	7.41
		Log i		-2.45	-2.40	-2.35	-2.25	-2.13
	Corogard (EC-843) over epoxy primer (BMS 10-79)	1		0.22	0.37	0.84	1.18	1.20
		2		0.15	0.27	0.67	0.78	0.95
		3		0.10	0.18	0.46	0.62	0.65
		4		0.10	0.15	0.26	0.54	0.77
		5		0.06	0.08	0.12	0.18	0.22
		Average		0.13	0.21	0.47	0.66	0.76
		Log i		-3.89	-3.68	-3.33	-3.18	-3.12
Test coatings	CAAPCO B-274 elastomeric polyurethane over epoxy primer (BMS 10-79)	1	Fastener 2 had slight corrosion current ≈ 0.3 μA					
		2						
		3						
		4						
		5						
		Average						
		Log i						
	Chemglaze M313 elastomeric polyurethane over epoxy primer (BMS 10-79)	1	Slight corrosion current on fastener 2 ≈ 1 μA					
		2						
		3						
		4						
		5						
		Average						
		Log i						
	Astrocoat Type I elastomeric polyurethane over epoxy primer (BMS 10-79)	1	Slight corrosion current on fastener 2 ≈ 1 μA					
		2						
		3						
		4						
		5						
		Average						
		Log i						

Table C-2. Potentiostat Test Data (Third Test)

	COATING	FASTENER	CURRENT, mA, AT TIME, min					
			0	2	4	6	8	10
Control coatings	Polyurethane enamel (BMS 10-60) over polysulfide primer (PR 1432GP)	1	0.60	9.00	9.40	9.00	9.40	9.00
		2	0.80	4.80	6.10	7.40	7.80	8.30
		3	5.20	5.60	6.60	6.80	7.20	7.60
		4	0.12	1.00	2.30	3.50	5.00	6.40
		5	1.40	2.40	3.40	4.00	4.20	4.90
		Average	1.62	4.56	5.56	6.14	6.72	7.24
		Log i	-2.79	-2.34	-2.25	-2.21	-2.17	-2.14
	Polyurethane enamel (BMS 10-60) over epoxy primer	1	2.20	2.40	2.40	3.00	3.60	3.80
		2	—	6.30	8.00	9.60	9.60	10.00
		3	—	10.20	12.00	13.20	14.40	16.40
		4	3.00	6.00	6.50	7.50	8.20	8.70
		5	8.20	14.40	14.50	16.60	18.50	19.80
		Average	4.50	7.86	8.68	9.98	10.86	11.74
		Log i	-2.35	-2.10	-2.06	-2.00	-1.96	-1.93
	Corogard (EC-843) over epoxy primer (BMS 10-79)	1	—	0.47	0.87	0.94	1.22	1.56
		2	0.04	0.22	0.44	0.46	0.62	0.67
		3	0.01	0.10	0.12	0.16	0.20	0.25
		4	—	0.16	0.27	0.40	0.51	0.56
		5	2.00	3.00	3.80	4.50	5.50	5.60
		Average	0.68	0.79	1.10	1.29	1.61	1.73
		Log i	-3.17	-3.10	-2.96	-2.89	-2.79	-2.76
Test coatings	CAAPCO B-274 elastomeric polyurethane over epoxy primer (BMS 10-79)	1, 2, 3, 4, 5, Average, Log i	On fastener 2, a small current of 0.27 μA; otherwise, never a positive current					
	Chemglaze M313 elastomeric polyurethane over epoxy primer (BMS 10-79)	1, 2, 3, 4, 5, Average, Log i	Never a positive current					
	Astrocoat Type I elastomeric polyurethane over epoxy primer (BMS 10-79)	1, 2, 3, 4, 5, Average, Log i	On fastener 2, a small current of 0.27 μA; otherwise, never a positive current					

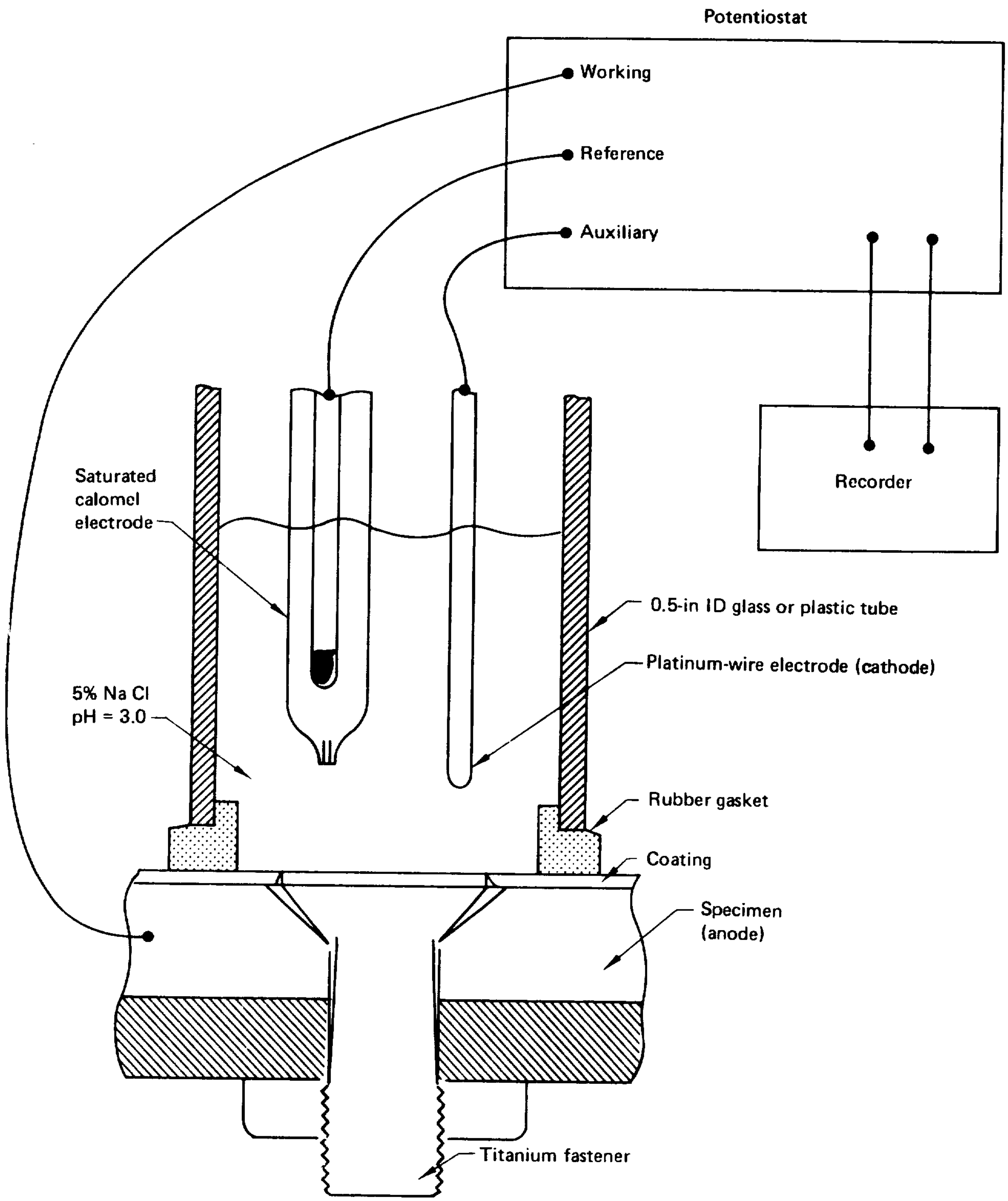

Figure C-3. Schematic Diagram of Potentiostat Test Apparatus

1. Report No.	2. Government Accession No.	3. Recipient's Catalog No.
NASA CR 165928		

4. Title and Subtitle

Aircraft Surface Coatings

5. Report Date

June 1982

6. Performing Organization Code

7. Author(s)

Boeing Commercial Airplane Company (BCAC)
Preliminary Design Department

8. Performing Organization Report No.

D6-49355

9. Performing Organization Name and Address

Boeing Commercial Airplane Company
P.O. Box 3707
Seattle, Washington 98124

10. Work Unit No.

11. Contract or Grant No.

NAS1-15325

12. Sponsoring Agency Name and Address

National Aeronautics and Space Administration
Washington, D.C. 20546

13. Type of Report and Period Covered

Contractor Report—Final
January 1980—February 1982

14. Sponsoring Agency Code

15. Supplementary Notes

Technical Monitor: D. B. Middleton
NASA Langley Research Center

16. Abstract

Liquid, spray-on elastomeric polyurethanes were selected from previous work (reported in NASA CR 158954 and CR 159288) as best candidates for aircraft external protective coatings. Flight tests were conducted to measure drag effects of these coatings compared to paints and a bare metal surface. The durability of two elastomeric polyurethanes, CAAPCO B-274 and Chemglaze M313, was assessed in airline flight service evaluations. Laboratory tests were performed to determine corrosion protection properties, compatibility with aircraft thermal anti-icing systems, the effect of coating thickness on erosion durability, and the erosion characteristics of composite leading edges - bare and coated.

A cost and benefits assessment was made to determine the economic value of various coating configurations to the airlines.

17. Key Words (Suggested by Author(s))

Surface coatings
Elastomeric polyurethanes
Leading-edge erosion
Corrosion protection
Drag reduction

18. Distribution Statement

[redacted]

Subject Category—05

19. Security Classif. (of this report)	20. Security Classif. (of this page)	21. No. of Pages	22. Price
Unclassified	Unclassified	171	

N 305 [redacted]